



UNIVERSITEIT VAN PRETORIA
UNIVERSITY OF PRETORIA
YUNIBESITHI YA PRETORIA

Denkleiers • Leading Minds • Dikgopolo tša Dihlalefi

Exploring the kinase inhibitor chemical space for dual active and gametocyte-focussed antimalarials.

by

Mariëtte van der Watt (neé Botha)

Submitted in the partial fulfilment of the requirements for the degree

Philosophiae Doctor

(Specialisation in Biochemistry)

In the Faculty of Natural and Agricultural Sciences
Department of Biochemistry, Genetics and Microbiology

University of Pretoria

Pretoria

South Africa

December 2018

I, **Mariëtte van der Watt**, declare that the thesis, which I hereby submit for the degree ***Philosophiae Doctor*** in the Department of Biochemistry, at the University of Pretoria, is my own work and has not previously been submitted by me for the degree at this or any other tertiary institution.

SIGNATURE:.....

DATE:.....

PLAGIARISM DECLARATION

University of Pretoria
Faculty of Natural and Agricultural Science
Department of Biochemistry

Full names of student: Mariëtte Elizabeth van der Watt

Student number: 04272528

Title of work: Exploration of the kinase inhibitor chemical space for dual active and gametocyte-focussed antimalarials.

Declaration

1. I understand what plagiarism is and I am aware of the University's policy in this regard.
2. I declare that this thesis is my own original work. Where other people's work has been used (either from a printed source, internet or any other source), due acknowledgement was given and reference was made according to departmental requirements.
3. I did not make use of another student's previous work and submit it as my own.
4. I did not allow and will not allow anyone to copy my work with the intention of presenting it as his or her own work.

SIGNATURE STUDENT:.....

DATE:.....

ACKNOWLEDGEMENTS

I would like to extend my deepest gratitude to my heavenly Father for the abundant grace I experienced during this time, and for giving me the strength and courage to endure the process and complete this degree.

To my husband, Jan van der Watt, thank you for all the sacrifices you made in order to make this PhD achievable. Also, thank you for being a constant source of support, love and encouragement and for your unsuspected surprises and broad shoulders during tough times. I am eternally grateful to my parents, Pieter and Elsa Botha, for always believing in me and loving me without bounds.

I am grateful to my supervisor, Prof. Lyn-Marie Birkholtz, for her mentorship through what has been an invaluable intellectual and emotional learning curve. Thank you for being a continuous source of insight, novel ideas and patience. To my co-supervisor, Dr. Jandeli Niemand, thank you for your input and advice towards shaping this project and thesis into a valuable research contribution.

I would like to thank all the members at the Drug Discovery and Development Centre (H3D) at the University of Cape Town (UCT), involved in the synthesis and provision of the kinase-focussed inhibitor library. Thank you to Dr. Claire Le Manach and Dr. Tanya Paquet, for providing physicochemical and biological data (asexual stage activity, cytotoxicity) for these compounds. I am grateful to my colleagues and friends, Dr. Janette Reader, Dr. Dina Coertzen and Dr. Bianca Brider, for their constant reassurance and research support, as well as “office antics” that kept me motivated. A special acknowledgement to Dr. Janette Reader for her insight on the speed-of-action assay and her contribution towards confirming the gametocyte stage-specific distribution achieved with the luciferase reporter cell lines.

To my funding body, the South African Medical Research Council Strategic Health Innovation Partnership, thank you for providing the funds and infrastructure for completing this study.

SUMMARY

The success achieved in controlling malaria in recent years [1, 2], has caused a focal shift to elimination of the disease, with renewed interest in the discovery of novel chemotherapeutics with unique modes of action (MoAs) able to target the asexual pathogenic forms of the disease-causing parasite, *Plasmodium falciparum*, even in resistant strains. Moreover, to eliminate the disease, these chemotherapeutics are now also expected to block transmission of the parasite between human hosts and mosquito vectors [3]. Particularly, *P. falciparum* mature gametocytes form an attractive, pharmaceutically tractable target for transmission-blocking antimalarials. Current drug discovery programmes therefore aim to identify novel chemical entities that either i) have dual activity against both asexual parasites and gametocytes or ii) are selective towards gametocytes [4].

To continue populating the global pipeline of novel antimalarials, this study aimed to evaluate the kinase inhibitor chemical space for its antiplasmodial profile and identify compounds useful in malaria elimination strategies. To screen for compounds with gametocytocidal activity requires enabling technologies, including the bulk production of viable gametocytes, and the development of robust assay platforms to evaluate activity in screening endeavours. An optimised gametocyte production protocol was developed, resulting in high-yield (~5% on day 11, n=10), tightly synchronised stage-specific gametocytes. This allowed subsequent parallel assays (ATP, pLDH, luciferase reporter and PrestoBlue[®]) which indicated that different assay platforms were not able to screen variant chemotypes with the same efficiency, due to their interrogation of different biological systems. Altogether, this evaluation accurately dissected the key parameters for gametocytocidal assays towards determining the transmission-blocking potential of chemical entities.

A kinase-focussed inhibitor library was subsequently screened using the same cross-validative approach, but also including additional gametocytocidal hit profiling assays, e.g. stage-specificity, speed-of-action and determination of *ex vivo* efficacy. Compounds (90) with submicromolar activity towards late stage gametocytes were validated across several assay platforms. From these, 21 potent ($IC_{50} < 100$ nM) dual active kinase inhibitors were identified; targeting late stage gametocytes within 48 hours and blocking transmission to

mosquitoes. These potent hits were additionally active against early stage gametocytes and asexual stages, with >1000-fold selectivity for the parasite over mammalian cells and no *in vitro* or *ex vivo* cross-resistance. Moreover, the chemogenomic fingerprint of lead kinase inhibitors revealed the importance of targeting kinases in asexual and gametocyte stages. Towards target candidate profile (TCP)-5 elucidation, an uncomplicated cheminformatic approach was created, validated and used to identify unique dual active (TCP-1 and TCP-5) and gametocyte-selective (TCP-5) chemotypes from the kinase-focussed library. This uncomplicated strategy entailed the combination of a novel TCP-5 selectivity factor, structure-activity landscape analysis and R-group deconvolution, which together enabled easily-interpreted gametocyte SAR. This led to the identification of a distinctive gametocyte-selective scaffold, an enticing chemical starting point for the development of either combination or single, gametocyte-selective therapies, vital to achieve malaria elimination.

Collectively, this doctoral study represents the most extensive exploration of kinase-focussed inhibitors for antiplasmodial action against both asexual and gametocyte stages of *P. falciparum*. Enabling technologies were established that are useful to the antiplasmodial drug discovery community and here, led to the discovery of potent hit compounds with transmission-blocking capacity. The data contribute greatly to our understanding of screening for dual active and gametocyte-selective antimalarials as well as the chemical space required for kinase inhibitors within malaria elimination agendas.

TABLE OF CONTENTS

PLAGIARISM DECLARATION	ii
ACKNOWLEDGEMENTS	iii
SUMMARY	iv
TABLE OF CONTENTS	vi
LIST OF FIGURES	ix
LIST OF TABLES	xi
ABBREVIATIONS	xii
Chapter 1: Literature review	1
1.1 The socio-economic impact of malaria	1
1.2 The multifaceted <i>Plasmodium</i> life cycle	4
1.3 Gametocytogenesis	6
1.3.1 Gametocyte morphology and localisation	6
1.3.2 Sexual commitment	9
1.3.3 Gametocyte developmental biology	12
1.4 Malaria control	14
1.4.1 Vector control	15
1.4.2 Vaccine development	16
1.4.3 Contemporary chemotherapeutics and resistance	16
1.4.5 Drug discovery towards novel treatments	18
1.4.5.1 Drug discovery for malaria elimination	21
1.5 Eukaryotic protein kinases (ePKs) as drug targets	24
1.6 The <i>P. falciparum</i> kinome	29
1.7 Work leading up to this investigation	33
1.7.1 Diaminothienyl-pyrimidines (DTPs)	35
1.7.2 2-aminopyridines and 2-aminopyrazines (2-APs)	36
1.7.3 Imidazopyridazines (IMPs)	37
1.7.4 Imidazopyridines (IPs)	39
1.8 Hypothesis	41
1.9 Aim	41
1.10 Objectives	41
1.11: Outputs generated	41
Chapter 2: Establishment of an optimised gametocyte production protocol and confirmation of viability on orthogonal assay platforms	43
2.1 Introduction	43
2.2 Methods and materials	46
2.2.1 Ethics	46
2.2.2 <i>In vitro</i> cultivation of asexual stage <i>Plasmodium falciparum</i> parasites	46
2.2.3 Induction of gametocytogenesis and general maintenance of gametocyte cultures	47
2.2.4 Characterisation, cultivation, genotypic and phenotypic profiling of clinical isolates of southern African origin	47
2.2.5 Male gamete exflagellation	48
2.2.6 Validation of stage-specific gametocyte production by flow cytometry and cell sorting	48
2.2.7 Gametocytocidal activity assays	49
2.2.7.1 Anti-malarial compounds	49
2.2.7.2 Resazurin-based dye assay	49

2.2.7.3	pLDH assay	50
2.2.7.4	ATP bioluminescence assay	50
2.2.7.5	Luciferase reporter assay	51
2.2.8	Data analysis	51
2.3	Results	52
2.3.1	Optimisation of <i>P. falciparum</i> gametocyte production	52
2.3.2	Phenotyping, genotyping and characterisation of gametocyte production from contemporary African clinical isolates	56
2.3.3	Validation of stage-specific gametocyte production	58
2.3.4	Assays for gametocytocidal activity	60
2.3.5	ATP assay as an indicator of parasite viability	60
2.3.6	pLDH assay as an indicator of metabolic activity in viable parasites	61
2.3.7	PrestoBlue [®] assay as an indicator of parasite respiration	62
2.3.8	Luciferase reporter assay as an indicator of stage-specific gametocyte gene expression	63
2.3.9	Assay comparisons for gametocytocidal screens	64
2.4	Discussion	69
2.5	Conclusions	75
	Chapter 3: Potent <i>Plasmodium falciparum</i> gametocytocidal compounds identified by exploring the kinase inhibitor chemical space for dual active antimalarials	78
3.1	Introduction	78
3.2	Methods and Materials	79
3.2.1	Chemistry	79
3.2.2	Ethics	79
3.2.3	<i>In vitro</i> cultivation of asexual stage parasites and induction of gametocytes	80
3.2.4	<i>In vitro</i> <i>P. falciparum</i> antiplasmodial activity and cytotoxicity evaluation	80
3.2.5	<i>In vitro</i> gametocytocidal activity evaluation	80
3.2.6	Luciferase reporter assay	81
3.2.7	Semi-quantitative RT-PCR	81
3.2.8	Resazurin-based dye assay	81
3.2.9	ATP bioluminescence assay	81
3.2.10	Phenotypic profiling of clinical isolates of southern African origin	83
3.2.11	Gametocytocidal stage-specificity and speed of action	83
3.2.12	Standard membrane feeding assay (SMFA)	84
3.2.13	DNA microarray analysis	84
3.3	Results	85
3.3.1	Hit identification	85
3.3.2	Hit profiling	90
3.3.4	Functional evaluation of dual active kinase inhibitors	100
3.4	Discussion	103
3.5	Conclusions	105
	Chapter 4: Evaluation of cheminformatic approaches towards the identification of dual active and gametocyte-selective scaffolds	107
4.1	Introduction	107
4.2	Methods and materials	111
4.2.1	Datasets	111
4.2.2	Biological and physicochemical data acquisition	111
4.2.3	Chemical clustering of the TCAMS dataset	112
4.2.4	Physicochemical properties and activity associations	112

4.2.5	Prediction of the physicochemical parameters that contribute to asexual and gametocyte-selective activity within the TCAMS dataset	112
4.2.6	Determination of SARs within the kinase-focussed series	113
4.3	Results	113
4.3.1	Interrogation of cheminformatic approaches using the TCAMS dataset	113
4.3.1.1	Chemical clustering	113
4.3.1.2	Physicochemical space extraction	116
4.3.1.3	Quantitative evaluation of the physicochemical contribution to asexual and gametocyte-selective activity	119
4.3.2	Establishment of the cheminformatic approach using a kinase-focussed inhibitor series	120
4.3.2.1	Physicochemical space extraction	121
4.3.2.2	R-group deconvolution of the kinase-focussed inhibitor series	127
4.4	Discussion	132
4.5	Conclusion	136
	CHAPTER 5	137
	REFERENCES	142
	APPENDIX	177

LIST OF FIGURES

Chapter 1

Figure 1.1: Malaria incidence status as indicated by region for 2015.	3
Figure 1.2: <i>Plasmodium</i> life cycle	5
Figure 1.3: Morphologically distinct stages of <i>P. falciparum</i> gametocyte development	8
Figure 1.4: Epigenetic regulation of sexual commitment	11
Figure 1.5: The pipeline of antimalarial drugs aligned to target candidate profiles (TCPs)	20
Figure 1.6: Malaria control and elimination are currently entirely dependent on the use of chemical interventions	22
Figure 1.7: SAMTC test cascade for screening of transmission-blocking antimalarial compounds	24
Figure 1.8: Structure of the eukaryotic protein kinase (ePK) catalytic domain	25
Figure 1.9: Structure of the eukaryotic protein kinase (ePK) catalytic domain	28
Figure 1.10: Phylogenetic classification of the <i>P. falciparum</i>	29
Figure 1.11: Life cycle transition involvement of <i>Plasmodium</i> kinases	32
Figure 1.12: SAR optimisation highlights for the diaminothienyl pyrimidine series.	36
Figure 1.13: SAR optimisation highlights for the 2-aminopyridine series.	37
Figure 1.14: SAR optimisation highlights for the imidazopyridazine series.	38
Figure 1.15: SAR optimisation highlights for the 2,6-imidazopyridine series.	40

Chapter 2

Figure 2.1: Visual evaluation of <i>P. falciparum</i> kinetics of conversion, gametocyte production, and asexual elimination.	54
Figure 2.2: Influence of gentamicin on gametocyte viability and drug assays.	55
Figure 2.3: <i>Pfap2-g</i> transcript levels mirror gametocyte production.	57
Figure 2.4: Stage-specific, quantitative analysis of gametocyte populations	58
Figure 2.5: Functional validation of gametocyte viability.	59
Figure 2.6: ATP assay evaluation	61
Figure 2.7: pLDH assay evaluation	62
Figure 2.8: PrestoBlue [®] assay evaluation	63
Figure 2.9: Luciferase reporter assay evaluation for early stage (EG) and late stage (LG) gametocytes	64
Figure 2.10: Comparative analysis of the performance of four assay platforms for gametocytocidal compounds.	66
Figure 2.11: Dual activity of the 10-compound set (MMV) toward <i>P. falciparum</i> early and late gametocyte stages.	67
Figure 2.12: Gametocytocidal activity of MMV 10-compound set against <i>ex vivo</i> clinical isolates of <i>P. falciparum</i> .	68

Chapter 3

Figure 3.1: Schematic of the synthesis of the 6,9-IPs	79
Figure 3.2: Stage-specific gametocyte production and speed-of-action assay	84
Figure 3.3: Description of the critical path followed for the screening of select scaffolds from kinase libraries for gametocytocidal activity.	86
Figure 3.4: Primary hit identification for late stage gametocytocidal activity.	87
Figure 3.5: Biological profiles of the evaluated compounds.	90
Figure 3.6: Late stage gametocytocidal activity of the lead compounds against <i>ex vivo</i> <i>P. falciparum</i> clinical isolates.	91
Figure 3.7: Stage-specific gametocyte production.	92
Figure 3.8: Dual reactivity of the lead compound series toward different <i>P. falciparum</i> gametocyte developmental stages.	94
Figure 3.9: Speed-of-action evaluation for the most potent compounds.	96
Figure 3.10: Stage-specific expression of 18 individual descriptors in late (>95% stage IV/V) and mature (>95% stage V) gametocytes.	97
Figure 3.11: Late (>90% stage IV/V) and mature (>95% stage V) stage-specific activity of the hit compounds.	99
Figure 3.12: Transmission-blocking capacity of MMV642943 evaluated during indirect SMFA.	100
Figure 3.13: Transcriptional response evaluation of parasites treated with kinase inhibitors.	102

Chapter 4

Figure 4.1: Spectrum of activity of compounds screened for gametocytocidal activity	109
---	-----

Figure 4.2: Identification of gametocyte-selective chemotypes through chemical clustering.	115
Figure 4.3: Structure-dual activity landscape analysis of the TCAMS subset	116
Figure 4.4: Inter-cluster structure activity landscape interrogation of gametocyte-selective nodes 5-8.	118
Figure 4.5: Intra-cluster structure activity landscape interrogation of groups 3 (A) and 4 (B).	119
Figure 4.6: Inter-series delineation of multi-stage activity of kinase chemotypes.	122
Figure 4.7: Intra-series structure activity landscape interrogation of the DTPs	123
Figure 4.8: Intra-series structure activity landscape interrogation of the 2-APs.	124
Figure 4.9: Intra-series structure activity landscape interrogation of the IMPs.	125
Figure 4.10: Intra-series structure activity landscape interrogation of the IMPs.	126
Figure 4.11: Intra-series structure activity landscape interrogation of the 2,6-IPs.	127
Figure 4.12: R-group deconvolution of the 2-aminopyridine and 2-aminopyrazine series.	128
Figure 4.13: R-group deconvolution of the representative IMP cores	129
Figure 4.14: R-group deconvolution of the 6,9-IP series.	130
Figure 4.15: R-group deconvolution of the 2,6-IP series.	131
Figure 4.16: A unique, gametocyte-selective scaffold from the 6,9-IP and 2,6-IP series	132

LIST OF TABLES

Chapter 1

Table 1.1: Hit chemical starting points from the diaminothienyl-pyrimidine, 2-aminopyridine, imidazopyridazine, 6,9-imidazopyridine and 2,6-imidazopyridine series	34
--	----

Chapter 2

Table 2.1: Overview of the optimised gametocyte production protocol	53
Table 2.2: Evaluation of various <i>in vitro</i> gametocytogenesis induction methods using <i>P. falciparum</i> parasites under different conditions	53
Table 2.3: Origin and drug resistance genotypes of southern African clinical isolates producing gametocytes.	56
Table 2.4: Phenotyping of a panel of 5 <i>P. falciparum</i> clinical isolates using a standard panel of antimalarial compounds	57
Table 2.5: Performance indicators of the four assay platforms	60

Chapter 3

Table 3.1: Transcripts and oligonucleotides used during the stage-specific validation of gametocyte maturity.	82
Table 3.2: Asexual and late stage profiles of the evaluated compounds	89
Table 3.3: Origin and drug resistance genotypes of southern African clinical isolates producing gametocytes	91

Chapter 4

Table 4.1: Criteria for the characterisation of gametocyte-selective compounds	113
Table 4.2: Multiple linear regression of asexual parasites versus stage V gametocyte IC ₅₀ related to physicochemical descriptors	120

ABBREVIATIONS

ACT	Artemisinin-based combination therapy
ADMET	Absorbtion, distribution, metabolism, excretion and toxicity
APAD	3-Acetyl pyridine adenine dinucleotide
ApiAP2	Apicomplexan Apetala 2 DNA-binding
aPK	Atypical protein kinases
2-AP	2-aminopyridine
ATP	Adenosine triphosphate
ATP4	P-type cation transporter ATPase4
cAMP	Cyclic adenosine monophosphate
CCp	Complement control proteins
CDK	Cyclin dependent kinase
CDPK	Calcium-dependent protein kinases
CHMI	Controlled human malaria infection
cGMP	Cyclic guanosine monophosphate
CNV	Copy number variations
CK1	Casein kinase 1
CLK	CDK-like kinases
cLogP	Octanol-water partition coefficients
CSP	Circumsporozoite protein
CV	Coefficient of variation
DAG	Diacylglycerol
DANQ	Diaminonaphthoquinones
DAPI	4'-6-diamidino-2-phenylindole
DGFA	Dual gamete formation assay
DHA	Dihydroartemisinin
DHODH	Dihydroorotate dehydrogenase
DHFR	Dihydrofolate reductase
DHPS	Dihydropteroate synthase
DTP	Diaminothienyl-pyrimidine
EGFR	Epidermal growth factor receptor
EG	Early stage gametocyte
ePK	Eukaryotic protein kinase

ER	Endoplasmic reticulum
ETC	Electron transport chain
EWG	Electron withdrawing groups
FDR	False discovery rate
G6PD	Glucose-6-phosphate dehydrogenase
Gdv-1	Gametocyte development protein 1
GEXP	Gametocyte exported protein
GFP	Green fluorescent protein
GMAP	Global Malaria Action Plan
GPCR	G-protein coupled receptor
GSEA	Gene set enrichment analysis
GSK	GlaxoSmithKline
GTP	Guanosine triphosphate
H2L	Hit-to-lead
H3D	Drug Discovery and Development Centre
H3K9me3	H3-trimethylated residues on lysine 9
HBA	Hydrogen bond accepting
HBD	Hydrogen bond donors
HCI	High content imaging
Hda2	Histone deacetylase 2
HMT	Histone methyltransferase
HP1	Heterochromatin protein 1
hpi	Hours post invasion
HTS	High-throughput screening
IDC	Intra-erythrocytic developmental cycle
IMC	Inner membrane complex
IMP	Imidazopyridazine
IP	Imidazopyridine
IP ₃	Inositol-(1,4,5)-trisphosphate
IRS	Indoor residual spraying
ITN	Insecticide treated bednet
LG	Late stage gametocyte
LysoPC	Lysophosphatidylcholine
malERA	Research and development agenda for malaria eradication
MDA	Mass drug administration

MMV	Medicines for Malaria Venture
MoA	Mode of action
mSAT	Mass screening and treatment
MTS	Medium-throughput screening
MW	Molecular weight
NAG	N-acetyl glucosamine
NBT	Nitro blue tetrazoliumchloride
NIMA	Never in mitosis/Aspergillus
PCA	Principal component analysis
PCR	Polymerase chain reaction
PES	Phenazine ethosulphate
PI	Phosphoinositide
PI3K	Phosphatidylinositol 3-kinase
PI3P	Phosphatidylinositol 3-phosphate
PI4P	Phosphatidylinositol 4-phosphate
PI4K	Phosphatidylinositol 4-kinase
PIP ₂	Phosphatidylinositol-(4,5)-bisphosphate
PIP5K	Phosphatidylinositol-4-phosphate-5-kinase
PIKK	Phosphoinositide lipid kinase kinase
PKA	Protein kinase A
PKB	Protein kinase B
PKG	Protein kinase G
PLC	Phospholipase C
pLDH	Parasite lactate dehydrogenase
PSA	Polar surface area
PVM	Parasitophorous vacuolar membrane
RBM	Roll Back Malaria
RFLP	Restriction fragment length polymorphism
RLU	Relative light unit
RT	Room temperature
RT-PCR	Real-time reverse transcriptase polymerase chain reaction
SAM	S-adenosylmethionine
SAMTC	South African Malaria Transmission-blocking Consortium
SAR	Structure-activity relationship
SALI	Structure–activity landscape index

S/B	Signal to background ratio
SEC	Single exposure chemoprotection
SERCaP	Single exposure radical cure and prophylaxis
SFI™	BioFocus® SoftFocus® Ion Channel
SFK™	BioFocus® SoftFocus® Kinase
SI	Selectivity index
SMFA	Standard membrane feeding assay
SMILES	Simplified molecular-input line-entry system
SMKI	Small molecule kinase inhibitors
S/N	Signal to noise ratio
SNP	Single nucleotide polymorphisms
SOM	Self-organising maps
SS	Sum of squares
TCA	Tricarboxylic acid
TCAMS	Tres Cantos Antimalarial Set
TCP	Target candidate profile
TKL	Tyrosine kinase-like
TPP	Target product profile
UCT	University of Cape Town
WGS	Whole genome sequencing
WHO	World Health Organization
XA	Xanthurenic acid

CHAPTER 1

LITERATURE REVIEW

1.1 The socio-economic impact of malaria

Malaria remains one of the most prominent diseases in the third world, with 92% of cases occurring in the World Health Organization (WHO) African region [5]. Infections with *Plasmodium* genus parasites (kingdom Protista, phylum Apicomplexa, class Hematozoa, order Haemosporidia) [6] lead to absenteeism (from schools and universities), reduced productivity in the workplace, lost opportunities for joint economic ventures and tourism and ultimately leads to losses in income [7]. Cost implications for governments include maintenance, supply and staffing of healthcare facilities, the acquisition of drugs and other provisions as well as public health interventions (indoor residual spraying, IRS; insecticide-treated bed nets, ITNs). Malaria results in US\$12 billion annual losses (economic productivity, foreign investment, tourism and trade) for sub-Saharan Africa [8], but by contrast, government and international partners' investments amounted only to US\$2.7 billion in control and elimination efforts in 2016, reflecting that more investment is still required to offset losses. This economic burden incurred is further increased by co-morbidities of two other African diseases viz. acquired immunodeficiency syndrome, caused by the human immunodeficiency virus and tuberculosis, caused by the bacterium *Mycobacterium tuberculosis* [1].

Malaria parasites are vectored by mosquitoes of the *Anopheles* genus. The *Anopheles gambiae* species complex are major vectors of malaria in sub-Saharan Africa and represent a clade of morphologically identical, closely related species, including *Anopheles gambiae* sensu stricto, *Anopheles arabiensis* and *Anopheles coluzzii* [9]. The primary malaria vector in South Africa is *An. arabiensis*, although *Anopheles funestus* is also implicated [10]. Human malaria is caused by five species of the parasite: *Plasmodium falciparum*, *Plasmodium vivax*, *Plasmodium malariae*, *Plasmodium ovale*, and *Plasmodium knowlesi*. The latter, together with a recent report describing the detection of *Plasmodium cynomolgi* in humans, make up two zoonotic species [11]. *P. vivax* parasites are the most geographically widespread [12], but only responsible for ~4% of global malaria cases [1], whereas *P. falciparum* is responsible for the majority (99%) of deaths in humans in sub-Saharan Africa [13, 14].

The research and development agenda for malaria eradication (malERA) was established in 2007 to identify research areas to support elimination of the disease globally [15]. This concept galvanized the malaria community and a global malaria elimination agenda was defined within the Global Malaria Action Plan (GMAP; a collaboration between the WHO and the Roll Back Malaria (RBM) Partnership), the RBM Global Strategic Plan 2005-2015 and the WHO Framework for Malaria Elimination to eliminate the disease in at least 8-10 regions within an eight year timeframe [16-18]. The main goals of the GMAP were to (i) achieve universal coverage for populations at risk using locally appropriate interventions for prevention and case management, (ii) reduce global malaria cases by 75%, and (iii) reduce global malaria deaths to ~zero towards 2015 [16].

Encouragingly, the 2000-2015 period saw remarkable progress towards global malaria elimination with a 40% and 60% decrease observed in malaria incidence and mortality rates, respectively. Countries exhibiting ≥ 3 years of zero indigenous cases (no local malaria transmission) are classified as having eliminated malaria, and 17 countries achieved this status [1] (grey areas, Figure 1.1). In addition, in 2016, the WHO identified 21 countries with the potential to eliminate malaria by 2020 [2] and 46 countries reporting fewer than 10 000 annual cases in 2017 [5], a 24% improvement since 2010 when only 37 countries reported this decrease [19]. These successes were achieved through better surveillance, enhanced community education, diagnoses, improved treatment and vector control, implemented through the scale up of three core interventions *viz.* ITNs, IRS and artemisinin-based combination therapies (ACTs), respectively responsible for 69%, 10% and 21% of the reductions in morbidity and mortality [2].

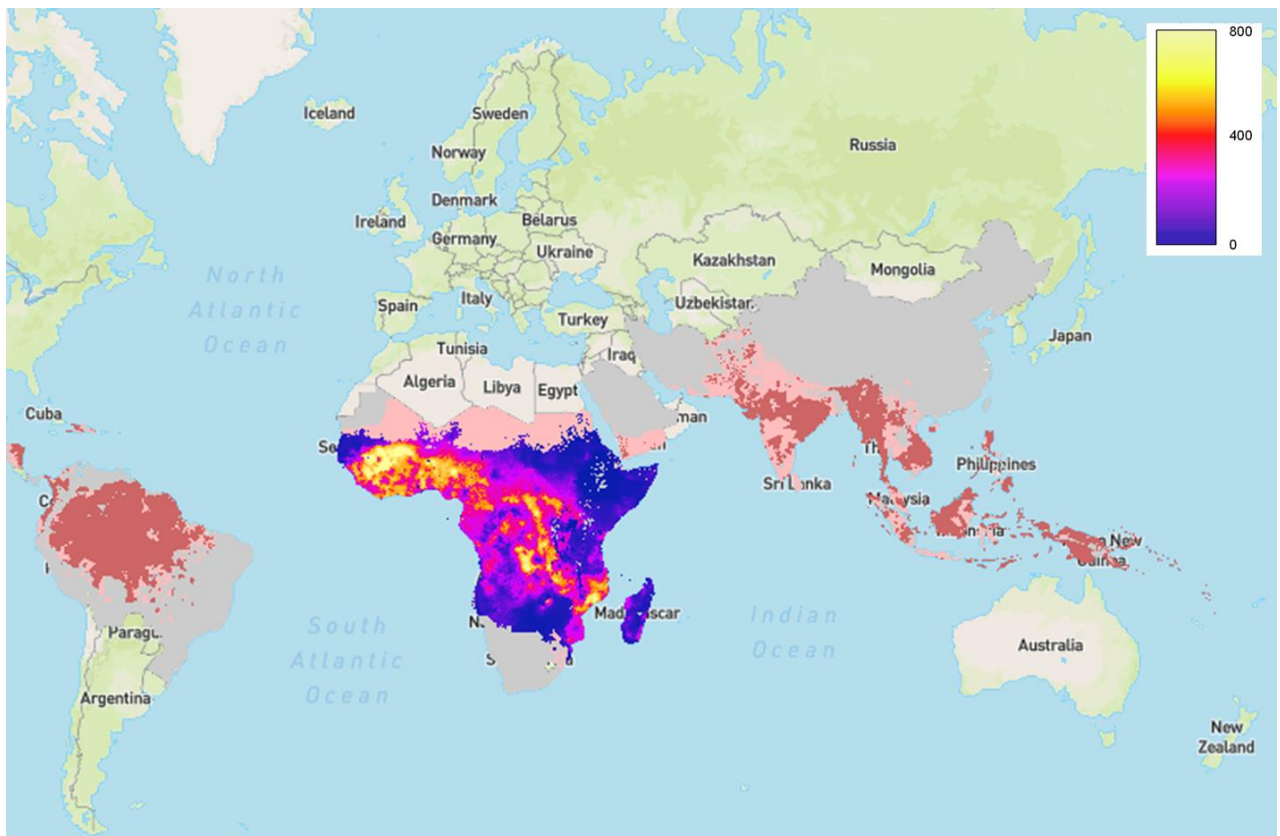


Figure 1.1: Malaria incidence status as indicated by region for 2015. This image is in the public domain as part of the Malaria Atlas Project, under licence: Creative Commons Attribution 3.0 (<https://creativecommons.org/licenses/by/3.0/>). Clear: no malaria (non-endemic). Grey: zero cases (malaria-free) since 2000. Pink: annual case incidence <1/10 000. Red: annual case incidence >1/10 000 (stable malaria transmission). The scale represents the number of cases per 1000 individuals, focussed on the African continent.

However, from 2014-2017, a stagnation in progress towards global elimination was observed, with only an 18% global reduction in incidence rates [5]. Alarmingly, the WHO Americas, Southeast Asia, Western Pacific and African regions reported significant increases in case incidence over this time [2]. Furthermore, where the 2016 WHO Malaria Report stated that 212 million cases and 429 000 deaths occurred in 2015 [20], the 2018 WHO Malaria Report states an increase to 219 million cases and 435 000 deaths for 2017 [5]. In South Africa, similar trends were observed with an increase of 3768 cases for the 2015-2016 season from 2572 cases in 2013 [1], including cases classified as both local and imported, curbing the progress in this country towards elimination, and setting the elimination target back to 2020 [2, 21]. Several factors are postulated to be involved in these global trends including favourable climatic conditions, increased movement across borders, the prevalence of drug-resistant parasites and insecticide-resistant vectors (*An. funestus*) as well as a concomitant plateau in the usage and coverage of vector control measures such as ITNs and IRS [2].

However, despite the underlying reasons, the current situation emphasizes that the fight against malaria is becoming increasingly complicated. This highlights the need to develop novel, effective and inexpensive tools with curative and prophylactic properties. Additionally, it is becoming increasingly evident that malaria elimination requires innovative tools to block the transmission cycle of the parasite between the human host and mosquito vector, in the face of our inability to completely remove either the mosquito vector or pathogenic parasite [22]. Indeed, in 2016, malERA was refreshed with the aim of accelerating malaria elimination in as many as possible regions and to drive global eradication. malERA Refresh promotes a multidisciplinary research agenda including two critical areas: (i) iterative improvements in drugs and vector control and (ii) tools and strategies to prevent transmission of the parasite [23].

1.2 The multifaceted *Plasmodium* life cycle

The unique *P. falciparum* life cycle takes place in both the human host (asexual replication) and insect vector where sexual reproduction occurs (Figure 1.2). An infected *Anopheles* mosquito vector transmits sporozoite stages of the parasite to the human host during a blood meal. These sporozoites invade hepatocytes within 30-60 minutes where they replicate *en masse* to produce hepatic schizonts in a process known as exo-erythrocytic schizogony. After roughly seven days, an infected hepatic schizont ruptures releasing 40 000-60 000 merozoites [24, 25] into the bloodstream where they infect erythrocytes to initiate asexual schizogony, known as the intra-erythrocytic developmental cycle (IDC). During the IDC, the parasite progresses from the 'ring' stage (based on morphology of chromatin as ring-like structures) to progressively metabolically more active trophozoite stages (associated with macromolecular synthesis), followed by asexual replication (endocytic schizogony) to form multinucleated schizonts, typically containing 8-32 daughter merozoites [26]. After a single cytokinetic event, the infected erythrocyte lyses to release merozoites and start another round of asexual replication in newly infected erythrocytes. As result of this developmental cycle, the asexual density in an infected human ranges from 100 to 250 000 parasites per μl of blood [27, 28].

In infections originating from a single bite and sporozoite population, the patient presents with fever every 48 hours corresponding to the completion of the IDC and erythrocyte rupture. Fever occurs as a result of the activation of an inflammatory response and concomitant release of cytokines (such as tumor necrosis factor) upon erythrocyte lysis [29]. Symptoms arise roughly 10-15 days after initial infection and additionally include

muscle aches and digestive indications in children [30]. Disease severity is classified as either uncomplicated (mainly symptomatic without organ dysfunction) or complicated malaria that manifests as vomiting, clinical jaundice, an increase in the respiratory rate [31] and cerebral manifestations [26].

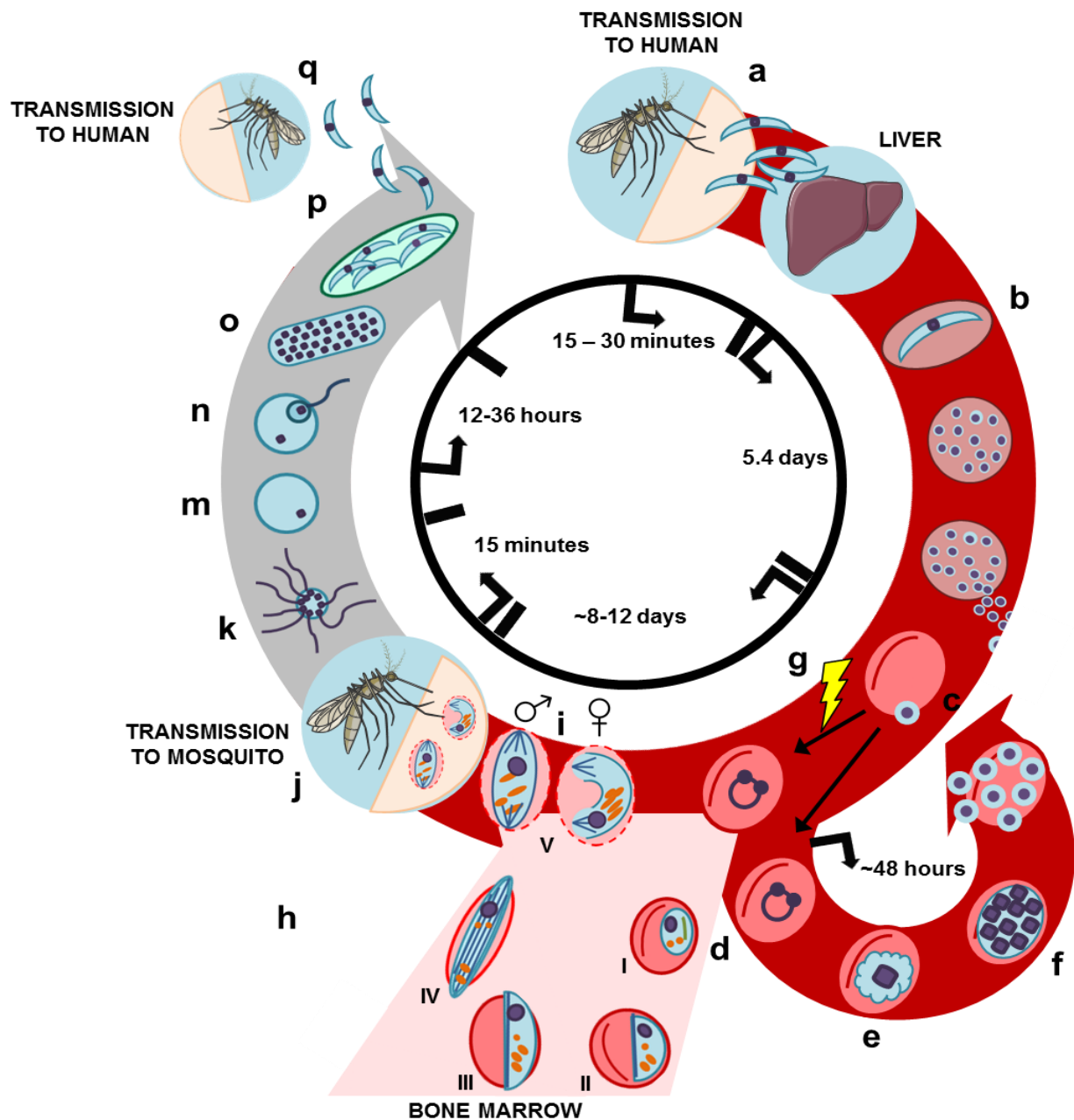


Figure 1.2: *Plasmodium* life cycle (created with information from [32]). The sporozoite is transmitted to the host during a blood meal (a); they invade liver cells, replicate and divide into merozoites (b), released after liver cell rupture. Merozoites invade erythrocytes (c), form ring stages (d) which develop into trophozoites (e) and then schizonts (f) which rupture, releasing new merozoites. Merozoites can either continue the asexual cycle or enter sexual differentiation upon external signals (g). Stage I–IV gametocytes sequester and mature in the bone marrow (h). Stage V gametocytes (i) re-enter peripheral circulation to be taken up by the mosquito vector (j). In the mosquito midgut, a motile microgamete (k) and macrogamete (m) fuse forming a diploid zygote (n), which elongates into an ookinete (o) and crosses the midgut epithelium to form an oocyst (p). After replication in the oocyst, sporozoites move from the mosquito abdomen to the salivary glands (q), reinitiating the cycle. The start-stop indicators (black) indicate the duration of each life cycle phase.

Parasite survival relies on the ability to perform a crucial binary decision: merozoites can either invade other erythrocytes to continue the IDC or commit to sexual differentiation (gametocytogenesis) during the next erythrocytic cycle [33, 34]. Commitment is thought to occur shortly before schizogony, due to the involvement of environmental factors (e.g. anaemia, certain drugs), transcription factors as well as other epigenetic regulators [35-37]. Commitment is a stochastic event in a minor subset (~1-10%) of parasites [38, 39]. After a prolonged development period (8-12 days), unique to *P. falciparum* parasites [40], mature gametocytes are released into the bloodstream as stage V female (macro) and male (micro) gametocytes and concentrate in subdermal capillaries to be taken up from the host by the next mosquito vector to continue transmission [33]. As sexual differentiation in the human host is the main topic of this thesis, it is discussed in more detail in a subsequent section.

Environmental factors in the mosquito midgut such as the presence of xanthurenic acid (XA), an increase in pH from ~7.4 to 8.2 [41] and a 5°C drop in temperature, trigger gametogenesis in the mosquito vector. During exflagellation, each male gametocyte undergoes three rounds of mitotic division and axoneme assembly to produce eight motile microgametes [42, 43]. The female gametocyte matures and rounds up to form a single macrogamete. The gametes fuse and form a diploid zygote, which transforms to an elongated, motile ookinete that will subsequently cross into the midgut epithelium and exit as an oocyst [34]. The oocyst undergoes several sporogonic replication cycles (sporogony; ~2 weeks), bursts open and releases sporozoites which collect in the mosquito salivary glands, ready to re-initiate the life cycle [44-46].

1.3 Gametocytogenesis

1.3.1 Gametocyte morphology and localisation

Gametocytogenesis is distinct for different *Plasmodium* spp., based on timeframe of development, morphologically detectable stage-differentiation as well as biological compartments of development. For *P. vivax*, *P. knowlesi*, *P. malariae* and *P. ovale*, gametocytes vary from morphologically round to oval whereas mature *P. falciparum* gametocytes are characterised by a unique falciform shape. Uniquely, gametocytogenesis in *P. falciparum* is prolonged (8-12 days) and immature stages show tissue sequestration localised to specific niches [47, 48], whereas other human (*P. vivax*) or murine (*P. berghei*,

P. yoelli) parasites have short developmental periods (24-48 hours), and remain in circulation (reviewed in [49]).

The earliest stage of gametocyte development (~14 hours post invasion (hpi) of committed merozoites) is known as committed ring stages, which cannot be visually distinguished from asexual ring stages. Stage I gametocytes (~40 hpi) have a rounded shape mostly indistinguishable from young asexual trophozoites, except for a pointed end and unique pigmentation pattern in the food vacuole (Figure 1.3) [33]. Stage IIa can be distinguished from the trophozoite by its larger round format and granular pigment distribution. Numerous food vacuoles and polyribosomes slightly extend stage IIb and a network of sub-pellicular inner membranes (inner membrane complex, IMC), subtended by microtubules, leads to this stage resembling a D-shape [50]. Stage III is further elongated (length to width ratio 2:1), more oval-shaped and has one straight and one curved side [51]. Vacuoles and clefts in the erythrocyte cytoplasm as well as the presence of Laveran's bib reflect the distortion of erythrocyte morphology [50]. Sexual dimorphism is apparent from stage III when crucial sex-specific genes are expressed [51, 52], but is more evident in the succeeding stage. Stage IV gametocytes resemble a thin spindle shape with pointed ends. A relatively small nucleolus, concentrated pigment pattern and rough extended endoplasmic reticulum (ER) network characterises the female, whereas the male gametocyte has a larger nucleus, smooth ER and diffuse pattern of pigmentation [52]. Garnham bodies are often present in the coagulated cytoplasm [50].

In order to avoid splenic clearance and elude the host immune system, immature (stage I-IV) gametocytes sequester in the extravascular space of the bone marrow and spleen, as confirmed by field and clinical reports (autopsies and *ex vivo* studies) [53-57]. Moreover, the localisation of immature gametocytes to erythroblastic islands within the bone marrow parenchyma, suggests that sexual development occurs in erythroid progenitor cells either before or after commitment [55]. Indeed, in *P. berghei*, asexual parasites establish a cryptic cycle in erythroid progenitors, characterised by early-onset sexual commitment [58]. Unlike asexual stages, gametocytes do not modify the erythrocyte membrane during, and sequestration is *P. falciparum* erythrocyte membrane protein 1 [53, 59], intercellular adhesion molecule-1 and cluster of differentiation 36 [47] independent, however, multigene families STEVOR or RIFIN, gametocyte exported proteins (*Pf*GEXPs) and mechanical retention are postulated to be involved [60-62]. Overall, the bone marrow provides a

nutrient-rich, anaerobic environment with haematopoietic progenitors [63, 64], ideal for the development of early gametocytes.

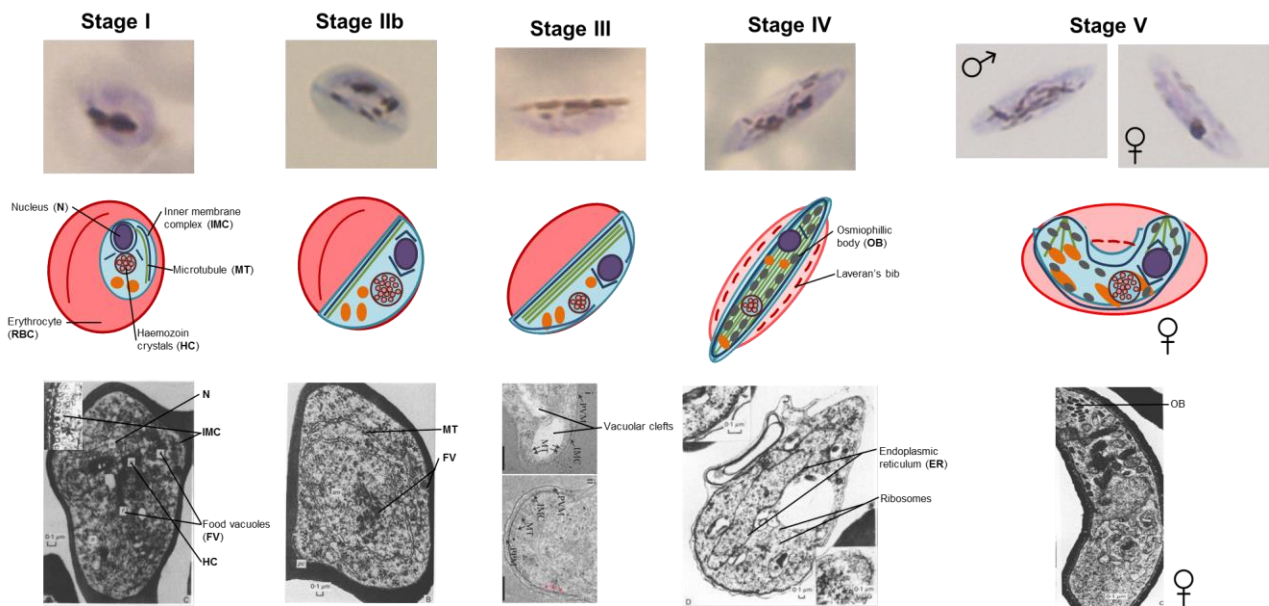


Figure 1.3: Morphologically distinct stages of *P. falciparum* gametocyte development (created with information from [65], [52] and [66]). Shown are the rounded shape of stage I, D-shape of stage II due to the formation of subpellicular microtubules (schematics, middle panel), elongated shape of stage III (photomicrograph, top panel), osmiophilic bodies and extensive rough endoplasmic reticulum (ER) of female stage IV gametocytes (electron micrographs, bottom panel) as well as the differential pigmentation pattern of stage V gametocytes. Photomicrographs (1000x magnification) were obtained from Giemsa stained smears. N: nucleus; RBC: red blood cell (erythrocyte); IMC: inner membrane complex; MT: microtubule; HC: haemozoin crystals; FV: food vacuoles; ER: endoplasmic reticulum.

Stage V male gametocytes (2:1 length to width ratio) appear thicker with pale blue cytoplasm after staining with Giemsa, whereas females are more elongated (~3:1 length to width ratio) with darker cytoplasmic staining due to the presence of ribosomes [33, 52]. Female gametocytes additionally exhibit a high frequency of osmiophilic bodies at the cytoplasmic periphery; specialised organelles involved in gametocyte egress from the erythrocyte during gametogenesis [67, 68]. The IMC is crucial for the development and maintenance of the falciform shape [57], determining the curved edge, whereas longitudinally oriented microtubules determine the long axis of the cell and F-actin fibrils become reorganised leading to the rounding-up of gametocyte tips [50, 66, 69-72]. This deformability switch releases stage V gametocytes from bone marrow or splenic retention and they subsequently return to peripheral circulation [24, 53-55, 66, 73, 74]. Dermal scarification smears, direct skin feeding assays and blood meal gametocyte counts confirm enrichment of these forms in the subdermal capillaries (density of mature gametocytes: ~100 cells per μl of blood [47]) ready for mosquito uptake [75-77].

1.3.2 Sexual commitment

Commitment takes place during the schizogonic phase of the preceding erythrocytic cycle, after which the merozoite progeny of a single schizont will become either all male or all female gametocytes [38, 59, 78, 79]. The 4:1 (female: male) gametocyte sex ratio of *P. falciparum* is the result of the biased production of committed schizonts, indicating that both commitment and sex determination occur before the schizont stage [78]. A variety of host or environmental stress factors can trigger sexual commitment and influence the sex ratio [80-82], including high parasitaemia, anaemia, microRNAs from sickle-cell erythrocytes [83], the host immune response, high densities of lymphocytes or reticulocytes [57, 63, 84], antibodies [85], haemolysis [86], haemoglobin variants [87, 88], ER stress [79], drug treatment (e.g. steroid hormones [89], fansidar [90], chloroquine and sulphadoxine-pyrimethamine [81]) and co-infections [91]. Recent studies indicated that erythrocyte-derived exosomes or microvesicles increase sexual conversion rates *in vitro* and *in vivo* in a dose-dependent manner [92, 93], suggesting that extracellular vesicles are involved in a direct cell-to-cell signalling mechanism, possibly mediating commitment. Another suggestion is that classical signal transduction mechanisms (e.g. protein kinase (PK), G-protein coupled receptor (GPCR) signalling or phorbol-ester induced pathways, mediated by cyclic adenosine monophosphate (cAMP) and adenylyl cyclase [33, 64, 94]), are involved in environmental sensing. However, the molecular mechanism of sexual commitment remains unclear [95].

Even though environmental cues affect sexual commitment, it is postulated that the basal level of gametocytogenesis is regulated by the stochastic expression of AP2-G, a unique transcription factor considered as the master regulator of sexual commitment. *PfAP2-G* is part of the apicomplexan Apetala 2 DNA-binding (ApiAP2) family, characterised by the presence of an AP2/ethylene response factor DNA-binding domain [96]. Gametocyte non-producing cell lines bear single nucleotide mutations in *pfap2-g*, whereas targeted *pfap2-g* gene disruption results in loss of sexual commitment and gametocyte production, as well as the down-regulation of early gametocytogenesis markers such as *Pfs25/27* and *Pfs16* [97-99], emphasising the important role of *PfAP2-G* in sexual commitment.

PfAP2-G expression triggers a transcriptional cascade resulting in the expression of a myriad of genes driving gametocytogenesis [65, 97, 98, 100]. The *PfAP2-G* palindromic DNA binding motif (GxGTAC/GTACxC) is present in the promoter region of many gametocytogenesis genes, however, it is unclear which of these marked genes are

functionally associated with *PfAP2-G*, or if any of these genes regulate the transcription of *PfAP2-G* [49]. The presence of this domain in the *ap2-g* gene itself, suggests regulation of the transcript through feedback inhibition [97]. Interestingly, one candidate transcriptional regulator of *PfAP2-G* is *PfAP2-G3* (PF3D7_1317200), an ApiAP2, mutation of which reduces gametocyte numbers [101] even though several early gametocyte markers are still expressed [102]. Furthermore, when *ap2-g* was disrupted, *ap2-g3* transcript levels remained unchanged, suggesting that AP2-G3 might act upstream as a *PfAP2-G* activator [97, 102]. The presence of *PfAP2-G3* in both the nucleus and cytosol, suggests that it might shuttle between these two compartments, potentially offering a link between environmental cues and the transcriptional regulation of commitment [49].

The localisation of *PfAP2-G* as a heterochromatic island at the nuclear periphery [103] supports an epigenetic model of regulation for this master switch of sexual commitment. This occurs through the involvement of heterochromatin protein 1 (*PfHP1*), histone deacetylase 2 (*PfHda2*), gametocyte development protein 1 (*Pfgdv-1*) and putative epigenetically-linked environmental signalling mechanisms (Figure 1.4). The histone reader, *PfHP1*, maintains heterochromatic gene silencing by binding to histone 3-trimethylated residues on lysine 9 (H3K9me3), resulting in the suppression of gametocyte commitment [97]. Heterochromatic features (less accessible to transcription factors such as *PfAP2-G*) are conserved in developing gametocytes with 40% of sexual stage genes *PfHP1*-bound [35, 104]. Histone methylation and *PfHP1* binding are facilitated by histone deacetylation by *PfHda2* [34]. Coleman *et al.*, (2014) proved that *PfHda2* is located in the perinuclear space and overlaps with *PfHP1* [35], validating its co-operative function in maintaining the heterochromatic state [100, 103, 105]. Conditional depletion of *PfHP1* [100] or *PfHda2* knockdown [36] leads to the de-repression of *PfAP2-G*, up-regulation of euchromatic early gametocytogenesis genes and the concomitant hyper-production of viable gametocytes [35, 36, 100], validating *PfHP1* and *PfHda2* as epigenetic regulators of gametocyte commitment [35].

Endogenous and ectopic overexpression of *pfgdv-1* enhanced *pfap2-g* expression and gametocyte production, whereas knockdown resulted in a block of gametocytogenesis [106]. Gene editing and ChIP-Seq analysis revealed that *Pfgdv-1* antagonises *PfHP1* by evicting it from H3K9me3 sites in the parasite genome, leading to the de-repression of *PfAP2-G* and induction of gametocytogenesis [37] (Figure 1.4). Co-immunoprecipitation and co-localisation experiments proved the interaction between *Pfgdv-1* and *PfHP1* and

RNA-Seq analysis showed that *Pfgdv-1* is regulated by an antisense RNA mechanism [37, 107].

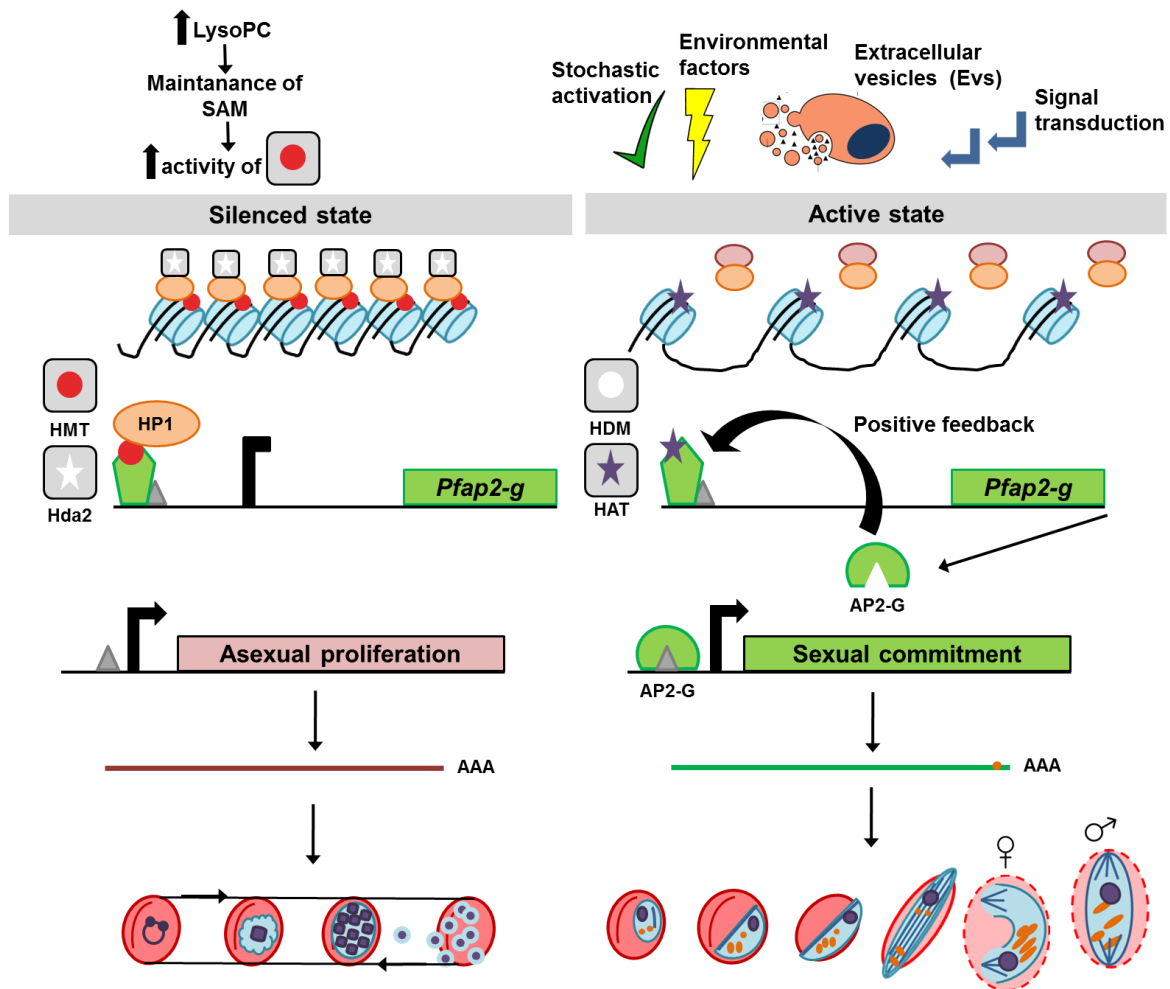


Figure 1.4: Epigenetic regulation of sexual commitment (created with information from [108] and [109]). In parasites undergoing gametocytogenesis, the lack of bound *gdv-1* (pink oval) allows HP1 (orange oval) to maintain the repressed heterochromatic state through H3-trimethylated residues on lysine 9 (H3K9me3) mediated by an unidentified histone methyltransferase (HMT, red dot) and deacetylation by Hda2 at various loci, including AP2-G. This prevents AP2-G expression, allowing asexual development. HMT activity is maintained through the availability of S-adenosylmethionine (SAM) as a result of the exogenous addition of lysophosphatidylcholine (lysoPC). In a subset of parasites, *gdv-1* evicts HP1, enriching the *ap2-g* locus in H3K9Ac sites (purple star). Without HP1 driven maintenance of H3K9 methylation, chromatin returns to a euchromatic state, mediated by an unidentified histone demethylase (HDM, white dot) and histone acetyltransferase (HAT, purple star), leading to AP2-G expression and sexual commitment.

Brancucci *et al.*, (2017) recently elucidated a possible environmental sensing mechanism linked to the epigenetic regulation of gametocyte commitment. Lysophosphatidylcholine (LysoPC), a common component of human serum, inhibited gametocyte production *in vitro* [110] and explains why conditioned culture medium (depleted of LysoPC) aids gametocyte induction. LysoPC is thought to regulate commitment not by acting as a direct trigger of a signalling cascade, but by causing metabolic changes in the cell, thereby influencing

epigenetic regulation. This is thought to occur through a shift of S-adenosylmethionine (SAM) to phosphatidylcholine production via the Kennedy pathway in the absence of LysoPC. This results in less SAM being available to histone methyltransferases in the nucleus, a concomitant decrease in histone methylation, de-repression of *ap2-g* and an increase in sexual commitment [49]. The full complex of regulatory factors involved in the epigenetic control of commitment still needs to be identified, including clearly understanding the contribution of lysine methyltransferases and demethylases that establish the conditions for asexual and sexual differentiation.

1.3.3 Gametocyte developmental biology

Gametocytogenesis is a highly coordinated process characterised by the hallmarks of cellular differentiation. Committed asexual stages or young gametocytes have a haploid genome and experience a brief period in G₁ of the cell cycle [33, 52]. Stage I and early stage II gametocytes (~day 1-2 of development) do have some DNA synthesis activity for ~48 hours [50] whereas RNA and protein synthesis characterises stage II-III development [50]. The late stages (IV/V; ~day 6 of development onwards) enter quiescence (G₀), characterised by the repression of RNA and protein synthesis [50]. Indeed, ~10% of the *P. falciparum* transcriptome in mature female gametocytes is translationally repressed until subsequent mosquito stages when the rapid translation of a plethora of transcripts occurs [111, 112] and pre-translated proteins are also used [113]. This halt in RNA synthesis [112, 114] and decrease in genes responsible for protein biosynthesis and haemoglobin catabolism [111, 115], results in mature stage V gametocytes being metabolically hypoactive and terminally differentiated [40, 46] and partly explains the difficulty in discovering active compounds to inhibit the viability of these stages [116-119]. Finally, upon entering the mosquito midgut, stage Vs enter successive S- and M-phases during which their genome replicates three times (octaploidy) and *de novo* protein synthesis occurs [42, 50]. Haploidy is restored during the oocyst stage when the genome undergoes meiosis [62].

Following transcriptional reprogramming, approximately 20-25% of the *Plasmodium* genome (consisting of ~5500 genes) is expressed specifically in the sexual stages [120-123]. *PfAP2-G* regulates early transcriptional control, whereas *PfAP2-G2* (another ApiAP2 family member) functions downstream of *PfAP2-G* [98, 101, 124]; together these mechanisms manifest in the expression of stage- and sex-specific markers as well as unique metabolic adaptations vital to gametocyte development, transmission and

subsequent fertilisation [46, 115, 125, 126]. Early gametocyte development can be traced through several genetic markers, the first of which is *PfGEXP5*, detected at 14 hpi of the committed merozoite [127]. *Pfs16* is used as an early marker, already detectable in stage I gametocytes, maintained throughout development, localised to the parasite vacuolar membrane (PVM) and a key regulator of gametocyte activation [128-133]. Stage I and II gametocytes are characterised by *Pfg27* (a homodimeric RNA-binding phosphoprotein with no other orthologues [133-135]), *PfPeg3*, *PfPeg4* and six additional complement control proteins (CCp's) [136]. CCp's possess adhesive properties and localise to the PVM in gametocytes as well as the female gamete surface post-emergence, where they play a role in cell-to-cell communication [125, 126, 137, 138].

Sex-specific transcripts are expressed from stage II onwards with 66.4% of genes expressed differentially between male and female gametocytes [111]. To date, 19 male- and female-specific transcripts each have been identified [111, 139]. The osmiophilic body protein *Pfg377* [140, 141] and ookinete surface antigen precursor, *Pfs25*, are specific to female gametocytes [136]. Male-specific transcripts include the 6-cysteine proteins, *Pfs45/48* and *Pfs230* (located as a complex on the gametocyte plasma membrane) [142-145], cytoskeletal proteins α -tubulin II and actin II [146, 147] and *PfMR5* (*PfB0040w*) [136, 143], all involved in the motility and viability of exflagellating gametes [140, 141, 146, 147]. Disruption of either *PfPuf2* (a RNA binding protein) or *PfPPM2* (a protein phosphatase) results in significantly male-biased sex ratios, suggesting a role for these proteins in the determination of the sex ratio [148, 149].

The transcriptional regulation discussed above manifests on a metabolic level, firstly to adapt the gametocyte to aerobic energy production and secondly, to enable lipid biosynthesis towards eventual fertilisation. During gametocytogenesis, the parasite moves from a glycolytic state to a state where the tricarboxylic acid (TCA) cycle and aerobic energy production via the electron transport chain (ETC) are the primary mechanisms of energy production in gametocytes [52]. Glucose and glutamine, host-derived carbon skeletons, enter the TCA cycle as acetyl-CoA, subsequently generating a proton flux and adenosine triphosphate (ATP) via ATP synthase [150]. Gametocytes are characterised by the upregulation of 15 of the 16 transcripts involved in TCA metabolism [111, 115, 151]. Moreover, the gametocyte can be distinguished by the presence of a single, large and branched mitochondrion with multiple tubular cistae, observable from stage II onwards. Additionally, a 7-fold increase in the activity of cytochrome b is observed in gametocytes

compared to their asexual stage counterparts [152]. This manifests in the efficacy of ETC inhibitors, atovaquone and primaquine, against gametocytes [150, 153, 154]. Although the sexual stages have a preference for the TCA cycle for glucose metabolism, it is not the sole metabolic process used for energy production. Early stage gametocytes also make use of glycolysis, whereas in late stages the genes required for this process are decreased in expression [115].

The gametocyte lipidome varies significantly from other life cycle stages, as well as during gametocyte maturation [155]. Phosphatidylserine, ceramides, and dihydroceramides are enriched (>8-fold) in gametocytes [156] and able to induce gametocytogenesis *in vitro* [156, 157]. Cholesterol and sphingomyelin are significantly enriched in late stage gametocytes [157] and responsible for membrane fluidity/deformability during splenic passage [66, 158]. Neutral lipids such as cholesterol esters, diacylglycerol (DAG) and triacylglycerol are enriched (up to 60-fold) in gametocytes and associated with the presence of fatty acid-rich and osmiophilic bodies at the gametocyte periphery [157]; here they serve as energy storage to fuel the increases in protein and phospholipid biosynthesis during gametogenesis and subsequent fertilisation [159]. Phosphatidylethanolamine and PC were also found to play a role during osmiophilic body formation [160], whereas phosphatidylinositol (PI) lipids have essential roles in vesicle trafficking and as secondary messengers in gametocyte activation and ookinete gliding motility, through the deployment of intracellular Ca^{2+} stores [161].

1.4 Malaria control

Malaria control is typically achieved by vector control (e.g. ITNs and IRS), chemoprevention and chemotherapy. However, current global malaria elimination efforts have been revised in the Global Technical Strategy on malaria for 2016-2030 and the RBM Partnership's Action and Investment to defeat Malaria 2016-2030 stratagem. Three pillars underlie the strategy: (i) ensuring global access to malaria prevention, diagnosis and treatment, (ii) accelerating efforts toward elimination and attainment of malaria-free status and (iii) transforming malaria surveillance into a core control intervention [2, 162, 163].

The first pillar includes vector control via the timely provision and replacement of tools such as long-lasting insecticide-treated bed nets and IRS. This approach includes entomological surveillance to assess the impact of interventions, emergence of insecticide

resistance, vector behaviour as well as larval source management. Seasonal chemoprevention is used intermittently in areas of moderate-to-high transmission for children and pregnant women [164] and has proven effective in the Sahel region [165-169]. Chemoprotection is used to protect non-immune travellers and migrants entering an area of high endemicity. Diagnosis includes effective microscopic and rapid diagnostic tests of all suspected cases in order to prevent the over-use of current treatments. Access to trained health workers that distribute WHO recommended antimalarials is also suggested [163].

The second pillar is focussed on improving legislation to drive compulsory reporting of all confirmed cases using a centralised, global reporting system. Future endeavours include mass drug administration (MDA) in high-transmission areas, the implementation of transmission-blocking chemotherapies, the use of endectocides as well as the development of *P. vivax*-targeted strategies. Active surveillance is a core strategy towards attaining elimination in the third pillar. This includes pharmacovigilance to monitor the efficacy of approved antimalarials and the removal of inappropriate medicines from the private sector, in order to contain resistance. Surveillance is also required to identify the re-establishment of infection through imported cases and identify foci of transmission [162].

1.4.1 Vector control

Current vector control approaches include the widespread use of insecticides such as dichlorodiphenyltrichloroethane and larvicides (pyrethroids, organophosphates) [2]. To date, the most efficient vector control method remains ITNs with 54% of the global population protected by this intervention [170]. Inappropriate use, mosquito behavioural changes (e.g. daytime and outdoor biting) and insecticide resistance [171], threatens the efficacy of ITNs; pyrethroid resistance is already present in *An. gambiae* [172-174]. Vector behavioural changes might be due to genetic changes or phenotypic adaptation to a changing environment, such as imposed by climate change [175]. Novel vector control approaches include the development of slow-release polymer-based wall linings [176, 177], the use of endectocides (TCP-6; section 1.4.5) as well as gene editing techniques (such as CRISPR-Cas9) that result in mosquito progeny being either sterile (lethal gene transfer) [178, 179] or refractory to *Plasmodium* spp. infection [180].

1.4.2 Vaccine development

Plasmodium spp. have evolved effective immune evasion strategies (e.g. cell surface protein variants such as the *var* gene family), thereby hampering clinical vaccine development towards chemoprotection. However, a variety of antigens are currently in pre-clinical assessment. These include a conjugate vaccine targeting the female gametocyte marker, *Pfs25* [181-183], vaccines targeting gametocyte and gamete surface proteins (*Pfs230*, *Pfs45/48*, HAP2), zygote and ookinete stages (*Pfs28*) [184, 185] and alanyl aminopeptidase (AgAPN1) a mosquito midgut surface antigen that mediates ookinete recognition [186-191]. Combination vaccines have also recently been considered, with the blend of the circumsporozoite protein (CSP), *Pfs25* and glutamate-rich protein being the most recent endeavour [192-194]. The most advanced vaccine to date is the RTS,S vaccine in phase III clinical trials (trade name Mosquirix, GlaxoSmithKline; GSK) [195]. RTS,S contains a large segment of the *P. falciparum* CSP (RTS protein), hepatitis B virus surface antigen (S), as well as a proprietary (AS01/AS02A) adjuvant [196]. It was recently approved by the European Medicines Agency (EMA) for use in young patients (6 weeks to 18 months of age) [197], however, it fails to provide long-term protection [198] and displays significant differences in the responses of vaccinated individuals, both in the field and in controlled human malaria infection models (CHMI).

1.4.3 Contemporary chemotherapeutics and resistance

Chemotherapeutics are the most successful approach towards targetting the parasite, both for chemoprotection and chemotherapy. There are three currently recommended medicines for chemoprotection *viz.* atovaquone-proguanil (Malarone[®], GSK), doxycycline or mefloquine (Lariam[®], Roche) [26].

WHO recommended chemotherapy regimens are based on ACTs due to the clinical failure and spread of resistance of the parasite to all previously used classes of antimalarials including the 4-aminoquinolines (chloroquine, amodiaquine, piperaquine), the amino alcohols (quinine, mefloquine, halofantrine, lumefantrine), the antifolates (sulphadoxine, pyrimethamine, proguanil), the hydroxynaphthoquinone (atovaquone) and the antibiotics (clindamycin, doxycycline and tetracycline) [199-206]. Artemisinin is the active component of “Qinghao”, the Chinese name for sweet wormwood (*Artemisia annua* L) from which it was extracted [207]. Clinically applied ACTs rely on fixed-dose combinations of one

artemisinin derivative (e.g. artesunate, artemether and dihydroartemisinin with short plasma half-life) with one partner drug (long plasma half-life; >4 days) [208].

Resistance development has a strong genetic basis with the parasite genome characterised as highly permissive and displaying great plasticity [209]. Additionally, the limited chemical and target diversity of current drug scaffolds, and cross-resistance profiles observed for certain classes (e.g. 4-aminoquinolines and amino alcohols), contribute to resistance development and restrict the scope of combination therapies [210-212]. Current resistance phenotypes are the result of copy number variations (CNVs) and single nucleotide polymorphisms (SNPs) in transporters and enzymes associated with direct changes in enzyme activity or processes that mitigate drug-induced toxicity. As an example, toxic Fe³⁺-containing protoporphyrin IX (oxidised from Fe²⁺-containing haem in the blood meal) usually converts to non-toxic haemozoin in the digestive vacuole, a process disrupted by antimalarials such as chloroquine. Resistance occurs by efflux, mediated by mutations of the chloroquine resistance transporter, *pfcr1*^{K76T} [213-216], as well as the multidrug resistance protein, *pfmdr1*^{N86Y; D1246Y}. The latter is a ubiquitous efflux pump, associated with resistance to many antimalarials, including ACTs [217]. Mutations in the mitochondrial electron donor cytochrome b (*pfcytb*^{Y268S/C/N}) [218] mediate clinical resistance to atovaquone. CNVs or mutations of dihydropteroate synthase (*pfdhps*^{A437G, K540E}) and dihydrofolate reductase (*pfdhfr*^{N51I, C59R, S108N}) mediate resistance to the antifolates [219-221]. Quintuple mutations of the latter have been observed in Africa [222, 223].

Artemisinin resistance presents as a reduced parasite clearance rate, or shift in the half-maximal inhibitory response (IC₅₀), upon the use of artemisinin monotherapy or ACTs. Resistance to the partner drug piperazine [224] and partial resistance to artemisinin has been observed in the Greater Mekong sub-region, whereas isolated reports of artemisinin resistance have come from Africa [225, 226]. Although there is no evidence for full artemisinin resistance [2], more than 200 non-synonymous mutations in *pfkelch13*, a regulator of protein quality control, have been identified as associated with reduced drug efficacy [2, 227]. Additionally, two avant-garde modes of artemisinin resistance were recently proposed, including the unfolded protein response [228] and proteostatic dysregulation of phosphatidylinositol 3-kinase (*PfPI3K*), leading to increased levels of phosphatidylinositol 3-phosphate (PI3P) [200]. Increased PI3P abundance positively correlates with artemisinin resistance in several clinical and laboratory *P. falciparum*

strains, supporting this mechanism [200, 216, 229]. Mutations in *pfkelch13* are therefore aimed to restore proteostasis in the parasite after free radical damage by alkylating agents, induced after cleavage of the artemisinin endoperoxide bridge [230, 231]. Because there have only been isolated reports of delayed parasite clearance in Africa and non-synonymous mutations to *pfkelch13* are diverse [2, 225, 226], ACTs remain the frontline treatment in South Africa.

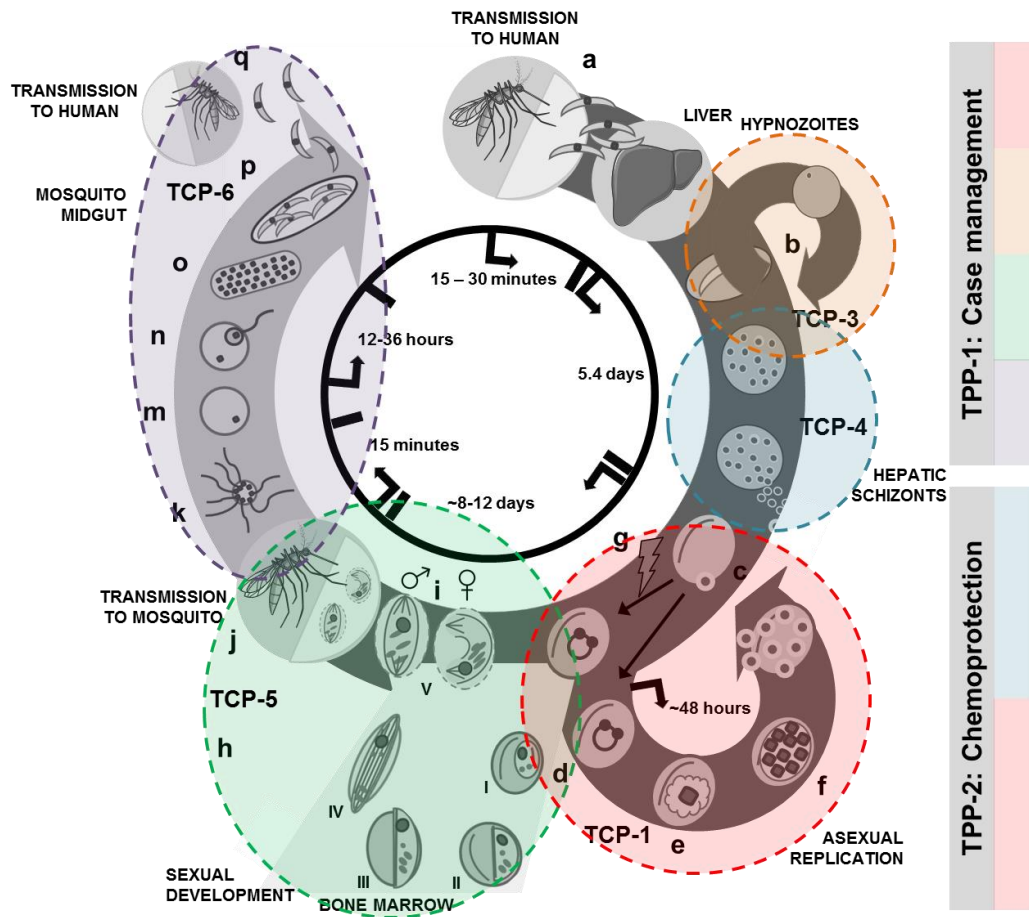
1.4.5 Drug discovery towards novel treatments

The emergence of ACT-resistant phenotypes suggests that current treatment regimens are not sustainable. The WHO [232] and the UN Special Envoy for Malaria's Aspiration to Action [233] have increased clarity with regards to the role of current and novel compound classes in control and elimination strategies. The single exposure radical cure and prophylaxis (SERCaP) was defined as the ideal antimalarial by the malERA initiative in 2011 [3], and would contain at least two active molecules with the aim of preventing the emergence of resistance in blood schizonticides. Given that the most advanced novel schizonticides will only be approved into policy in the late 2020s, this was recently revised to single-exposure radical cure (SERC) and single-exposure chemoprotection (SEC) [3]. These treatments should entail multi-stage activity towards asexual blood stages, sexual gametocyte stages as well as liver hypnozoites responsible for relapse in *P. vivax* infection (radical cure). Preferably, new chemical entities need to be active against novel targets, and diverse scaffold back-up compounds should be available in order to circumvent the resistance mechanisms the parasite has already developed. Partner drugs in combination therapy should also be of different chemical classes, have different MoA targeting different biological pathways, and target at least one asexual as well as one sexual stage in order to prevent transmission. Epitome drugs in SERC/SEC application should ideally reduce the emergence and spread of resistance (increase therapeutic lifespan) and be safe and well tolerated, especially in vulnerable populations such as young children and pregnant women in order to improve patient compliance [3, 234-236].

The Medicines for Malaria Venture (MMV) is a not-for-profit public-private partnership with the goal of discovering, developing and facilitating the delivery of new, effective and affordable antimalarials. The MMV has defined criteria for the types of individual molecules (target candidate profiles; TCPs) and treatment formulations (target product profiles; TPPs), thereby setting clear goals for drug development. Each TPP requires multiple biological activities, defined by the TCPs (Figure 1.5A). TPP-1 entails case

management, with a specific focus on treating acute infections and might include a combination of molecules with asexual blood stage (TCP-1) activity, transmission-blocking ability (TCP-5, gametocytes and vector stages) and the ability to prevent relapse via hypnozoite stage incapacitation (TCP-3). Alternatively, this can be a TCP-1 only formulation for the treatment of severe (complicated) malaria. TPP-2 is defined as SEC and involves molecules with both TCP-1 and TCP-4 (hepatic schizont) activity in order to protect individuals migrating to endemic regions. Additionally, TPP-2 formulations might serve to protect populations from developing epidemics during the final stages of elimination as chemoprevention in MDA scenarios. A new profile, TCP-6, has been defined as endectosides; molecules that target the insect vector when given to the host and taken up during the blood meal [3]. Ivermectin is a potential endectocide under investigation [237].

A



B

Drug	Drug class/scaffold	Target/MoA	Clinical phase	TCP(s) targeted
MK4815	NA	Mitochondrial electron transport chain		TCP-1
MMV253	Triaminopyrimidines	Vacuolar ATP-synthase sub-unit D		TCP-1
JPC3210	Aminomethylphenol	NA		TCP-1
ACT-451840	Phenylalanine-based	NA		TCP-1
N-tert butyl isoquine	Quinine	NA		TCP-1
Artemisone	Endoperoxide	Oxidant drugs		TCP-1
CDRI 9778	1,2,4 trioxane	Inhibit phospholipid metabolism		TCP-1
SAR97276	albitiazolium bromide	Choline antagonist		TCP-1
SAR121	NA	NA		TCP-1
AQ13	4-aminoquinoline	Inhibitits haem detoxification	NA	TCP-1
NPC1661B	NA	NA	NA	TCP-3
DSM421	Triazolopyrimidine	Dihydroorotate dehydrogenase inhibitor		TCP-1, TCP-4
P218	Triazolopyrimidine	<i>Pfdhfr</i> inhibitor, human volunteers		TCP-1, TCP-4
DSM265	Triazolopyrimidine	Dihydroorotate dehydrogenase inhibitor		TCP-1, TCP-4
GSK030	Thiotriazole	<i>Pf</i> ATP4 inhibitor		TCP-1, TCP-5
SJ(557)733	Tetrahydroisoquinoline	<i>Pf</i> ATP4 inhibitor, human volunteers		TCP-1, TCP-5
GSK607	Dione	<i>Pf</i> ATP4 inhibitor		TCP-1, TCP-5
PA92	Aminopyrazole	<i>Pf</i> ATP4 inhibitor		TCP-1, TCP-5
KAE609	Spiroindolone	<i>Pf</i> ATP4 inhibitor		TCP-1, TCP-5
Methylene Blue	Quinine derivative	Changes redox potential	NA	TCP-1, TCP-5
OZ439	Endoperoxide	Haem detoxification		TCP-1, TCP-5
Tafenoquine	8-aminoquinoline	Clinical		TCP-4, TCP-5
AN13762	Oxaborole	NA		TCP-1, TCP-4, TCP-5
DDD498	NA	Elongation factor 2		TCP-1, TCP-4, TCP-5
UCT943	2-aminopyrazine	Phosphatidyl-4-inositol kinase (<i>Pf</i> P4K)		TCP-1, TCP-4, TCP-5
MMV390048	2-aminopyridine	Phosphatidyl-4-inositol kinase (<i>Pf</i> P4K)		TCP-1, TCP-4, TCP-5
KAF156	Imidazolopiperazine	Mutations: cyclic amine resistance locus, uridine diphosphate galactose and acetyl coenzyme A transporters		TCP-1, TCP-4, TCP-5

Figure 1.5: The pipeline of antimalarial drugs aligned to target candidate profiles (TCPs) (created with information from [3, 26, 32, 238-244]). (A) Individual TCPs collectively form the two high-level target product profiles (TPPs). Target product profile 1 (TPP-1) focusses on treating already infected patients as well as chemoprevention (mass drug administration in endemic areas). TPP-1 consists of TCP-1 (asexual stages, red), TCP-3 (relapse causing liver stages, orange), TCP-5 (gametocytes and gametes, green) and TCP-6 (endectosides, purple). TPP-2 covers chemoprotection (TCP-1 and TCP-4 (hepatic schizonts, blue) and is aimed at travellers to endemic areas. (B) Pre-clinical compounds or compounds currently in clinical development. Compounds in pre-clinical () and clinical () development are indicated, as well as those in the patient exploratory phase (). The TCPs targeted are indicated.

With these useful strategic tools in mind, the MMV and partners in academia and industry, have created the most comprehensive antimalarial portfolio to date. Novel antimalarials in the pipeline, together with their MoAs (if known) and the TCPs they adhere to, appear in Figure 1.5B. These promising compounds have been identified using hypothesis-driven drug design, target-based screening as well as a combination of phenotypic screening and rational drug design. New chemical classes have activity across different life cycle stages (including transmission-blocking activity) and with novel MoAs, such as inhibition of dihydroorotate dehydrogenase (DHODH) by the triazolopyrimidines DSM421 and DSM265 [245], elongation factor 2 by DDD498 [3] and the P-type cation transporter ATPase4 (*Pf*ATP4) by the spiroindolone Cipargamin (KAE609) [246]. Additionally, future drug combinations have been suggested, consisting of novel chemotypes such as the trioxolanes (artefenomel, OZ439) or imidazolopiperazines (KAF156) combined with the novel 4-aminoquinoline ferroquine [3, 247], piperaquine or DSM265 [248]. This armamentarium additionally includes two compounds (MMV390048 and MMV642943) targeting phosphatidylinositol 4-kinase (*Pf*PI4K) [249-252], a mechanism of action that is investigated in Chapter 3 of this thesis.

1.4.5.1 Drug discovery for malaria elimination

For antimalarial drugs to be useful in elimination agendas [3], they will likely have to be dual active (with TCP-1 and TCP-5 activities) or selective towards mature gametocytes (TCP-5). Singular, dual active compounds (Figure 1.6A) with the same potency, provide the opportunity to consolidate TCP-1 and TCP-5 activities, but have the potential to increase resistance development due to the expected prolonged therapeutic regime of such compounds to ensure TCP-5 activity. Combining separate compounds with either TCP-1 or TCP-5 activity (Figure 1.6A, B) could overcome this, but might be restricted by developmental cost and pharmacological difficulties in combination compatibility and safety assessments (clinical observation, metabolic modelling) [3]. A TCP-5 gametocyte-selective compound (Figure 1.6A, B) could be used prophylactically in a MDA/mass screening and treatment (mSAT) scenario or as treatment of identified gametocyte carriers [4]. The identification and development of TCP-5 selective drugs will require novel strategies tailored for these unique transmission stages.

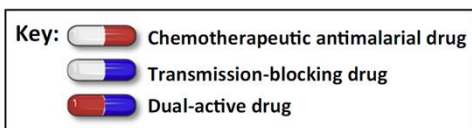
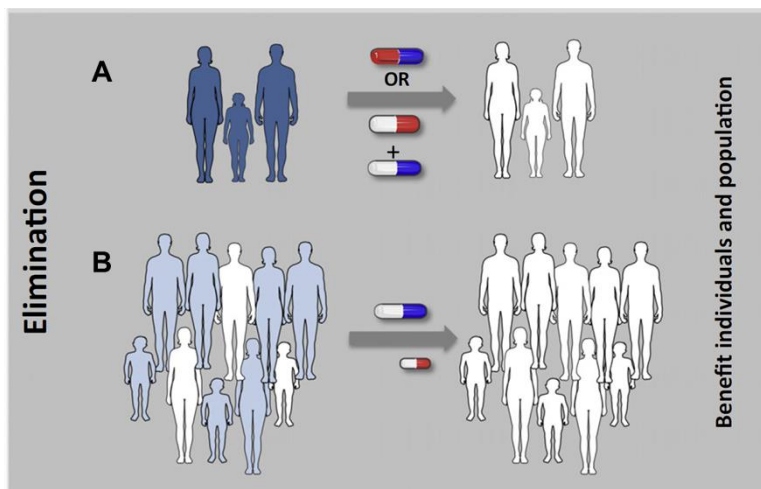
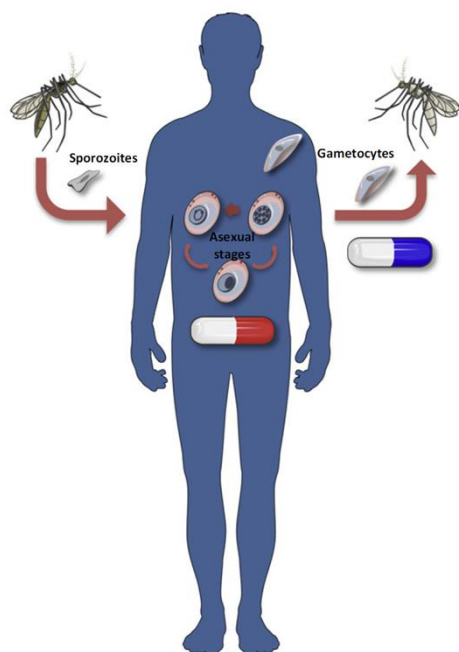


Figure 1.6: Malaria control and elimination are currently entirely dependent on the use of chemical interventions (adapted from [4]). (A) Thus, patients with malaria may be treated with either a dual acting drug or a combination of a curative drug plus a transmission-blocking drug. **(B)** At the population level, administration of a transmission-blocking drug to asymptomatic gametocyte carriers will eliminate gametocytes, which will prevent transmission and thereby disrupt the parasite lifecycle. However, this will only be achieved if these asymptomatic patients do not carry low-level asexual parasites, in which case they should be treated concomitantly with a chemotherapeutic drug. This figure is freely available for academic purposes from the journal.

As discussed, one of the key points where the parasite life cycle can be broken to achieve elimination, is human-to-vector transmission, embodied by TCP-5, which entails activity towards all gametocyte stages as well as inhibition of oocyst and sporozoite formation in the mosquito [3]. The WHO currently recommends a low-dose primaquine (0.25 mg/kg)-ACT combination to reduce the transmissibility of *P. falciparum* through targeting both gametocytes from all *Plasmodium* spp. as well as dormant liver stages of *P. vivax* and *P. ovale* [253]. A recent compendium of 25 controlled trials concluded that either low (0.2-0.25 mg/kg), medium (0.4-0.5 mg/kg) or high (0.75 mg/kg; previously suggested by the WHO [19]) dose primaquine reduced the number of individuals infective to mosquitoes from 14% and 4%, to 2% and 1% by days 3-4 and day 8, respectively [254] and reduced gametocyte prevalence, however, patients remained infective post-treatment. Haemolytic events (in glucose-6-phosphate dehydrogenase (G6PD) deficient individuals [255]; usually the major clinical concern) were only reported for a few cases [256-262]. The value of primaquine as radical cure is therefore dubious since it is equipotent at all doses, does not

deliver long-term protection (beyond day 8), resistance can be introduced at the currently recommended low dose if enduringly used at a population level, and there is no clinical evidence of the latter improving on sole ACT treatment [254, 263]. The identification of novel transmission-blocking chemical entities to support or replace primaquine is therefore of utmost importance.

Unfortunately, the quiescence of mature (stage V) gametocytes leads to insensitivity to most current antimalarials [264], hampers the development of cell-based assays specific to this stage, and the limited metabolic repertoire further confines the biochemical pool of targets available in this parasite [4]. Drug development is further encumbered by the sex-specificity of compounds, with females only sensitive to a quarter of the chemical entities tested thus far [265]. However, the narrow toolkit of clinical interventions available, and increased risk of resistance to antimalarial drugs and insecticides, makes targeting TCP-5 an opportune strategy. This is mainly due to the comparative population bottleneck ($\sim 10^2$ gametocytes vs. $\sim 10^{10-11}$ circulating asexual stages [266, 267]) for targeting transmission stages in *Plasmodium*, the larger window of opportunity to target the parasite (longevity of these stages) [268], and the comparatively invariant nature of genes expressed in the sexual stages [269, 270], conceptually resulting in reduced resistance development.

A novel, gametocyte-selective screening cascade (Figure 1.7) was therefore designed to interrogate for TCP-5 transmission-blocking activity [4]. This comprehensive screening cascade was designed as part of the South African Malaria Transmission-blocking Consortium (SAMTC) [4] and the core approach was validated by the MMV [271] and Crimalddi Consortium [272]. Each tier of the cascade is progressively more costly and delivers lower throughput, but provides additional information to guide hit prioritisation and progression, through sequentially more stringent (generally by 10-fold) selection criteria that act as “stop/go” verdicts [273]. Tier 1 focusses on late stage (IV/V) activity using orthogonal assay platforms, with activity towards the earlier stages only contributing towards reducing the gametocyte pool. Hits are further prioritised in Tier 2 based on ease or cost of production and cheminformatic/toxicity profiles, and subsequently screened for potential cross-resistance on gametocytes from laboratory-adapted strains as well as for *ex vivo* efficacy on clinical isolates. These hits are further prioritised for stage-specificity and kill kinetics as well as male and female gamete assays to determine the sex-specificity of compounds. Tier 3 entails the validation of transmission-blocking activity via the standard membrane feeding assay (SMFA) and *in vitro* liver stage assays [4].

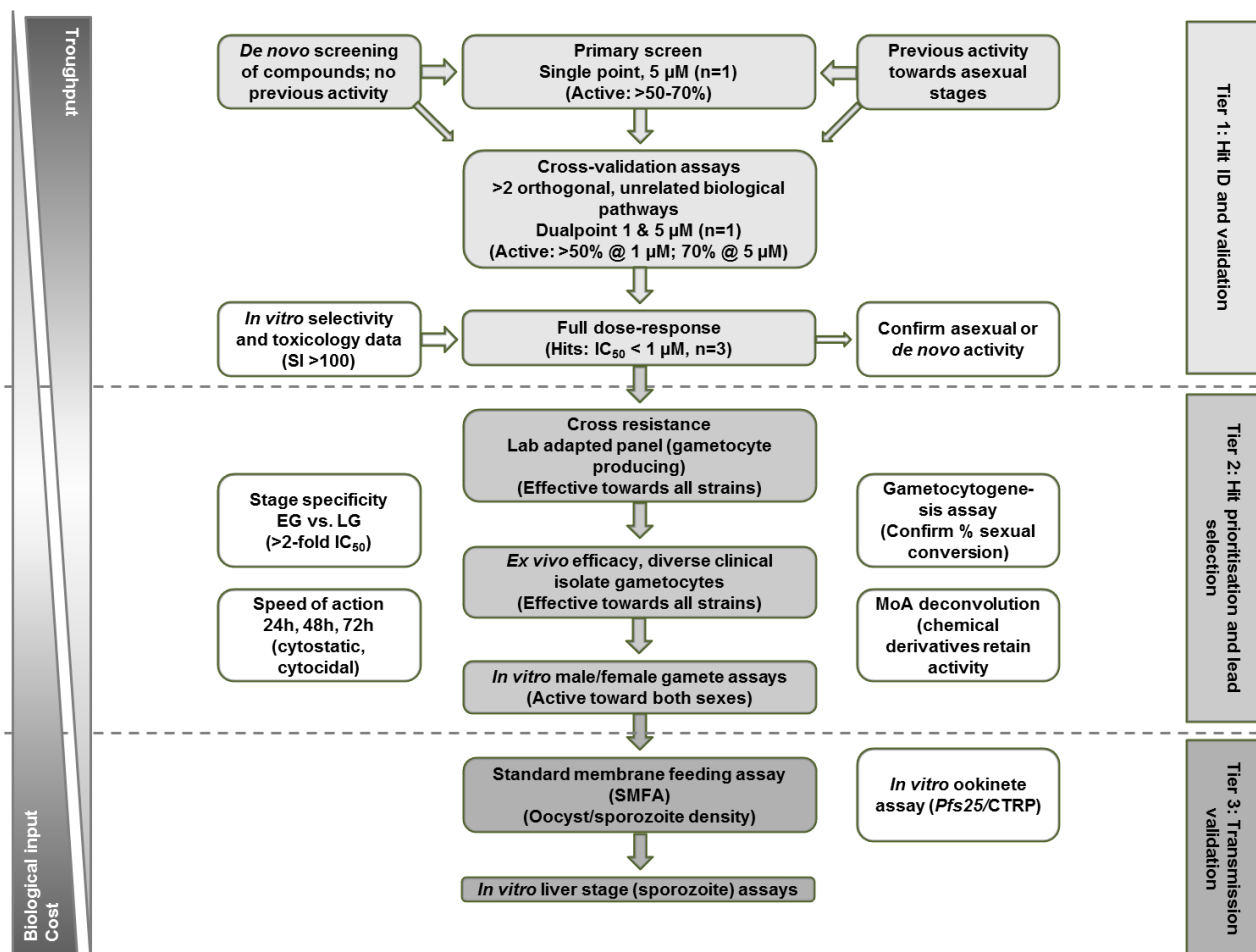


Figure 1.7: SAMTC test cascade for screening of transmission-blocking antimalarial compounds (Adapted from [4]). The proposed three-tiered screening cascade provides biologically richer information because compounds progress through each tier with more involved assays, albeit with decreased throughput. Application of strict selection criteria (indicated in the italic text) guides the progression of compounds through the cascade. The primary cascade is indicated in the centre in dark grey, with parallel (and in some cases optional) investigations indicated in white blocks. This figure is freely available for academic purposes from the journal.

Outputs from this screening cascade contributed to the identification of *Pf*PI4K inhibitors, MMV390048 [252] and MMV642943 [274] as well as the data in Chapter 3 of this thesis.

1.5 Eukaryotic protein kinases (ePKs) as drug targets

Reversible phosphorylation is an essential post-translational modification regulating many aspects of protein function, e.g. folding, localisation, binding potential, enzymatic activity, cell signalling, and protein kinases (catalysing phosphate transfer from ATP/guanosine triphosphate (GTP) to certain amino acids e.g. serine, threonine and tyrosine), play an essential role in these processes [275, 276]. ePKs are a large superfamily (518 members) [277] of evolutionary and structurally related enzymes, harbouring highly conserved residues and motifs, which determine their catalytic activity [276]. The active PK domain consists of a small N-terminal lobe and large C-terminal lobe (Figure 1.8A), which

comprise the following catalytic moieties: an ATP-binding lysine in subdomain II (β -sheet), two aspartates in either the catalytic loop (subdomain VIb) or the activation segment (N-terminal, subdomain VII) [278, 279], a glutamate (subdomain IX) in the α C helix which forms a salt bridge with the aforementioned lysine residue in active conformation, as well as a glycine-rich ATP-phosphate binding loop between the β 1 and β 2 strands [280] (Figure 1.8A,B).

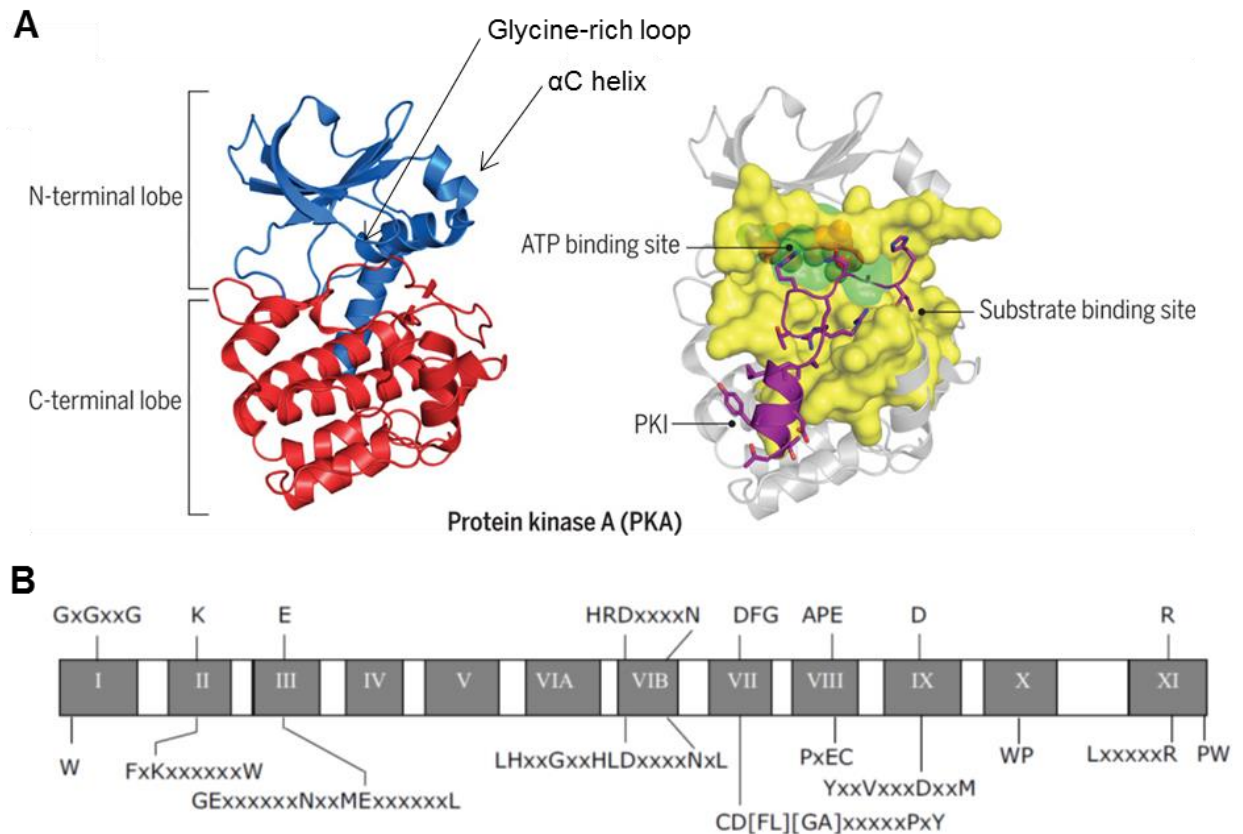


Figure 1.8: Structure of the eukaryotic protein kinase (ePK) catalytic domain (taken from [281] and [282]). (A) Classical division of the catalytic domain showing the N-terminal (blue) and C-terminal (red) lobes on the left-hand side, as well as the adenosine triphosphate (ATP, green), substrate binding site and PK inhibitor (PKI) (purple) on the right-hand side. (B) The eleven subdomains of the PK catalytic domain are indicated. Note the conserved residues required for catalytic activity: the lysine (K) in subdomain II and aspartates (D) in either subdomain VIb or VII. This figure is freely available for academic purposes from the journal.

The dysregulation and mutation of PKs play causal roles in human illnesses such as Alzheimer's disease (CDK, MAPK and AGC families) and cancer (AGC, CMGC and lipid kinases; sustaining the proliferative signal, evading growth suppressors, activating metastasis and angiogenesis as well as resisting cell death) [281, 283]. Moreover, when the chromosomal kinase map is compared to loci associated with specific diseases, 164 kinases map to sites frequently observed in tumours and 80 kinases map to other disease loci [277, 284], highlighting the important role of kinases in the initiation and progression of

signalling disorders which include cardiovascular disease, diabetes and inflammation (autoimmune disorders) [285].

PKs are only second to GPCRs in the number of screening targets that are used by the pharmaceutical industry to identify new therapeutic chemical entities [286] with 25-30% of these targets representing PKs [287]. The targetability of PKs is due the size of this enzyme superfamily [277], the structural similarity of the ATP binding site enabling polypharmacological drug design [287], the involvement of single kinases in different disorders, as well as the availability of allosteric sites (hydrophobic pockets) unique to specific kinases [288]. Indeed, 31 small molecule kinase inhibitors (SMKIs, including tyrosine, serine/threonine, lipid kinases (PI3K) and three macrolide [289] inhibitors of the mammalian target of rapamycin (mTOR)) have been approved as treatments for a variety of cancers [290]. At least half of these drug approvals occurred in the last four years [291] and in excess of 250 kinase inhibitors are currently in clinical trials [290], further validating the extraordinary scope of this enzyme superfamily as viable drug targets.

However, the design of selective PK inhibitors is complicated by the fact that these enzymes share the same protein fold (catalytic domain), have high sequence identities, use the same ubiquitous cofactor (ATP/GTP), employ the same catalytic mechanism and are closely associated in signal transduction cascades [276], the dysregulation of which might lead to the disruption of normal cellular homeostasis and undesired phenotypic effects [281]. As a result of these structural and mechanistic similarities, inhibitors typically contain a hydrogen bond accepting (HBA) group that mimics N1 of the ATP purine ring and interacts with the backbone amide group of the hinge residue which links the N- and C-terminal lobes of the kinase, as well as a moiety that interacts with the gatekeeper residue. The latter is either bulky (e.g. methionine) in human orthologues or much smaller (e.g. glycine, alanine or threonine) in *Plasmodium* orthologues [275], occurs at the start of the hinge region and controls access to a hydrophobic pocket at the back of the ATP binding site cleft.

Even though there are certain shared functional groups, vital to the activity of kinase inhibitors, they are tailored to inhibit a specific kinase or conformational state. SMKIs are classified based upon the activation state of the PK target, i.e. the disposition of specific residues or structural elements including the N-terminal lobe, α C helix (α C-helix-in, active; α C-helix-out, inactive), the C-terminal lobe DFG-D (DFG-D-in, active; DFG-D-out, inactive)

and the C-terminal lobe activation segment (AS-open, active; AS-closed, inactive). Type I (classical) kinase inhibitors target the active, phosphorylated (DFG-D-in, α C helix-in) enzyme in an ATP-competitive, reversible fashion [292](Figure 1.9A), contain at least one HBA/hydrogen bond donating (HBD) group to facilitate binding to the hinge region, induce very little conformational change, are promiscuous, and their selectivity can be improved by addressing the hydrophobic back pocket (Figure 1.9A). Type I $\frac{1}{2}$ inhibitors are similar to type I, but bind reversibly to inactive state kinases (DFG-D-in, α C helix-variable) and extend into the back cleft of the ATP binding site [280, 293] (Figure 1.9B). Type II-IV inhibitors are non-ATP competitive, often displaying better potencies and pharmacokinetic properties than type I and I $\frac{1}{2}$ inhibitors [276, 294, 295]. Type II allosteric inhibitors bind to kinases in a DFG-D-out, α C-helix-variable conformation [280] and extend into the hydrophobic deep pocket unavailable in active state kinases [276] (Figure 1.9C), leading to improved structural complementarity and the design of highly selective inhibitors inducing significant conformational change [296]. Type III inhibitors bind allosterically to the hydrophobic deep pocket of inactive (DFG-D-variable, α C-helix-out) kinases (Figure 1.9D) and do not require any specific hinge- or adenine-binding motifs [280], whereas type IV inhibitors bind to allosteric sites distant from the ATP binding or hydrophobic, peptide binding sites mentioned [297-299] (Figure 1.9E). Type V are bivalent (linked allosteric and covalent) inhibitors which bind via a Michael acceptor electrophile (e.g. cysteine) in the hinge region of the binding pocket [276, 280] (Figure 1.9F). This reinforces affinity and selectivity, but requires prior knowledge of PK substrates or binding motifs [297]. Type VI inhibitors are small molecules that form covalent Michael adducts within the ATP binding site [280], via an α,β -unsaturated carbonyl moiety [300] (Figure 1.9G).

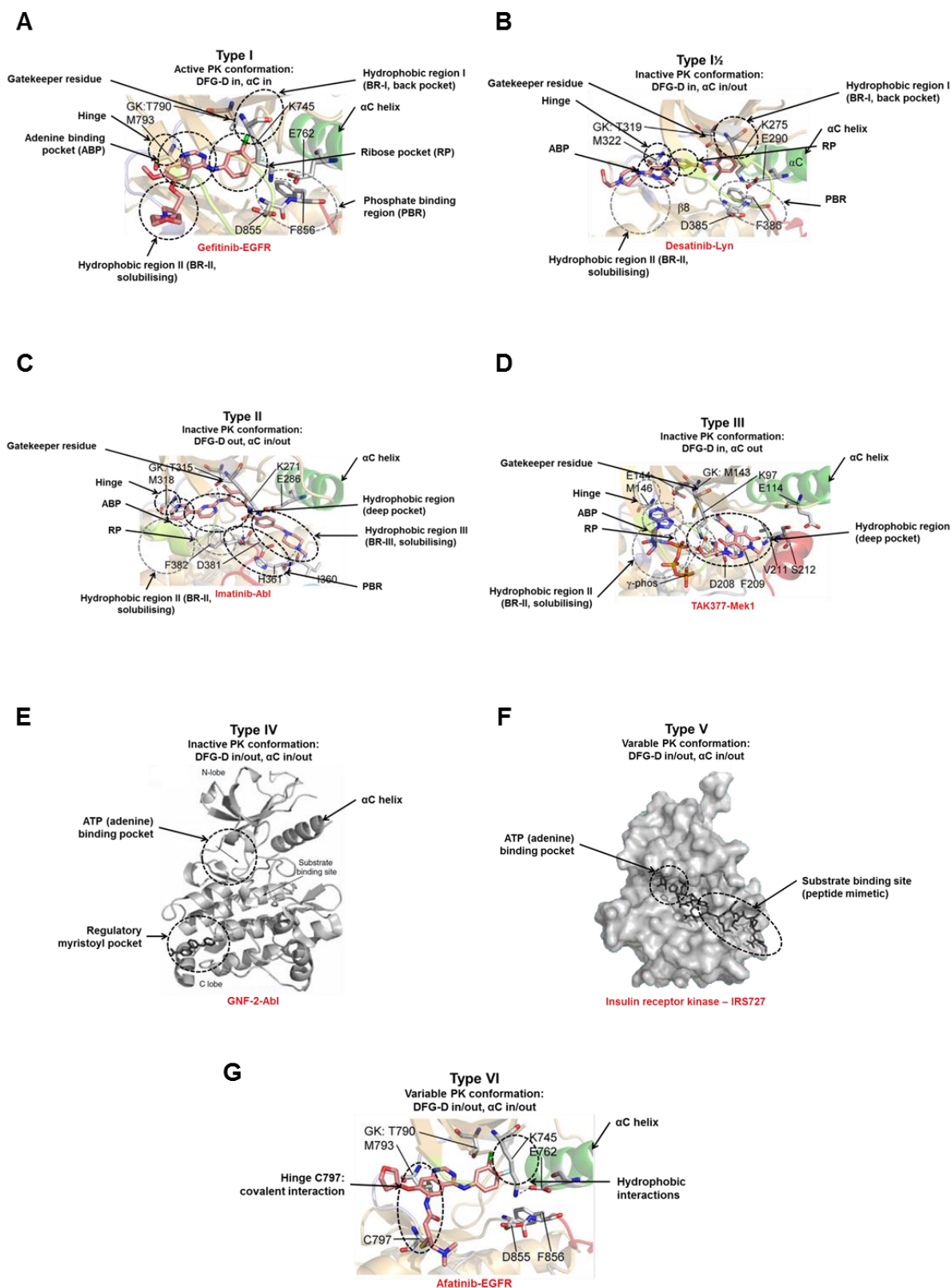


Figure 1.9: Structure of the eukaryotic protein kinase (ePK) catalytic domain (Adapted from [276], [280] and [297]). Drug carbon atoms are indicated in orange for A, B, C, D and E and black for E and F, whilst enzyme carbons are indicated in grey. The pharmacophore models are indicated by binding of the inhibitor to specific sites (dashed circles) and include type I (A), type I½ (B), type II (C), type III (D), type IV (E), type V (F) and type VI (G) inhibitors. EGFR: epidermal growth factor receptor, Lyn: tyrosine protein kinase Lyn, Abl: nonreceptor tyrosine kinase Abl, Mek1: dual specificity mitogen-activated protein kinase 1, IRS727: peptide substrate of insulin receptor kinase.

1.6 The *P. falciparum* kinome

The kinome and phosphatome constitute ~1.7% of the *Plasmodium* transcriptome and are thought to play significant roles during life cycle transitions in the parasite [301, 302]. Whole genome sequencing (WGS) of *Plasmodium* spp. identified 85-99 kinase-associated transcripts, including 65 confirmed ePKs, which cluster with human orthologues, but also orphan kinases with no human orthologues, including 20 kinases belonging to the FIKK family (Phe-Ile-Lys-Lys motif) [301, 302] and various other atypical protein kinases (aPKs) [301, 302] (Figure 1.10).

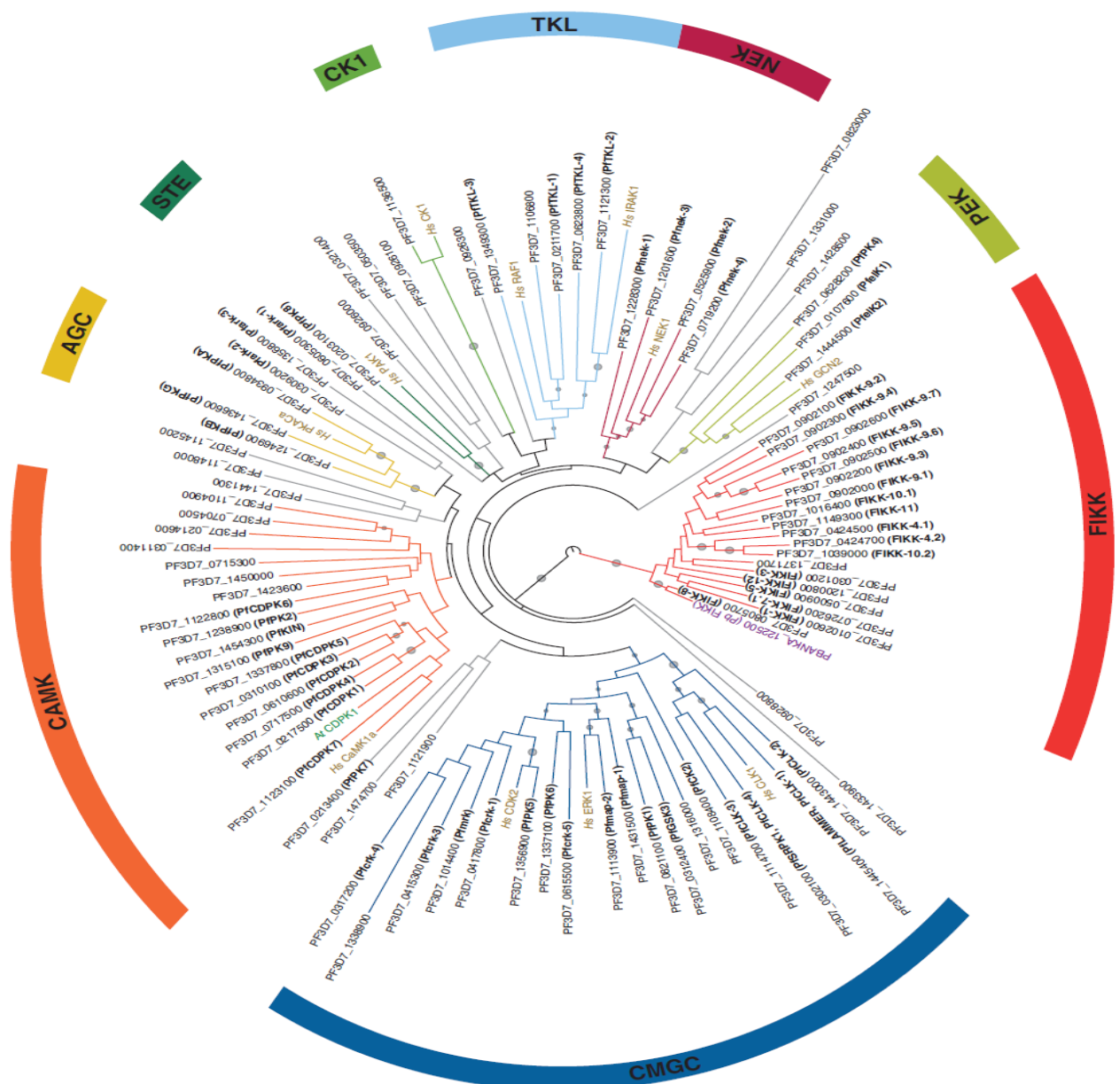


Figure 1.10: Phylogenetic classification of the *P. falciparum* kinome (taken from [278]). Circular tree of eukaryotic protein kinases (ePK). Representative genes from human (*Homo sapiens*; Hs), *Arabidopsis thaliana* (At) and *P. berghei* (Pb) are indicated with labels coloured gold, green and purple, respectively. Branch and arc colours indicate kinase classification by ePK major group. CK1: casein kinase 1. TKL: tyrosine-like kinases. NEK: never in mitosis/Aspergillus (NIMA)-related kinases. CamK: calcium/calmodulin-dependent kinases. The figure is freely available for academic purposes.

The regulation of kinase-mediated signal transduction processes in *Plasmodium* spp. is only partially clarified, possibly due to the involvement of atypical mechanisms. However, the functions of many *Plasmodium* spp. kinases have been resolved using phosphoproteomic and reverse genetics approaches [303-306], and reflect the importance of these enzymes in processes vital to the development of all parasite stages (Figure 1.11). Examples of kinases essential to completion of the IDC [303, 307] include casein kinase 1 (*PfCK1*) and the tyrosine-like kinases (TKL), *PfTKL1* and *PfTKL3* [302]. The FIKK kinases (largest kinase family, 20-25% of the *Plasmodium* kinome) [308, 309] phosphorylate unique substrates involved in erythrocyte membrane rigidity [310] and parasite virulence [310-313]. The CMGC group (termed after the four kinase families cyclin dependent kinase (CDK), mitogen-activated protein kinase (MAPK), glycogen synthase kinase-3 (GSK3) and CDK-like kinases (CLK) associate to cyclins [314] and are essential regulators of cell cycle progression [279, 303]. *Pfcrk-1*, *Pfcrk-3* and *Pfmrk* regulate the DNA replication machinery during asexual proliferation [315-319], whereas *PfPK6* is essential for erythrocytic schizogony through possible involvement in the G₁/S-phases of the cell cycle [320]. *PfMap-1* and *PfMap-2* are essential to erythrocytic schizogony [321] as well as cytokinesis during exflagellation [113, 322]. The three Aurora kinases (*PfArk-1*, *PfArk-2* and *PfArk-3*) are vital for cell division by transiently associating with duplicated spindle pole bodies and mitotic organisation centres [323], whereas *PfPK7* and *PfPK8* are essential regulators of the IDC and oocyst development [316].

AGC group protein kinases (*PfPKA*, *PfPKB* and *PfPKG*) are regulated by secondary messengers cAMP, cyclic guanosine monophosphate (cGMP) or DAG [301] and essential for erythrocytic schizogony [324, 325], gametocytogenesis [326], gamete egress [281] ookinete motility and hepatocyte invasion [161]. *PfPKG* additionally maintains Ca²⁺ homeostasis upon cGMP, guanylyl cyclase and phospholipase C (PLC) activation during exflagellation [110, 161]. The calcium/calmodulin-dependent (CamK) group are involved in a number of calcium-mediated signalling processes [327-335]. *PfCDPK1* regulates myosin function towards gametocyte motility [330], whereas *PfCDPK3* and *PfCDPK4* are required for ookinete gliding motility and mosquito midgut invasion [330, 331, 336, 337]. *PfCDPK4* is also regulated by PLC [338] and mediates XA-induced exflagellation and subsequent transmission in a manner similar to *PfPKG* [331]. *PfCDPK5* is essential for merozoite egress [339], whereas *PfCDPK6* is involved in liver cell invasion [333]. *PfCDPK7* associates with vesicular structures (transport) during asexual development [223, 301, 340], similar to *PfPK5*, an important cell cycle control kinase [320, 341].

Knockout of the never in mitosis/Aspergillus (NIMA)-related kinases, *PfNek-2* and *PfNek-4*, results in aberrant ookinete and oocyst development due to incomplete meiosis [113, 342-347]. The phosphoinositide lipid kinase kinases (PIKKs), part of the aPK classification, phosphorylate inositol lipids thereby generating PIs, important cell cycle regulators [348]. *PfPI4K* is responsible for vesicular trafficking towards the ingressing plasma membrane during exflagellation [349, 350]. Phosphatidylinositol-4-phosphate-5-kinase (*PfPIP5K*) is a possible bifunctional enzyme and produces phosphatidylinositol-(4,5)-bisphosphate (PIP_2), an essential substrate of PLC during gametocyte activation [351], exflagellation [352, 353], sporozoite gliding motility [354], egress and hepatocyte invasion [355]. *PfPK4* and *PfIK1* (PEK kinases) are part of the haem-regulated inhibitory class of eukaryotic initiation factor 2 kinases [356], involved in translational repression in schizonts and gametocytes [357].

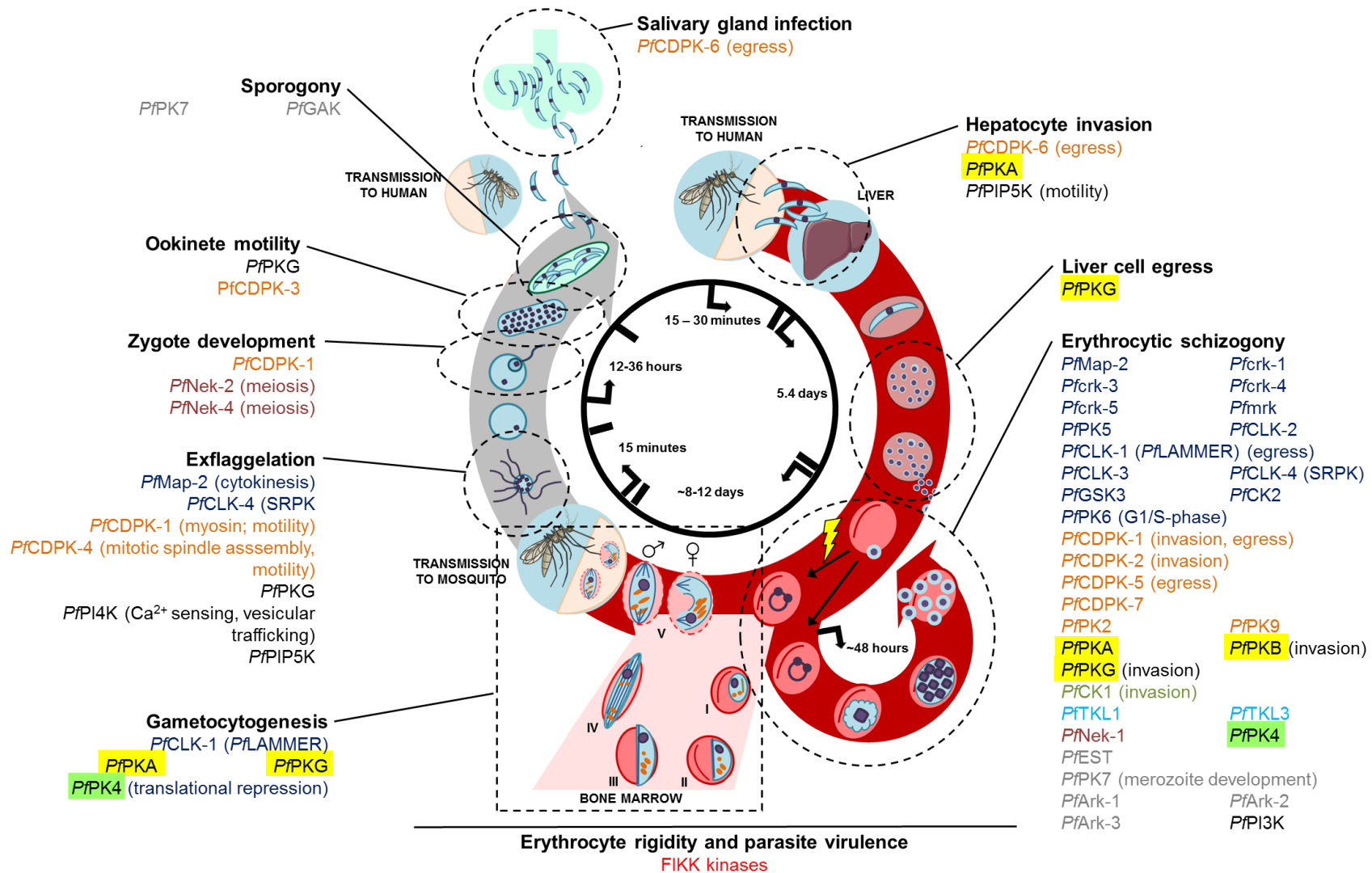


Figure 1.11: Life cycle transition involvement of *Plasmodium* kinases (created with information from [281] and additional literature). The involvement of kinases at various stages of the life cycle are indicated. The major ePK classifications are indicated for the CMGC (blue text), CamK (orange text), AGC (yellow highlight), CK1 (mid green text), TKL (turquoise text), NEK (maroon text) and PEK (light green highlight) groups. The aPKs are indicated in black text and the orphan kinases either in grey or red text (FIKK kinases).

This broad spectrum of functions, spanning the entire life cycle, together with the unique features of this enzyme class, makes *Plasmodium* kinases a highly targetable niche. *Plasmodium* kinases share the bi-lobed 3D structure and conserved catalytic domain architecture with other ePKs [358], however, due to the phylogenetic distance between *Plasmodium* and human kinase orthologues, parasite-specific kinase properties (sequence diversity, composition, organisation of signalling pathways, regulatory and functional roles) can be exploited to increase potency and specificity whilst decreasing the toxicity of PK inhibitors [275, 359]. One example is the gatekeeper loop which contains smaller amino acids (e.g. glycine, alanine or threonine), allowing larger substituents to fit into the pocket behind the gatekeeper residue, thereby permitting increased target specificity [275]. More unique features include large, low-complexity extensions and insertions within the catalytic domain, rich in charged, polar residues at the loops between secondary structure elements [360, 361]; these might serve as novel target sites selective for the parasite. Additionally, the distinctive allosteric sites outside of the ATP binding cleft can be targeted using small molecule analogues of cGMP or cAMP, thereby inhibiting the active state conformation induced by effector binding or phosphorylation (as for the AGC group) [362].

Even with the advancements in the functional elucidation of *Plasmodium* kinases [303-306] and kinase inhibitor screening campaigns [324, 363-380], only a single lipid kinase, *Pf*PI4K, is currently the target of compounds in pre-clinical (MMV642943) [274] and clinical (MMV390048) [252] antimalarial development.

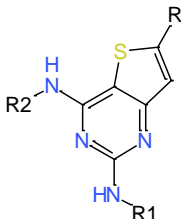
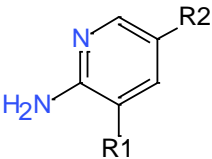
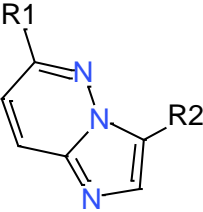
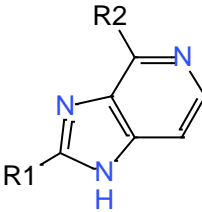
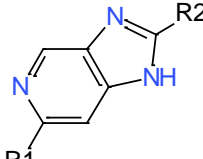
1.7 Work leading up to this investigation

The inhibitor scaffolds investigated in this manuscript were originally derivatised from kinase and voltage-gated ion channel target-focussed compound libraries known as the BioFocus[®] SoftFocus[®] Kinase (SFK[™]) and BioFocus[®] SoftFocus[®] Ion Channel (SFI[™]) libraries [381]. BioFocus[®] applied either a Helical Domain Recognition Analysis[™] or ligand-based design strategy to develop the SFI[™] series [381]. For the SFK[™] series, all public domain crystal structures were grouped according to active and inactive protein conformations as well as ligand binding modes and a single structure selected from each group representing human kinase families. Scaffolds were designed to mimic ATP-binding in the hinge region through correctly orientated hydrogen donating/accepting pairs [275, 381, 382]. Minimally substituted versions of each scaffold were docked into the kinase subset and selected based on the ability to bind multiple kinases in different conformational states. Side chains were selected to reflect the size and environment of

the kinase binding pocket [381]. The scaffolds were subsequently screened *in vitro* against 17 human enzymes representing major kinase families (AGC, TKL, thymidine kinase, STE, CK1, CGMC and CAMK) in order to determine the specificity and promiscuity of each scaffold.

The resulting BioFocus[®] DPI SoftFocus[®] library (36 608 compounds, covering more than 200 scaffolds [383]) was screened using an image-based (fluorescence-based confocal imaging of 4'-6-diamidino-2-phenylindole (DAPI) stained parasites) [384] high-throughput screen (HTS). This revealed 222 selective hits against asexual blood stage *P. falciparum* drug-sensitive (3D7) and -resistant (Dd2) strains [385] representing various scaffold series. Hit compounds were identified where >80% inhibition of asexual proliferation was achieved at a screening concentration of 1.82 μ M (Table 1.1). Hits displayed no cytotoxicity with potent activity towards *P. falciparum* asexual stages and therefore provided high-quality starting points with physicochemical, pharmacological and pharmacokinetic characteristics representative of 'druggable' compounds [383, 386]. These starting points were subsequently exploited in a hit-to-lead (H2L) and lead optimisation programme, established by the Drug Discovery and Development Centre (H3D) located at the University of Cape Town (UCT). Novel hit scaffolds included four kinase-focussed inhibitor series: 2-aminopyridines (2-APs), imidazopyridazines (IMPs), 6,9-imidazopyridines (6,9-IPs) and 2,6-imidazopyridines (2,6-IPs), as well as an ion-channel-focused series of diaminothieryl-pyrimidine (DTP) compounds.

Table 1.1: Hit chemical starting points from the diaminothieryl-pyrimidine, 2-aminopyridine, imidazopyridazine, 6,9-imidazopyridine and 2,6-imidazopyridine series.

Series	DTP	2-AP	IMP	6,9-IP	2,6-IP
Scaffold					
Hit rate: >80% inhibition @ 1.82 μ M	118/554 (21%)	8/739 (1%)	153/488 (31%)	NA	NA

NA: Not available

1.7.1 Diaminothienyl-pyrimidines (DTPs)

DTP-like scaffolds have been applied as antimalarials as well as anticancer agents [387-390]. The 5-methyl-6-phenyl derivative of a 2,4-diaminothieno[2,3-d]pyrimidine series was active against *P. berghei in vivo* at 640 mg/kg and identified as DHFR inhibitor [387]. Desroches *et al.*, (2017) synthesised a series of thienopyrimidines based on the structure-activity relationship (SAR) of the parent trichloromethylquinazoline scaffold; derivatives displayed submicromolar antiplasmodial activity but were generally cytotoxic [391]. Derivatisation around the lapatinib scaffold (a human tyrosine kinase (TK) inhibitor) led to potent activity ($IC_{50} = 27$ nM) against the *P. falciparum* D6 strain [392].

Initial SAR analysis and derivatisation of the DTPs (Figure 1.12) revealed that this series had potent asexual stage activity (25-600 nM), displayed low *in vitro* cytotoxicity, good to moderate metabolic stability in human liver microsomes, excellent solubilities [393] as well as a fast speed-of-action on both ring and schizont stages [394]. Derivatisation focussed mainly on changes at the R1 and R2 positions of the DTP core in order to improve pharmacokinetics and hERG (cardiovascular risks, K^+ channel) due to unwanted drug metabolites [393].

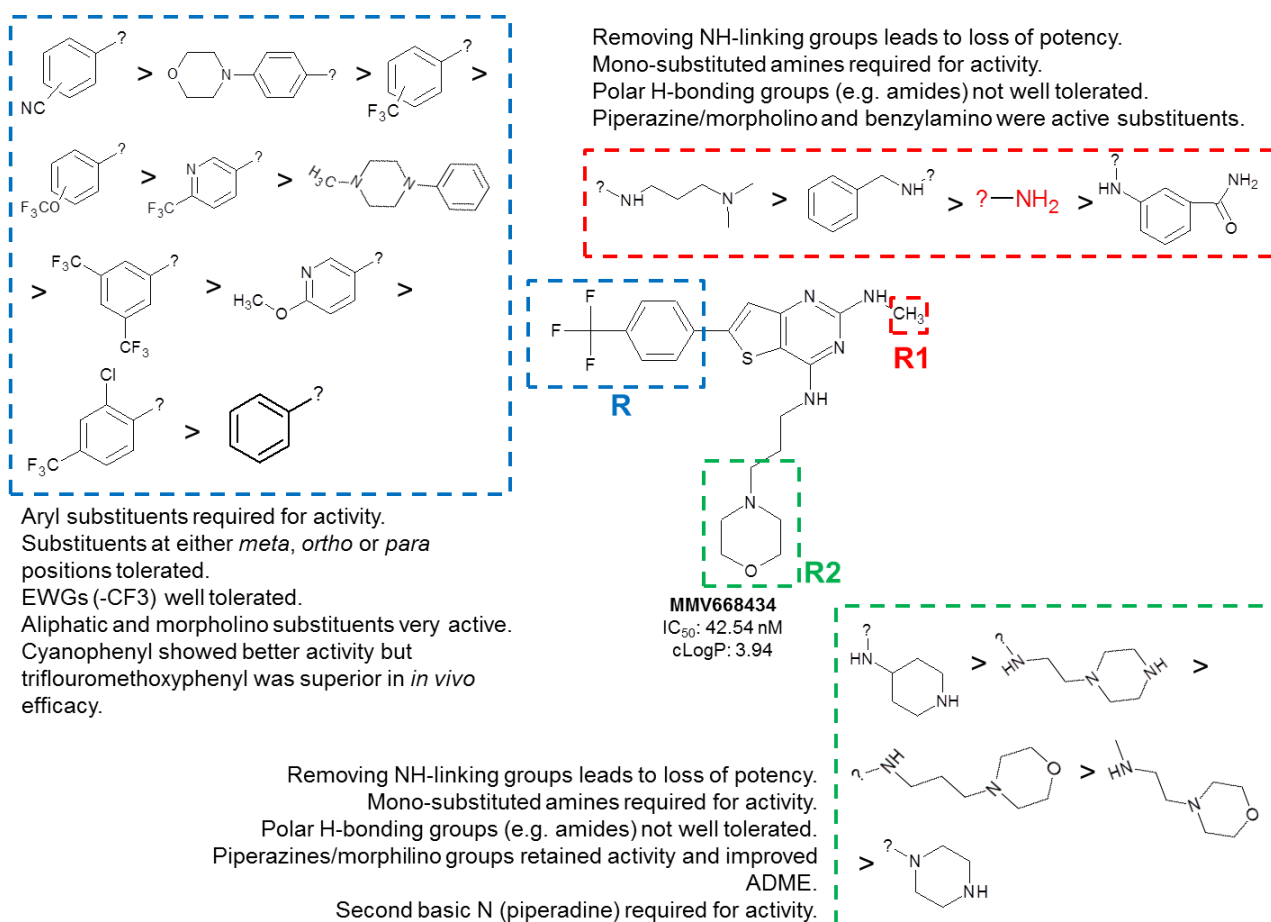


Figure 1.12: SAR optimisation highlights for the diaminothienyl pyrimidine series (created with personal information from our collaborators at H3D, UCT). An active representative from the series (MMV668434) is indicated with its asexual blood stage activity and physicochemical properties (cLogP). Substitutions at are indicated in red (R1), green (R2) and blue (R).

1.7.2 2-aminopyridines and 2-aminopyrazines (2-APs)

Aminopyridine- and aminopyrazine-like scaffolds are well-known kinase inhibitors [395, 396], GPCR antagonists [397], ion channel modulators [398] and antioxidants [399-401]. Analogues form part of the GSK Tres Cantos Antimalarial Set (TCAMS) and Novartis GNF libraries [402-404], and have been extensively explored as antimalarials displaying submicromolar activity [405].

SAR analysis of the 2-APs focussed on derivatisation around the 3 and 5-positions of the 2-aminopyridine core, as well as a core change resulting in the 2-aminopyrazines, in order to improve *in vivo* efficacy, kinetic solubility and hERG risks (Figure 1.13). The clinical candidate 2-AP, MMV390048, is active against all life cycle stages with a slow mode of action and reduced both primary and secondary transmission events. Chemoproteomic investigation identified PvPI4K as the target of MMV390048 [252], while WGS of *P. falciparum* resistant mutants, identified *pfpi4k* as the only mutated gene in all resistant

clones [252]. MMV390048 displayed transmission-blocking capacity in the male gamete formation assay (inhibition of exflagellation; $IC_{50} = 90$ nM) and SMFA ($IC_{50} = 111$ nM) [252]. The pre-clinical candidate 2-aminopyrazine, MMV642943, was highly soluble (31-3000 $\mu\text{g/ml}$), afforded complete cure in different animal models, was active against all life cycle stages [406] showed no cross-resistance and displayed transmission-blocking capacity in the dual gamete formation assay (DGFA) ($IC_{50} \sim 80$ nM) and SMFA ($IC_{50} = 96$ nM) ([274]; section 3.3.2 of this thesis). Chemoproteomic studies revealed *Pv*PI4K as its target with >200-fold specificity for the parasite enzyme and no potential risk to G6PD-deficient individuals [274].

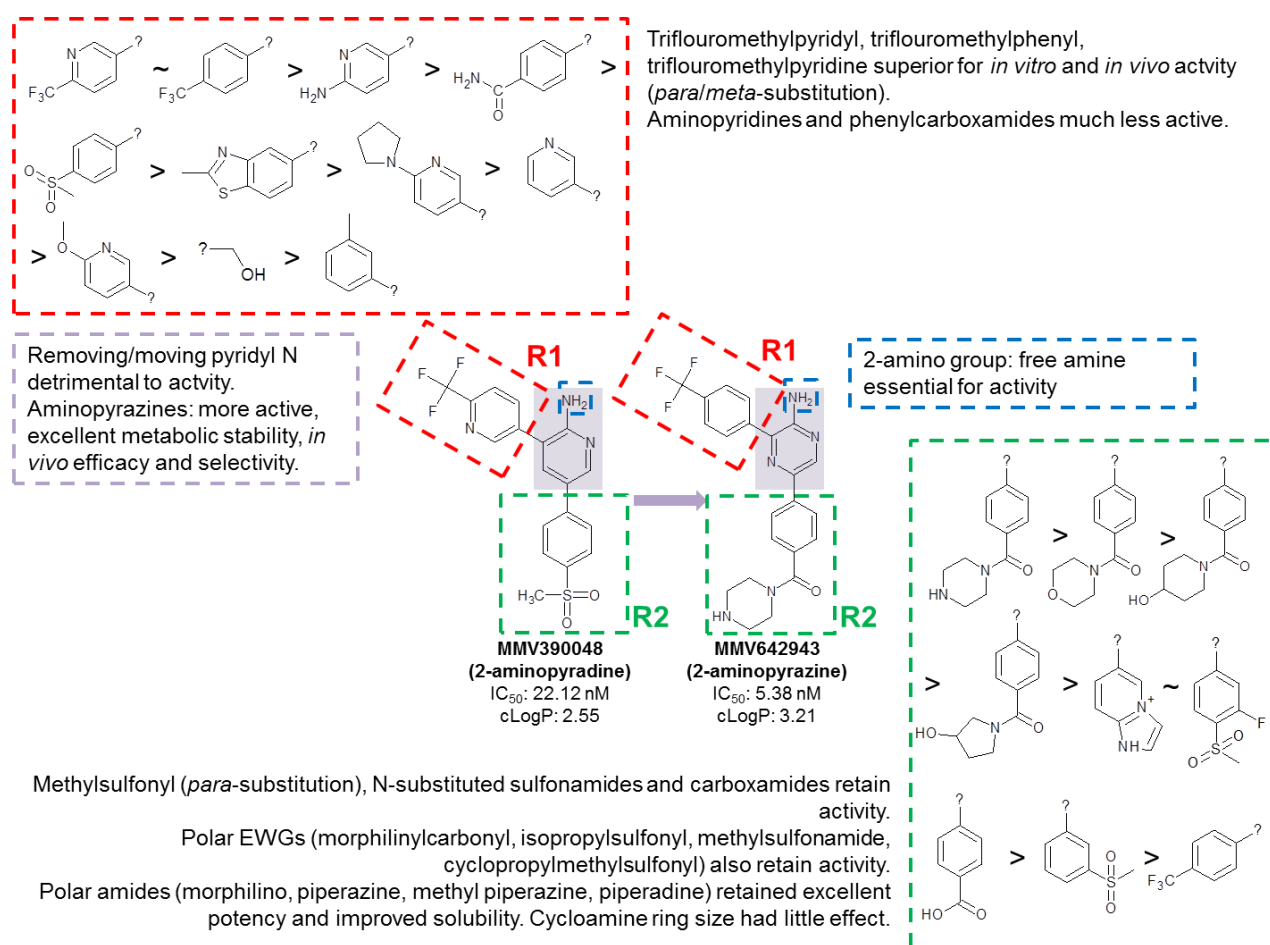


Figure 1.13: SAR optimisation highlights for the 2-aminopyridine series (created with personal information from our collaborators at H3D, UCT). Active representatives with both the 2-aminopyridine (MMV390048) and 2-aminopyrazine (MMV642943) cores are indicated with asexual blood stage activity and physicochemical properties (cLogP). Substitutions at are indicated in red (R1), green (R2) and other structural changes in blue. Core changes are indicated in purple.

1.7.3 Imidazopyridazines (IMPs)

Representatives from the IMP series displayed asexual stage activities comparable to chloroquine and artesunate. SAR investigations were performed around the IMP scaffold to improve pharmacokinetics, *in vivo* efficacy and selectivity over hERG [407]. This led to

the identification of the pyrazolopyridine, pyrazolopyrimidine and tetrahydropyrazolopyrimidine cores (Figure 1.14).

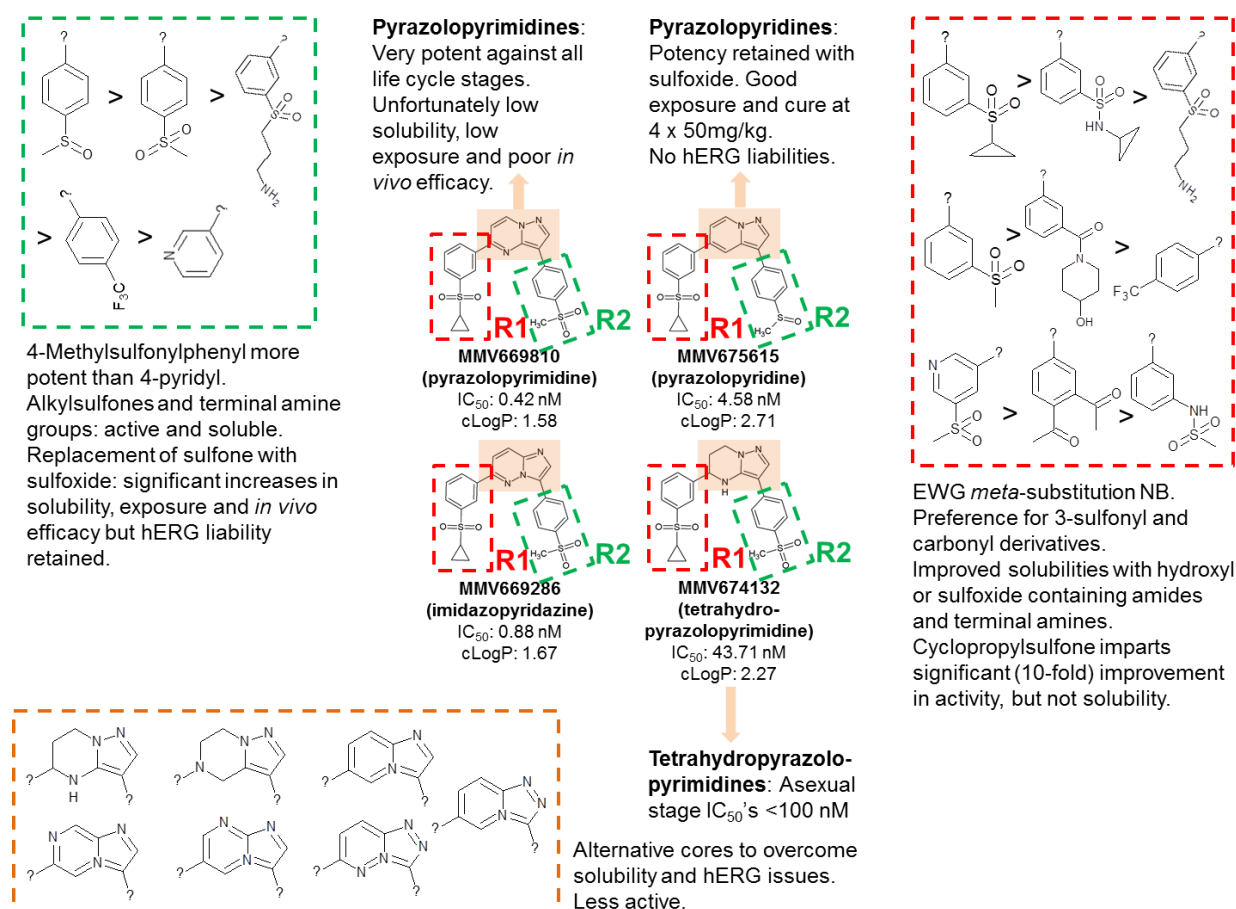


Figure 1.14: SAR optimisation highlights for the imidazopyridazine series (created with personal information from our collaborators at H3D, UCT). Active representatives of the pyrazolopyrimidine (MMV669810), pyrazolopyridine (MMV675615), imidazopyridazine (MMV669286) and tetrahydropyrazolopyrimidine (MMV674132) cores are indicated with asexual blood stage activity and physicochemical properties (cLogP). Substitutions at are indicated in red (R1) and green (R2), and core changes are indicated in orange.

IMPs have been identified as weak antiplasmodial (3D7; IC_{50} = 1-8 μ M) and *Pf*PK7 (IC_{50} = 0.131-11.6 μ M) inhibitors [364]. Active IMP (IC_{50} = 0.066-5 μ M) and pyrazolopyrimidine inhibitors of *Pf*CDPK1 displayed enhanced specificity due to the smaller size of this enzyme's threonine gatekeeper [365]. Substituted IMP analogues (bearing 2- or 3-aminoethylpyridyl and amide, cyano, fluoro or alkyl groups) displayed nanomolar IC_{50} s but were not selective for *Pf*CDPK1 and ineffective *in vivo* [366], whereas analogues harbouring heteroaryl substituents and basic amine side chains, displayed submicromolar anti-enzymatic (*Pf*CDPK1; IC_{50} <10 nM) and antiplasmodial (IC_{50} = 12 nM) activity [369], but with limited *in vivo* efficacy [367]. Moreover, 3,6-disubstituted IMPs were active towards *Tg*CDPK and parasites *in vitro* [366]. IMP-like compounds containing either a pyrimidine or non-pyrimidine linker were active towards mature asexual stages, confirmed

as *Pf*PKG inhibitors ($IC_{50} = 1.55$ nM), *Pf*CDPK1 inhibitors, and heat shock protein 90 (HSP90) binding partners [368]. Pyrazolopyrimidines with known *Tg*CDPK1 and *Cp*CDPK1 activity, blocked *Pf*CDPK4 activity and exflagellation (*P. falciparum* $EC_{50} < 40$ nM) [371]. 1-phenyl-1*H*-pyrazolo[3,4-*b*]pyridine derivatives bearing benzenesulfonamide substituents displayed moderate antiplasmodial activity (asexual IC_{50} : 3.5-9.3 μ M) [408].

1.7.4 Imidazopyridines (IPs)

IP-like scaffolds have been explored as antimalarials and antiprotozoal agents. A potent cGMP-dependent *Pf*PKG inhibitor, ML10 [409], displayed anti-enzymatic (160 μ M), asexual stage ($IC_{50} = 2.1$ nM) and transmission-blocking (IC_{50} SMFA = 41.3 nM) activity [410]. A 2-(3-aminophenyl) imidazopyridine displayed potent *in vitro* ($EC_{50} = 2$ nM) and *in vivo* efficacy against *Trypanosoma brucei*, with no clinical toxicity and favourable absorption, distribution, metabolism, excretion and toxicity (ADMET) parameters [411]. IP-like DHODH inhibitors from the Genzyme Corporation chemical library (N = 208 000) displayed submicromolar activity towards asexual stages (IC_{50} : 0.3-0.9 μ M) [412], whereas N-aryl-2-aminobenzimidazoles (pyridine-2-ylamino and basic piperazine substituents) from the AstraZeneca corporate collection (N = 500 000) displayed potent asexual stage activity (IC_{50} range: 36-59 nM), *in vivo* efficacy (99.9% reduction in parasitaemia; MSD >30) and excellent PK and ADMET profiles [234].

Initial SAR for the 2,6-IP series (Figure 1.15) resulted in the inclusion of mono- or trifluoromethoxy *ortho*-pyridyl substituents at R2 and difluorinated cycloalkanes at R1 [413]. Two early leads showed favourable pharmacokinetic parameters and *in vivo* efficacy in the *Pf*SCID mouse model [413], however, early derivatives displayed biphasic dose-response curves on drug-resistant *P. falciparum* (K1, Dd2, HB3, 7G8, TM90C2B, V1/S, FCB), alluding to incomplete kill or recrudescence [414]. Further derivatisations (piperazines with distal amides at R2; halogenated phenyls at R1) resulted in sigmoidal dose-response, but could not improve permeability or efflux [414], suggesting that the chemical space is too constricted to achieve both antiplasmodial activity and good pharmacokinetic properties.

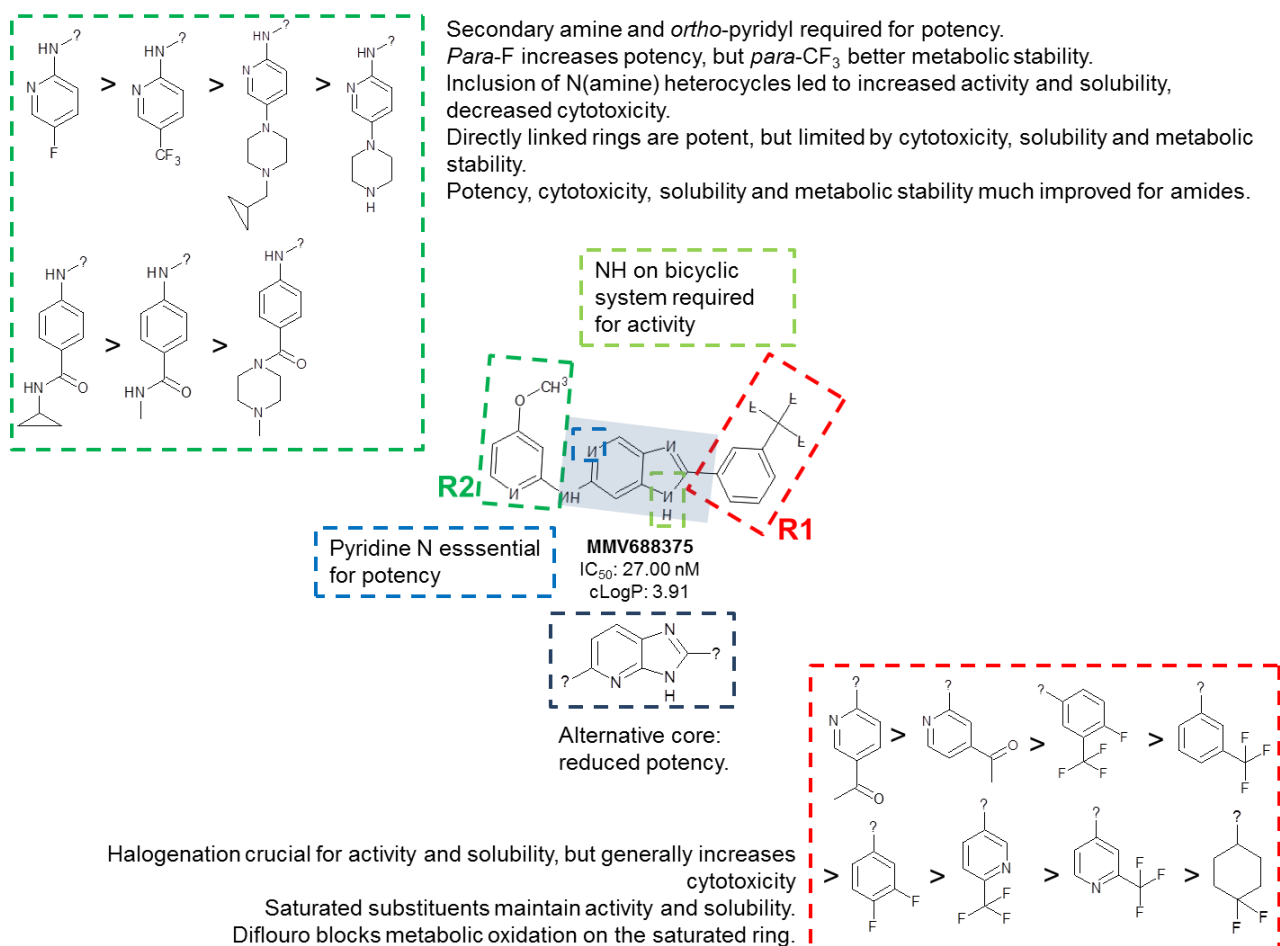


Figure 1.15: SAR optimisation highlights for the 2,6-imidazopyridine series (created with personal information from our collaborators at H3D, UCT). An active representative from the series (MMV688375) is indicated with its asexual blood stage activity and physicochemical properties (cLogP). Substitutions at are indicated in red (R1) and green (R2) whereas blue or light green indicate other structural changes). Core changes are indicated in dark blue.

In this thesis, the kinase-focussed library described above, was evaluated for activity against both asexual proliferative parasites (addressing TCP-1 criteria) as well as the gametocyte stages required for transmission (TCP-5). Literature indicated that similar scaffolds display potent activity towards the asexual stages of the parasite, as well as *P. falciparum* protein and lipid kinases, however the gametocytocidal activity of these chemotypes was unknown. Importantly, at least two of these compounds, MMV642943 and MMV390048, have gametocytocidal activity and are currently in pre-clinical and clinical assessment [252, 274]. Active compounds from this study might, therefore, serve as dual active or gametocyte-selective antimalarials, thereby providing a meaningful contribution to the global malaria elimination campaign.

1.8 Hypothesis

A kinase-focussed inhibitor library will demonstrate potent dual activity against the pathogenic asexual and sexual, transmissible stages of the *P. falciparum* parasite *in vitro*.

1.9 Aim

To interrogate the antiplasmodial activity of a kinase inhibitor library against the asexual and gametocyte stages of the *P. falciparum* parasite.

1.10 Objectives

1. Develop a robust and reproducible gametocyte production protocol towards screening gametocytocidal compounds on cross-validated assay platforms (Chapter 2).
2. Interrogate the asexual stage activity and gametocytocidal profile (stage-specificity, speed of action, *ex vivo* efficacy) of a kinase-focussed inhibitor library (Chapter 3).
3. Use cheminformatics to extract the physicochemical features and SAR of kinase-focussed inhibitor chemotypes towards predicting a potential gametocyte-selective scaffold (Chapter 4).

1.11: Outputs generated

Publications

1. Reader J, **Botha M**, Theron A, Lauterbach SB, Rossouw C, Engelbrecht D, Wepener M, Smit A, Leroy D, Mancama D, Coetzer TL, Birkholtz LM. (2015). Nowhere to hide: interrogating different metabolic parameters of *Plasmodium falciparum* gametocytes in a transmission-blocking drug discovery pipeline towards malaria elimination. *Malaria Journal*. May 22;14:213. Doi: 10.1186/s12936-015-0718-z.
2. **van der Watt M**, Reader J, Churchyard A, Nondaba S, Lauterbach S, Niemand J, Abayomi S, van Biljon R, Connacher J, van Wyk R, Le Manach C, Paquet T, Gonzales Cabrera D, Theron A, Leroy D, Duffy J, Street L, Chibale K, Mancama D, Coetzer T, Birkholtz LM. (2017). Potent *Plasmodium falciparum* gametocytocidal compounds identified by exploring the kinase inhibitor chemical space for dual active antimalarials. *Journal of Antimicrobial Chemotherapy*. Doi: 10.1093/jac/dky008.

Conferences

1. **Mariëtte Botha**, Janette Reader, Abayomi Sijuade, Theresa Coetzer and Lyn-Marie Birkholtz. (3 - 5 August 2015). *Plasmodium falciparum* gametocytogenesis: Target of Transmission-blocking antimalarial interventions. Poster presentation. 1st MOMR South African Malaria Research Conference, Durban, South Africa).
2. **Mariëtte Botha**, Janette Reader, Alisje Churchyard, Sindisiwe H. Nondaba, Sonja Lauterbach, Claire LeManach, Tanya Paquet, Diego González Cabrera, Anjo Theron, Didier Leroy, James Duffy, Leslie Street, Kelly Chibale, Dalu Mancama, Theresa L. Coetzer and Lyn-Marie Birkholtz. (15 – 18 November 2016). Potent *Plasmodium falciparum* gametocytocidal compounds identified by exploring the kinase inhibitor chemical space for

antimalarials. Poster presentation. 3rd H3D symposium *Malaria, Tuberculosis and Neglected Tropical Diseases: Progress in Drug Discovery and Development Cape Town, South Africa*.

3. **Mariëtte van der Watt**, Janette Reader, Alisje Churchyard, Sindisiwe Nondaba, Sonja Lauterbach, Jandeli Niemand, Sijuade Abayomi, Riëtte van Biljon, Jessica Connacher, Roelof van Wyk, Claire Le Manach, Tanya Paquet, Diego González Cabrera, Anjo Theron, Didier Leroy, James Duffy, Leslie J. Street, Kelly Chibale, Dalu Mancama, Theresa Coetzer and Lyn-Marie Birkholtz. (7 - 9 November 2017). Potent *Plasmodium falciparum* gametocytocidal compounds identified by exploring the kinase inhibitor chemical space for dual active antimalarials. 3rd Annual MOMR South African Malaria Research Conference, NICD, Johannesburg, South Africa).

CHAPTER 2

ESTABLISHMENT OF AN OPTIMISED GAMETOCYTE PRODUCTION PROTOCOL AND CONFIRMATION OF VIABILITY ON ORTHOGONAL ASSAY PLATFORMS.

The work in this chapter has been published as follows:

Reader J*, **Botha M***, Theron A, Lauterbach SB, Rossouw C, Engelbrecht D, Wepener M, Smit A, Leroy D, Mancama D, Coetzer TL, Birkholtz LM. (2015). Nowhere to hide: interrogating different metabolic parameters of *Plasmodium falciparum* gametocytes in a transmission-blocking drug discovery pipeline towards malaria elimination. *Malaria Journal*. May 22;14:213. Doi: 10.1186/s12936-015-0718-z.

* **Note:** This chapter was published as a **shared first author publication**, and therefore parts thereof also appear in the thesis of Dr J. Reader entitled: "Interrogation of the chemotherapeutic and transmission-blocking abilities of metalloodrugs against malaria parasites."

2.1 Introduction

Global efforts to eliminate malaria have achieved success in Europe and North America, but the disease remains a significant health problem in sub-Saharan Africa [2]. Mortality rates have been reduced due to the deployment of ITNs, IRS and ACTs, but an estimated 219 million cases still occurred in 2017 [5]. One of the major realisations from previous elimination attempts is that, compared to smallpox and poliomyelitis, no single strategy will pertain to control and eliminate malaria. Particularly evident is the fact that malaria elimination will not be achieved by focusing only on the treatment of the disease in humans or on vector control, but will require strategies to prevent transmission of the parasite between the human host and mosquito vector by targeting hepatic and gametocyte developmental stages [386, 415]. In 2007, the malaria eradication agenda was adopted by the global malaria community to galvanise coordinated efforts aimed not only to control malaria but also to eliminate it worldwide and ultimately eradicate this disease [2].

As pathogens, parasites of the genus *Plasmodium* have exquisitely adapted to varying biological environments in their human and mosquito hosts, with *P. falciparum* causing the most virulent form of the disease. *Anopheles* mosquitoes introduce sporozoites into humans, and these infect hepatocytes where, undetected, they replicate *en masse* and are released to initiate the pathogenic asexual cycle in human erythrocytes. Synchronised

egress of merozoites from erythrocytes results in the characteristic fever spells that typify the disease [416]. A portion of these *P. falciparum* parasites mature through five distinctive stages (I-V) in a process known as gametocytogenesis, lasting ~8 to 12 days, after which late stage V male and female gametocytes transmit to mosquitoes for sexual reproduction [416, 417]. Mosquito uptake initiates the necessary molecular and cellular changes in gametocytes, enabling adjustment from the human to insect host. Moreover, contact with midgut factors activates the developmentally arrested gametocytes, resulting in egress from the erythrocyte, gamete formation and subsequent fertilisation [46]. This is followed by the transformation of the fertilised zygote into the infective ookinete, succeeded by the oocyst that releases sporozoites for transmission back to humans [136].

Commitment to sexual development is postulated to take place in the first 20 hours of the preceding erythrocytic cycle [33]. All merozoites from a single schizont will become either male or female gametocytes [59]. Gender is predetermined in the schizont committed to gametocytogenesis and typically female-biased [38, 80]. Several population bottlenecks occur during the complete *Plasmodium* life cycle, including the sexual developmental stages in the mosquito (e.g. only ~10 oocysts per mosquito midgut) as well as the hepatic sporozoite and intra-erythrocytic sexual gametocyte stages in humans. These, therefore, represent critical areas that could be successfully targeted for the ambitious goal of malaria elimination [418, 419]. A strategy which targets the vector stages would require a drug to be present at pharmacologically relevant concentrations for as long as late gametocytes circulate (up to 30 days). The most appropriate point of intervention is therefore to target gametocytes in the host and eliminate the parasite population, thus interrupting transmission. Currently, only ACTs and primaquine have therapeutic activity against late stage gametocytes, but these are threatened by emerging resistance and toxicity concerns (e.g. for primaquine in G6PD deficient patients) [255]. The development of new gametocytocidal compounds has, therefore, become a priority.

SMFAs remain the ultimate indicator of the transmission-blocking ability of new compounds against *P. falciparum* parasites, but due to the highly demanding nature of this approach, gametocyte assays are vital filters to identify transmission-blocking molecules [255]. However, there is a lack of standardisation of methods to produce gametocytes and of assays to screen compounds. This makes it difficult to compare results from different laboratories and has hampered the discovery of new chemotherapeutics targeting gametocytes. The *in vitro* production of pure, viable, stage-specific *P. falciparum*

gametocytes in high yield and a consistent, reproducible manner for downstream screening assays is challenging, however, several methods have recently been published [255, 264, 420-428]. *In vivo* gametocyte production generally increases when the human host is anaemic and reticulocytosis augmented [429]. Gametocytogenesis is induced *in vitro* by nonspecific “stress” to the parasite, including a drop in haematocrit [90], the use of spent nutrient deficient culture medium [423], lymphocytes [57], mammalian hormones [89], reticulocytes [63], some inhibitors of nucleic acid synthesis (including antifolates) [90, 430, 431], Berenil, Fansidar, chloroquine, amodiaquine, sulphadoxine-pyrimethamine, ammonia compounds [82, 432, 433] and cholera toxin [429]. However, many of these methods are cumbersome, costly, not robust, and the gametocytes are not suitable for evaluating potential transmission-blocking compounds.

Gametocyte screening assays should be reproducible and amenable to scaling up to medium- or high throughput systems. Since gametocytocidal activity cannot be monitored with cellular multiplication markers, recent screens have typically relied on phenotypic assays. Systems developed thus far range from determination of gametocyte viability through the detection of ATP [118, 434-436], parasite lactate dehydrogenase (pLDH) [427], colourimetric detection [118, 435, 437-439], flow cytometry [440], fluorescence-based high content imaging [264, 265, 405, 441-443] and transgenic reporter lines, which are useful for monitoring stage-specific effects [426, 428, 438, 444, 445]. Some of these platforms have been developed into reproducible medium/high throughput screening (MTS/HTS) assays [439, 446, 447]. However, since these assays interrogate different metabolic pathways in the parasite, notable discrepancies regarding the identification of compounds with gametocytocidal activity have been observed in the literature [448]. Potential target compounds may, therefore, be missed if only one assay system is used. One such example, is the gametocytocidal compound methylene blue which displays variant potencies on late stage (III-IV) gametocytes using the pLDH ($IC_{50} = 29$ nM) [449], luciferase ($IC_{50} = 38$ nM) [428], ATP ($IC_{50} = 490$ nM) , alamarBlue[®] ($IC_{50} = 307$ nM) [447] as well as dye-based ($IC_{50} = 170$ nM) [443] and antibody-based ($IC_{50} = 920$ nM) [442] high content imaging (HCI) assays. Direct comparison of assay platforms using a reference set of gametocytocidal compounds has been reported. D’Allesandro *et al.*, (2016) stated an excellent correlation between readouts from the luciferase and pLDH assays using the MMV Validation Set [426]. Similarly, a comparison between luciferase as well as green fluorescent protein (GFP)-Mitotracker[®] Red and GFP-Acridine Orange HCl readouts using a selection of compounds from the MMV Malaria Box, revealed good inter-assay

correlations. Assay-specific hits were, however, identified and revealed the value of utilising multiple assay platforms interrogating different viability parameters [450]. These comparisons are highly informative for the evaluation of the robustness and validity of individual assay platforms in drug discovery programmes.

This report evaluated a system for the production of gametocytes that addresses several issues including (i) increasing the number of parasites that commit to gametocytogenesis, (ii) isolating large numbers of pure and viable gametocytes of a specific stage and (iii) reducing variability in gametocyte production, resulting in a robust system. Moreover, these gametocytes were subsequently used in a comparative study of four different assay platforms on a single set of antimalarial compounds provided by the MMV. The ability of compounds to inhibit gametocytes was measured by detecting changes in the redox status of the parasite (modified alamarBlue[®] assay [435, 446]), energy production (measurement of ATP levels [118, 425, 436, 437]), active glycolysis reflecting metabolic activity (pLDH [449]) and stage-specificity with a luciferase reporter assay [438]. Uniquely, all of the assays were performed on the same gametocyte population, with the same drug pressure applied for 48 hours. This work enabled interrogation of the biological consequence of gametocytocidal compounds, irrespective of assay platform influences.

2.2 Methods and materials

2.2.1 Ethics

All *in vitro* parasite and blood collection work has ethics approvals (University of Pretoria 120821–077; CSIR Ref 10/2011; University of the Witwatersrand M130569). *Ex vivo* culture adaptation of clinical isolates was performed under ethical clearance (University of Pretoria 417/2013, University of the Witwatersrand M140995).

2.2.2 *In vitro* cultivation of asexual stage *P. falciparum* parasites

In vitro *P. falciparum* parasite cultures were maintained at 37°C in human erythrocytes at a haematocrit of 5% suspended in complete culture medium [RPMI 1640 medium (Sigma-Aldrich) supplemented with 25 mM HEPES (Sigma-Aldrich), 0.2% D-glucose (Sigma-Aldrich), 200 µM hypoxanthine (Sigma-Aldrich), 0.2% sodium bicarbonate, 24 µg/ml gentamicin (Invitrogen)] with either 0.5% AlbuMAX[®] II (Invitrogen) or 10% human serum (Interstate Blood Bank, Chicago, USA) and flushed with 90% N₂, 5% O₂, and 5% CO₂ (Afrox, Johannesburg, South Africa) as described elsewhere [451, 452]. Medium was

aspirated daily and replaced with fresh medium pre-warmed to 37°C and parasite proliferation was monitored with microscopy of Giemsa-stained smears. Various *P. falciparum* strains (NF54, 3D7, FCR3, W2, HB3 and 7G8) were cultured in the same manner. In cases where asexual synchronicity was required, standard 5% D-sorbitol synchronisation was applied to ring stage parasites [422, 453].

2.2.3 Induction of gametocytogenesis and general maintenance of gametocyte cultures

This method was adapted from Carter *et al.* [454]. Gametocytogenesis was induced by a combination of nutrient starvation and a drop in haematocrit. Asexual parasites were cultured to a 6-10% parasitaemia, which was then decreased to 0.5% [39] (at 6% haematocrit [59]) and the culture transferred to glucose-deprived medium (complete culture medium without glucose). Cultures were maintained in an atmosphere of 5% CO₂, 5% O₂ and 90% N₂, at 37°C, without shaking. Cultures were also kept at 37°C during daily medium changes. On day -2, the culture underwent no medium change in order to introduce an additional stressor (depleted or spent medium). The ring population on day -1 received glucose-deprived medium with a drop in haematocrit on day 0 (from 6 to 4%). Gametocytogenesis was subsequently monitored microscopically with daily medium (glucose-deprived) changes. On days 6-9, residual asexual parasites were eliminated by continuous 50 mM N-acetyl glucosamine (NAG), Sigma-Aldrich) treatment, in complete culture medium. The cultures were maintained in complete culture medium from day ten onwards and gametocytes monitored daily by microscopy until used in the various assays.

2.2.4 Characterisation, cultivation, genotypic and phenotypic profiling of clinical isolates of southern African origin

Isolates were sampled between February and April 2014 from the Steve Biko Academic Hospital, Tshwane District Hospital, and Kalafong Hospital. These clinical isolates represent a pool of current southern African parasites. *Ex vivo* cultures were initiated from intravenous blood samples within 2-24 hours [455], and parasites only maintained for a maximum of five *in vitro* passages. Cryopreserved stocks were prepared throughout to maintain polyclonal variability for all subsequent gametocyte inductions. All of the isolates were phenotyped for drug resistance against artemisinin, chloroquine, DHA, mefloquine, pyrimethamine and amodiaquine using SYBR[®] Green I fluorescence assays [456] and genotyped using polymerase chain reaction (PCR) and restriction fragment length

polymorphisms (RFLPs) for asexual drug resistance markers *dhfr* (codons 50, 51, 59, 108, 164); *dhps* (codons 436, 437, 540, 581), *pfcr1* (codon 76) and *pfmdr1* (codon 86) [457]. Gametocytogenesis was induced as above (section 2.2.2) and the MMV 10-set evaluated for activity on the resultant late stage ($\geq 95\%$ stage IV/V) gametocytes for a panel of five gametocyte-producing *ex vivo* African clinical isolates using the pLDH assay as described below (section 2.2.7.3).

Further characterisation of the conversion of asexual parasites to sexual commitment was achieved by microscopic examination of Giemsa stained slides as well as the determination of *pfap2-g* transcript abundance in committed schizonts [97]. Briefly, a population of $>80\%$ early schizonts were harvested from committed cultures on day 0 of gametocytogenesis (Table 2.1). Infected erythrocytes were centrifuged and the pellets stored (-70°C) for RNA isolation and cDNA synthesis. Real-time reverse transcriptase polymerase chain reaction (RT-PCR) was used to confirm *pfap2-g* differential transcript abundance for the panel of clinical isolates. The *PfAP2-G* forward (5'-AACACGTTTCATTCAATAAATAAGG-3') and *PfAP2-G* reverse (5'-ATGTTAATGTTCCCAAACAACCG-3') primers were used [458]. Analysis was performed using the LightCycler[®] 480 and KAPA SYBR[®] Fast qPCR kit (Kapa Biosystems, USA) using 5 pmol of each primer in 384-well plates; with cycling after pre-incubation at 95°C for 10 min for 45 cycles (95°C for 3 seconds, 55°C for 7 seconds and 72°C for 4 seconds). Relative expression was calculated using LightCycler[®] 480 software (version 1.5) and the comparative Ct ($2^{-\Delta\Delta\text{Ct}}$) method [459] used to analyse transcript abundance.

2.2.5 Male gamete exflagellation

Gametogenesis was assessed by treating samples with 50 μM XA; Sigma-Aldrich) in exflagellation buffer (RPMI 1640 with 25 mM HEPES, 0.2% sodium bicarbonate, pH 8.0) followed by a >15 -minute incubation at room temperature (RT). Exflagellation was visualised by phase contrast microscopy at 40x magnification.

2.2.6 Validation of stage-specific gametocyte production by flow cytometry and cell sorting

Flow cytometry was used to distinguish asexual parasites from different gametocyte populations. Gametocytes were enriched on CS-columns by magnetic separation in a VarioMACS magnetic system (Miltenyi Biotec) according to the manufacturer's

recommendations. Parasites were stained with Thiazole Orange (1 μ M) for 20-30 minutes in the dark at 37°C. Flow cytometry acquisition was performed for at least 50 000 events with a Beckman Coulter Gallios flow cytometer (excitation at 488 nm; emission with 525/540 bandpass filter at 525 \pm 20 nm). Gating of uninfected and infected erythrocytes was previously established and confirmed by Giemsa-stained microscopy of sorted populations. Uninfected erythrocytes were used as the negative control to determine background DNA fluorescence. Post-acquisition analyses were performed with Beckman Coulter Kaluza (v1.1) software.

Note: This work was contributed by Dewaldt Engelbrecht as part of the published manuscript.

2.2.7 Gametocytocidal activity assays

2.2.7.1 Anti-malarial compounds

A 10-compound set was provided by the MMV, blinded until after data analysis. All other drugs were purchased from Sigma-Aldrich. Compounds were dissolved in DMSO and diluted fresh for each assay with complete culture medium to achieve a final concentration of 1 μ M (final DMSO concentration \leq 0.5 %). All assays were performed in parallel using the same stock of compounds, diluted fresh at the same time under the same conditions. Gametocytocidal activity was controlled by H₂O₂ (0.5% continuous or 200 mM added at endpoint) as well as drug controls, including methylene blue (1 μ M) and dihydroartemisinin (DHA; 1 μ M). Untreated gametocytes and uninfected red blood cells or culture medium were used to monitor viability and background, respectively.

2.2.7.2 Resazurin-based dye assay

The PrestoBlue[®] (Life Technologies) assay was based on an adaptation of the method described by Tanaka and colleagues [435, 446]. Drug dilutions were placed in triplicate in 96-well plates in a volume of 50 μ l/well. Semi-synchronous gametocyte cultures (50 μ l/well, stage IV/V) were added to the 96-well plates to achieve a final gametocytaemia and haematocrit of 2% and 5% respectively, in a total incubation volume of 100 μ l. The plate was placed on a shaker for 10-20 seconds before being encased in an airtight chamber and gassed for 5 minutes with a 5% CO₂, 5% O₂, balance N₂ mixture (Afrox, Johannesburg, South Africa). Following incubation at 37°C for 48 hours, 10 μ l of PrestoBlue[®] reagent was added to each well, the plate mixed on a shaker for 10-20 seconds and left to incubate at 37°C for 2 hours. Finally, the plate was centrifuged at 120g (1 minute), and 70 μ l of the supernatant transferred to a clean 96-well plate before reading

in a multi-well spectrophotometer (Infinite F500, Tecan, USA) by fluorescence detection at 612 nm.

Note: This work was contributed by Anjo Theron as part of the published manuscript.

2.2.7.3 pLDH assay

Drug dilutions were placed in triplicate in 96-well plates in a final volume of 100 µl/well. Semi-synchronous stage IV and V gametocyte cultures (100 µl/well) were added to the 96-well plates to achieve a final gametocytaemia and haematocrit of 2% and 1% respectively, in a total incubation volume of 200 µl. The plates were incubated at 37°C for 48 hours. Gametocyte viability was determined spectrophotometrically by measuring the activity of pLDH [449], according to a modified version of the method of Makler and Hinrichs [460]. Briefly, 100 µl of Malstat reagent (0.21% v/v Triton-100; 222 mM L-(+)-lactic acid; 54.5 mM Tris; 0.166 mM APAD; Sigma-Aldrich); adjusted to pH 9 with 1 M NaOH) was transferred into a clean 96-well plate. A fixed volume of 20 µl parasite suspension/well was added to the Malstat plate, followed by the addition of 25 µl PES/NBT (1.96 mM nitro blue tetrazoliumchloride NBT; 0.239 mM phenazine ethosulphate PES). Absorbance was measured with a Multiskan Ascent 354 multi-plate scanner (Thermo Labsystems, Finland) at 620 nm.

2.2.7.4 ATP bioluminescence assay

Mature gametocytes, predominantly stage V, were enriched using density gradient centrifugation and magnetic separation. For density gradient separation, gametocytes were pelleted and resuspended in 10 ml of complete culture medium, loaded onto 5 ml preheated (37°C) NycoPrep™ 1.077 cushions (Axis- Shield) and centrifuged at 800g for 20 minutes at 37°C. The gametocyte-containing bands were collected, concentrated by centrifugation and the pellet resuspended in 5 ml complete culture medium. This was loaded on equilibrated LS-columns for magnetic separation in a MidiMACS magnetic system (Miltenyi Biotec) to purify and enrich the gametocytes, which were counted in a Neubauer chamber. Drug dilutions were placed in triplicate in 96-well plates. Approximately 30 000 gametocytes in complete culture medium were added to each well in a final volume of 100 µl and the plates incubated for 24 hours in a humidified gas chamber (90% N₂, 5% O₂, and 5% CO₂) at 37°C. Subsequently, the BacTiter-Glo™ assay (Promega) was performed according to the manufacturer's instructions at RT, in the dark, with assay substrate incubation for 10 minutes and shaking for the first two minutes, to detect ATP levels. Bioluminescence [118, 421, 425] was detected at an integration

constant of 0.5 seconds with the GloMax[®]-Multi + Detection System with Instinct[®] Software.

Note: This work was contributed by Janette Reader as part of the published manuscript.

2.2.7.5 Luciferase reporter assay

The Luciferase reporter assay was established to enable accurate, reliable and quantifiable investigations of the stage-specific action of gametocytocidal compounds for each of the early and late gametocyte marker cell lines; NF54-Pfs16-GFP-Luc and NF54-Mal8p1.16-GFP-Luc (kind gift from David Fidock, Columbia University, USA) [438]. Gametocytogenesis was induced on synchronised asexual parasites as described above, with the exception that NAG treatment was initiated from day 1-4 to remove asexual parasites early and allow more synchronised early stage gametocytes. Drug assays were set up on day 5 and 10 (representing early stage II/III and late stage IV/V gametocytes, respectively). In each instance, assays were set up in triplicate using a 2% gametocytaemia, 2% haematocrit culture and 48 hour drug pressure in a gas chamber (90% N₂, 5% O₂, and 5% CO₂) at 37°C. Luciferase activity was determined in 20 µl parasite lysates by adding 50 µl luciferin substrate (Promega Luciferase Assay System) at RT and detection of resultant bioluminescence at an integration constant of 10 seconds with the GloMax[®]-Multi+ Detection System with Instinct[®] Software.

2.2.8 Data analysis

Assay quality was measured for all assays by defining the standard deviation (SD); standard error of the mean (SEM); percent coefficient of variation (%CV); signal to background ratio (S/B), signal to noise ratio (S/N) and the Z'-factor, which were calculated according to the formulae below [449]. The Z'-factor is a measure of statistical effect size. The result is given as a numerical value (0 to 1), being more favourable as it approaches 1 [118, 461]. %CV is acceptable at <20% [462]. All parameters were calculated from at least three independent experiments for each assay, each time performed in triplicate. Results were expressed as the percentage inhibition compared to untreated controls.

$$Z' = 1 - [3(SD_{\text{positive}} + SD_{\text{background}}) / (\text{Mean}_{\text{positive}} - \text{Mean}_{\text{background}})]$$

$$S/N = [(\text{Mean}_{\text{positive}} - \text{Mean}_{\text{background}}) / SD_{\text{background}}]$$

$$S/B = \text{Mean}_{\text{positive}} / \text{Mean}_{\text{background}}$$

$$\%CV = (SD / \text{Mean}) \times 100$$

$$\text{Percentage gametocyte viability (\% Viability)} = \frac{[(\text{Signal} - \text{Mean}_{\text{background}})/(\text{Mean}_{\text{positive}} - \text{Mean}_{\text{background}})] \times 100}{\% \text{Inhibition} = 100 - (\% \text{viability})}$$

2.3 Results

2.3.1 Optimisation of *P. falciparum* gametocyte production

Various parameters were investigated for their ability to influence gametocyte production including (i) the influence of stationary versus shaking culturing conditions; (ii) AlbuMAX[®] II versus human serum in culture medium; (iii) evaluating different methods for removal of asexual parasites; and (iv) evaluating strain-specific differences in gametocyte production. This resulted in the following optimised protocol: the application of physiological stress to a starting asexual culture by increasing parasitaemia to 6-10% in a parasite population of >80% rings. The induction of gametocytogenesis by a combination of both nutrient starvation (glucose deprivation) and a decrease in haematocrit under stationary culturing conditions in the presence of AlbuMAX[®] II and gentamicin, while maintaining a 37°C environment throughout. Gametocytogenesis required growth under stationary conditions, from asexual cultures grown either under stationary or shaking conditions. Upon microscopic observation of gametocytes, asexual parasites were removed from a predominantly stage II gametocyte population by applying NAG pressure for at least two asexual developmental cycles (from day 6–9), while maintaining gametocyte viability in a nutrient-rich environment (Table 2.1).

Table 2.1: Overview of the optimised gametocyte production protocol.

Day	Early stage gametocytes (> 90% stage II/III)	Late stage gametocytes (> 95% stage IV/V)
-3	Initiate culture at 6% haematocrit and 0.5% parasitaemia using glucose-deprived medium	
-2	No medium change (additional stressor)	
-1	Replace spent medium with glucose-deprived medium	
0	Replace spent medium with glucose-deprived medium and drop haematocrit to 4%	
1	Resuspend in NAG medium Ensure culture >80% rings	Resuspend in glucose-deprived medium
2	Resuspend in NAG medium	Resuspend in glucose-deprived medium
3	Resuspend in NAG medium	Resuspend in NAG medium Ensure culture >80% rings
4	Resuspend in NAG medium	Resuspend in NAG medium
5	Day of assay (> 90% stage II/III) Complete culture medium	Resuspend in NAG medium
6		Resuspend in NAG medium
7		Resuspend in NAG medium
8		Resuspend in NAG/complete culture medium (depending on residual asexual stage presence)
9		Resuspend in NAG/complete culture medium (depending on residual asexual stage presence)
10		Day of assay (> 95% stage IV/V) Complete culture medium

This optimised protocol produced an average gametocytaemia of $5.1 \pm 1.0\%$ on day 11 using the NF54 strain. A gametocyte conversion factor of $33.3 \pm 1.9\%$ was obtained, indicating a high proportion of asexual parasites committed to gametocytogenesis (Table 2.2).

Table 2.2: Evaluation of various *in vitro* gametocytogenesis induction methods using *P. falciparum* parasites under different conditions. Data are representative of (n) biological experiments, each performed in triplicate, \pm SEM. Data indicate maximal levels of gametocytaemia obtained.

		Gametocytaemia ^a	Conversion factor ^b
Shaking vs. Stationary (serum medium)			
Asexual culture	Gametocyte culture		
Stationary	Stationary	1.3 \pm 0.6% (n=4)	15.8 \pm 0.6%
Stationary	Shaking	NA	NA
Shaking	Stationary	3.3 \pm 1.4% (n=22)	34.2 \pm 3.4%
Shaking	Shaking	NA	NA
Medium composition (shaking asexual cultures, stationary gametocyte cultures)			
Asexual culture	Gametocyte culture		
AlbuMAX [®] II	AlbuMAX [®] II	5.1 \pm 1.0% (n=10)	33.3 \pm 1.9%
AlbuMAX [®] II	Serum	1.9 \pm 0.8% (n=3)	8.2 \pm 2.2%
Serum	Serum	1.3 \pm 0.6% (n=4)	20.7 \pm 3.3%
Serum	AlbuMAX [®] II	3.7 \pm 1% (n=3)	22.7 \pm 1.1%
Asexual parasite elimination			
	Sorbitol	5.3 \pm 0.2% (n=2)	32.3 \pm 1.4%
	NAG	4.9 \pm 1.0% (n=2)	37.7 \pm 1.7%
Induction of other <i>P. falciparum</i> strains			
	3D7	1.5 \pm 0.2% (n=3)	11.2 \pm 2.0%
	W2	1.1 \pm 0.2% (n=3)	8.9 \pm 0.5%
	7G8	1 \pm 0.7% (n=2)	ND
	FCR3	0% (n=3)	ND
	HB3	0% (n=3)	ND

ND: not detected/determined

NA: not applicable

^a Day 11 after induction

^b Conversion factor =

$$\frac{\text{Number of stage 2 gametocytes on day 4}}{\text{Number of rings on day 2}}$$

This procedure was highly robust as validated across three independent laboratories (Figure 2.1A) that generated high quality, viable gametocytes in a high average yield of $3.9 \pm 0.2\%$ using the NF54 strain. Moreover, gametocytes could also be produced using other known gametocyte-producing *P. falciparum* strains (Table 2.2). The kinetics of conversion to gametocytes followed the expected maturation to stage IV-V gametocytes, achieved at day 10-12 (Figure 2.1A). The number of asexual forms increased to a maximum parasitaemia of 5.4% on days 2 (before NAG treatment) and declined steadily thereafter. Sexual forms were first detected on day 2, with gametocytaemia reaching an average of 5.1% on day 11 (Figure 2.1B).

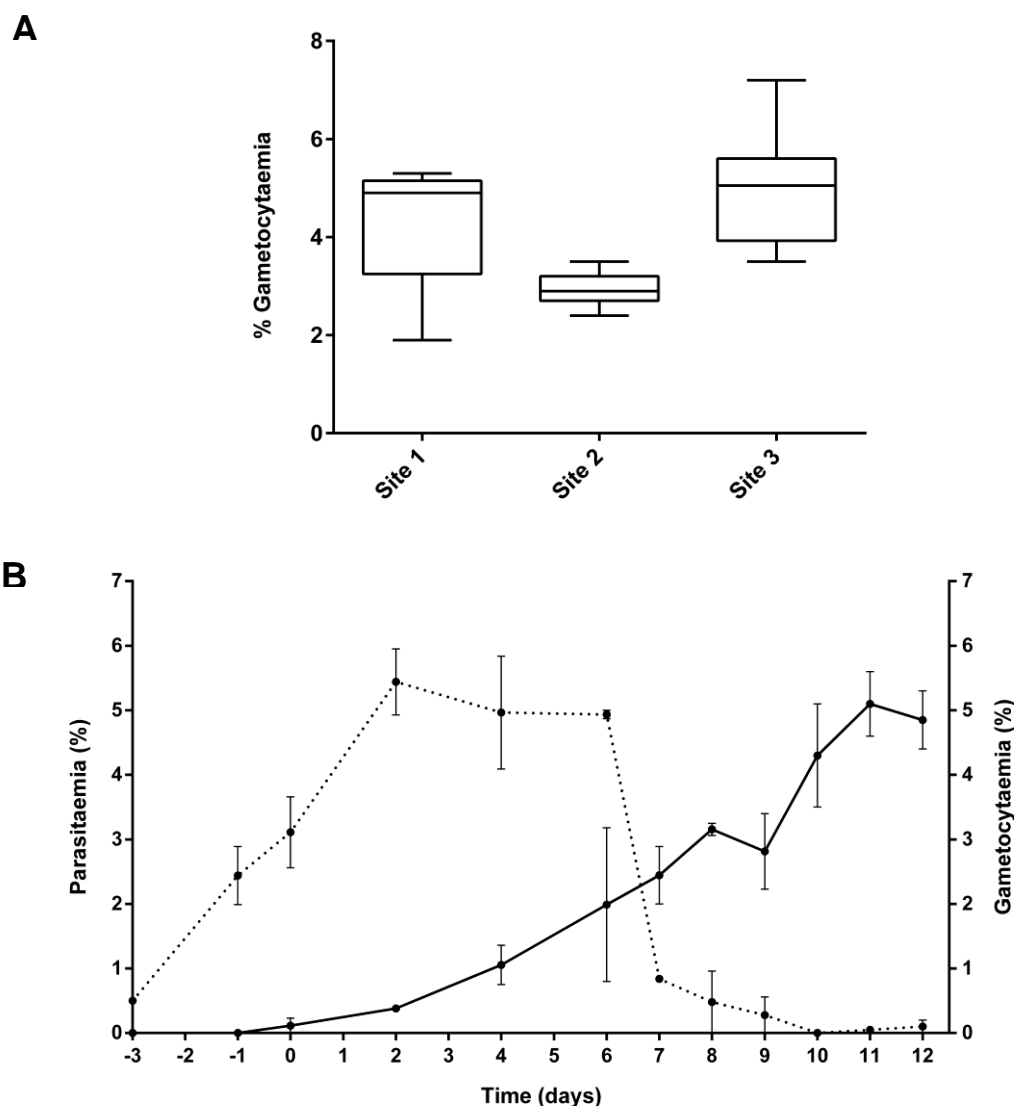


Figure 2.1: Visual evaluation of *P. falciparum* kinetics of conversion, gametocyte production, and asexual elimination. Parasites (*P. falciparum* NF54) were cultured in medium with 0.5% AlbuMAX[®] II for both asexual and gametocyte cultures. **(A)** Box and whisker plots of gametocytaemia (% stage III-V gametocytes) obtained with the same optimised protocol across three independent sites (site 1: n=6; site 2: n=17; site 3: n=14). **(B)** Kinetics of parasitaemia (asexual stages; dashed line) and gametocytaemia (gametocytes; solid line) during gametocytogenesis. Data are from n≥4 independent biological experiments each performed in triplicate, ± SEM.

Normal exflagellation and ATP production were used as gametocyte viability indicators. The addition of the broad-spectrum antibiotic, gentamicin, to the culture medium as preservative did not influence gametocyte production or viability (Figure 2.2A). However, gentamicin might influence downstream antimalarial assays, particularly in the context of screening unknown test compounds. The viability of late stage IV-V gametocytes grown in the presence and absence of gentamicin was determined after treatment with DHA to investigate possible gentamicin interference (Figure 2.2B). Treatment in the presence of gentamicin revealed the expected dose-response indicating no detrimental effect of gentamicin under these conditions and for this compound. Gentamicin was therefore included in the culture medium for the duration of the study.

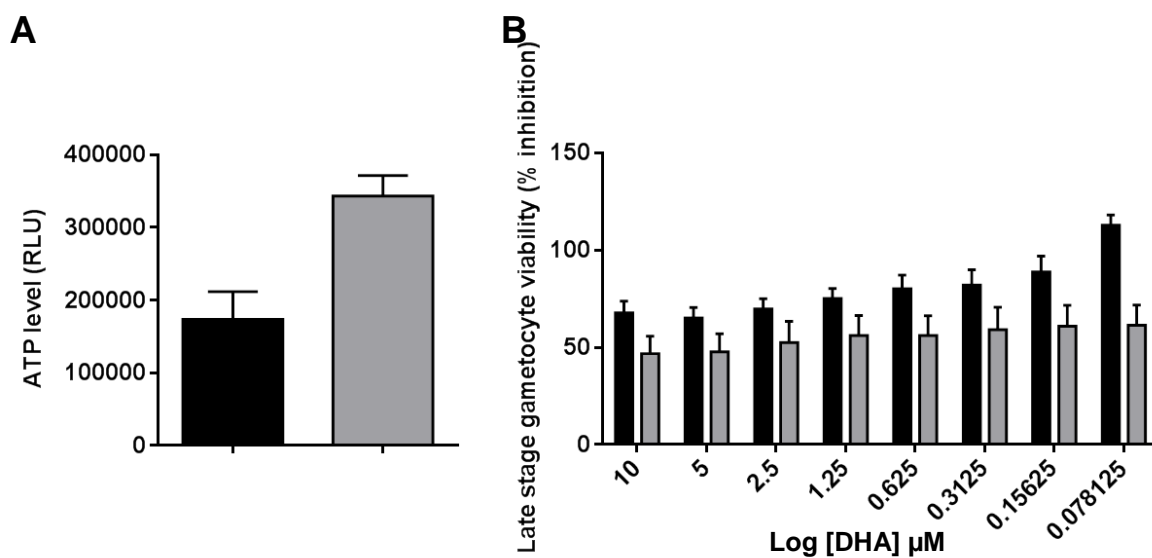


Figure 2.2: Influence of gentamicin on gametocyte viability and drug assays. (A) Gametocyte viability measured as a factor of ATP production in relative light units (RLU) in gametocytes grown either in the presence (black bars) or absence (grey bars) of gentamicin. (n=6, SEM indicated) **(B)** Dose-response curve for DHA on gametocytes in the presence and absence of gentamicin. Data are from n=2 independent biological experiments each performed in triplicate, \pm SEM. (Note: This work was contributed by Janette Reader as part of the published manuscript).

As previously reported, gametocytogenesis is strain dependent, and this held true for the tested strains, where the ability to produce gametocytes varied under the same optimised culture conditions [423, 463]. Of the *P. falciparum* strains tested, drug-sensitive NF54 parasites remained superior in producing gametocytes, with the chloroquine-resistant W2 strain, the chloroquine sensitive and sulphadoxine-resistant 3D7 strain, and the chloroquine- and antifolate-resistant 7G8 strain producing low levels of gametocytes. No detectable gametocytes were observed in the pyrimethamine resistant HB3 strain and the FCR3 strain (chloroquine and cycloguanil resistant (Table 2.2). Maximal gametocytogenesis (1.5% gametocytaemia, 11% conversion factor) could only be

achieved in freshly thawed 3D7 parasites, and this decreased as parasites were kept in routine culture for more than seven generations to 0.1% gametocytaemia (~4% conversion rate). For optimal gametocyte production on all strains, gametocytes were induced from freshly thawed asexual cultures within 2-3 generations after thawing but never from asexual parasites maintained for more than 6-9 generations.

2.3.2 Phenotyping, genotyping and characterisation of gametocyte production from contemporary African clinical isolates

Several intravenous blood samples were obtained from malaria patients reporting to Steve Biko Academic Hospital, Kalafong Hospital and Tshwane District Hospital during February to April 2014. A 100% success rate for *in vitro* culture adaptation was obtained for all the clinical samples. The robust gametocyte production protocol developed here was used to initiate gametocytogenesis from the clinical isolates. All of the isolates produced viable gametocytes (Table 2.3) at levels comparable to laboratory-adapted strains (Table 2.2). All of the isolates were genotyped using PCR and RFLP analysis (Table 2.3) and were found to harbour single SNPs in *pfcr*, *pfdhfr* and *pfdhps*, representing chloroquine, folate and sulfadoxine resistance respectively, except TD_01 that only harboured *pfcr* and *pfdhfr* mutations.

Table 2.3: Origin and drug resistance genotypes of southern African clinical isolates producing gametocytes.

Strain	Origin	Resistance phenotype	Resistance mechanism (genotype)	Gametocyte production (Y; %)
KF_01	Mozambique	Pyrimethamine	<i>pfdhfr</i> , <i>pfdhps</i> , <i>pfcr</i>	2.4 ± 0.3% (n=4)
TD_01	Mozambique	Pyrimethamine	<i>Pfdhfr</i> , <i>pfcr</i>	0.9 ± 0.1% (n=4)
SB_04	Malawi	Pyrimethamine, mefloquine	<i>pfdhfr</i> , <i>pfdhps</i> , <i>pfmdr1</i> (mixed)	1.4% (n=1)
SB_05	Mozambique	Pyrimethamine	<i>pfdhfr</i> , <i>pfdhps</i> , <i>pfcr</i>	1.1 ± 0.4% (n=4)
SB_07	Malawi	Pyrimethamine, methylene blue	<i>pfdhfr</i> , <i>pfdhps</i> , <i>pfcr</i>	0.5% (n=1)

The asexual stages were phenotyped for drug resistance using the SYBR[®] Green I fluorescence assay. All *ex vivo* clinical isolates exhibited artemisinin and DHA sensitivity in addition to sensitivity against the quinolones (Table 2.4). The only compounds presenting failure against specific isolates were mefloquine and methylene blue failing (IC₅₀>10-fold of reported values) against SB_04 and SB_07, both originating from Malawi.

Table 2.4: Phenotyping of a panel of 5 *P. falciparum* clinical isolates using a standard panel of antimalarial compounds. IC₅₀ values are representative of a single biological experiment, performed in triplicate.

Strain	Origin	ART	CQ	DHA	MQ	AQ	MB
SB_04	Malawi	1.4 nM	<1 nM	<1 nM	>250 nM	1.4 nM	<1 nM
SB_05	Mozambique	2.8 nM	2.9 nM	<1 nM	4.7 nM	2.2 nM	<1 nM
SB_07	Malawi	3.2 nM	2.6 nM	1.4 nM	6.5 nM	2 nM	>250 nM
TD_01	Mozambique	3.7 nM	2.1 nM	<1 nM	6.1 nM	2.2 nM	<1 nM
KF_01	Mozambique	3.5 nM	3.5 nM	1.1 nM	9.8 nM	3.1 nM	<1 nM
NF54	Netherlands	41.6 ± 12 nM	6.8 ± 0.1 nM	2.1 ± 0.6 nM	133 ± 41 nM	255 ± 65 nM	21.9 ± 0.1 nM

Relative *pfap2-g* (a transcriptional regulator of gametocytogenesis) transcript abundance in early schizonts correlated to final gametocytaemia and percentage commitment for all clinical isolates (Figure 2.3).

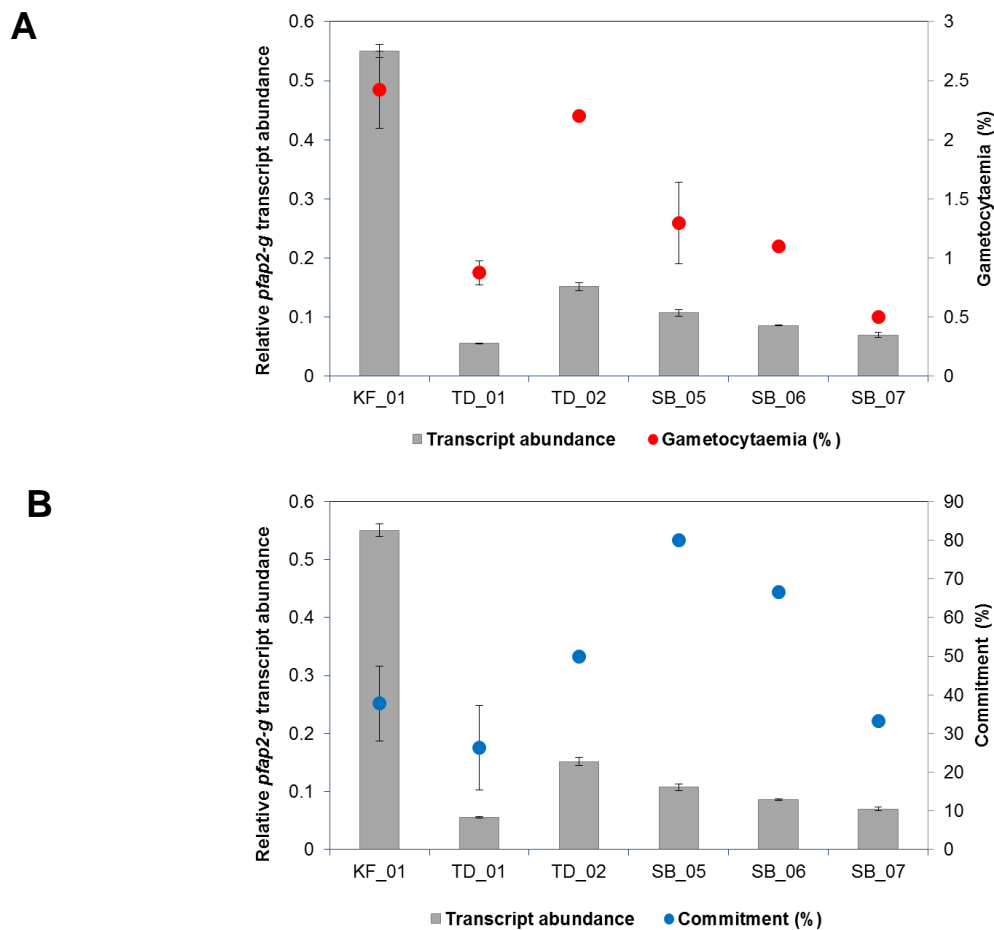


Figure 2.3: *Pfap2-g* transcript levels mirror gametocyte production. *Pfap2-g* relative transcript abundance in synchronised (early schizont stage) cultures as measured by qPCR of clinical isolates. Values are normalised against seryl transfer RNA synthetase (n=1, SD shown). **(A)** Gametocytaemia and **(B)** percentage commitment to gametocyte differentiation reflect relative *pfap2-g* transcript levels (n≥2, SEM shown). %Commitment = (number of stage 2 gametocytes on day 4)/ number of rings on day 2.

2.3.3 Validation of stage-specific gametocyte production

The production of gametocytes, synchronised to a small stage-specific window, is important in gametocytocidal drug discovery efforts, as evidence indicates differential susceptibility of gametocytes in different stages of development towards a variety of compounds [264, 438, 439]. Stage-specific gametocyte production was ensured through the use of synchronised (>80% rings) starting populations of asexual parasites and the application of NAG pressure at defined time points during gametocytogenesis. Developmental stages of gametocytes were evaluated morphologically based on the description of Hawking 1971 (Figure 2.4A) [48]. Synchronicity was quantified to >90% late stage IV/V gametocytes with <10% contaminating early stage (II and III) gametocytes (Figure 2.4B).

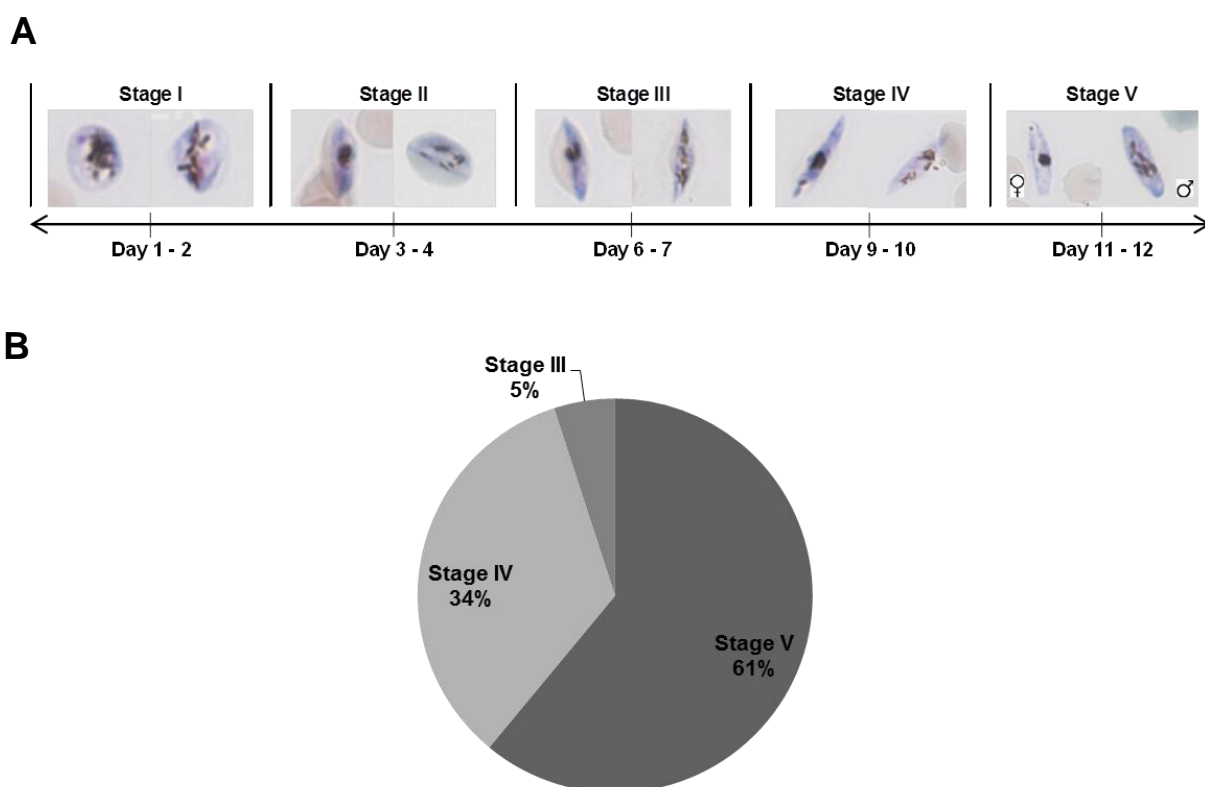


Figure 2.4: Stage-specific, quantitative analysis of gametocyte populations. (A) Giemsa stained smears, obtained at 1000x magnification, indicate the morphology of different stages. (B) Stage distribution of gametocyte populations; $n \geq 6$ independent gametocyte cultures on day 10.

The viability and functionality of the gametocyte populations were confirmed by real-time microscopic observation of male gamete exflagellation induced by XA and a decrease in temperature (Figure 2.5A). Moreover, the mature gametocyte populations produced, mimicked the *in vivo* female bias [33] with a 4:1 ratio of female: male gametocytes, as evaluated morphologically. Flow cytometry was used as an explorative technology to

differentiate and quantify gametocyte populations. Asexual parasites were easily distinguishable from gametocytes, and various gametocyte populations (stages) could be identified based on their morphological and density differences (Figure 2.5B). Subsequent gating of various populations within the enriched gametocyte sample allowed cellular sorting of between 100 000 and 5 000 000 cells. Samples were analysed microscopically to confirm the identity of the suggested populations and discriminate between asexual and gametocyte populations. Additionally, to distinguish the mature male and female gametocytes, ~500 000 cells were treated with XA to induce gametogenesis. This produced two separate gamete populations, and in this manner, clear gamete populations were distinguishable (Figure 2.5B). Although informative from a qualitative point of view regarding quality control for gametocyte production, the flow cytometric method is however not amenable to continuous application in a screening programme.

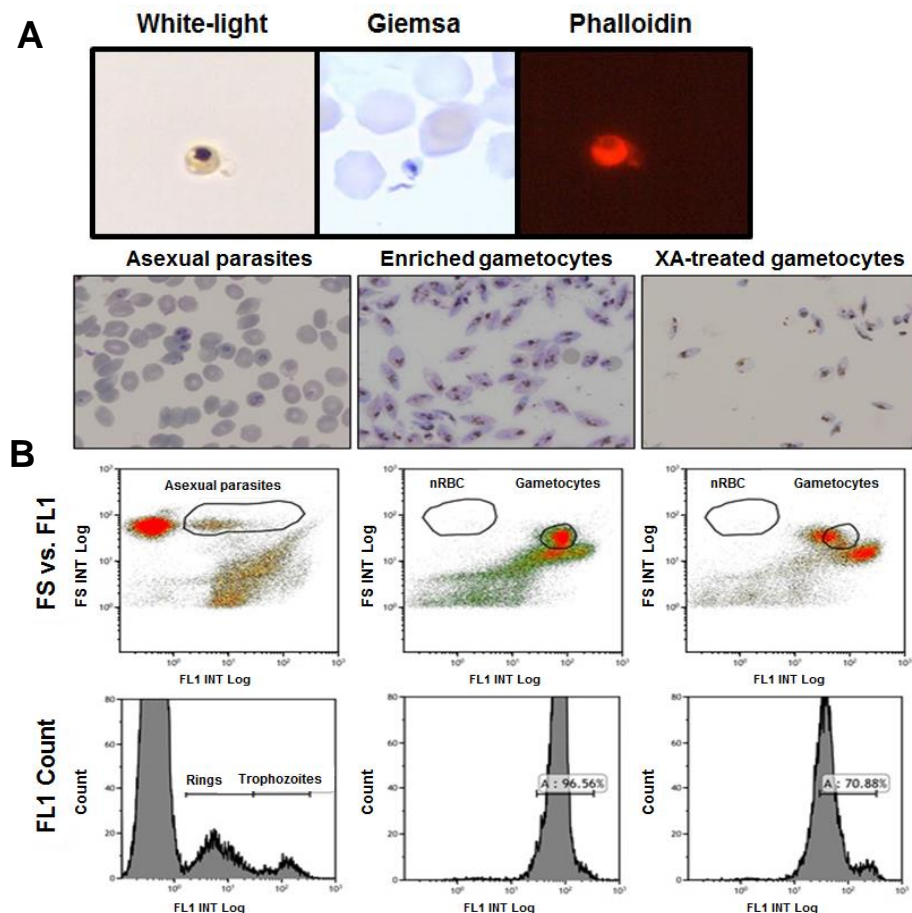


Figure 2.5: Functional validation of gametocyte viability. (A) Male exflagellation. White-light, Giemsa and Phalloidin stained real-time imaging of an exflagellating microgamete. Visualised at 200x magnification. **(B)** Flow cytometric evaluation of asexual parasites and gametocytes by thiazole orange nuclear marker analysis. Gametocytes were purified on magnetic columns and treated with xanthurenic acid (XA) to induce exflagellation of male gametes. (Note: This work was contributed by Dewaldt Engelbrecht as part of the published manuscript).

2.3.4 Assays for gametocytocidal activity

Four different gametocytocidal screening assays were evaluated and compared on late stage IV-V gametocytes. The assays were chosen based on their ability to detect different biological activities as indicators of parasite viability. The bioluminescent ATP assay reflects energy status; pLDH is an indicator of active glycolysis; the colourimetric resazurin dye is a redox indicator, and the luciferase reporter assays (under control of gametocytogenesis-specific promoters for *Pfs16* and *mal8p1.16*) determine stage-specific action of gametocytocidal compounds. Assay performance was evaluated for linearity, detection range, reproducibility, the assay screening window coefficient (Z' -factor) [461] and inter-assay reproducibility via %CV [462] (Table 2.5). Moreover, drug incubation time (24 or 48 hours), optimal haematocrit and optimal gametocytaemia were determined for each assay platform.

Table 2.5: Performance indicators of the four assay platforms. Each assay was performed after 48 hour drug exposure, and comparative quality control parameters determined, using standardisation of DHA activity as a common factor between all the assay platforms. Methylene blue interfered with the PrestoBlue® assay and was not used as a control. For each assay platform, data are from 4 independent biological experiments, performed in triplicate.

Assay performance parameters (average)	ATP (n=4)	pLDH (n=4)	PrestoBlue® (n=4)	Luciferase reporter (n=4)
S/N	>15 000	>300	>900	16 000 (early stage gametocytes; <i>Pfs16</i>) 500 (late stage gametocytes; <i>mal8p1.16</i>)
S/B	500	3.2	15	175
Z' -factor	0.79	0.87	0.91	0.81
%CV (intra-assay)	8.8%	2.4%	3.15%	0.73%
Average DHA activity at 1 μ M (% inhibition)	37.19 \pm 7.67%	62 \pm 6%	83.48 \pm 8.58%	73.56 \pm 5.58% (average early/late stages)
IC ₅₀ DHA	14.9 μ M ^a	20 nM	11 nM	43 nM (early stages) 11 nM (late stages)
IC ₅₀ MB	900 nM ^a	800 nM		195 nM (early stages) 143 nM (late stages)

DHA: dihydroartemisinin

MB: methylene blue

^aunpaired experiments; 24 h incubation

2.3.5 ATP assay as an indicator of parasite viability

The bioluminescent ATP assay measured luciferin-luciferase as an indicator of parasite viability, directly correlating ATP levels to luminescence output. Because ATP is present in erythrocytes, the assay requires almost 100% pure gametocytes that are free of contaminating, uninfected erythrocytes. The assay proved to be linear over the range of 4 000-62 000 purified gametocytes ($R^2 = 0.99$). S/N and S/B were high at >15 000 fold and >500 fold, respectively (Figure 2.6). The assay was routinely performed on 30 000 gametocytes and 24 hour drug treatment. Late stage IV-V gametocytes were successfully

enriched to >95% purity with yields of $\sim 677\,500 \pm 83\,815$ gametocytes/ml original culture volume (n=4). The assay incubation time was monitored, with a dramatic decrease in ATP levels observed directly after enrichment, which then stabilised around 16-24 hours. However, an average decrease of $\sim 50\%$ was seen in ATP levels of untreated parasites between 24 and 48 hours, with linearity decreasing from $R^2 = 0.99$ at 24 hours to 0.85 at 48 hours. The assay produced good intra-assay variability with average Z'-factors of 0.84 and 0.79 at 24 and 48 hours, respectively. However, a relatively high average %CV of 8.8% was observed (Table 2.5).

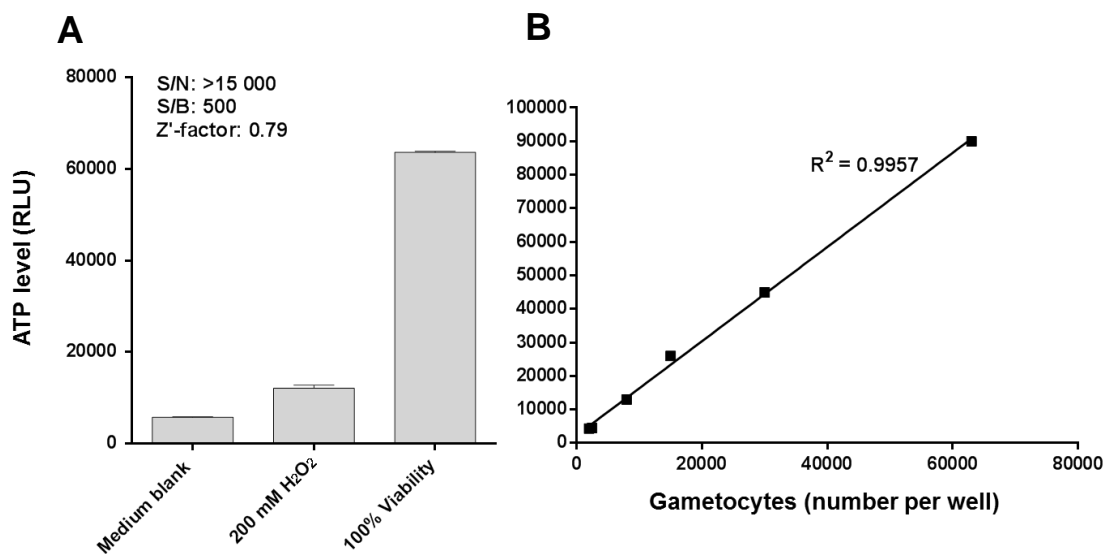


Figure 2.6: ATP assay evaluation . The ATP readout was obtained after 24 hour incubation of enriched late (stage IV/V) gametocytes. **(A)** Signal to noise (S/N) and signal to background (S/B) values for the ATP luminescence readout. Data are from three independent biological experiments, each performed in technical triplicates \pm SEM. **(B)** The linearity of ATP luminescence readout compared to the number of isolated gametocytes. Data are from a single biological experiment performed in technical triplicates.

2.3.6 pLDH assay as an indicator of metabolic activity in viable parasites

The pLDH assay relies on the rapid use of APAD (an NAD⁺ analogue) as a coenzyme by *P. falciparum* lactate dehydrogenase, a reliable auxiliary for gametocyte viability [426, 427, 449], in the reaction leading to the conversion of lactate to pyruvate [460, 464]. The pLDH assay revealed acceptable linearity profiles of $R^2=0.95$ and 0.96 achieved at 0.5% and 1% haematocrit, respectively (Figure 2.7). At 24 hours, the Z'- factor, S/N and S/B ratios were markedly less than after 48 hours of incubation (S/N of 28 vs 300 at 24 vs 48 hours, respectively, Table 2.5). Z'-factor values decreased with decreasing gametocytaemia and haematocrit with the optimal gametocytaemia and haematocrit for the pLDH assay determined as 4.5% gametocytaemia and 0.5% haematocrit, based on a Z'-factor of 0.90.

However, due to the typical gametocytaemia produced without enrichment, the assay was optimised to 2% gametocytaemia and 1% haematocrit with an acceptable Z'-factor of 0.87 still attained at 2.3% gametocytaemia and 0.5% haematocrit. Average %CV was 2.4% between independent experiments for the control compounds (Table 2.5).

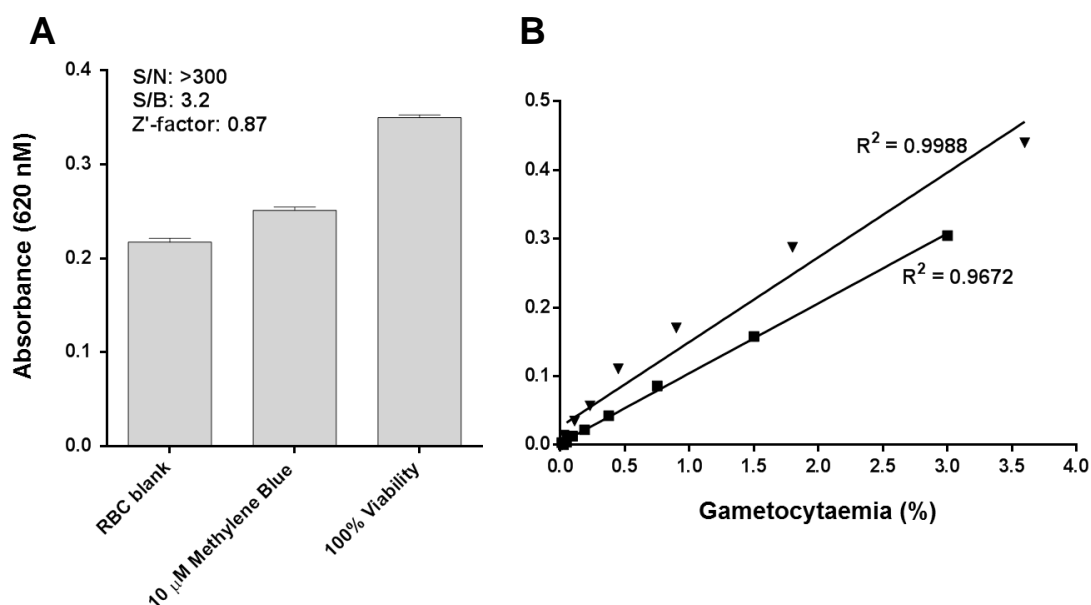


Figure 2.7: pLDH assay evaluation. The pLDH readout was obtained after 48 hour exposure of late (stage IV/V) gametocytes (2% gametocytaemia and 1% haematocrit) to 10 μ M methylene blue. **(A)** Signal to noise (S/N) and signal to background (S/B) values for the pLDH readout. Data are from three independent biological experiments, each performed in technical triplicates \pm SEM. **(B)** The linearity of absorbance (620 nm) readout compared to gametocytaemia, at 0.5% haematocrit (triangles) and 1.0% haematocrit (squares). Data are from a single biological experiment performed in technical triplicates.

2.3.7 PrestoBlue[®] assay as an indicator of parasite respiration

PrestoBlue[®] is a colourimetric reagent whose spectral features reflect the metabolic activity of cells. It is based on resazurin, a cell-permeant blue dye, which functions as a cell viability indicator when reduced to resorufin (red) by the metabolic activity of living cells. Resazurin reduction correlates almost entirely with cellular respiration. Resorufin is around 12 times more fluorescent than resazurin and has an emission maximum of 584 nm [465, 466]. The colourimetric assay displayed a good linearity profile in the absence or presence of the drugs tested ($R^2 = 0.97$) using a 2% gametocytaemia and 5% haematocrit (Figure 2.8). Upper and lower detection limits were estimated to be 97% and 21%, respectively, and the average %CV between independent experiments was estimated to be 3.15%. On average, the Z'-factor was estimated to be 0.91 (Table 2.5). Modifying the final gametocytaemia (using 0.5%, 1%, or 3%), or by decreasing the drug incubation duration (24 hours instead of 48 hours) led to a general reduction in assay performance as determined by the Z'-factor.

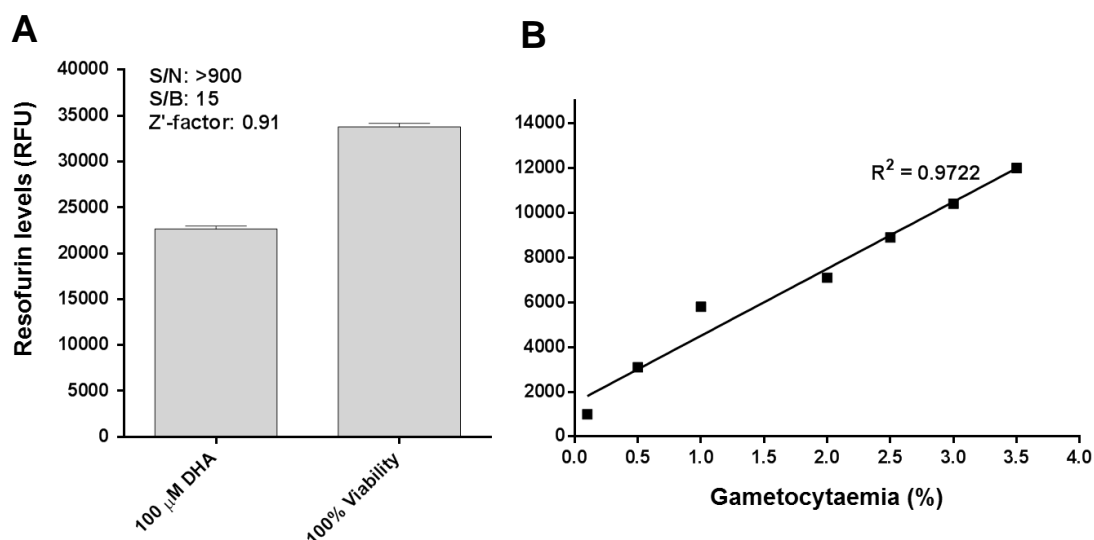


Figure 2.8: PrestoBlue® assay evaluation. The PrestoBlue® readout was obtained after 48 hour exposure of late (stage IV/V) gametocytes (2% gametocytaemia and 5% haematocrit) to 100 μM DHA. Data are from three independent biological experiments, each performed in technical triplicate ± SEM. **(A)** Signal to noise (S/N) and signal to background (S/B) values for the fluorescence readout. **(B)** The linearity of fluorescence readout compared to gametocytaemia. Data are from a single biological experiment performed in technical triplicates.

2.3.8 Luciferase reporter assay as an indicator of stage-specific gametocyte gene expression

Two transgenic parasite lines were employed in the luciferase assays *viz.* NF54-PfS16-GFP-Luc and NF54-Mal8p1.16-GFP-Luc [438], expressing a GFP-luciferase fusion reporter gene under the control of two gametocytogenesis-specific genes. *Pfs16* reporter expression in NF54_{Pfs16} peaks on day 2 of gametocytogenesis and then gradually declines [119]. *Mal8p1.16* reporter expression in NF54_{mal8p1.16} is specific for late stage gametocytes, increasing only at day 6-8 and peaking at day 10-12 after gametocytogenesis [438]. These lines accurately and reproducibly allowed detection and quantification of early gametocytes (stage II/III) from late gametocytes (stage IV/V) [438]. Luciferase activity was determined for a stage II/III culture (day 5; 89% stage II/III; 11% stage I; n=6) as well as late stage IV/V gametocytes (day 11; 91% stage IV/V; 9% stage III; n=6). This assay exhibited good intra-assay reproducibility (Z'-factor of 0.77 and 0.83 on average for early and late stage gametocyte markers, average of 0.81) as well as high sensitivity (S/N >500 or >16 000 for the late and early marker assays, respectively) and a %CV of 0.73% (Figure 2.9 and Table 2.5).

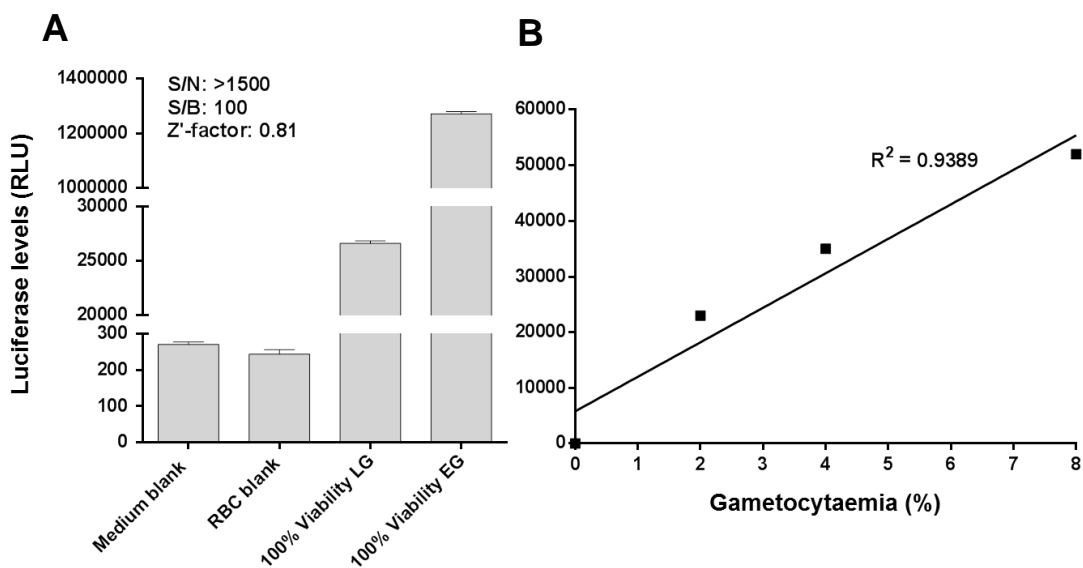


Figure 2.9: Luciferase reporter assay evaluation for early stage (EG) and late stage (LG) gametocytes. The luminescence readout was obtained using early (EG; stage II/III) and late (LG; stage IV/V) gametocytes (2% gametocytaemia and 1.5% haematocrit). Data are from three independent biological experiments, each performed in technical triplicate \pm SEM. **(A)** Signal to noise and signal to background values for the luminescence readout. **(B)** The linearity of luminescence readout compared to gametocytaemia. Representative linearity is based on the readout achieved for late stage gametocytes. Data are from a single biological experiment performed in technical triplicates.

2.3.9 Assay comparisons for gametocytocidal screens

The different assay platforms were also evaluated and compared for their ability to accurately determine the IC_{50} of known gametocytocidal compounds DHA and methylene blue. Late stage gametocytocidal potency of DHA has been reported to be in the range of 2-26 nM whereas methylene blue potency is poorer, ranging between 12 and 490 nM [255, 439]. The pLDH, luciferase reporter and PrestoBlue[®] assays all reported comparably low nM activities for DHA whereas the luciferase reporter assay seemed more sensitive to determine methylene blue IC_{50} compared to the pLDH and ATP assays (Table 2.5).

Taking assay platform differences into account, and relying on good intra-assay variability for each assay, the ATP, pLDH, luciferase reporter and PrestoBlue[®] assays were compared in the context of a 10-compound set provided by the MMV (Figure 2.10). A single population of late stage IV/V gametocytes were produced from *P. falciparum* (NF54) and split such that all the assays were performed in parallel on the same gametocytes. The only differences were that a proportion of these gametocytes were enriched to enable the ATP assay. Additionally, gametocytes were produced in parallel from the luciferase reporter lines. The remaining parameters for each assay were all comparable: in each instance, single point assays were performed at 1 μ M drug for 48 hours of continuous drug

pressure for at least three replicates. Reproducibility was maintained with Z'- factors ≥ 0.8 . The assays were performed on late stage gametocytes (>95% stage IV/V) in all instances, except for the luciferase reporter assay that was also performed on early stage gametocytes (>90% stage II/III). To enable comparisons, significant inhibition of gametocyte viability is defined as >70% and >50% inhibition at 5 and 1 μM , respectively, whereas no activity is defined as <50% inhibition at both screening concentrations. Inhibition of 50-70% at 1 or 5 μM is seen as moderate.

Although direct comparison of absolute inhibition values is difficult between assay platforms, similar trends were observed (Figure 2.10) including comparable performance of the luciferase marker assay and the PrestoBlue[®] assay for compounds such as DHA and methylene blue. At the concentration tested (1 μM), these compounds resulted in >70% inhibition of parasite viability. The ATP and pLDH assays consistently did not detect the same level of inhibition of parasite viability for the endoperoxides (artemether and DHA, <50% inhibition) compared to the other assay platforms, however, the luciferase and PrestoBlue[®] assays detected >50% inhibition on these compounds. Interestingly, only the luciferase reporter assay detected any activity for OZ439 (>70% inhibition) whereas all the other assays defined this compound as inactive (<50% inhibition). The ATP assay could not detect any inhibitory activity for the 4-aminoquinolines, chloroquine and halofantrine, and may, therefore, be more sensitive to indicating the known inability of these compounds to inhibit gametocytes. The signal obtained for these compounds in the PrestoBlue[®] assay may therefore instead reflect the inability of this assay in discriminating the activity of compounds against earlier stages of gametocytes, whereas the ATP assay (working on an enriched late stage gametocyte population) more accurately reflects these compounds' activity. The PrestoBlue[®] and pLDH assays seem to provide what may be falsely enhanced activity for compounds such as tafenoquine and lumefantrine, respectively. However, the PrestoBlue[®] assay did not correlate to the other assays for atovaquone, reporting poor activity of this compound.

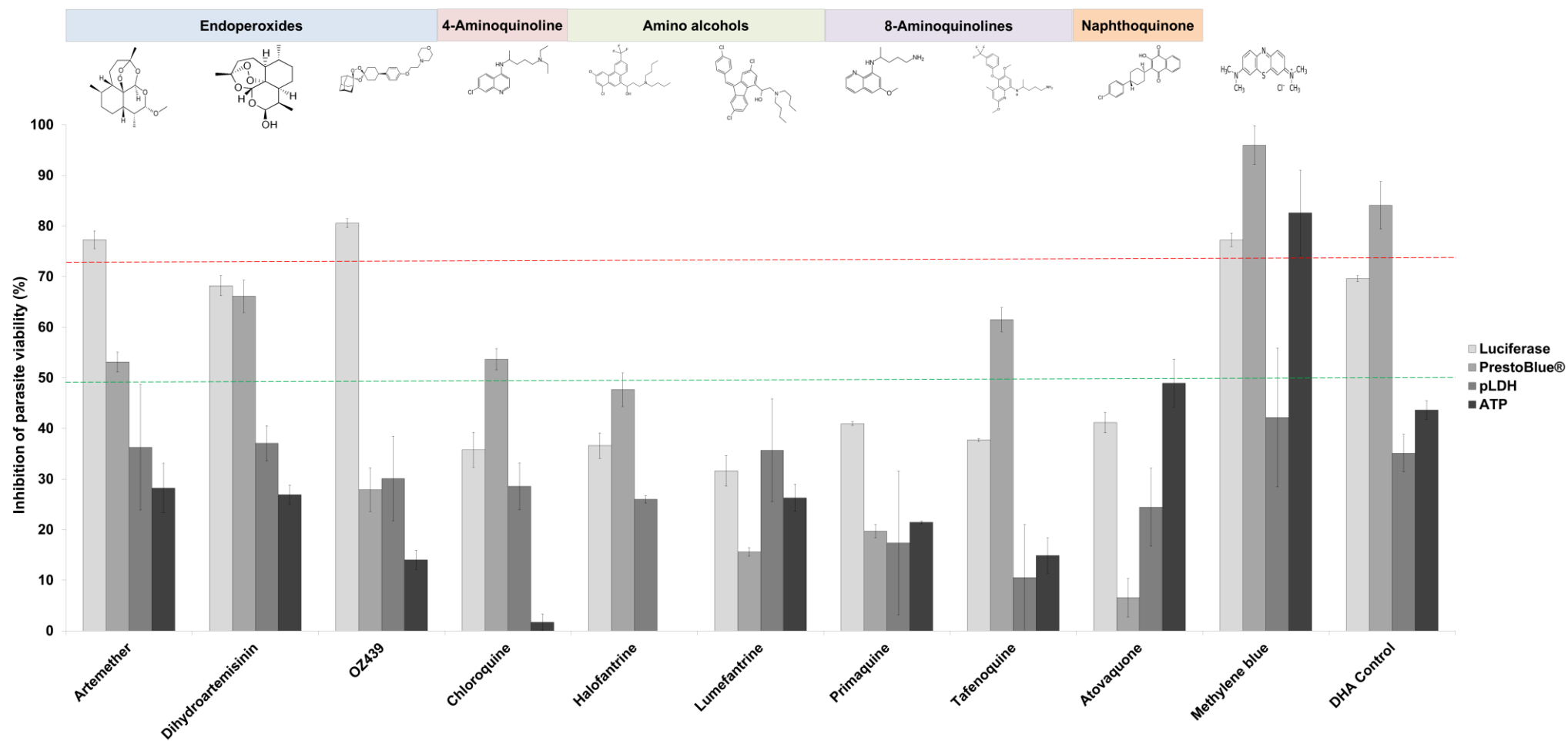


Figure 2.10: Comparative analysis of the performance of four assay platforms for gametocytocidal compounds. Late stage IV/V gametocytes were assayed after 48 hours (ATP assay, 24 hours) continuous exposure to 1 μ M drug in the four different assay platforms indicated based on the optimal conditions for each platform. The ATP data for halofantrine approximated zero. Data are from at least three independent biological experiments, each performed in technical triplicate \pm SEM.

Data from the early and late stage luciferase reporter assays indicated that these compounds were indeed not highly active against late stage gametocytes (30-50% inhibition at 1 μ M) (Figure 2.11).

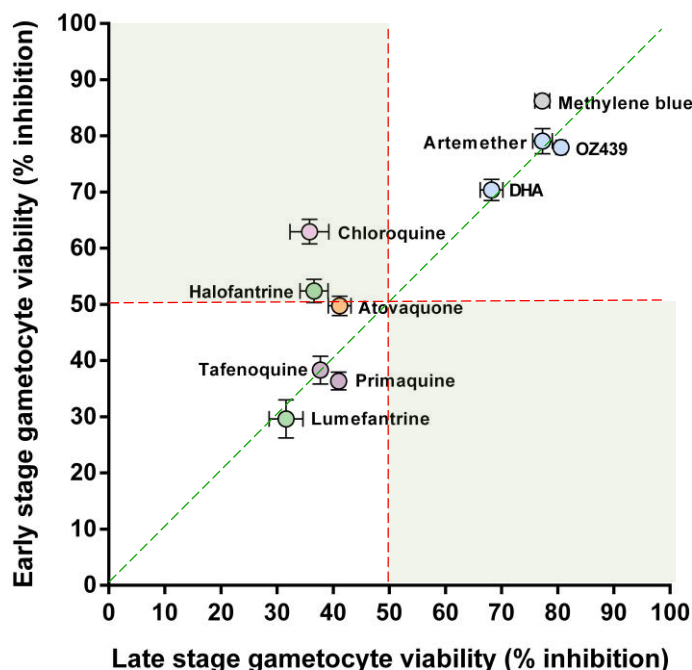


Figure 2.11: Dual activity of the 10-compound set (MMV) toward *P. falciparum* early and late gametocyte stages. Early (>90% II/III; y-axis) and late stage (>95% IV/V; x-axis) gametocytes were assayed after 48 hour continuous exposure to drug (1 μ M) using the luciferase reporter assay. Compound classes are coloured according to the scheme provided in figure 2.10. Dual active compounds are situated on the trend line (dotted, green).

The MMV 10-compound set was further profiled for cross-resistance using a panel of clinical isolates. A single population of late stage IV/V gametocytes were produced from each isolate and phenotyped using the pLDH assay (Figure 2.12). Methylene blue performed best against all clinical isolates. Some clinical isolates seemed highly sensitive to all compounds tested (e.g. SB_07, Malawi) whereas other isolates, particularly TD_01 and TD_02 (Mozambique) were poorly inhibited. No indication of cross-resistance was observed when taking both the genotypic and phenotypic diversity of these isolates into account.

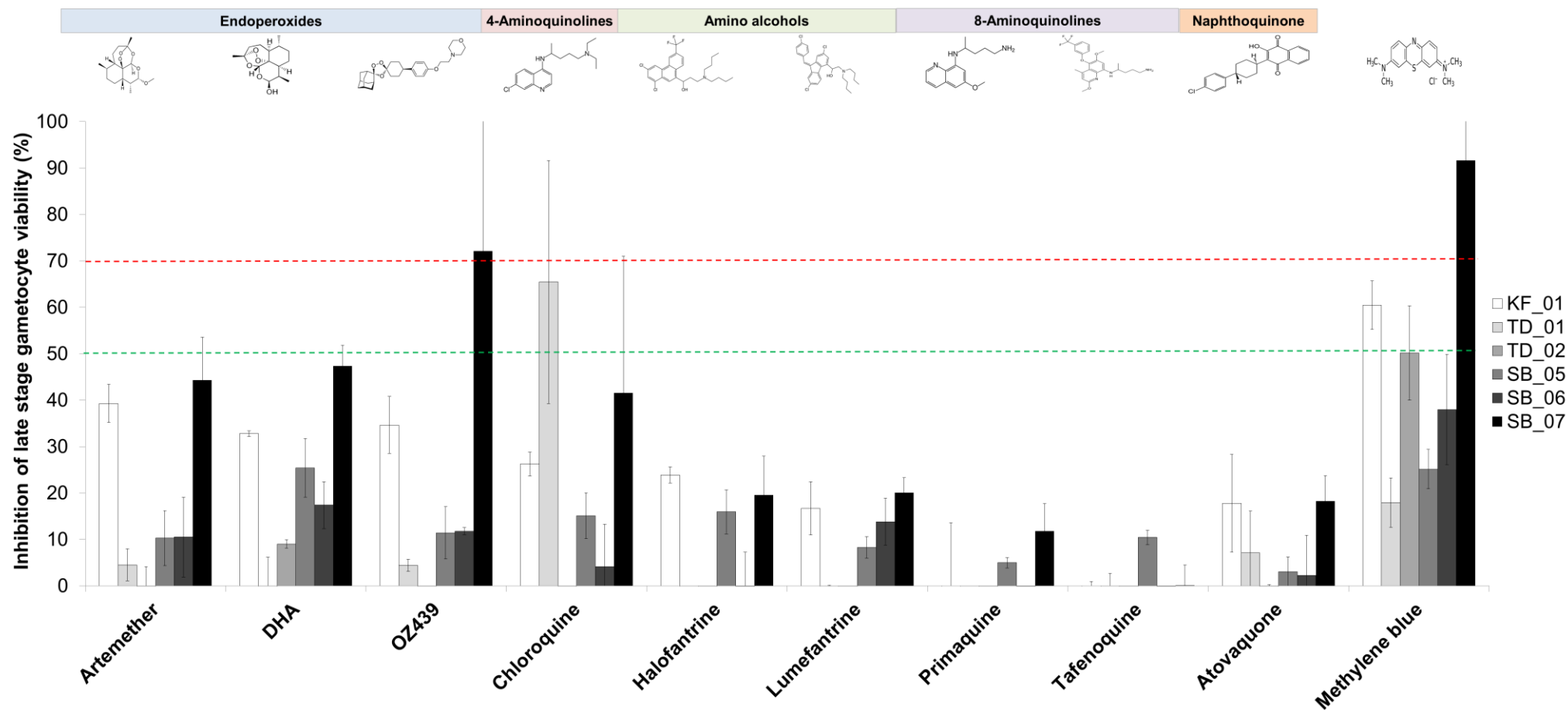


Figure 2.12: Gametocytocidal activity of MMV 10-compound set against *ex vivo* clinical isolates of *P. falciparum*. Clinical isolates were adapted to limited *ex vivo* culturing and gametocytes produced from each isolate. The pLDH assay was performed for each compound (1 μ M) for a 48 hour incubation against late stage (IV/V) gametocytes. Data are representative of a single biological experiment, performed in triplicate \pm S.D., average Z'-factor = 0.71.

2.4 Discussion

Sustainable malaria control dictates the integration of therapeutic strategies targeting the pathogenic asexual forms with the transmissible sexual gametocyte forms of malaria parasites. Drug discovery is a long, arduous and expensive process, and to avoid duplication in screening libraries for gametocytocidal compounds, especially in the face of limited resources, it would be useful to compare assay results generated in different laboratories. Currently there are often discrepancies in the data, which hampers progress in this field. Two significant challenges in this regard are the lack of standardisation in culturing reproducible batches of pure, stage-specific gametocytes in high yield and assays for the metabolically hypoactive gametocytes.

Gametocytogenesis is mimicked *in vitro* under very diverse conditions, which makes standardisation difficult and also reflects our lack of knowledge of the *in vivo* biological process by which *P. falciparum* parasites generate gametocytes. One of the major problems with current gametocyte production protocols is that they are frequently not reproducible and are not robust when applied in different settings. Furthermore, the inherent biological variability in different parasite populations in culture introduces additional challenges. In this study, a protocol was optimised which consistently generated high-quality gametocytes in three different laboratories, confirming the robustness of the method. These gametocytes were used to evaluate and directly compare different screening assays using a set of 10 drugs supplied by the MMV. Furthermore, this method could be applied to contemporary African *ex vivo* clinical candidates without any changes to the protocol and allowed phenotypic evaluation using the MMV 10-compound set and pLDH assay.

The optimised method exploited the inherent biological conversion of asexual parasites to gametocytes, confirming that not all asexual parasites will convert to gametocytes even under optimal conditions. Recently, gametocyte conversion has been shown to be under the control of a transcriptional regulator (*PfAP2-G*) that is activated in a stochastic manner, leading to a typically low frequency (~1-10%) of gametocyte conversion [49, 97]. The high conversion of approximately 33% obtained in the current study, therefore, points to the direct response of the parasites to external stressors to obtain at least a doubling in gametocyte conversion in the *in vitro* system. Indeed, evaluation of the *pfap2-g* transcript abundance, gametocytaemia and percentage commitment achieved from *ex vivo* clinical isolates reflected this relationship and crucial role of *PfAP2-G*. The increased production

of gametocytes did not change the gender ratio of approximately 4:1 females: males as has been observed *in vivo* [33, 80]. For gametocytes produced *in vitro* to be used to evaluate the gametocytocidal activity of compound libraries, it is important to monitor the quality of the parasites prior to performing the assay, including assessment of gametocyte viability and functionality (e.g. ability to form male gametes); purity (absence of asexual parasites) and stage specificity (>90% of stage IV/V in this study).

Endeavours to find transmission-blocking antimalarials are currently hindered by a lack of understanding of the basic biological processes governing gametocytogenesis in the human host, which makes an informed choice of an assay system problematic. Gametocytes are suggested to be terminally differentiated and metabolically less active [118]. There is no replication of the gametocyte genome during development and gametocytes arrest in phase G_0 of the cell cycle [42]. After the first ~48 hours of development, nucleic acid synthetic activity is likely restricted to RNA synthesis, and genetic evidence shows that gametocytes are haploid. Synthesis of RNA is reported to stop after day 6 of development, and there is no haemoglobin digestion and protein synthesis in mature gametocytes [40, 467]. Any assay for gametocytocidal activity therefore currently relies on measuring changes in metabolic status or stress responses in gametocytes, performed against the background of a metabolically quiescent cell.

Several groups have published platforms allowing the evaluation of gametocytocidal activity of a compound series. Other groups have recently attempted to compare gametocyte assay platforms from various laboratories using different assay readouts [426, 448]. However, a direct comparison of the data from these studies is fraught with difficulty due to differences in parameters such as (i) parasite strains used; (ii) different gametocyte induction protocols; (iii) composition of culture medium used; (iv) gametocyte isolation protocols; (v) stage of development of gametocytes; (vi) assay platforms; (vii) presence or absence of erythrocytes; (viii) number of gametocytes per assay well; (ix) panel of compounds; (x) concentration of compounds; (xi) drug exposure times; (xii) presentation of data, e.g. % inhibition at single concentrations or only IC_{50} values, etc.

The production of viable and functional gametocytes using a standardised, robust gametocyte production protocol was used here to overcome the limitations listed above. These gametocytes were subsequently used, for the first time, in a parallel, comparative interrogation of four different gametocytocidal assays (ATP, pLDH, PrestoBlue[®] and the

luciferase reporter) for their ability to detect the gametocytocidal activity of a single set of 10 compounds from the MMV. The compound set was provided blinded and only unblinded after completion of all the assays and data analysis. The parallel nature of the assays performed on the same gametocyte population uniquely allowed direct comparisons of the assay platforms in this study.

The TCA cycle is highly active in gametocytes, especially in females that are characterised by a rapidly expanding mitochondrion in preparation for gametogenesis [113, 468]. A recent study found 15 of 16 mRNA transcripts of the mitochondrial TCA cycle enzymes upregulated in gametocytes [115]. Increased TCA cycle activity implies increased levels of cytoplasmic ATP. In the luminescent ATP assay, ATP content reflects the functional integrity of living cells, as injured/dead cells will display drastically reduced ATP levels [469]. This platform should, therefore, be reliable for the assessment of compounds for their ability to inhibit gametocytes. However, the assay requires the downstream manipulation of gametocytes (enrichment and isolation), which compromises gametocyte viability. ATP levels decrease by as much as 50% within the first 16 hours after enrichment, and this level steadily decreases as gametocytes incubate further after enrichment, to a total level of only 20% remaining at 48 hours, which is the usual timeframe for assaying drug effects. This influences the number of viable gametocytes remaining in the population used to detect drug effects. Moreover, although this manipulation results in high S/N ratios due to gametocytes enriched above background, it could contribute to higher inter-assay variability. However, the ATP assay is possibly less prone to artefacts compared to fluorescent viability assays [470].

One key advantage of the pLDH assay is that it is performed directly on parasite cultures, therefore minimising manipulation of gametocytes. pLDH has been shown to be present in the blood of malaria patients and to be a reliable marker for gametocyte viability as the enzyme is present at high levels throughout gametocytogenesis [471, 472]. pLDH catalyses the conversion of pyruvate, the final product of glycolysis, to lactate. This flux is vital for the regeneration of NAD^+ , itself an essential cofactor for glycolysis. Only when increased fermentative glycolysis is possible, do cells exhibit increased proliferation through the anabolic capacity of glycolysis [150]. However, late stage gametocytes exhibit decreased expression of genes responsible for glycolysis, protein biosynthesis and haemoglobin catabolism [115]. As mentioned, terminally differentiated gametocytes make use of a canonical TCA cycle, and less glucose is metabolised by fermentation to lactate.

Reduced glycolytic activity suggests that less pyruvate is converted to lactate by pLDH, which might explain the relatively low S/B values obtained for the pLDH assay. A direct comparison of the pLDH activity in asexual parasites, early and late stage gametocytes will be valuable in confirmation of assay reliability. Additionally, the continued presence of pLDH activity even after parasite death has to be taken into account [427].

Redox reactive (oxidoreductive indicators) cell permeable dyes like alamarBlue[®], and PrestoBlue[®] have previously been reported as robust assays amenable to high-throughput screens, more sensitive than traditionally used tetrazolium dyes [435, 446]. These assays enable ease of use when screening gametocyte populations due to the direct addition of reagent to the parasite suspension after incubation. However, care must be taken with these assay platforms in the case where compounds target the redox state of the parasite, as it may interfere with the assay readout. Moreover, compounds routinely used as controls (e.g. methylene blue) cannot be used in this assay platform due to colourimetric interference.

Despite the drawbacks of each assay, the ATP, pLDH and PrestoBlue[®] assays are useful for assaying the gametocytocidal activity of compounds on non-genetically modified laboratory strains as well as clinical isolates. This information will become increasingly important in drug development programmes, enabling early detection of cross-resistance or efficacy failure of lead gametocytocidal compounds. Assay cascades may also be influenced from an economic point of view, with the PrestoBlue[®] the least expensive (~\$1 per compound) followed by the pLDH and lastly the ATP luminescence and luciferase assays (up to a 7-fold increase in cost). The luciferase assay platform was robust in all cases resulting in high S/N ratios and in the quantification of the internal signal. This platform has recently been further optimised to a dual-colour assay (green and red luciferases) to simultaneously and quantitatively assay the viability of different stages of gametocyte populations [445]. Also, the blinded nature of the study and the fact that the assays were performed in parallel, allowed for a situation where assay platforms could be compared directly. The data were validated since the DHA control included in the study correlated very well for all assay platforms with the blinded DHA control included in the 10-compound panel.

As reported [439, 464], the endoperoxides were able to target both the early and late stage gametocytes equally and were the most active compounds tested with IC₅₀s in the nM

range in some assay platforms. The equipotency of the endoperoxides to early and late stage gametocytes was confirmed here mainly with the luciferase reporter assay (for artemether, DHA and OZ439). These data are also comparable to the late stage gametocytocidal activity of endoperoxides (artemether and DHA) [427]. The endoperoxides are amongst the most potent antimalarials, fast acting and thought to act through alkylation of haem or other biomolecules [473] and require iron-mediated activation of the endoperoxide bridge. The ability of artemisinin, particularly to oxidise cofactors of parasite flavoenzymes, contributes to generating cytotoxic metabolites and reactive oxygen species, resulting in oxidative damage to cells [474, 475]. The PrestoBlue[®] assay was able to detect comparable levels of activity to the luciferase reporter assay particularly for DHA, indicating that the oxidoreductive dye can measure drug response in the context of oxidative cellular stress, at least for the compounds tested here. It has however been postulated that another target for the endoperoxides may be direct interaction with *Pf*ATP6, interfering with ATP synthesis [475]. As mature gametocytes do not metabolise haemoglobin effectively, the latter may indeed be the physiological mode of action of these compounds in the sexual parasites.

Interestingly, the ATP assay indicated poor activity of the endoperoxides compared to the luciferase and PrestoBlue[®] assays, previously reported as a good indicator [425, 436]. Within the endoperoxide group, OZ439 was shown to have potent gametocytocidal activity with the luciferase reporter assay in the low nM range, however, none of the other assay platforms was able to detect this activity. This confirmation of the ability of the endoperoxides to target both immature and mature gametocytes sheds light on ACTs as transmission-blocking drugs, an effect that should not solely be ascribed to the extremely rapid clearance of asexual parasites and young gametocytes. Surprisingly, the endoperoxides seem to target male gametocytes preventing male gamete formation exclusively; the exact reason for this is unclear [116]. The ATP assay has been reported to be a poor indicator of the gametocytocidal activity of endoperoxides [425, 436] and this was confirmed here with IC₅₀s of 15 µM obtained for DHA compared to nanomolar IC₅₀s seen with the pLDH, PrestoBlue[®] and luciferase assays. Alternatively, gametocytes may stay viable in the presence of endoperoxides or at least maintain their ATP pool and pLDH activities while some gene promoters are not as active, explaining the difference between reporter gene and metabolic readouts.

The 4-aminoquinoline, chloroquine, was confirmed to be more active against asexual parasites and early stage gametocytes, confirming their targeting of haemozoin formation in these stages of the parasite. While the PrestoBlue[®] and pLDH assays did seem to indicate some activity against late stage parasites; the ATP assay is possibly more informative for this chemotype. Comparatively, the 8 aminoquinolines tested here (primaquine and tafenoquine) performed poorly against both early and late stage gametocytes. However, for these compounds, the ATP assay was able to detect low inhibitory activities, implying differences in the mode of action between the 4- and 8-aminoquinolines on mature gametocytes or interference of the compounds tested (primaquine and tafenoquine) with the assay platform.

The 8-aminoquinolines are known to be metabolically activated by liver enzymes, hence eliciting activity against liver stage hypnozoite forms of malaria parasites [476]. However, in the assay systems employed here, such metabolic activation is not possible but could be resolved by pre-exposure of the drugs to liver cell extracts before analysing their gametocytocidal activity. Such metabolic activation is not considered in medium- to high-throughput screening assays of unknown compounds. Although the PrestoBlue[®] assay seems to report “enhanced” activity of particularly tafenoquine compared to the other assay systems used, this was not the case for primaquine. Primaquine is known to have activity against liver stages of *P. falciparum*, *P. vivax* and *P. ovale* and is, therefore, of interest in transmission-blocking strategies. Primaquine has been shown to be gametocytocidal against all *Plasmodium* species for late stage gametocytes through targeting the parasites’ mitochondria but is not clinically useful against *P. falciparum* asexual stages. However, at *in vitro* gametocytocidal IC₅₀ values of 1-15 µM [255, 477], this compound would be identified as not active, as confirmed by the data presented here (<50% inhibition observed on all assay platforms). This discrepancy between activity observed *in vivo* and the lack thereof *in vitro* supports the notion of metabolic activation of primaquine *in vivo* and thus hampers the use of *in vitro* assay systems for this class of compounds.

The naphthoquinone atovaquone was able to inhibit ~50% of immature gametocytes with the previously proposed action, i.e. targeting of the ETC through the cytochrome b ubiquinol oxidation site [478]. Gametocytes do however have active mitochondria [33, 150] and according to the ATP levels measured, these parasites are still 50% viable and may indicate static arrest of the gametocytes after atovaquone treatment. The

PrestoBlue[®] assay was unable to detect this inhibitory capacity at a primary screening concentration of 1 μ M, which may be a concern when such assay platforms are solely used to derive chemical signatures of libraries for gametocytocidal activity [118, 464]. As this assay theoretically provides a direct readout of cellular respiration, this is either a more sensitive probe of decreased glycolysis and respiration of the parasite upon atovaquone treatment or an indication of pluri-pharmacology of atovaquone in gametocytes. When atovaquone was re-screened against the PrestoBlue[®] assay at 10 μ M, gametocytocidal activity was however noted for this compound, highlighting the need to define an optimal concentration threshold for primary screens that minimises both false-negative and false-positive hit rates. In the case of synthetic compound library screens, the effects of false negative losses may be reduced if related compounds of the same basic scaffold are identified to be active [479].

When compared to the reference strain NF54, and considering the data from the ATP, pLDH and PrestoBlue[®] assay platforms, the *ex vivo* clinical isolates showed slightly reduced susceptibility to the compounds evaluated. When considering only the pLDH data for the NF54 strain, the inhibitions achieved correlated well. Exceptions were SB_07 that was highly susceptible to all of the compounds tested and TD_01 which by contrast was inversely resistant. These profiles could not be related to the genotypic data reported since these were restricted to chloroquine and antifolate resistance.

2.5 Conclusions

The standardised protocol produced a reproducible, high gametocytaemia and these parasites were viable, functional and could be used in gametocytocidal assays. An important point that emerged from this study is that unlike asexual parasite assays measuring parasite proliferation, greater variability in end-point readout exists between gametocytocidal assays that interrogate different parasite biological functions. Drug mode of action is likely to be an essential factor in this outcome. This suggests that compounds targeting a specific biological pathway may fail in one assay, but be active when evaluated in a different assay. Reliance on a single assay platform to screen different pharmacophores may, therefore, result in false negative results. However, an assay that has been demonstrated to be sensitive to a particular pharmacophore/MoA may be used to screen compounds of the same series and additionally provide data that is informative from a biological perspective, thereby giving indications of the drug MoA. This study,

therefore, highlights the necessity of taking care when screening broad chemotypes with a single assay platform against gametocytes for which the biology is not clearly understood.

The robust gametocyte production protocol and assay platforms established in this chapter contributed greatly to transmission-blocking antimalarial development as illustrated by the following published articles that incorporated the methods:

1. Le Manach C, Paquet T, Brunschwig C, Njoroge M, Han Z, González Cabrera D, Bashyam S, Dhinakaran R, Taylor D, Reader J, **Botha M**, Churchyard A, Lauterbach S, Coetzer TL, Birkholtz LM, Meister S, Winzeler EA, Waterson D, Witty MJ, Wittlin S, Jiménez-Díaz MB, Santos Martínez M, Ferrer S, Angulo-Barturen I, Street LJ, Chibale K. (2015) A Novel Pyrazolopyridine with *in Vivo* Activity in *Plasmodium berghei* – and *Plasmodium falciparum*-Infected Mouse Models from Structure-Activity Relationship Studies around the Core of Recently Identified Antimalarial Imidazopyridazines. *J Med Chem.* 12;58(21):8713-22. Doi: 10.1021/acs.jmedchem.5b01605.
2. Le Manach C, Nchinda AT, Paquet T, González Cabrera D, Younis Y, Han Z, Bashyam S, Zabiulla M, Taylor D, Lawrence N, White KL, Charman SA, Waterson D, Witty MJ, Wittlin S, **Botha ME**, Nondaba SH, Reader J, Birkholtz LM, Jiménez-Díaz MB, Martínez MS, Ferrer S, Angulo-Barturen I, Meister S, Antonova-Koch Y, Winzeler EA, Street LJ, Chibale K. (2016) Identification of a Potential Antimalarial Drug Candidate from a Series of 2-Aminopyrazines by Optimization of Aqueous Solubility and Potency across the Parasite Life Cycle. *J Med Chem.* 10;59(21):9890-9905.
3. Moyo P, **Botha ME**, Nondaba S, Niemand J, Maharaj VJ, Eloff JN, Louw AI, Birkholtz L. (2016) *In vitro* inhibition of *Plasmodium falciparum* early and late stage gametocyte viability by extracts from eight traditionally used South African plant species. *J Ethnopharmacol.* 5;185:235-42. Doi: 10.1016/j.jep.2016.03.036.
4. Singh K, Okombo J, Brunschwig C, Ndubi F, Barnard L, Wilkinson C, Njogu PM, Njoroge M, Laing L, Machado M, Prudêncio M, Reader J, **Botha M**, Nondaba S, Birkholtz LM, Lauterbach S, Churchyard A, Coetzer TL, Burrows JN, Yeates C, Denti P, Wiesner L, Egan TJ, Wittlin S, Chibale K. (2017) Antimalarial Pyrido[1,2-a]benzimidazoles: Lead Optimization, Parasite Life Cycle Stage Profile, Mechanistic Evaluation, Killing Kinetics, and *in vivo* Oral Efficacy in a Mouse Model. *J Med Chem.* 23;60(4):1432-1448. Doi: 10.1021/acs.jmedchem.6b01641.
5. Paquet T, Le Manach C, Cabrera D, Younis Y, Henrich P, Abraham T, Lee M, Basak R, Ghidelli-Disse S, Lafuente-Monasterio M, Bantscheff M, Ruecker A, Blagborough A, Zakutansky S, Zeeman A, White K, Shackelford D, Mannila J, Morizzi J, Scheurer C, Angulo-Barturen I, Martínez M, Ferrer S, Sanz L, Gamo F, Reader J, **Botha M**, Dechering K, Sauerwein R, Tungtaeng A, Vanachayangkul P, Lim C, Burrows J, Witty M, Marsh K, Bodenreider C, Rochford R, Solapure S, Jiménez-Díaz M, Wittlin S, Charman S, Donini C, Campo B, Birkholtz L, Hanson K, Drewes G, Kocken C, Delves M, Leroy D, Fidock D, Waterson D, Street L, Chibale K. (2017) Antimalarial efficacy of MMV390048, an inhibitor of *Plasmodium* phosphatidylinositol 4-kinase. *Sci Transl Med.* Apr 26;9(387). Doi: 10.1126/scitranslmed.aad9735.
6. Harmse R, Coertzen D, Wong H, Smit FJ, **van der Watt ME**, Reader J, Nondaba SH, Birkholtz L, Haynes RK, N'Da D. (2017) Activities of 11 Azaartemisinin and N-sulfonyl Derivatives against Asexual and Transmissible Malaria Parasites. *ChemMedChem*, 12;24:2086

7. Coertzen D, Reader J, **van der Watt M**, Nondaba SH, Gibhard L, Wiesner L, Smith P, D'Alessandro S, Taramelli D, Wong HN, du Preez JL, Wu RWK, Birkholtz LM, Haynes RK. (2018) Artemisone and Artemiside Are Potent Panreactive Antimalarial Agents That Also Synergize Redox Imbalance in *Plasmodium falciparum* Transmissible Gametocyte Stages. *Antimicrob Agents Chemother.* Jul 27;62(8). Doi: 10.1128/AAC.02214-17.
8. Brunshwig C, Lawrence N, Taylor D, Abay E, Njoroge M, Basarab GS, Le Manach C, Paquet T, Cabrera DG, Nchinda AT, de Kock C, Wiesner L, Denti P, Waterson D, Blasco B, Leroy D, Witty MJ, Donini C, Duffy J, Wittlin S, White KL, Charman SA, Jiménez-Díaz MB, Angulo-Barturen I, Herreros E, Gamo FJ, Rochford R, Mancama D, Coetzer TL, **van der Watt ME**, Reader J, Birkholtz LM, Marsh KC, Solapure SM, Burke JE, McPhail JA, Vanaerschot M, Fidock DA, Fish PV, Siegl P, Smith DA, Wirjanata G, Noviyanti R, Price RN, Marfurt J, Silue KD, Street LJ, Chibale K. (2018) UCT943, a Next-Generation *Plasmodium falciparum* PI4K Inhibitor Preclinical Candidate for the Treatment of Malaria. *Antimicrob Agents Chemother.* Aug 27;62(9). Doi: 10.1128/AAC.00012-18

CHAPTER 3

POTENT *PLASMODIUM FALCIPARUM* GAMETOCYTOCIDAL COMPOUNDS IDENTIFIED BY EXPLORING THE KINASE INHIBITOR CHEMICAL SPACE FOR DUAL ACTIVE ANTIMALARIALS

The work in this chapter has been published as follows:

van der Watt ME, Reader J, Churchyard A, Nondaba SH, Lauterbach SB, Niemand J, Abayomi S, van Biljon RA, Connacher JI, van Wyk RDJ, Le Manach C, Paquet T, González Cabrera D, Brunshwig C, Theron A, Lozano-Arias S, Rodrigues JFI, Herreros E., Leroy D, Duffy J, Street LJ, Chibale K, Mancama D, Coetzer TL, Birkholtz L (2018). Potent *Plasmodium falciparum* gametocytocidal compounds identified by exploring the kinase inhibitor chemical space for dual active antimalarials. *Journal of Antimicrobial Chemotherapy*. 2018 May 1;73(5):1279-1290. doi: 10.1093/jac/dky008

3.1 Introduction

Most antimalarial drugs targeting the asexual blood stages of the most lethal malaria parasite, *P. falciparum*, are not clinically useful against the transmissible, sexual gametocyte forms [416, 417]. Robust *in vitro* gametocyte production and screening platforms [117, 255, 480] have allowed the evaluation of compound libraries to target *P. falciparum* gametocytes [264, 265, 363, 428, 439, 443, 444, 447, 464, 481, 482] and the identification of compounds with dual activity against both asexual parasites and gametocytes [3, 4, 271] or, alternatively, with strategy-specific abilities, targeting either asexual parasites or gametocytes [3, 4].

An image-based (fluorescence-based confocal imaging of DAPI stained parasites) high-throughput screen of 36 608 compounds of the BioFocus[®] DPI SoftFocus[®] library revealed 222 selective hits against *P. falciparum* parasites [385]. These provided high-quality starting points with potent activity against *P. falciparum* asexual stages and physicochemical characteristics representative of “druggable” compounds [383]. Five lead scaffolds, including four kinase-focussed inhibitor series: 2-aminopyridines (2-APs), imidazopyridazines (IMPs), 6,9-imidazopyridines (6,9-IPs) and 2,6-imidazopyridines (2,6-IPs) as well as an ion-channel-focussed series of diaminothienyl-pyrimidine (DTP) compounds were used in H2L and LO programmes. These scaffolds fit into the kinase

inhibitor chemical space, the latter being the property space bridged by the compounds, and defined by construction principles and border conditions limited by this target enzyme class. This led to the identification of several lead compounds for the IMPs [407, 480, 483], DTPs [393, 394, 483], IPs and 2-APs [394, 484-486]. Leads included MMV390048 and MMV642943, *Pf*PI4K inhibitors currently in pre-clinical and clinical assessment [252]. Based on the success of the compounds mentioned above against asexual stage malaria parasites and proof that at least two of them additionally have gametocytocidal activities, [252, 406] representative compounds from the 2-AP, IMP, IP and DTP series were further interrogated here for their gametocytocidal activity. Several 2-APs, IMPs and IPs were active against both asexual and gametocyte stages and profiled through sequential and increasingly more demanding chemical and biological filters to identify potent chemical scaffolds, useful as dual active antimalarial agents.

3.2 Methods and Materials

3.2.1 Chemistry

Aminopyridine and aminopyrazine (APs) derivatives were prepared from commercially available 2-amino-5-bromopyridine and 2-aminopyrazines, respectively, as described [484-487]. The IMPs were synthesised from 3-amino-6 chloropyridazine [407, 488]. Likewise, the DTPs [393, 483] and 2,6-IPs [413, 414] were synthesised as reported. Synthesis of the 6,9-IPs is briefly described (Figure 3.1). The kinase-focussed inhibitors were designed with developable, druggable assets in mind, adhering to the following physicochemical cut-offs [489]: molecular weight (MW) <500 g/mol, cLogP <5, number of HBA <10, number of HBD <5 and polar surface area (PSA) <140 Å.

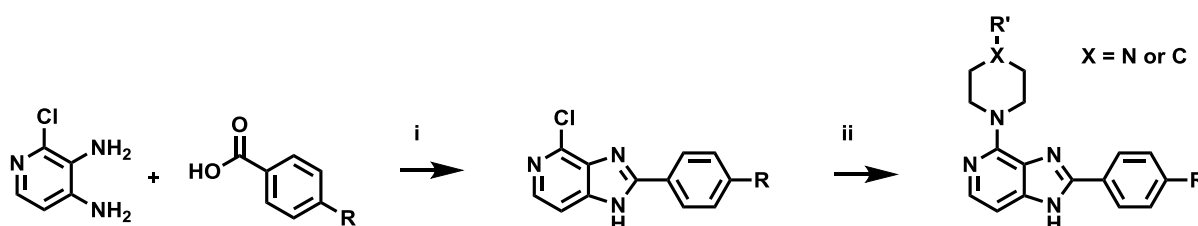
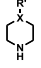


Figure 3.1: Schematic of the synthesis of the 6,9-IPs.

Reagents and conditions include: i) Eaton's reagent (100°C, 98%) and ii)  (160°C). An additional deprotection step may be required if there is a Boc-protection group on the amine. Figure courtesy of Claire Le Manach.

3.2.2 Ethics

All *in vitro* parasite and blood collection work has ethics approvals (University of Pretoria 120821–077; CSIR Ref 10/2011; University of the Witwatersrand M130569).

3.2.3 *In vitro* cultivation of asexual stage parasites and induction of gametocytes

P. falciparum asexual cultures were maintained as described before [117, 455] (section 2.2.2), including the initiation, induction and maintenance of gametocyte cultures (section 2.2.3) from reference strains (drug susceptible NF54).

3.2.4 *In vitro* *P. falciparum* antiplasmodial activity and cytotoxicity evaluation

Compounds were screened against *P. falciparum* K1 (chloroquine, mefloquine and pyrimethamine-resistant) and NF54 strains *in vitro* using a modified [³H]hypoxanthine incorporation assay [490] or pLDH assay [460] (section 2.2.7.3). *In vitro* cytotoxicity was determined by screening compounds against Chinese Hamster Ovarian (CHO) cells, using 3-(4,5-dimethylthiazol-2-yl)-2,5-diphenyltetrazolium bromide [491], with emetine as reference drug. Cells (10⁵ cells/ml) were exposed to 10-fold compound serial dilutions for 48 hour incubation, in triplicate for two biological replicates. Non-linear dose-response curve fitting analysis [492] allowed IC₅₀ deduction (GraphPad Prism6, GraphPad Software Inc.).

3.2.5 *In vitro* gametocytocidal activity evaluation

Gametocytocidal activity was evaluated independently with a gametocyte-luciferase reporter assay (section 2.2.7.5), an ATP assay (section 2.2.7.4) or a PrestoBlue[®] assay (section 2.2.7.2) as previously described [117]. All assays were performed in parallel using the same stock of compounds, diluted fresh with complete culture medium from 10 mM stock solutions in DMSO (final DMSO concentration ≤0.5%). Drug controls included methylene blue (25 μM for the ATP assay, 5 μM for the luciferase reporter assay) and MMV390048 (5 μM for the luciferase reporter assay). Untreated gametocytes and uninfected erythrocytes/complete culture medium were used to monitor viability and background, respectively. Primary screen data were analysed using GraphPad Prism 6 and quality parameters determined by %CV, S/B, S/N and Z'-factor. IC₅₀s were generated with GraphPad Prism 6, represented as means ± SEM for n≥3 independent biological replicates.

3.2.6 Luciferase reporter assay

A luciferase reporter assay for early (NF54-pfs16-GFP-Luc) and late (NF54-mal8p1.16-GFP-Luc) gametocyte marker cell lines [438] (section 2.2.7.5) enabled stage-specific analyses of synchronous gametocyte cultures (2% gametocytaemia, 1.5% haematocrit). Drug assays were performed on early ($\geq 90\%$ stage II/III; EG) and late ($\geq 95\%$ stage IV/V; LG) gametocytes with 48 hour drug pressure as described [117]. The assay was additionally performed on mature ($>95\%$ stage V) gametocytes. Drug assays were set up on day 5, 10 and 13 (representing early stage II/III, late stage IV/V and mature stage V gametocytes, respectively). In each instance, assays were set up in triplicate using a 2% gametocytaemia, 1.5% haematocrit culture and 48 hour drug pressure in a gas chamber (90% N₂, 5% O₂, and 5% CO₂) at 37°C. Luciferase activity was determined in 20 μ l parasite lysates by adding 50 μ l luciferin substrate (Promega Luciferase Assay System) at RT and detection of resultant bioluminescence at an integration constant of 10 seconds with the GloMax[®]-Multi+ Detection System with Instinct[®] Software.

3.2.7 Resazurin-based dye assay

The PrestoBlue[®] (Life Technologies) assay was performed on semi-synchronous gametocyte cultures (2% gametocytaemia, 5% haematocrit) for 48 hour drug pressure on late stage (IV/V; LG) gametocytes [117] (section 2.2.7.2).

3.2.8 ATP bioluminescence assay

Late stage gametocytes (95% stage IV/V, LG) were enriched using density gradient centrifugation and magnetic separation as described [117] (section 2.2.7.4). Approximately 50 000 gametocytes were exposed to drug for 24 hours.

3.2.9 Semi-quantitative RT-PCR

RT-PCR was used to confirm the gametocyte stages by evaluating differential transcript abundance in late (stage IV/V) and mature (stage V) gametocyte populations as compared to asexual stages, using primers for asexual and gametocyte-specific genes. Analysis was performed using the LightCycler[®] 480 and KAPA SYBR[®] Fast qPCR kit (Kapa Biosystems, USA) on 18 transcripts of interest (Table 3.1) using 5 pmol of each primer in 384-well plates; with cycling after pre-incubation at 95°C for 10 min for 45 cycles (95°C for 3 seconds, 55°C for 7 seconds and 72°C for 4 seconds). Relative expression was

calculated using LightCycler® 480 software (version 1.5) and the comparative Ct ($2^{-\Delta\Delta Ct}$) method [459] used to analyse transcript abundance.

The same protocol was applied to confirm the stage-specific production of early (stage II/III) and late (stage IV/V) gametocytes, applied in the luciferase reporter assay. For early and late stage gametocyte comparisons, the differential transcript abundance of an early stage marker (*pfs16*; forward primer: 5'-TGCTTATATTCTTCGCTTTTGC-3'; reverse primer: 5'-TAGTCCACCTTGATTAGGTCCA-3') and late stage marker (*pfs25*; forward primer: 5' CCGTTTCATACGCTTGTAATG-3', reverse primer: 5'-TGCCTATATTACATGAGCAAACCTCC-3') were determined.

Table 3.1: Transcripts and oligonucleotides used during the stage-specific validation of gametocyte maturity.

PlasmoDB identifier	Gene description	Stage-specific abundance	Primer sequence (5'-3') forward and reverse
Pf3D7_0831400	<i>Plasmodium</i> exported protein, unknown function	Early trophozoite, ookinete	5'-TAAGAAATGAAATTATGGATG-3' 5'-CCTCGTTTTATATTTACCTG C-3
Pf3D7_1250100	Osmiophilic body protein G377 (female marker)	Stage V, ookinete	5'-GCGACAGATGAACAACAGGT-3' 5'-CACTTGGTTTTGATTATCTCCC-3'
Pf3D7_0406200	Sex specific protein precursor Pfs16	Stage II	5'-TGCTTATATTCTTCGCTTTTGC-3' 5'-TAGTCCACCTTGATTAGGTCCA-3'
Pf3D7_1038400	Gametocyte-specific protein PF11-1	Stage IV/V, ookinete	5'-ATCATTTACGCTTTAGAGG-3' 5'-CTTCTTATGTTTCGGTTTTA-3'
Pf3D7_0209000	6-cysteine protein P230	Ring stage	5'-CCACTTATTTTATTATTCCCAC-3' 5'-GTTCTTTGTTTTATTTTACGG-3'
Pf3D7_1228300	NIMA related kinase 1 NEK1	Trophozoite/ Schizont	5'-GTGCTTACAGTGTTTGGGA-3' 5'-TTAATACATCATTCGGATGAGC-3'
Pf3D7_1302100	Gamete antigen 27/25 G27/25	Stage II	5'-CCTCGTATTAGAAAAGTTGGG-3' 5'-ATCTATTTTGATTCTTGCGAAC-3'
Pf3D7_0617900	Histone H3 variant H3.3	Schizont, stage II	5'-CCCCAAGAAAACAACCTCGC-3' 5'-AAAGCAACAGTTCCTGGACG-3
Pf3D7_0625100	Sphingomyelin synthase 2 SMS2	Stage V	5'-TTACCCGCAACATTAGAAAC-3' 5'-TTGTTGAAAAAGAATATGTCCTG-3
Pf3D7_0621400	PF77 protein ALV7	Stage V, ookinete	5'-GAAAAAGAGGACGATGGTT-3' 5'-CATTAAAAACGGGTTGATCT-3'
Pf3D7_0501200	Parasite infected erythrocyte surface protein PIESP2	Early trophozoite	5'-TACGCCAAGAATCAAGAAC-3' 5'-GGGTCAAGTGCCTAACTAA-3'
Pf3D7_1477300	<i>Plasmodium</i> exported protein Pfg14-744	Stage I/II	5'-AGTGAAACTGAACCACCG-3' 5'-GATTTTCTTCCGTCAAC-3'
Pf3D7_0500800	Mature parasite infected erythrocyte surface antigen	Stage I	5'-ATGAAATAATTCGTGCGA G-3' 5'-CTGTAACAACCGAACCCC-3'
Pf3D7_0525800	IMC protein 1g	Stage V, ookinete	5'-GTTCCAGAAGTTAATTGCC-3' 5'-GCAAGACTTATGGTTTGG-3'
Pf3D7_1035800	Probable protein, function unknown M712	Stage I	5'-AAATTCGGATTCTAATGTG-3' 5'-CAACTCATCTTCTTCGC-3'
Pf3D7_0309100	Conserved <i>Plasmodium</i> protein, unknown function	Stage II	5'-CTCAAAAAGACTCGTACAAT-3' 5'-GCTGAACATTAATCAGC-3'
Pf3D7_0717500	Calcium dependent protein kinase 4 CDPK4	Stage III	5'-CCTTTCAACGGTTCGAACG-3' 5'-GCGTCCCTTGCCGATATCC-3'
Pf3D7_0411700	Conserved <i>Plasmodium</i> protein, unknown function	Stage IV	5'-TGGAAATATTAATTCGAGCG-3' 5'-TGGCTTTATGGAACCTGTC-3'

Data derived from the Lopez-Barragan *et al.* and Young *et al.* 2005, datasets on PlasmoDB v. 24, accessed on 30 April 2015.

3.2.10 Phenotypic profiling of clinical isolates of southern African origin

The cultivation, genotypic and phenotypic profiling of the panel of clinical isolates are described in section 2.2.4 of this thesis, with the only exception that additional clinical isolates (collected from the Charlotte Maxeke Johannesburg Academic Hospital and Chris Hani Baragwanath Hospital; JZA notation) were included in this chapter. Gametocytogenesis was induced as above and hit compounds evaluated for activity on the resultant late stage ($\geq 95\%$ stage IV/V) gametocytes for a panel of nine gametocyte-producing *ex vivo* African clinical isolates using either the ATP assay (compound evaluated at $1\ \mu\text{M}$) or with a previously reported pLDH assay at $1 \times \text{IC}_{50}$ of each compound [427].

3.2.11 Gametocytocidal stage-specificity and speed of action

Highly synchronised asexual parasites ($>97\%$ rings) were used to induce gametocytogenesis to produce compartmentalised early ($>90\%$ stage I-III), late stage gametocytes ($>95\%$ stage IV/V) or mature stage V gametocytes ($>95\%$ stage V gametocytes). Full dose-response analysis was performed for each compound after 48 hour exposure, after which the luciferase activity was measured as described above (section 3.2.6). More detailed descriptions of this approach can be found in sections 2.2.7.5 and 2.3.8 of this thesis. To determine the speed of action, early and late stage gametocytes were exposed to compounds for 24, 48 and 72 hours at IC_{50} (determined during 48 hour incubation; mid-point for temporal evaluation) to allow chronological evaluation of IC_{50} fluctuations (Figure 3.2). Inhibition ratios were subsequently determined and used (together with the curve slope) to determine the speed of action. All assays were performed on three independent biological replicates (technical triplicates, GraphPad Prism 6).

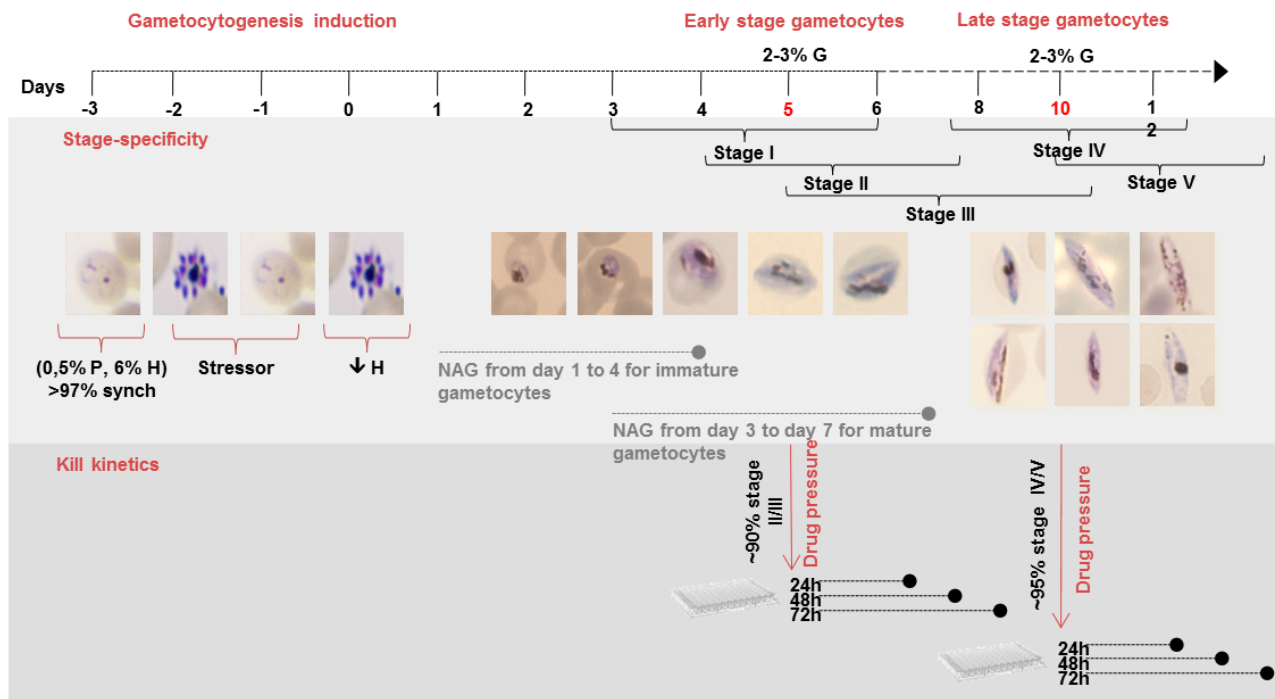


Figure 3.2: Stage-specific gametocyte production and speed-of-action assay. Asexual parasites (0.5% parasitemia, 6% hematocrit) were sorbitol synchronised for two consecutive cycles to ensure a highly synchronised (>97%) ring population on day -3. Initiation of gametocytogenesis was induced on day 0 by a decrease in the haematocrit. Asexual elimination was achieved with NAG treatment from day 1 to 4 for early gametocytes and day 3 to 7 for mature gametocytes. Assays were performed on day 5 and 10 for early and late stage gametocytes and incubated for 24, 48, and 72 hours. P: parasitaemia, H: haematocrit, G: gametocytaemia. Figure courtesy of Janette Reader.

3.2.12 SMFA

SMFA was used to determine the infectiousness of gametocytes as previously described [493]. Mature (>95% stage V) *P. falciparum* gametocytes were exposed to various concentrations of MMV642943 (0.001 to 1 μM) for 24 hours prior to feeding to *Anopheles stephensi* mosquitoes. Both the exflagellation assay and SMFA were performed as previously described [116, 405]. Note: This work was contributed by Sonia Lozano-Arias, Janneth Rodrigues and Esperanza Herreros (GSK, Tres Cantos) as part of the published manuscript.

3.2.13 DNA microarray analysis

Late stage gametocytes were enriched by density centrifugation using Nycoprep 1.077 cushions (Axis-Shield) before RNA isolation as described [494]. DNA microarray was performed using 3-12 μg total RNA for reverse transcription and aminoallyl incorporation for each sample to be used in a reference design (reference pool of equal amounts of all cDNA samples coupled to Cy3, hybridized to samples coupled to Cy5; 17 hours at 65°C while rotating) performed on *P. falciparum* custom Agilent 60-mer 8x15k arrays (AMADID#037237,[495]). Post washing, arrays were scanned on a GenePix 4000B scanner (10 μm resolution) at wavelengths of 532 nm (Cy3) and 635 nm (Cy5). Signal

intensities that passed GenePix standard background filters ($p < 0.05$) were normalised by robust spline and GQuantile using limma Log₂. (Cy5/Cy3) expression values were used to calculate the log fold change in gene expression ($\log_2(T/UT)$) with differential expression set at >0.5 or <-0.5 . Data were clustered hierarchically according to Euclidean distance with average linkage clustering using TIGR MeV 4.9.0. Pearson correlation coefficients were calculated and visualised using the corrplot package in R (v3.2.3). Gene ontology annotations were obtained from the Gene Ontology Consortium (<http://www.geneontology.org/>) and combined with genes involved in different metabolic pathways from the Malaria Parasite Metabolic Pathways (MPMP) database (<http://mpmp.huji.ac.il/>), and INTERPRO domains for *P. falciparum* proteins were obtained from UniProt (<http://www.uniprot.org/>). Gene set enrichment analysis (GSEA) was applied to determine the enriched processes using GSEA v2.2.4 (<http://www.broad.mit.edu/gsea/index.jsp>) ($p < 0.05$, false discovery rate (FDR) $< 0.1\%$) and interaction networks visualised with Cytoscape v3.5.0. Note: This work was contributed by Jessica Nepomuceno (née Connacher), Roelof van Wyk and Riëtte van Biljon as part of the published manuscript.

3.3 Results

3.3.1 Hit identification

In total, 379 compounds belonging to the 2-AP (31 representatives), IMP (23 representatives), DTP (12 representatives) and IP (158 and 155 representatives respectively) series were evaluated for their activity against late stage gametocytes ($>95\%$ stage IV/V). The 2-APs, IMPs and DTPs were cross-validated on three independent assay platforms (luciferase reporter, ATP and PrestoBlue[®] assays) to interrogate different biological endpoints and minimise assay interference. The IPs were treated similarly, with the exception that they were not validated on the PrestoBlue[®] platform. Strict selection criteria were imposed requiring primary hits to pass thresholds of $>50\%$ inhibition (1 μM) and $>70\%$ inhibition (5 μM) (Figure 3.3, section 1.4.5.1) [4].

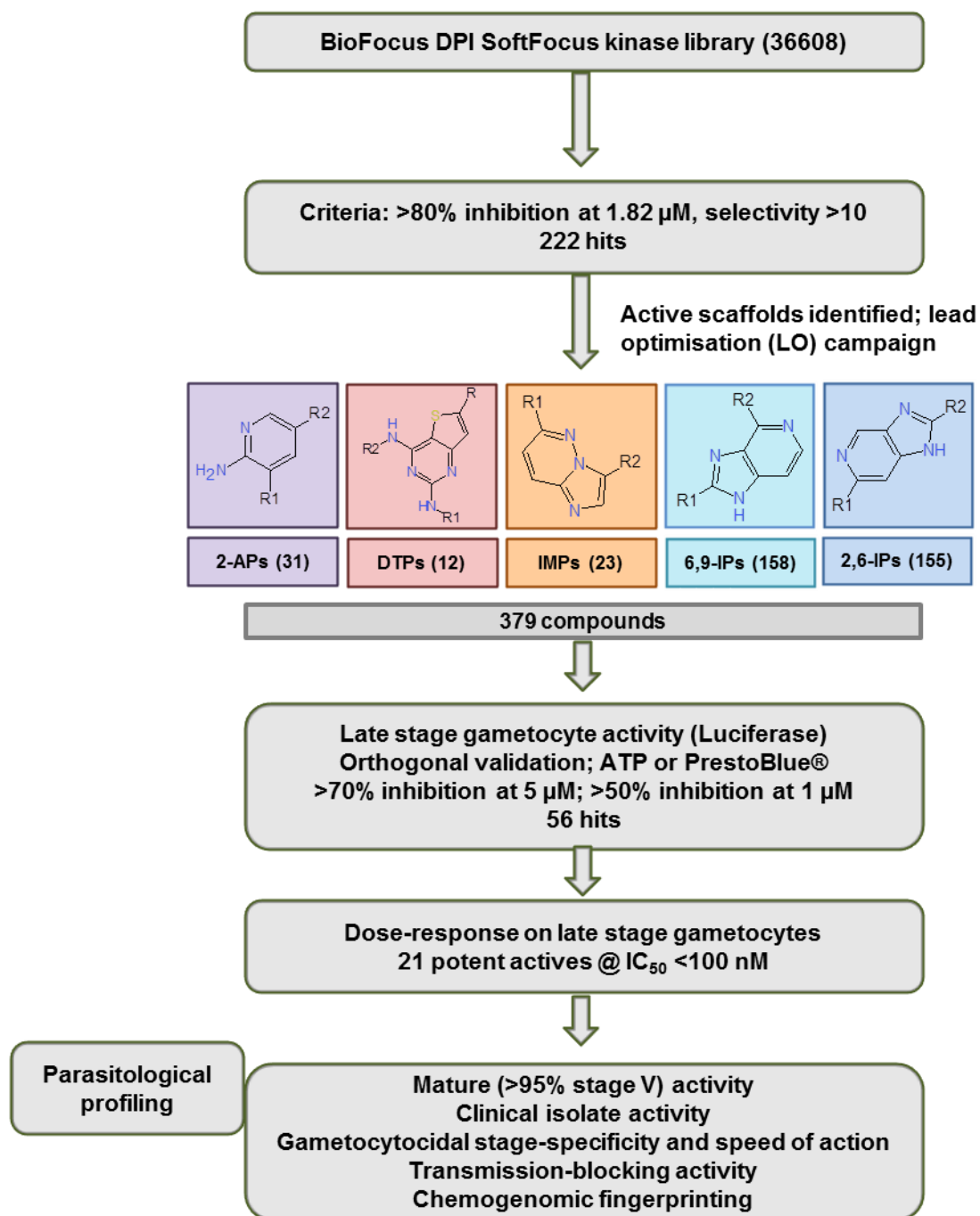


Figure 3.3: Description of the critical path followed for the screening of select scaffolds from kinase libraries for gametocytocidal activity. The DTPs series are indicated in pink, the APs in purple, the IMPs in orange, the 6,9-IPs in turquoise and the 2,6-IPs in blue. The number of compounds in each series is indicated in parentheses.

Overall, the 2-APs were the most active compounds, with a hit rate of 84% on the luciferase reporter assay at 1 μ M (Figure 3.4A). By contrast, the DTPs displayed a 33% hit rate on the ATP assay, whereas very similar hit rates of 30%-70% were observed for the IMPs, irrespective of the assay platform used.

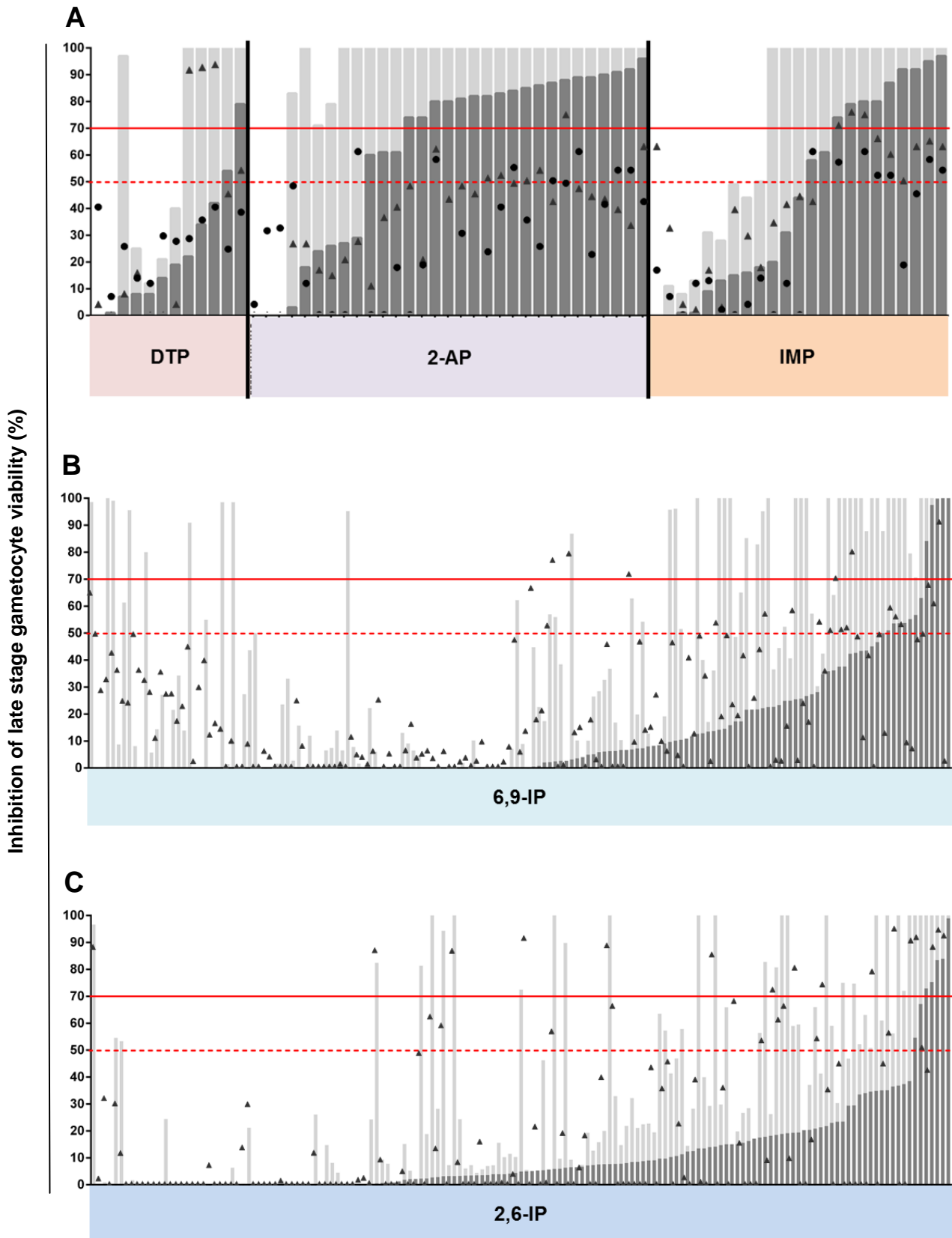


Figure 3.4: Primary hit identification for late stage gametocytocidal activity. Inhibition of *P. falciparum* late stage IV/V gametocyte viability after 48 hours continuous exposure to 1 and 5 μM drug (**A**) DTPs: pink, APs: purple, IMPs: orange, (**B**) 6,9-IPs: turquoise, (**C**) 2,6-IPs: blue, using the luciferase reporter assay (light and dark bars), PrestoBlue[®] (dots) and ATP (triangles) assay platforms. Data are organised per series and with increasing percentage inhibition on the luciferase platform (1 μM). The 70% (solid red line) and 50% (dotted red line) selection cut-offs are indicated. Results are expressed as percentage inhibition compared to the untreated controls and are representative of single biological experiment performed in technical triplicates, \pm SD. The full list of data, including compound names, can be found in Table A3.1 (appendix).

The 6,9-IPs (Figure 3.4B) and 2,6-IPs (Figure 3.4C) displayed 8.2% and 5.8% hit rates on the luciferase reporter platform, whereas 13.3% and 18.1% hit rates were achieved on the ATP assay platform. A comparison of the compound efficacy across the three assay platforms (at 1 μ M) indicated high similarity (Pearson $r^2 = 0.82$) between the luciferase reporter and ATP assays, whereas the PrestoBlue[®] assay showed a strong correlation for the IMPs with one or the other assay platforms (r^2 of 0.82 and 0.74, respectively). Both the 6,9-IPs ($r^2 = 0.44$) and 2,6-IPs ($r^2 = 0.50$) showed moderate correlations between the luciferase reporter and ATP datasets.

The selected primary hits were evaluated with dose-response to determine their IC₅₀ values on late (>95% stage IV/V) gametocytes, which corresponded well to the inhibition data obtained from the primary screen (Table A3.2, appendix).

Of these, 90 compounds had submicromolar IC₅₀s (Table 3.2), composed of 2% DTPs, 23% 2-APs, 12% IMPs, 27% 6,9-IPs and 36% 2,6-IPs. These compounds also maintained activity on asexual blood stages (Tables A3.1 and 3.2), with a 3- to 4-fold drop in inhibitory activity between asexual parasites and gametocytes. However, the rank order of compounds with activity against asexual parasites and activity against gametocytes differed, indicating that preference towards specific gametocyte stages is present, even within clusters of compounds with dual gametocyte-asexual activity (Table A3.2, appendix).

Table 3.2: Asexual and late stage profiles of the evaluated compounds. Stage-specific IC₅₀ data are organised per series as increasing IC₅₀ values on late stage gametocytes. The DTPs series are indicated in pink, the APs in purple, the IMPs in orange, the 6,9-IPs in turquoise and the 2,6-IPs in blue. Colour intensity represents increasing *in vitro* potency against *P. falciparum* asexual stages and late (stage IV/V) gametocytes (LG). Late stage gametocyte IC₅₀'s represent the lowest of each value obtained for the luciferase reporter (NF54-*mal8p1.16*-GFP-Luc) or ATP bioluminescence assays. The complete dataset, in support of Table 3.2, is available from Table A3.2 (appendix).

Compound	IC ₅₀		Compound	IC ₅₀		Compound	IC ₅₀	
	Asexual	LG		Asexual	LG		Asexual	LG
MMV668434	43	105	MMV666620	12	79	MMV688375	27	44
MMV666632	28	643	MMV672925	10	477	MMV910895	20	51
MMV642943	6	66	MMV670815	417	655	MMV688475	272	98
MMV674192	9	45	MMV672653	36	907	MMV676245	133	104
MMV642944	20	52	MMV689854	36	8	MMV1545672	20	140
MMV643110	23	72	MMV893002	46	62	MMV675812	34	145
MMV642942	10	135	MMV893195	41	70	MMV675617	44	158
MMV668647	21	137	MMV892998	63	96	MMV910833	82	195
MMV390048	22	140	MMV1558618	ND	177	MMV897781	40	196
MMV673927	15	146	MMV884980	64	194	MMV675717	40	239
MMV666810	5	179	MMV884979	52	222	MMV977480	25	256
MMV670930	14	190	MMV1557964	50	230	MMV897760	171	275
MMV394902	19	209	MMV982237	20	266	MMV688389	39	317
MMV642941	53	225	MMV1545775	20	271	MMV1545620	20	340
MMV642990	14	237	MMV893049	57	294	MMV676227	376	356
MMV670401	42	238	MMV893359	45	306	MMV675097	30	364
MMV668808	94	342	MMV892826	74	321	MMV675876	53	367
MMV668809	38	432	MMV1558759	ND	359	MMV897779	164	371
MMV670402	26	441	MMV884981	222	403	MMV688137	30	411
MMV672643	42	460	MMV032931	55	440	MMV982093	118	451
MMV668648	6	536	MMV892827	68	483	MMV676003	172	699
MMV675081	24	845	MMV693080	62	542	MMV910836	29	701
MMV668807	26	901	MMV910900	68	626	MMV1542261	117	745
MMV669810	0	1	MMV884692	230	626	MMV691888	94	774
MMV669286	1	3	MMV690981	127	660	MMV1542021	70	774
MMV672652	1	3	MMV982681	66	831	MMV893197	151	802
MMV652103	7	27	MMV884975	64	846	MMV982672	35	816
MMV674850	3	29	MMV982629	36	972	MMV676222	32	836
MMV674766	8	66	MMV688390	69	15	MMV1542775	26	842
MMV675615	4	72	MMV897780	35	38	MMV982673	87	987

Hit compounds were defined as those with late stage gametocyte activity at IC₅₀s <100 nM. The 21 most potent hit compounds on late stage gametocytes included eight IMPs, four 2-APs, four 6,9-IPs and five 2,6-IPs (Figure 3.5 and Table A3.2 and 3.2).

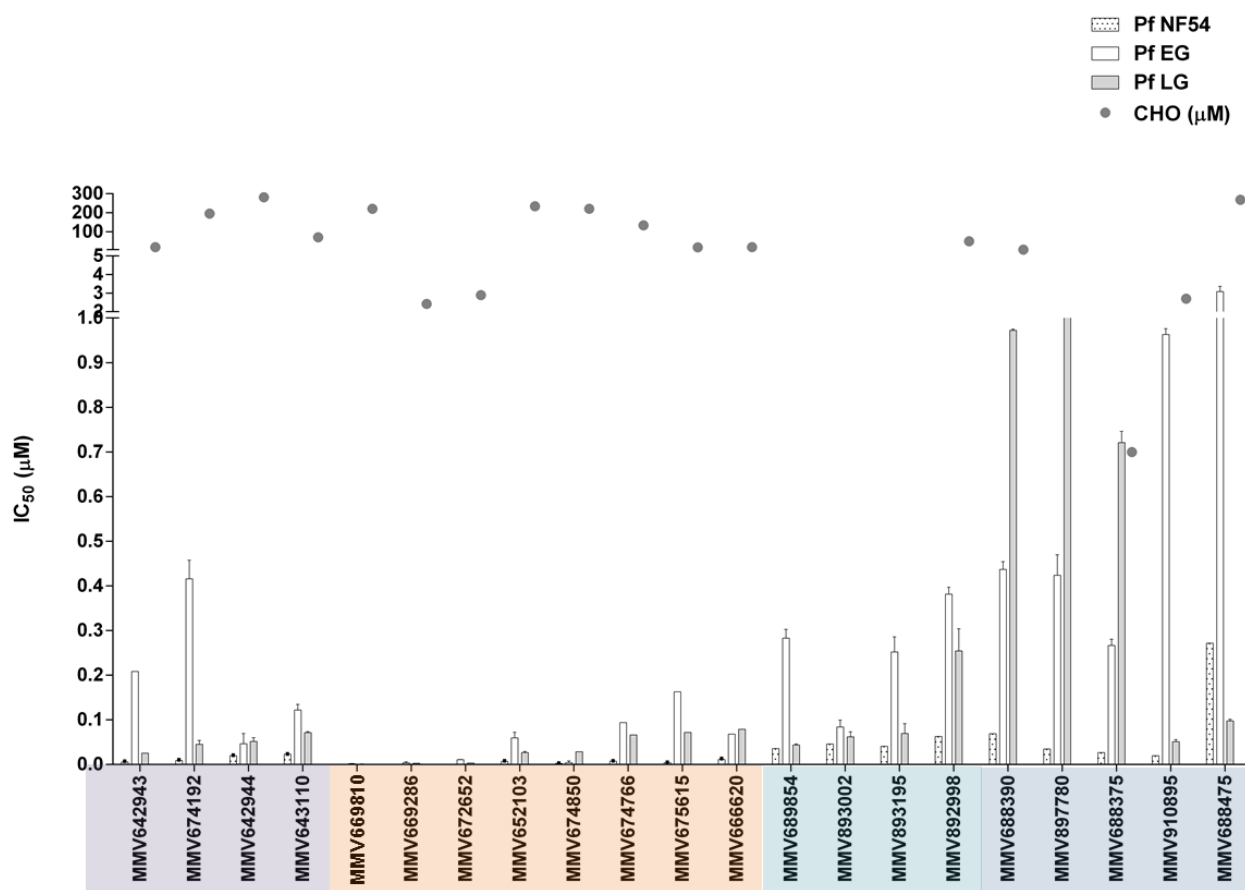


Figure 3.5: Biological profiles of the evaluated compounds. The DTP series are indicated in pink, the APs in purple, the IMPs in orange, the 6,9-IPs in turquoise and the 2,6-IPs in blue. Biological profiles of hits displaying late stage IC₅₀'s <100 nM are indicated. *P. falciparum* NF54 asexual (patterned), early stage gametocyte (white fill), late stage gametocyte (grey fill) and CHO IC₅₀ (dots) values are indicated. Data are representative of at least two biological experiments, each performed in technical triplicates, ± SEM. The complete dataset, in support of Figure 3.5, is available from Table A3.2 (appendix).

All of these compounds had dual activity between asexual parasites and gametocytes and displayed minimal cross-resistance to the *P. falciparum* multidrug-resistant K1 strain, with resistance indices <10 (Figure 3.5 and Table A3.2). The only exceptions were the 6,9-IPs MMV910900 (RI = 13.4), MMV892903 (RI = 13.0) and MMV892904 (RI = 11.5). Additionally, the majority of the DTP, 2-AP and IMP compounds were highly selective towards *P. falciparum* asexual parasites (SI >1000-fold) and late stage gametocytes (SI >10-fold) compared with mammalian cells (Figure 3.5, Table A3.2). By contrast, the 6,9-IPs and 2,6-IPs displayed moderate selectivities (SIs: 50 – 200), only slightly higher than the threshold (SI >10) required by the MMV [3].

3.3.2 Hit profiling

To obtain an indication of efficacy against various contemporary clinical and laboratory-adapted parasite lines, the activity of selected gametocytocidal compounds was evaluated against late stage gametocytes from currently circulating clinical isolates of southern

African origin as well as the drug sensitive reference strain, NF54. These clinical isolates were harvested between April and February 2014, genotyped and phenotyped for selected drug resistance markers on asexual parasites (section 2.3.2, Table 2.3 and Table 3.3) [496].

Table 3.3: Origin and drug resistance genotypes of southern African clinical isolates producing gametocytes. Data for the additional clinical isolates evaluated, can be found in Table 2.3, section 2.3.2.

Strain	Origin	Resistance phenotype	Resistance mechanism (genotype)	Gametocyte production (Y; %)
JZA15	NA	Pyrimethamine	<i>Pfdhfr, pfmdr1</i>	1.1% (n=1)
JZA20	NA	Pyrimethamine	<i>pfdhfr, pfdhps</i>	0.8% (n=1)
JZA25	NA	Pyrimethamine	<i>pfcr, pfdhfr, pfdhps</i>	0.8% (n=1)
JZA30	NA	Pyrimethamine, Mefloquine, atovaquone	<i>pfdhfr, pfdhps, pfcr</i>	0.8% (n=1)
JZA39	NA	Pyrimethamine, Lumefantrine	<i>pfdhfr</i>	1.3% (n=1)

The majority of 2-APs and IMPs (but not the DTPs) were comparably active against gametocytes from the clinical isolates and the *P. falciparum* NF54 reference strain, with the highest activity maintained even in isolates with resistant phenotypes (e.g. JZA 20 and TD_01, both antifolate-resistant) (Figure 3.6). MMV642944 and MMV642942 were consistently more active against the clinical isolates compared with the NF54 reference strain. Collectively, this indicates that the kinase inhibitors evaluated are active towards contemporary clinical isolates of geographical relevance.

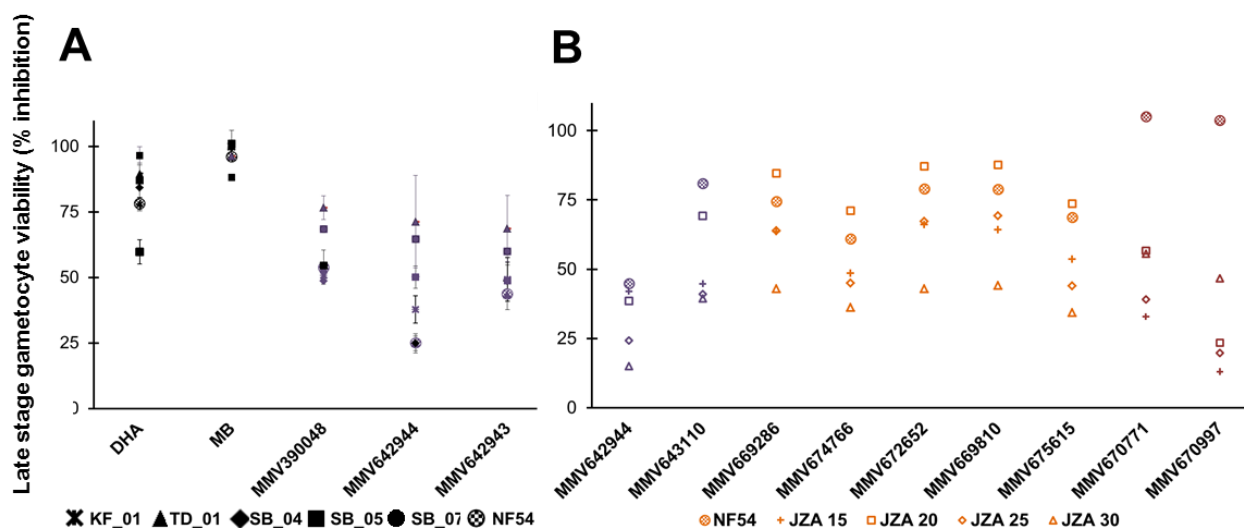


Figure 3.6: Late stage gametocytocidal activity of the lead compounds against *ex vivo* *P. falciparum* clinical isolates. (A) The pLDH assay was performed at 1 x IC₅₀ for each compound, as previously determined on the NF54-*mal8p1.16*-GFP-Luc strain using the luciferase reporter assay. (B) The ATP assay was performed at a single concentration of 1 µM. In all instances, *P. falciparum* NF54 was included as drug susceptible reference strain and (5 µM) and DHA (100 µM) as reference drug controls. Compounds are coloured according to classes as in Table A3.2. Data are representative of at least triplicate experiments ± SEM; a single biological repeat was performed for SB_07.

The parasitological properties (evaluation of gametocytocidal stage-specificity, speed-of-action and *ex vivo* efficacy) of the 90 compounds with late stage IC_{50} s $<1 \mu M$ (from Table 3.2) were additionally evaluated on both early ($>90\%$ stage I-III; EG) and late ($>95\%$ stage IV/V; LG) stage gametocytes (Figure 3.7). Morphological investigation validated the stage-specificity of the adapted gametocyte production protocol (Figure 3.7A). Stage-specificity was further confirmed by evaluating the expression of two stage-associated genes: *Pfs16* as stage-specific marker peaking in early stage gametocytes [497] and *Pfs25* as late stage marker peaking in gametocytes and gametes [498]. Five-fold increased expression was observed for *pfs25*, thereby confirming the presence of late stage gametocytes in these populations (Figure 3.7B). Increases in luciferase expression (relative light units, RLUs) also corresponded to promoter activity (Figure 3.7C).

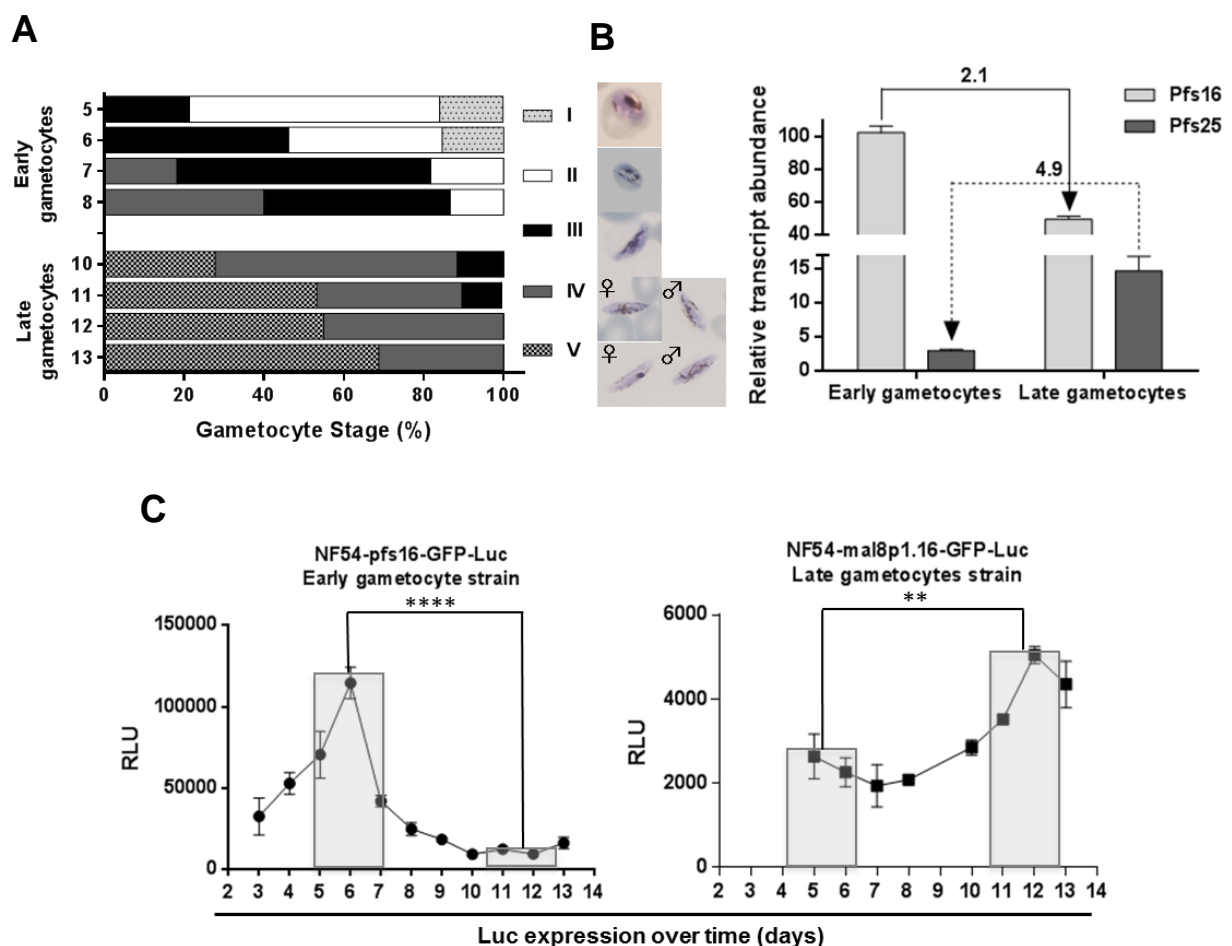


Figure 3.7: Stage-specific gametocyte production. (A) Gametocyte stage confirmation and percentage using Giemsa smears over the assay time periods. For the day 5 and 10 populations, data are from >49 individual experiments; the subsequent daily evaluation was performed once. (B) Semi-quantitative real-time PCR confirmation of the expression of the early gametocyte marker (*pfs16*) and late gametocyte marker (*pfs25*) on the day of assay (day 5 for early gametocytes and day 10 for late gametocytes ($p < 0.05$)). (C) Assessment of the luciferase expression (RLU) throughout gametocytogenesis of the two transgenic lines used (NF54-*pfs16*-GFP-Luc: $P < 0.0001$ and NF54-*mal8p1.16*-GFP-Luc: $p < 0.001$, $n = 3$, \pm SEM).

Within the 2-APs, the majority (88%) were significantly more active ($p < 0.005$, $n=3$) towards late stage gametocytes (Table A3.2, Figure 3.8), as was true for the two drug candidates MMV390048 (EG $IC_{50} = 214.6$ nM; LG $IC_{50} = 140.3$ nM) and MMV642943 (EG $IC_{50} = 134$ nM; LG $IC_{50} = 66$ nM) [252, 406]. Within the IMPs, the most active compounds showed comparable activity (<2-fold difference) for both early and late stage gametocytes (MMV669810 and MMV669286) (Figure 3.8A). The 6,9-IPs and 2,6-IPs were 1.3- and 1.4-fold more active towards late than early stages, respectively (Figure 3.8 B,C). However, the most potent representatives from these series were up to 30-fold more active towards late compared to early stage gametocytes and includes MMV689854 (EG $IC_{50} = 283.0$ nM versus LG $IC_{50} = 7.7$ nM), MMV688390 (EG $IC_{50} = 437.2$ nM versus LG $IC_{50} = 14.7$ nM), MMV910895 (EG $IC_{50} = 963.0$ nM versus LG $IC_{50} = 51.2$ nM) and MMV688475 (EG $IC_{50} = 3093.3$ nM versus LG $IC_{50} = 97.9$ nM).

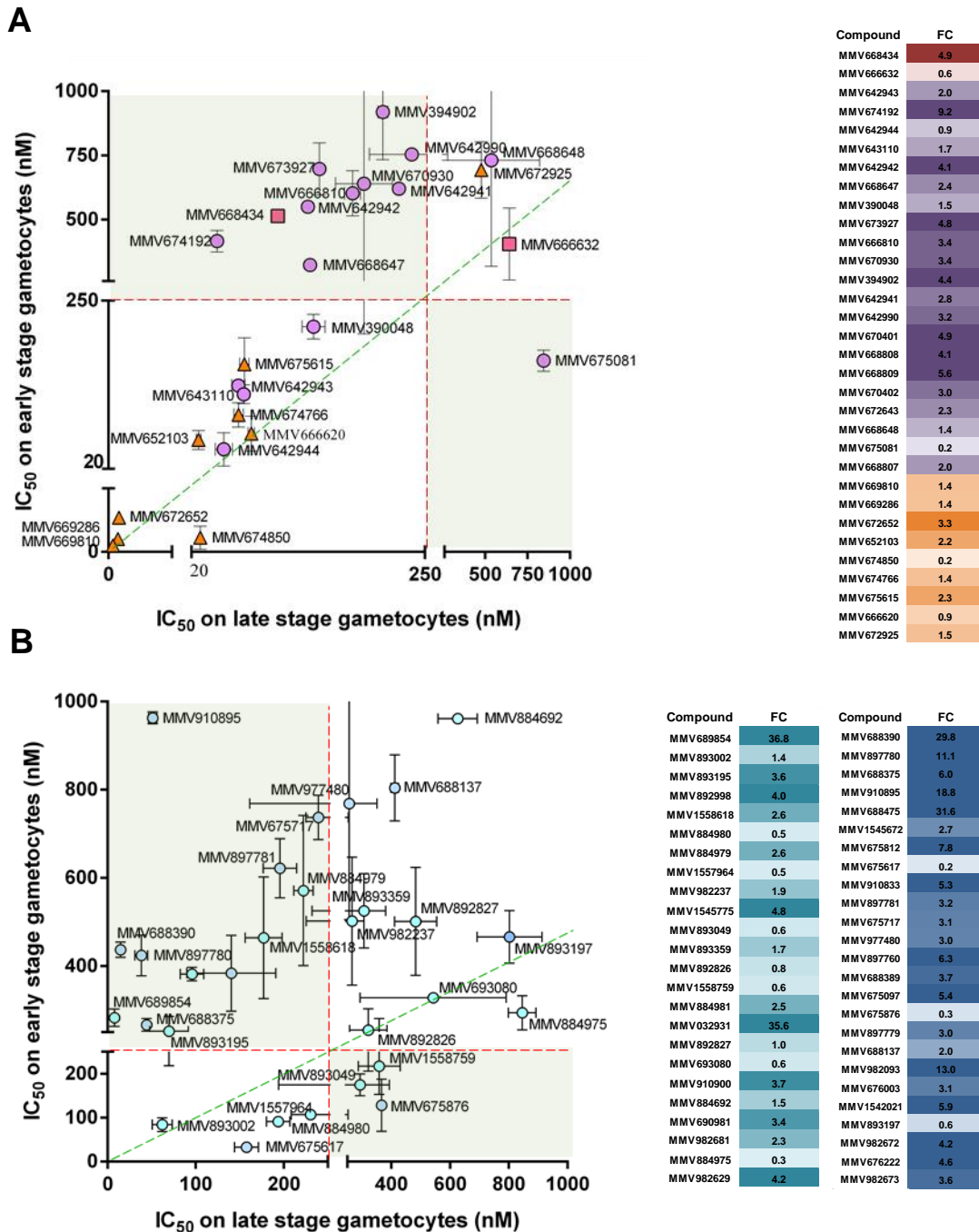


Figure 3.8: Dual reactivity of the lead compound series toward different *P. falciparum* gametocyte developmental stages. The DTPs series are indicated in pink, the APs in purple and the IMPs in orange in (A). The 6,9-IPs are indicated in turquoise and the 2,6-IPs in blue in (B). Early (>95% II/III; y-axis) and late stage (>95% IV/V; x-axis) gametocytes were assayed after 48 hour continuous exposure to drug using the luciferase reporter and/or ATP bioluminescence assays and the IC_{50} determined using GraphPad Prism. Dual active compounds are situated on the trend line (dotted, green). Fold changes (FCs; EG IC_{50} /LG IC_{50}) for stage-specificity towards late stage gametocytes are indicated to the right of each figure. Only compounds with submicromolar IC_{50} s are displayed on this graph. Data are representative of at least triplicate experiments \pm SEM. The complete dataset, in support of Figure 3.8, is available from Table A3.2 (appendix).

The stage-specific gametocytocidal activity of selected hits from all three series was confirmed via additional evaluation of their speed-of-action over 24, 48 or 72 hours (Figure

3.9) using each compound at $1 \times IC_{50}$ (determined at 48 hours). Treatment for shorter periods (<24 hours) did not result in accurate dose-responses for any compound. Within the 2-APs, MMV642943 and MMV643110 had a similar slow speed-of-action against both early and late stage gametocytes with a >48 hour lag observed. By contrast, MMV674594 required only 24 hours to affect early stage gametocytes, but 72 hours to affect late stage gametocytes. Within the IMPs, several of the hits had a similar speed-of-action with a lag of 48 hours on both early and late stage gametocytes (e.g. MMV669286, MMV672652 and MMV652103). MMV669286 preferentially targeted early stage gametocytes within 24 hours. The DTP compounds inhibited the viability of both early stage gametocytes with a slow, and late stage gametocytes with a fast speed-of-action. The 6,9-IPs displayed slow to moderate killing speeds on both early and late stage gametocytes, except MMV892998 which had a fast onset of 24 hours on early stage gametocytes. The 2,6-IPs displayed fast killing rates against early stage gametocytes but were surprisingly slow killing towards the late stages. The speed-of-action evaluation for 2,6-IP, MMV688475, could not be determined due to limited availability of the compound.

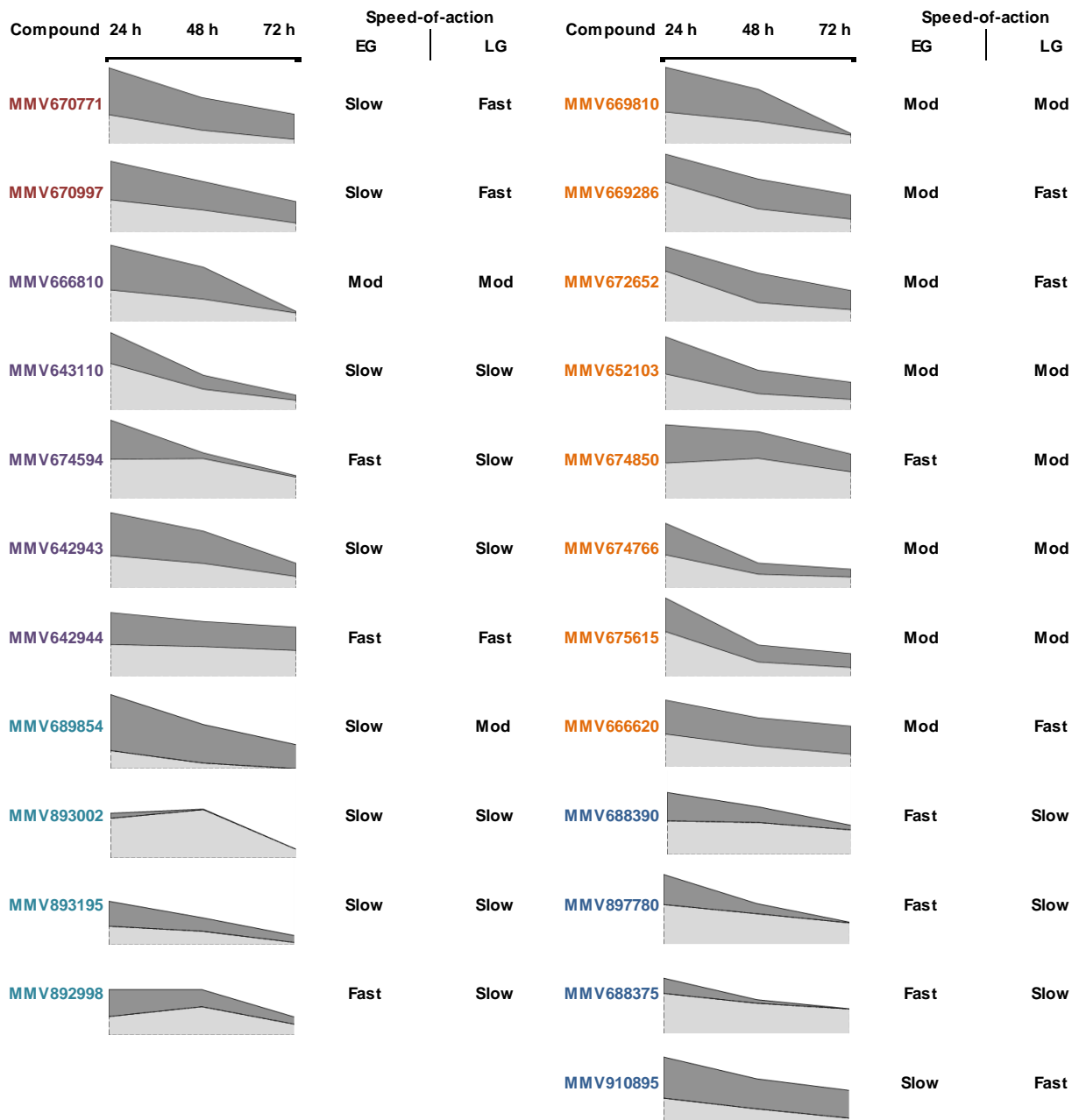


Figure 3.9: Speed-of-action evaluation for the most potent compounds. The DTP series are indicated in pink, the APs in purple, the IMPs in orange, the 6,9-IPs in turquoise and the 2,6-IPs in blue. Gametocyte viability (y-axis) was determined for 24, 48, or 72 hour (x-axis) drug pressure at $1 \times IC_{50}$ (determined at 48 hours). Dark grey = late stage gametocytes, light grey = early stage gametocytes. Speed-of-action was classified based on rate of onset of compound activity: fast ≤ 24 hour, moderate ~ 48 hour and slow ≥ 72 hours. EG: Early stage (II/III) gametocytes; LG: late stage (IV/V) gametocytes. Data are representative of at least three biological experiments, each performed in technical triplicates, \pm SEM.

To further interrogate late stage gametocyte activity, a subset of compounds was evaluated against $>95\%$ pure stage V, mature gametocytes. In order to confirm the maturity of these stages, obtained on day 13 of our gametocyte production protocol, the abundance of 18 transcripts of interest, usually more abundant in either late or mature gametocytes, was determined (Table 3.1). These 18 transcripts were selected from the Lopez-Barragan *et al.* and Young *et al.* datasets on PlasmoDB (v. 24; accessed on 30

April 2015) to represent all intra-erythrocytic life cycle stages of the parasite, including mature gametocytes [115, 499]. Transcripts such as Pf3D7_1302100, Pf3D7_0500800 and Pf3D7_0309100, expected in earlier gametocyte stages, were indeed more abundant in the day 10 (>95% stage IV/V) population. Similarly, transcripts that were expected in mature gametocytes (Pf3D7_1250100, Pf3D7_1038400 and Pf3D7_0411700) were upregulated in the mature, day 13 population (Figure 3.10). Additionally, the correlation ($r^2 = 0.18$) between the late and mature gametocyte expression profiles for this gene set was weak, reflecting the stage specificity of the populations produced.

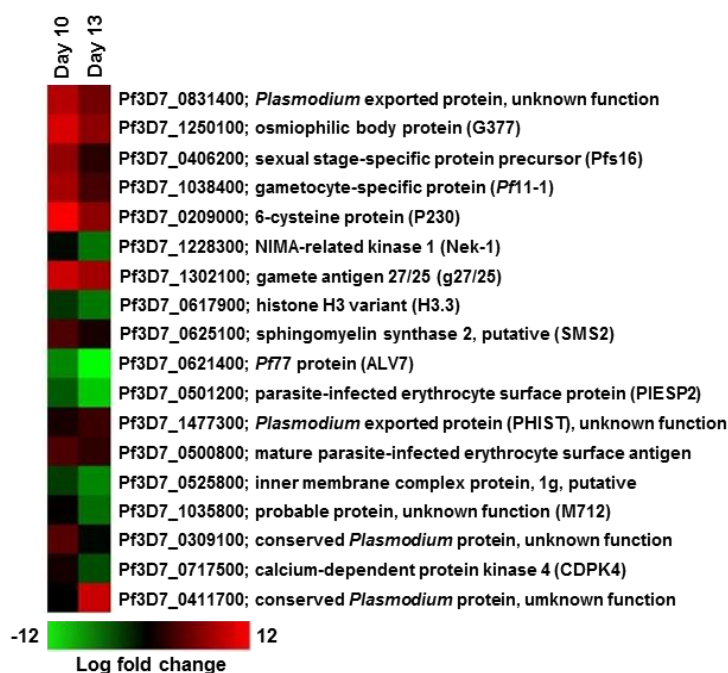


Figure 3.10: Stage-specific expression of 18 individual descriptors in late (>95% stage IV/V) and mature (>95% stage V) gametocytes. Semi-quantitative RT-PCR was performed, and data normalised to cyclophilin as household expression control and expressed as fold change relative to background expression of the transcripts in asexual parasites. Data are from $n \geq 4$ independent biological experiments each performed in triplicate. Under-expressed transcripts are presented in green and over-expressed transcripts in red.

The majority of 2-APs displayed <2-fold difference in activity between mixed stage IV/V and pure stage V, including pre-clinical candidate MMV642943 (Figure 3.11). Clinical candidate, MMV390048, displayed a 6.4-fold reduction in activity in mature compared to late stage gametocytes. The IMPs also displayed equipotent activity against stage IV and V gametocytes with MMV669810 at 1.4 nM versus 1.2 nM, respectively. Although the other IMP representatives displayed 2- to 10-fold losses in activity, the IC_{50} s were still in the low nanomolar range (<250 nM). The 6,9-IPs exhibited either decreased (MMV689854, MMV897780; 4 - 27-fold) or increased (MMV892998, MMV893002; 6 - 11-fold) activity towards mature gametocytes. The 2,6-IPs were exemplified by <10-fold

decreases in mature versus late stage activity. Mature stage IC₅₀s for both IP series were still in the nanomolar range, except MMV676245, which was only included in this analysis due to its borderline late stage gametocyte IC₅₀. This confirmed that these compounds can target and kill mature, transmissible gametocytes. The stage V gametocytocidal activity of the 2,6-IP, MMV688475, could not be determined due to limited availability of the compound.

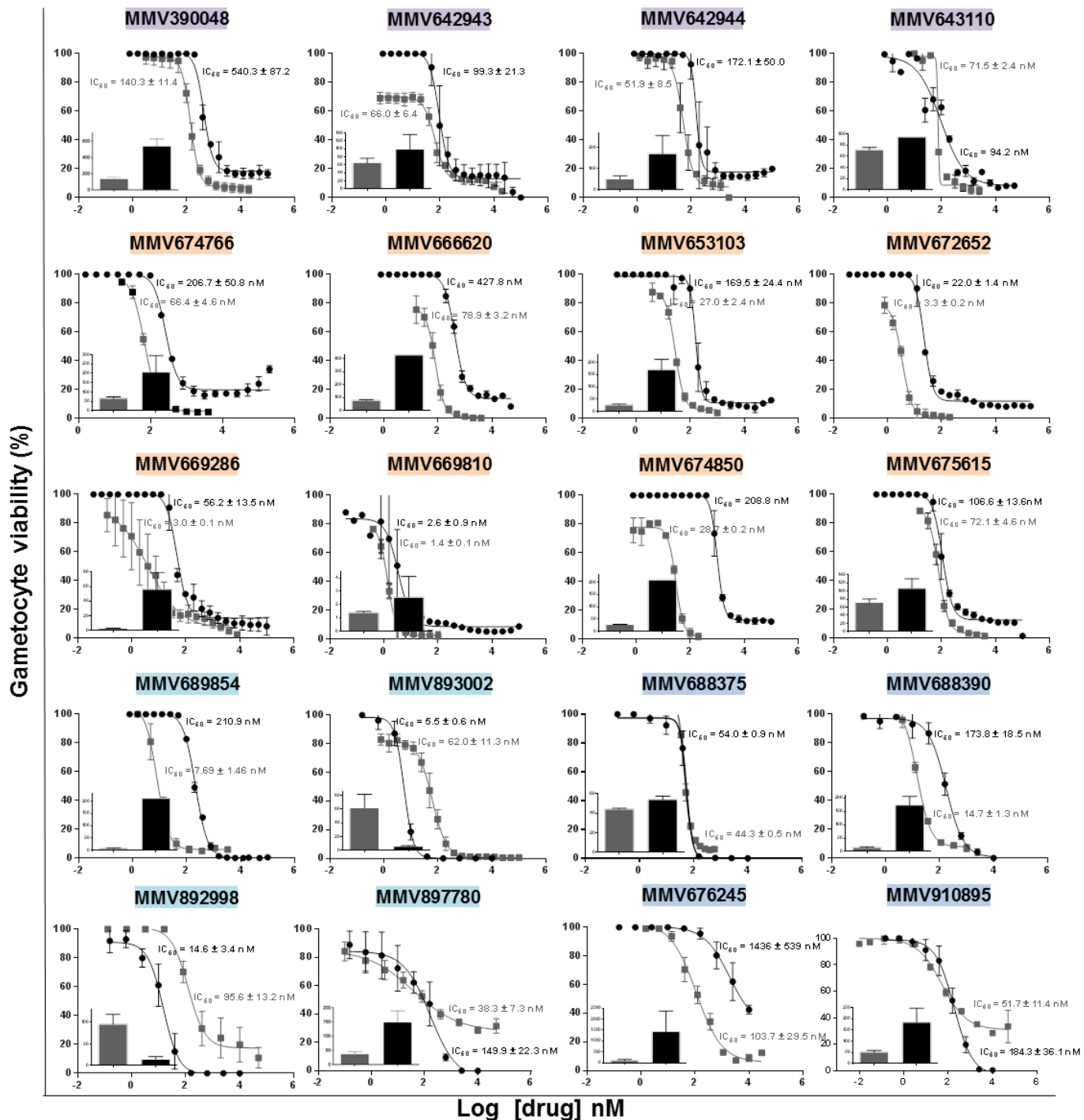
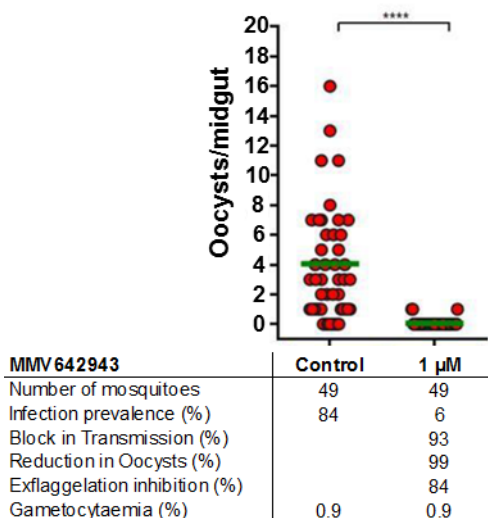


Figure 3.11: Late (>90% stage IV/V) and mature (>95% stage V) stage-specific activity of the hit compounds. The DTP series are indicated in pink, the APs in purple, the IMPs in orange, the 6,9-IPs in turquoise and the 2,6-IPs in blue. IC_{50} evaluation of the hit compounds (LG IC_{50} <100 nM) against the late (grey) and mature (black) gametocyte stages. The fold change in IC_{50} is indicated by the bar graph (bottom left of each dose-response curve). LG IC_{50} s for the 6,9-IPs and 2,6-IPs were obtained using the ATP bioluminescence assay. Data are representative of at least three biological experiments, each performed in technical triplicates, \pm SEM.

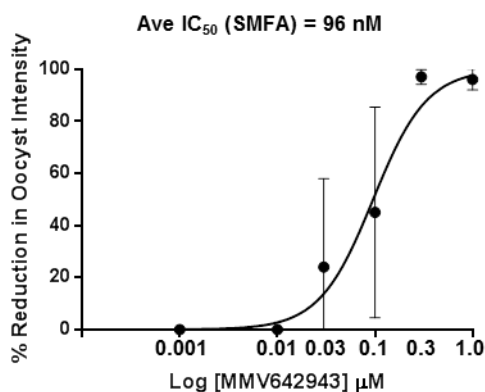
Late stage-specific activity translated directly into blocking transmission to mosquitoes, as evident from a significant reduction in oocyst density for both the 2-APs, MMV390048 [252] as well as MMV642943 (99% reduction in oocysts, Figure 3.12A). MMV642943

resulted in a 93% block in transmission (Figure 3.12A) with an IC₅₀ of 96 nM in SMFA (Figure 3.12B) compared with an IC₅₀ of 111 nM for MMV390048 [252].

A



B



MMV642943	Control	0.001 µM	0.01 µM	0.03 µM	0.1 µM	0.3 µM	1 µM
Number of mosquitoes	103	54	55	29	35	40	30
Infection prevalence (%)	80	54	69	84	59	16	10
Block in Transmission (%)		0	0	12	28	82	87
Reduction in Oocysts (%)		0	0	24	45	97	96
Exflagellation inhibition (%)		0	14	22	48	92	94

Figure 3.12: Transmission-blocking capacity of MMV642943 evaluated during indirect SMFA. (A) Effect of MMV642943 on oocyst intensity after 24 hour treatment (1 µM). The Mann Whitney Test was used to compare the statistical significance between the drug treatments and control. The total number of oocysts in a single mosquito midgut (red dots) and mean oocyst intensity of infection (green line) are indicated. $p < 0.0001$ as ****. **(B)** Dose-response of MMV642943 effect on oocyst intensity. Data are representative of at least three biological experiments, each performed in technical triplicates, \pm SEM, for a minimum of 17 fed mosquitoes at the highest concentration tested. (Note: This work was contributed by Sonia Lozano-Arias, Janneth Rodrigues and Esperanza Herreros (GSK, Tres Cantos) as part of the published manuscript).

3.3.4 Functional evaluation of dual active kinase inhibitors

To understand the functional consequence of inhibiting lipid kinases in the parasite, we used global gene expression analysis to evaluate the response of both asexual parasites and gametocytes following inhibition with the *Pf*PI4K inhibitors MMV390048 and

MMV642943. An appreciable and tractable drug-specific effect was observed on asexual parasite transcriptomes when treated for 48 hours, with 15-29% of the transcriptome differentially affected (\log_2 fold-change thresholds at >0.5 and <-0.5). However, a tractable transcriptional response was not observed at 24 hours, which confirms the described moderately slow action of these compounds, with a 24-48 hour lag period (see section 3.3.2; Figure 3.9) [252]. MMV390048- and MMV642943-treated asexual parasites responded nearly identically ($r = 0.96$, Figure 3.13A). The resultant transcriptional profiles were unique and did not show a close association with other antimalarials (Figure 3.13B) [500]. An enrichment map of the biological processes affected due to MMV390048 or MMV642943 treatment using moderately stringent statistical significance [$p < 0.05$, FDR $< 0.1\%$] included 47 gene sets over-represented after treatment (Figure 3.13C). A variety of different processes were affected as expected after inhibition of proteins involved in phosphatidylinositol 4-phosphate (PI4P) synthesis, which has pleiotropic functions involved in intracellular signalling and membrane maintenance. Protein phosphorylation, host cell invasion and intracellular signalling/transport were three particularly strongly affected communities, with multiple members within the nodes showing decreased gene expression after treatment, except for intracellular transport processes that showed increased abundance after treatment (Figure 3.13C).

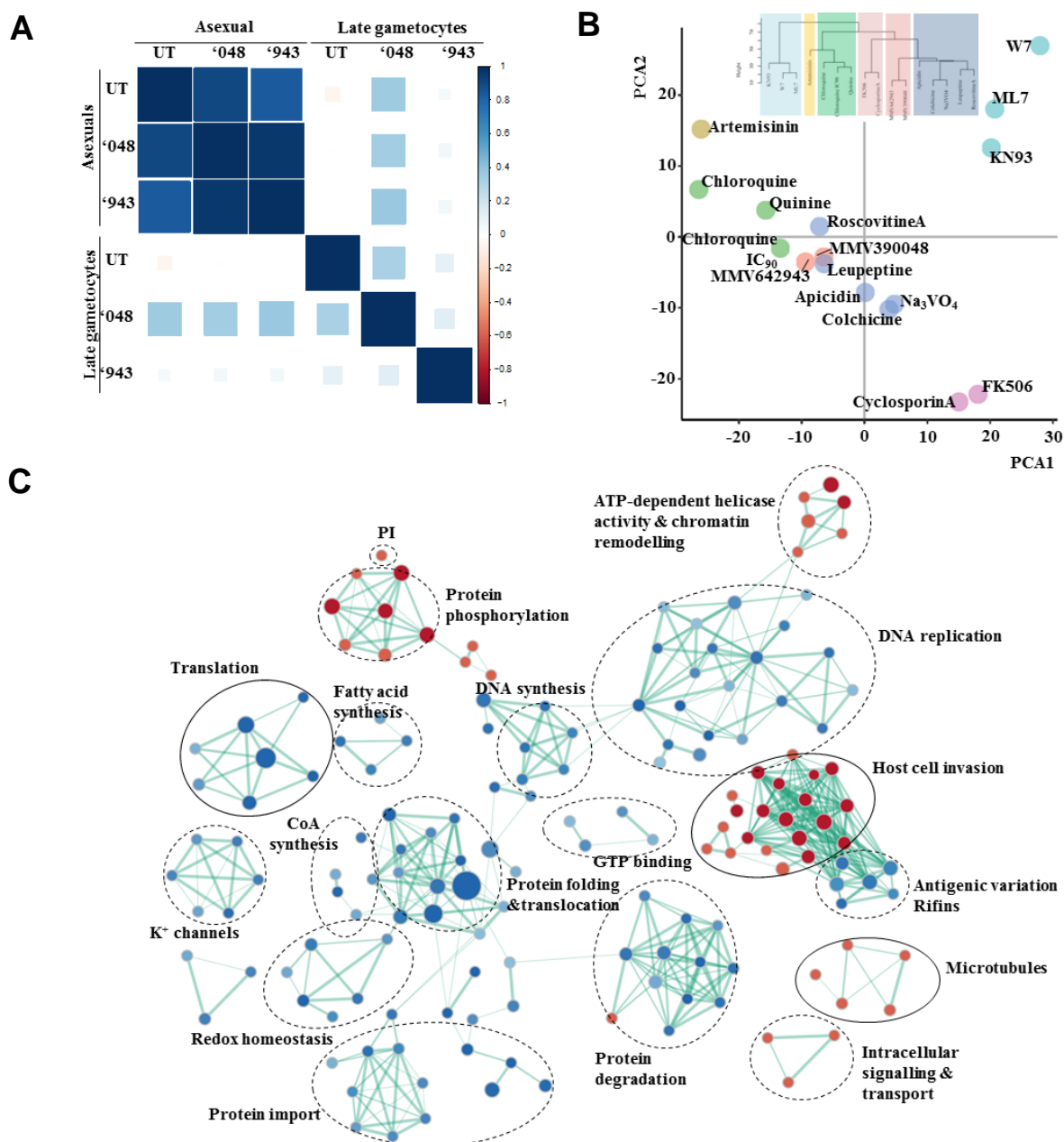


Figure 3.13: Transcriptional response evaluation of parasites treated with kinase inhibitors. (A) Pearson correlation analysis of the complete transcriptional profiles of either asexual parasites or late stage gametocytes treated with compound MMV390048 (048) or MMV642943 (943). (B) Principal component analysis (PCA) of MMV390048 and MMV642943 treated asexual parasites compared to the transcriptome of parasites with numerous other perturbations as described [500]. (C) Gene set enrichment map for *P. falciparum* parasites treated with MMV390048 and MMV642943. GSEA was performed with $p < 0.05$ and FDR $< 0.1\%$ using hierarchical clustering within nodes. Node sizes represent the number of members present in the node. Processes enriched in the treated population are indicated in red, while blue indicates processes enriched in untreated parasites. Hashed circles are processes only observed in asexual parasites, solid circles processes observed in both asexual parasites and in late stage gametocytes.

Moreover, processes like macromolecular synthesis, protein degradation, protein folding and translocation were severely affected in the treated populations, linked to *PfPI4K* inhibition. The transcriptional fingerprint for late stage gametocytes displayed similarly affected different biological processes including decreased macromolecular synthesis, lipid synthesis, gene expression and host cell invasion. However, life cycle differences

between asexual parasites and gametocytes were evident, as a reduction in protein degradation observed in asexual parasites was not enriched in gametocytes, which do not digest haemoglobin. This implies some divergence in the effect of inhibiting *Pf*PI4K in different life cycle stages.

3.4 Discussion

Dual active compounds are primary starting points for the generation of antimalarials that are able to treat clinical symptoms and are useful to eliminate malaria [4]. To our knowledge, this study provides the most in-depth evaluation of the lipid kinase inhibitor space for gametocytocidal activity and identifies compounds useful as starting points for the development of dual active antimalarials. Additionally, the potent activities observed against late stage gametocytes entice strategies prioritising gametocyte-selective activities as part of the newly defined target candidate profiles [3, 266, 501].

Our data indicate that, although some potential ion-channel modulators show potency against asexual blood stage parasites and gametocytes (e.g. *Pf*ATP4 inhibitors) [264, 502], those tested here (the DTP series) were generally poor inhibitors of gametocytogenesis. By contrast, compounds selected for their kinase inhibitor chemical background (2-AP, IMP, 6,9-IP and 2,6-IP series) yielded very active gametocytocidal compounds, while additionally maintaining their asexual activity. A 2- to 10-fold higher hit identification rate for the compounds tested here, compared with those typically seen by screening diversity-oriented libraries [264, 424, 443, 447, 482, 493, 503] supports the chemical signature for kinase inhibition previously alluded to as gametocytocidal [264, 405]. A total of 90 compounds were identified with submicromolar activity against late stage gametocytes, of which 21 were potent at <100 nM. Cross-validation of these hits on independent assay platforms and the presence of high selectivity towards the parasite provide confidence to the potency and usefulness of these hit compounds.

Gametocyte stage-specificity and speed-of-action of such potential transmission-blocking active compounds importantly confirmed that 85% of the hits (<100 nM activity) identified on stage IV/V populations maintained their inhibition against mature stage V gametocytes (fold change MG IC₅₀/LG IC₅₀ <10). The majority of the compounds acted after a 24 hour lag period on various stages of gametocytes, similar to the clinical candidate MMV390048 [252] and this effective time frame is sufficient to result in transmission blocking activity observed during SMFA, evident for the lead drug candidates (MMV390048 [252] and

MMV642943) reported here. The luciferase assay on late stage gametocytes, therefore, has some predictive capacity for transmission-blocking activity, confirming previous reports [426].

A subset of compounds preferentially targeted late stage gametocytes, similarly to what has been observed during other screens [264], raising questions as to the enhanced permeability of late stage gametocytes with a ghostlike erythrocyte and expression of perforin-like proteins that prepare the gametocyte for gamete egress [504, 505]. The different stage-specific preferences between compounds within the IMPs, 2-APs, 6,9-IPs and 2,6-IPs may indicate a propensity to target multiple members of structurally related parasite kinases while maintaining sufficient selectivity from human kinase inhibition [275, 363]. This scenario may indeed be preferable to inhibitors targeting single kinases that may be more prone to resistance development [275] as has been observed for IMPs and IPs that target multiple kinases depending on the different parasite stages during asexual development (e.g. Ca^{2+} -dependent protein kinase 1 [366, 368] and *Pf*PKG [368, 410]). The late stage gametocyte preference, observed for the 2-AP, 6,9-IPs and 2,6-IPs, provides appealing starting points from a transmission-blocking perspective for TCP-5 strategies [3]. Indeed, development of these as gametocyte-selective compounds would require new pharmacokinetic/pharmacodynamic models, independent of constraints that are associated with pharmacokinetic modelling of dual active antimalarials.

Several kinases that are associated with gametocytes/gametes [275] are clearly druggable [359], including lipid kinases like *Pf*PI3K and *Pf*PI4K, particularly in late stage gametocytes [249, 264, 447]. Chemogenomic fingerprinting of MMV390048 and MMV642943 revealed differentiated global effects between asexual parasites and gametocytes, as proteolysis required for haemoglobin digestion in asexual parasites is not observed as affected in gametocytes. Moreover, shared processes required for cytokinesis [249] are observed, resulting in dysregulation of invasion processes following schizogony and in late stage gametocytes in preparation for egress during gametogenesis.

Although the transcriptome of gametocytes differs from that of asexual parasites [115], the re-distribution of intracellular PI4P to the plasma membrane after *Pf*PI4K inhibition [249], does affect processes in gametocytes that rely on PI signalling and lipid transport (e.g. DNA replication, cytokinesis, axoneme motility, chromatin condensation and Rab11A-mediated membrane trafficking required for gametogenesis) [249, 351]. *Pf*PI4K and

*Pf*PIP5K synthesise PIP₂ from PI via PI4P. *Pf*PI4K and *Pf*PIP5K are, in turn, activated via phosphorylation by the cGMP-dependent kinase *Pf*PKG [161]. Phospholipid availability drives PI-specific PLC (PI-PLC)-mediated production of the secondary messenger molecules DAG and inositol-(1,4,5)-trisphosphate (IP₃) from PIP₂ [351]. This increase in IP₃ results in the rapid mobilisation of Ca²⁺ (within 10s of XA exposure) from the ER [506]. XA, a metabolic intermediate of the kynurenine pathway of tryptophan oxidation [507] as well as the ommochrome (eye pigment) synthesis pathway in insects [508], triggers guanylyl cyclase (GC α and GC β) activity in the gametocyte membrane, resulting in the synthesis of cGMP and *Pf*PKG activation [509, 510]. PIP₂ is subsequently re-synthesised at a rate similar to its hydrolysis, based on a positive feedback mechanism [351]. The intracellular Ca²⁺ increase potentially activates the calcium-dependent protein kinases *Pf*CDPK1 and *Pf*CDPK4 (cytokinesis) in male gametocytes [331], leading to the downstream activation of mitogen-activated protein kinase (*Pf*Map-2; gamete egress) and the cell division cycle protein CDC20 [322, 511, 512]. In female gametocytes, the Ca²⁺-mediated activation results in a sudden onset of protein synthesis due to the *Pf*CDPK1-regulated release of translationally repressed mRNAs [513]. *Pf*PI4K is, therefore, a key part of a phospholipid-driven signalling hub, involved in many core parasite processes. It represents a promising multi-stage target for antimalarial drug development.

3.5 Conclusions

In summary, a set of unique scaffolds with dual activity against both gametocytes and asexual parasites were identified from the gametocyte-selective screening of 379 ion-channel and kinase-focussed compounds. Dose-response yielded 21 hit kinase-focussed compounds with potent (<100 nM), moderate speed, late gametocyte-specific activity, maintained on mature gametocytes and translatable to transmission-blocking activity during DGFA and SMFA. Hit compounds additionally displayed *ex vivo* efficacy on contemporary African clinical isolates and were highly selective for the parasite. The functional evaluation of *Pf*PI4K inhibition on late stage gametocytes revealed that processes associated with PI4P re-distribution (e.g. macromolecular synthesis, lipid synthesis and gametocyte egress) were severely affected. Overall, the potent, late gametocyte preference of the 2-APs, IMPs, 6,9-IPs and 2,6-IPs expands the susceptibility profiles of these chemotypes, potentially targeting kinases in various stages of malaria parasites. This study entailed an in-depth evaluation of the kinase inhibitor space for gametocytocidal activity, highlighting the importance of targeting the kinase superfamily in malaria elimination strategies. Furthermore, the hit compounds reported here are enticing

starting points for the development of dual active antimalarial compounds or compounds targeting only gametocytes in transmission-blocking strategies.

CHAPTER 4

EVALUATION OF CHEMINFORMATIC APPROACHES TOWARDS THE IDENTIFICATION OF DUAL ACTIVE AND GAMETOCYTE-SELECTIVE SCAFFOLDS

4.1 Introduction

The focus of antimalarial drug development has shifted from control to elimination through targeting both the proliferative asexual stages and the non-proliferative sexual stages of the *P. falciparum* parasite. This is because the sexual stages maintain infection and facilitate the spread of evolutionary adaptations and drug resistance through meiotic recombination [3, 514]. The MMV has defined TCP-1 as entities with asexual stage activity and TCP-5 as transmission-blocking activity. The latter encompasses stage V gametocyte incapacitation, supported by early stage gametocytocidal activity as well as gamete and oocyst inhibition [3]. *P. falciparum* stage V (mature) gametocytes persist in circulation for up to 3 weeks with little morphological differentiation [256, 515], they are rarely affected by drugs active towards the asexual or early gametocyte stages [264, 438], male and female gametocytes are differentially susceptible [265] and compared to asexual parasites they are metabolically differentiated and quiescent [114, 516]. Even though these caveats drastically reduce the druggable pool of biochemical targets within this parasite, gametocytes still represent a highly targetable population bottleneck, due to the reduction in parasite numbers from $\sim 10^{11}$ to 10^2 from the replicative asexual to non-replicative sexual stages [266] as well as their presence in the blood compartment [33].

Currently, only artemether, artesunate, methylene blue and primaquine have activity towards gametocytes, with primaquine the only WHO clinically approved representative with late stage gametocytocidal activity [254]. Primaquine-ACT combinations are threatened by the emergence of ACT resistance in Asia [201, 205, 217, 224, 517] and Africa [225, 226, 518] and retain the possibility of toxicity of primaquine to G6PD deficient individuals [227]. Current compounds in the antimalarial development pipeline showing clinical efficacy against gametocytes include OZ439, KAE609 (spiroindolone; *Pf*ATP4 inhibitor), KAF156 (imidazolopiperazine; disphosphate galactose (*Pf*ugt) and coenzyme A (*Pf*act) transporter inhibitor), SJ733 (*Pf*ATP4 inhibitor), and DDD498 (elongation factor 2

inhibitor) [3]. However, with limited targets and scaffolds available and the continued risk of resistance development, unique non-endoperoxide chemotypes are required as essential components of novel antimalarials. These new drugs will likely have to be dual active (with TCP-1 and TCP-5 activities) or selective towards mature gametocytes (TCP-5 selective activity) [3]. Singular, dual active compounds with the same potency provide the opportunity to consolidate TCP-1 and TCP-5 activities, but have the potential to increase resistance development due to the expected prolonged therapeutic regime of such compounds to ensure TCP-5 activity. Combining separate compounds with either TCP-1 or TCP-5 activity could overcome this, but might be restricted by developmental cost, pharmacological difficulties in combination compatibility and safety assessments (clinical observation, metabolic modelling) [3]. A TCP-5, gametocyte-selective compound should display improved activity towards late stage (IV/V) gametocytes as compared to the asexual stage parasites, reflected by a fold change in IC_{50} .

Several diverse and target-focussed chemical entities with proven asexual stage activity have been screened using different assay readouts (Table A4.3). These compounds all have similar trends in activity, with maximal potency observed against the asexual stages, and typically a 4- to 10-fold reduction observed in activity against the gametocyte stages (Figure 4.1). However, dual active chemotypes have been identified and include diaminoanthraquinones (DANQ) [424], certain quinolines (including primaquine and mefloquine), anthracyclines, dihydroergotamine-type adrenergic agents, as well as inhibitors of kinases [405], protein biosynthesis, the proteasome, protein modification and membrane trafficking, phospholipid metabolism [519] and ion homeostasis [264, 446, 503] (Table A4.3). However, gametocyte-selective chemical classes include endoperoxides [439], acridines [482], tripeptide epoxyketones [436], carbamazide thioureas, naphthoquinones, dioxonaphthalen-acetamides [264], quinacridines [493], 2,4-diaminopyrimidines, 1,2,3,4-tetrahydroacridines, 3-amino-imidazo[1,2-a]pyridines, 3H-imidazo[4,5-b]pyridines [363] and novel artemisinin derivatives [520] (Figure 4.1 and Table A4.3). Moreover, TCP-5 selective representatives have been identified from diverse chemical collections such as the MMV box set [439], the Sytravon library [363] and the TCAMS library [405, 503].

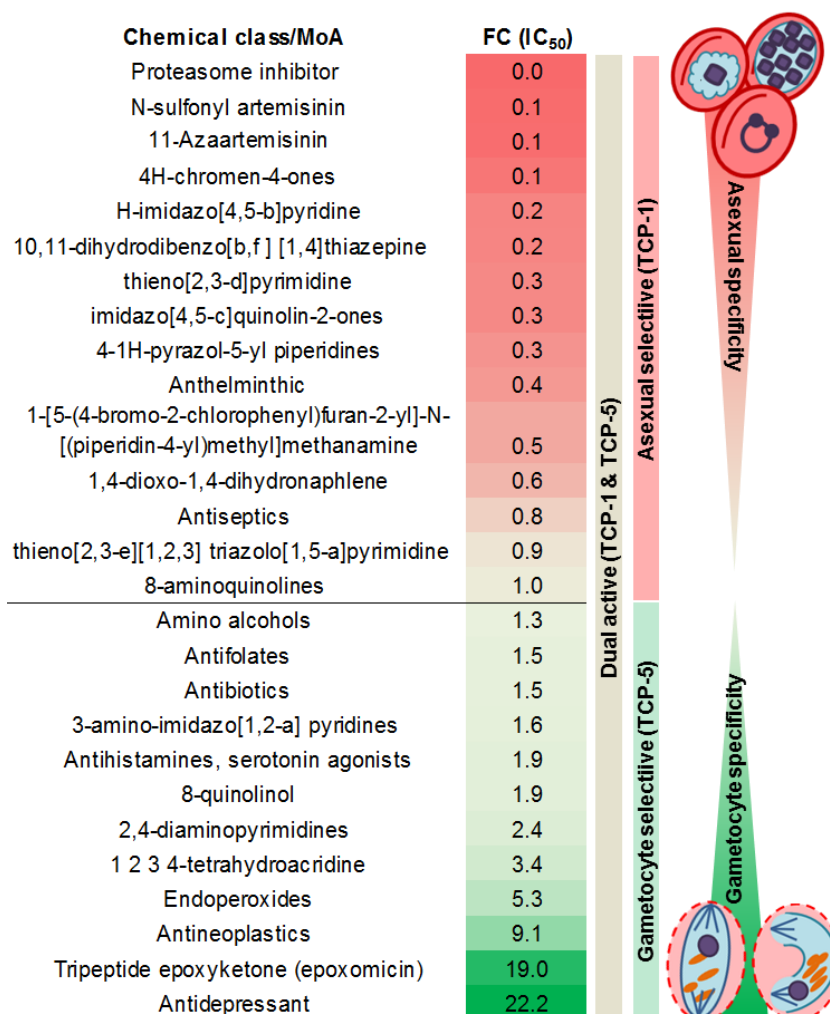


Figure 4.1: Spectrum of activity of compounds screened for gametocytocidal activity (created with information from [363, 436, 439, 441, 447, 482, 503, 519, 521, 522]). Scaffolds from diverse- and focussed collections, pre-screened for asexual stage activity, typically display a decreased gametocytocidal profile ($FC < 1.0$), but gametocyte-selective chemotypes have been identified ($FC > 1.0$). FC = ratio of asexual stage IC_{50} to late stage (III-IV) IC_{50} . MoA = mode of action.

Although numerous gametocytocidal compounds have been identified based solely on activity data, none have been promoted as gametocyte-selective and no chemical features have been directly associated with this activity. The large amount of data now available lend itself to meta-analysis, and cheminformatics encompasses semi-automated *in silico* techniques, key to the elucidation of SARs, that might therefore be useful towards the identification of novel TCP-5 selective compounds and/or scaffolds from these datasets.

Cheminformatics enables the processing of massive data collections by simple and sophisticated *in silico* mathematics in order to mine and navigate the chemical, property and bioactivity space for SAR associations [523, 524]. Basic cheminformatic tools enable molecular editing, automated chemical nomenclature, coding and annotation of chemical reactions, substructure searches [525, 526] and pattern recognition (Markush, fingerprint,

3D-pharmacophore, regression, decision tree, hierarchical and non-hierarchical clustering, self-organising maps (SOM) [525, 527]. More advanced tools include high throughput virtual screening, 2D and 3D molecular dynamics modelling (includes forecasting chemical and biological ADMET properties), docking, ligand and target-based pharmacophore modelling and quantitative structure-activity relationship elucidation [523, 525]. These basic and advanced approaches have been used in the identification of compounds with *P. falciparum* asexual stage activity [363, 402, 403, 528-536] as well as in target-based drug design towards TCP-1 focussed drugs [528, 531, 532, 537-551]. However, TCP-5 selective, transmission-blocking drug discovery is limited to scaffold clustering and analogue searches [264, 363, 405, 493] as well as fundamental network analysis [264]. This endeavour is additionally restricted by the low number of gametocytocidal compounds identified (typical hit rate: 0.3-9% [4], Table A4.3), which usually have reduced activity as compared to the asexual stages. Moreover, most of these hits are identified from diversity sets and therefore structurally dissimilar, making it difficult to define a gametocyte-selective (TCP-5) scaffold.

DataWarrior's [527] cheminformatics applications have been applied for drug discovery in the fields of virology [552-555], neuroscience [556-559], endocrinology [560], tuberculosis [561], cancer [562-570], herbicides [571], antibiotics [572], inflammation [573], industrial chemical safety assessments [574] as well as in the malaria field [575-578]. DataWarrior calculates molecule similarities by comparing two descriptors derived from the molecular structure. Both the nature of the descriptors and the algorithm applied to compare them, determines the similarity value which can then be applied during chemical clustering, SOMs and activity cliff analysis [527]. The structure-activity landscape index (SALI) analysis allows the correlation of functional motifs to measured properties (biological, physicochemical) as well as tiny structural changes to activity cliffs visible on an easily interpreted 2D map [527]. Inferring SARs is therefore greatly simplified as compared to chemical clustering which does not relate biological activity to structural characteristics.

In this study, we propose the use of simple cheminformatic approaches to identify novel chemical scaffolds that have either dual activity or display gametocyte-selectivity, from a chemically diverse training set as well as a series of kinase-focussed inhibitors, towards consolidating TCP-1 and TCP-5 criteria as set forth by the MMV. Both dual active and gametocyte-selective chemotypes were identified, which are chemically tractable, have

favourable physicochemical properties and are promising starting points for the development of transmission-blocking chemotherapies.

4.2 Methods and materials

4.2.1 Datasets

The first dataset comprised 13 533 compounds from the TCAMS set, data which was released by GSK after successful screening of the GSK Corporate Collection (~2 million compounds) [402]. The TCAMS set all displayed >80% inhibition at 2 μ M on asexual stages, and 405 of these compounds achieved >53% inhibition of stage V gametocytes at the same screening concentration [405]. This subset of 405 compounds, evaluated for dose-response, were used to interrogate various cheminformatic approaches, with the goal of identifying and validating a robust method for the identification of either dual active or gametocyte-selective chemotypes. The TCAMS set comprises structurally diverse compounds with physicochemical traits suitable for the discovery of orally active drugs [402, 579], with a few small deviations from Lipinski's rules [489] (Table A4.1, appendix). Unique identifiers, as well as structural information (simplified molecular-input line-entry system (SMILES) notations, molecular weights), were obtained from the ChEMBL-NTD database (<http://www.gsk.com/responsibility/downloads/GSK-CR-2009>). No data was available on the solubility of the TCAMS dataset. Compounds were included in the chemical clustering below, based on the following cut-off: gametocyte-selective activity: stage V IC_{50} <2500 nM and TCP-5 selectivity >1.0.

The second dataset contained all the compounds from the kinase-focussed inhibitor series (DTPs, 2-APs, IMPs, 6,9-IPs and 2,6-IPs) from Chapter 3. SMILES notations and limited physicochemical properties were obtained from our collaborators at H3D, UCT (Table A4.2). The kinase inhibitors were derivatised and/or selected with favourable physicochemical properties in mind.

4.2.2 Biological and physicochemical data acquisition

Biological data (asexual stage IC_{50} , stage V gametocyte IC_{50} and HepG2 IC_{50} (SI)) for the TCAMS set was obtained from Miguel-Blanco *et al.*, (2017) [405]. The kinase inhibitor series biological data were obtained from Chapter 3 as well as the ScienceCloud database (project number: MMV09/0002). Additionally required physicochemical properties were predicted *in silico* using Osiris DataWarrior v 4.2.2 (www.openmolecules.org). The TCP-5

selectivity factor was defined as the fold change between IC_{50} against asexual stages and either stage V gametocyte IC_{50} (TCAMS dataset) or final late (stage IV/V) gametocyte IC_{50} (kinase-focussed inhibitor series).

4.2.3 Chemical clustering of the TCAMS dataset

The reduced 83-compound subset that adhered to the cut-offs imposed (stage V IC_{50} <2500 nM and TCP-5 selectivity >1.0) was clustered using the *Skel/Spheres* descriptor and complete linkage clustering algorithm, by applying a Tanimoto similarity threshold of 0.55, implemented in Osiris DataWarrior v 4.2.2 (<http://www.openmolecules.org>).

4.2.4 Physicochemical properties and activity associations

SALI analysis of both the TCAMS and kinase-focussed datasets was performed using Osiris DataWarrior v 4.2.2 (www.openmolecules.org). DataWarrior applies a unique Rubberbanding Forcefield approach which translates similarity faster and better than PCA or SOM, uses the available space more efficiently and works with any of DataWarrior's similarity criteria [527]. During SALI analysis, a similarity map of all involved molecules is created, while modulating the similarity threshold from molecule to molecule in order to account for similar neighbour structures. Molecules are positioned in a 2D area such that similar neighbours are located close to each other and connected by a connecting line, the length of which represents the strength of the relationship. Compounds are further characterised within the landscape by superimposing stage-specific gametocytocidal activity using the size and colour intensity of markers as well as the background colour intensity to represent asexual stage activity. This enables the visualisation of hit compounds as activity cliffs in the 2D space. In this study, the *Skel/Spheres* descriptor was used as similarity criterion and takes into account stereochemistry, duplicate fragments and heteroatom depleted skeletons.

4.2.5 Prediction of the physicochemical parameters that contribute to asexual and gametocyte-selective activity within the TCAMS dataset

A selection of physicochemical parameters were chosen as predictor variables to describe the observed variation in either asexual stage IC_{50} or stage V IC_{50} as the response variable in a multiple linear regression approach. The physicochemical predictor variables included the cLogP (atomic cut-off: 20), PSA [580] as well as number of HBA, HBD, aromatic rings, amine moieties, amide moieties and electronegative atoms. These

properties were determined *in silico* using Osiris DataWarrior v 4.2.2 (www.openmolecules.org). The contribution of the predictors to the observed variation was assessed during a stepwise multiple linear regression analysis, applying backward elimination using Minitab 18 statistical software.

4.2.6 Determination of SARs within the kinase-focussed series

R-group deconvolution of the kinase-focussed inhibitors was performed in Osiris DataWarrior v 4.2.2. Core-based SAR Analysis was performed, involving manual core input and review of core and substituent outputs. Core scaffolds and R-group substituents were manually validated and edited where necessary. R-group deconvolution results were used to identify the structural core, scaffolds (based on the least substituted R-group) and substituents of hit compounds. The TCP-5 selectivity value was used to identify gametocyte-selective compounds and scaffolds (FC >1.0). The criteria in Table 4.1 were used to identify any possible liabilities of the compounds. These benchmarks were adapted from those defined by the MMV (partner meeting, October 2017, Geneva) [3] and Paquet *et al.*, (2012) [383] for gametocyte-selective, druggable compounds.

Table 4.1: Criteria for the characterisation of gametocyte-selective compounds.

Compound property	Criterion
Lipophilicity (cLogP)	<5
Solubility (pH 6.5)	≥40 μM
Asexual stage activity (NF54 IC ₅₀)	≤50 nM
Asexual cross resistance (K1 IC ₅₀)	≤50 nM
Late stage gametocyte IC ₅₀	≤100 nM
Cytotox IC ₅₀ /SI	>10 uM/>10
TCP-5 selectivity	FC >1.0
DGFA IC ₅₀ (female/male)	≤100 nM
Activity SMFA	@ 1 μM

TCP-5 selectivity = fold change of asexual stage IC₅₀ to late (stage IV/V) IC₅₀.

4.3 Results

4.3.1 Interrogation of cheminformatic approaches using the TCAMS dataset

4.3.1.1 Chemical clustering

To assess the chemical diversity of gametocyte-selective compounds, the 405 hits were filtered by imposing a cut-off of stage V IC₅₀ ≤2500 nM and TCP-5 selectivity ≥1.0. This resulted in an 83-compound subset that was subsequently clustered using a complete linkage clustering algorithm (Osiris DataWarrior) by applying a Tanimoto similarity threshold of 0.55, classifying the compounds into 12 clusters and 3 singletons. Clusters 1,

2, 5 and 7 as well as singletons 3 and 4, displayed mean TCP-5 selectivities of 20.42 ± 14.33 , 9.76 ± 9.69 , 6.91 ± 4.59 , 4.07 ± 1.87 , 27.13 and 20.69 (Figure 4.2A). Compounds within these clusters show structural similarity and are associated with mostly pyridyl, thioamide and amine moieties (Figure 4.2B). Representatives with the highest TCP-5 selectivity values (20- to 47 fold) were present in clusters 1 and 2, as well as singletons 3 and 4. Clusters with lower TCP-5 selectivity values (right-hand side of Figure 4.2B) were structurally separated from gametocyte-selective clusters and bore different functional groups, affirming the validity of the approach.

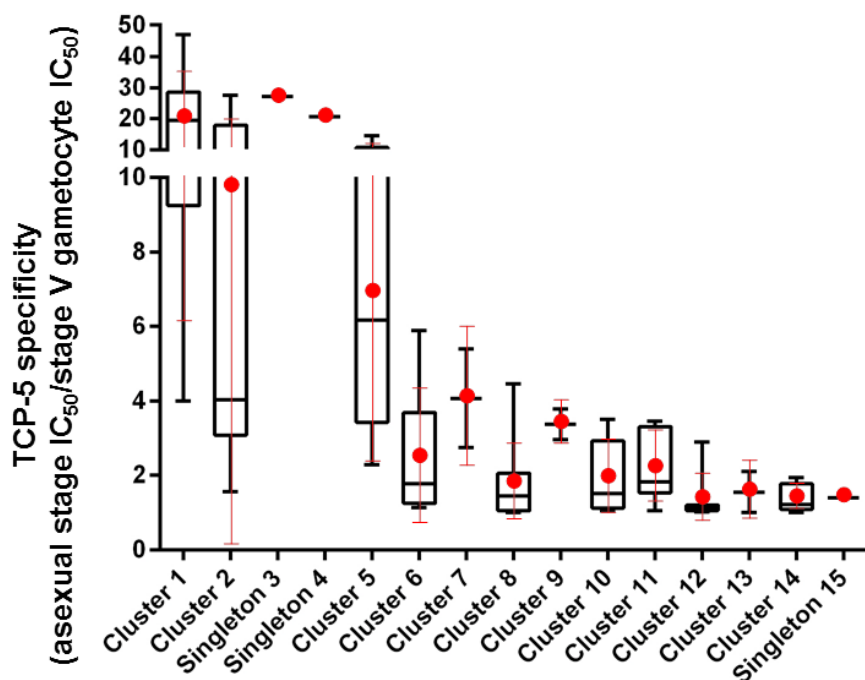
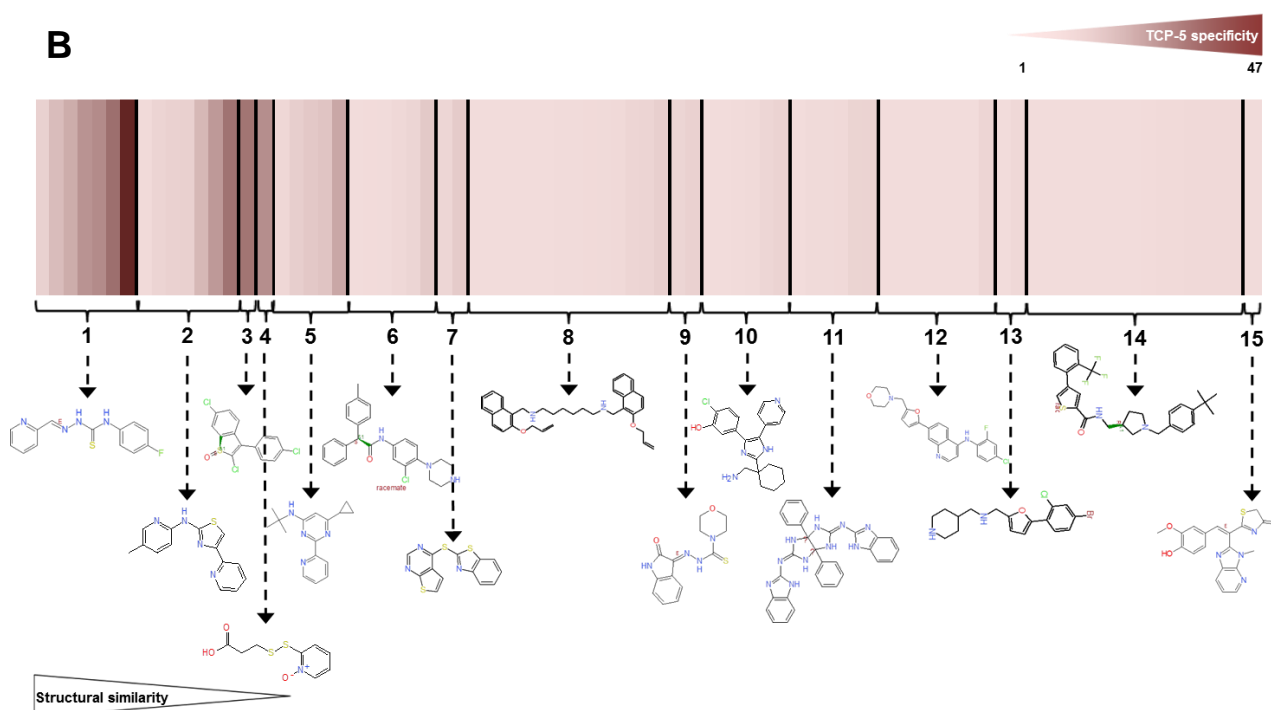
A**B**

Figure 4.2: Identification of gametocyte-selective chemotypes through chemical clustering. (A) Box and whisker plot of TCP-5 selectivity (asexual stage IC_{50} /mature (stage V) IC_{50}) over chemical clusters. The mean TCP-5 selectivity value and standard deviation are indicated in the overlaid graph (red). (B) Twelve clusters and three singletons belonging to the 83 compounds profiled. Members from each cluster are arranged in order of increasing mean TCP-5 selectivity. The cluster number is indicated together with a representative structure.

The chemical clustering approach was able to highlight TCP-5 selective clusters and gave preliminary information as to the functional moieties responsible for this selective activity. In order to derive finer SARs for the 83-compound TCAMS dataset, chemical feature

extraction and biological activity association was performed, using a similarity and activity cliff analysis.

4.3.1.2 Physicochemical space extraction

Towards elucidating SARs and associating this to either dual or gametocyte-selective activity, structure-activity landscape analysis was performed. The SALI analysis allows multiple levels of biological information to be incorporated, which permits finer inferences with regards to SAR to be made. Structure-activity landscape analysis of the 83-compound subset mirrored the diversity of the TCAMS dataset, as reflected by the limited connectivity between compounds and high number of singletons observed (Figure 4.3). The increased structural diversity seen is additionally due to the higher similarity threshold (Tanimoto >0.80) imposed during SALI analysis as compared to the complete linkage clustering (Tanimoto >0.55) in section 4.3.1.1. The latter was chosen to replicate the analysis in Miguel-Blanco *et al.*, (2017), whereas the SALI analysis was performed at the lowest possible threshold.

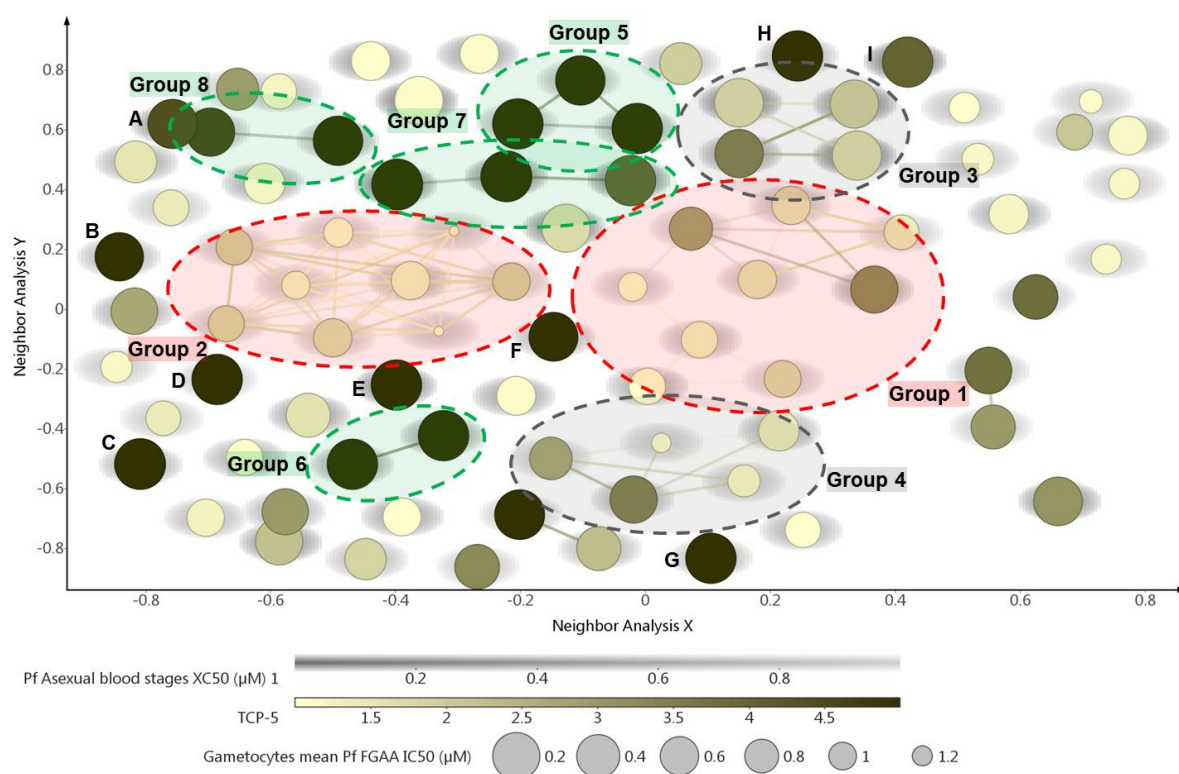


Figure 4.3: Structure-dual activity landscape analysis of the TCAMS subset. Pairwise stage V gametocyte activity to structural feature (*Skel/Sphere*) analysis was performed on 83 compounds with activity cliff analysis (Osiris DataWarrior v 4.2.2), at a stringency of 80% in structural characteristics. Increasing mature (stage V) potency is indicated by increasing marker size, TCP-5 selectivity by increasing colour intensity and asexual potency by increasing background colour intensity. Potential asexual actives are shaded by red ellipses, dual active by grey and gametocyte selective shaded by green. A = TCMDC-137908; B = TCMDC-125529; C = TCMDC-125752; D = TCMDC-124011; E = TCMDC-123745; F = TCMDC-125826; G = TCMDC-141973; H = TCMDC-125854; I = TCMDC-139725.

The SALI analysis resulted in seven groups which could be classified as either asexual selective, dual active or gametocyte-selective based on (i) number of connections between neighbouring compounds, (ii) dual activity or (iii) TCP-5 selectivity. Although groups 1 and 2 were highly connected with high structural similarity, these groups contained compounds with primarily asexual activity. Groups 3 and 4 are associated with mostly dual active compounds, whereas TCP-5 selectivities (>5) are reflected strongly in groups 5-8. Members in these groups displayed TCP-5 selectivity values as high as 28. Although these groups contain the least number of compounds and are structurally diverse, the sensitivity of the SALI analysis allowed finer structural nuances to be defined. For instance, groups 5 and 7 clearly separate on the SALI analysis, but were clustered together during the previous analysis (cluster 1, Figure 4.2). Moreover, the SALI analysis identified additional singletons with TCP-5 selectivity such as TCMDC-124011 (TCP-5 selectivity = 27; D on Figure 4.3), TCMDC-141973 (TCP-5 selectivity = 21; G on Figure 4.3) and TCMDC-125854 (TCP-5 selectivity = 28; H on Figure 4.3). The most gametocyte-selective singleton (TCMDC-125752; TCP-5 selectivity = 47, C on Figure 4.3) is structurally far removed from any other nodes, indicating the potential use of this compound as distinctive chemical starting point for transmission-blocking drugs.

The TCP-5 enriched groups (5-8) and dual active groups 3 and 4 were subsequently interrogated separately to reveal inter- and intra-cluster relationships. SALI analysis of the gametocyte-selective groups confirmed the abundance of pyridyl, thioamide and amine moieties (Figure 4.4), presumed to be required for the TCP-5 selective activity of the TCAMS dataset.

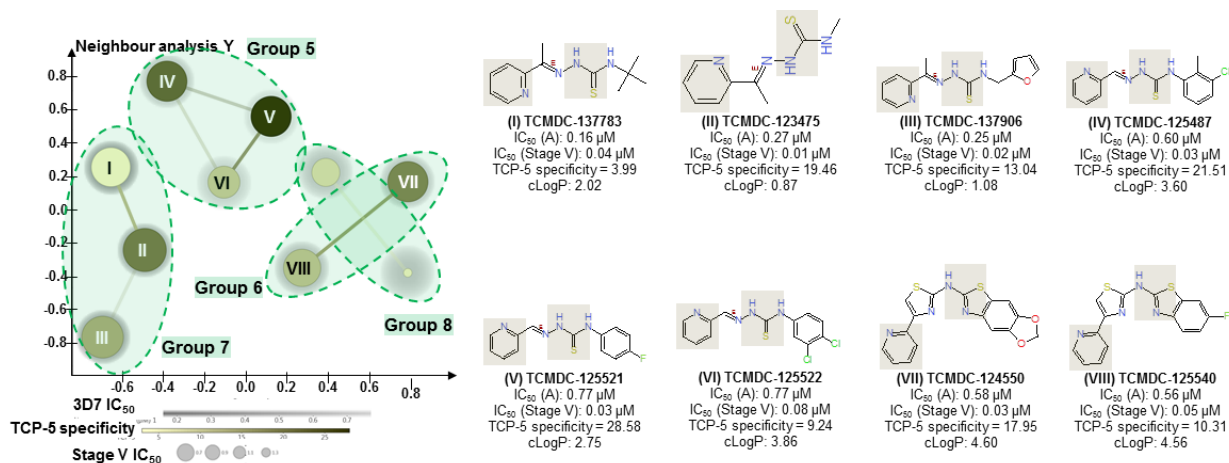


Figure 4.4: Inter-cluster structure activity landscape interrogation of gametocyte-selective nodes 5-8. Pairwise stage V gametocyte activity to structural feature (*SkelSphere*) analysis was performed with superimposed activity cliff analysis (Osiris DataWarrior v 4.2.2) at a stringency of 80% in structural characteristics. Increasing mature (stage V) potency is indicated by increasing marker size, TCP-5 selectivity by increasing colour intensity and asexual potency by increasing background colour intensity. R-groups are indicated (light brown). A = asexual parasites; Stage V = mature stage V gametocytes.

Intra-cluster SALI analysis of potential dual active groups revealed that the TCP-5 selectivity of compound TCMDC-139089 (group 3) is due to the electron-withdrawing chloro-phenyl moiety at R3 (Figure 4.5A). Similar interrogation of group 4 showed that cycloalkyl groups bearing terminal amines (R2) are responsible for the gametocyte-selectivity observed here (Figure 4.5B).

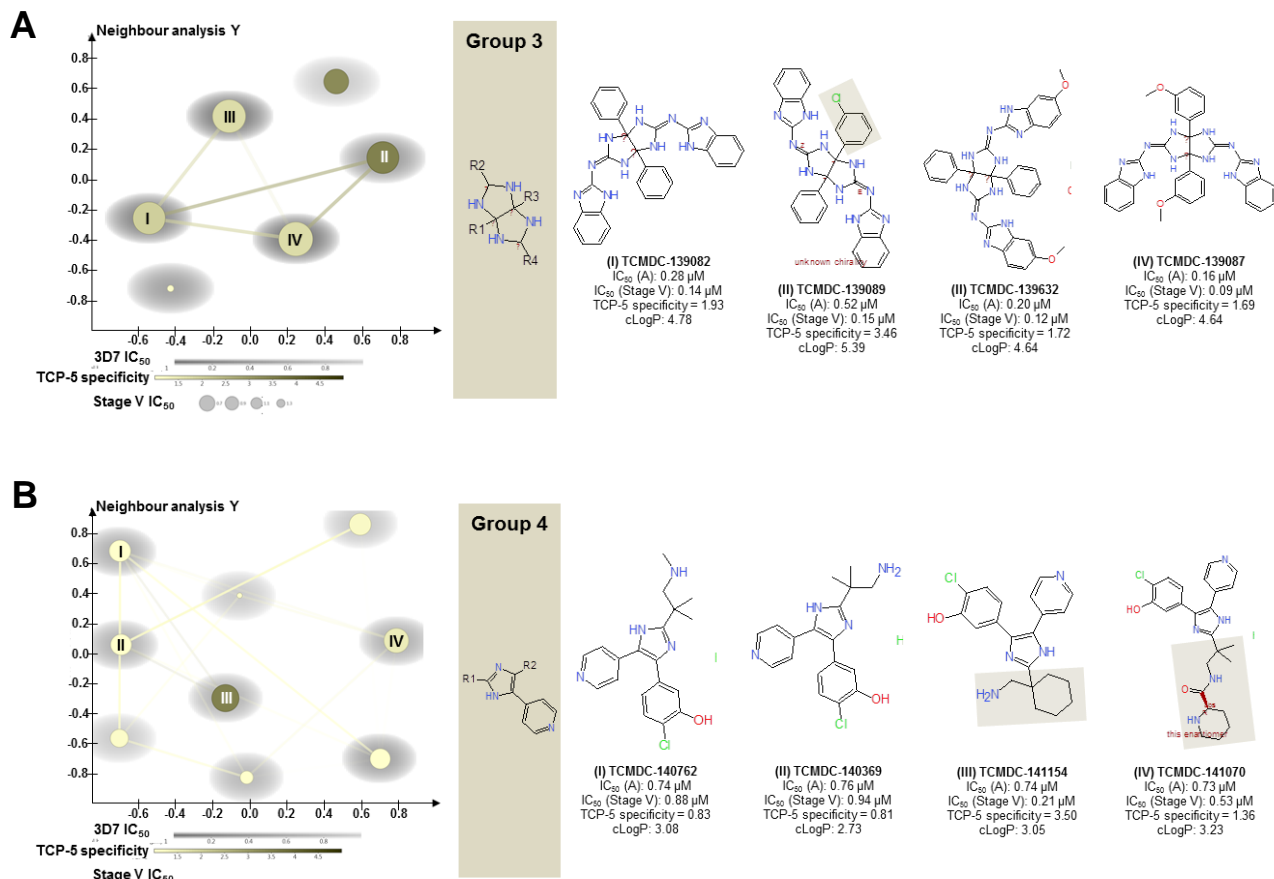


Figure 4.5: Intra-cluster structure activity landscape interrogation of groups 3 (A) and 4 (B). Pairwise stage V gametocyte activity to structural feature (*Ske/Sphere*) analysis was performed with superimposed activity cliff analysis (Osiris DataWarrior v 4.2.2) at a stringency of 80% in structural characteristics. Increasing mature (stage V) potency is indicated by increasing marker size, TCP-5 selectivity by increasing colour intensity and asexual potency by increasing marker colour intensity. R-groups are indicated (light brown). A = asexual parasites; Stage V = mature stage V gametocytes.

Both the inter- and intra-cluster SALI analyses revealed that predictive lipophilicity is not an indicator of the differential activity or TCP-5 selectivities observed, as cLogP values ranged from 0.9-5.6 for gametocyte-selective compounds. This discrepancy prompted further evaluation of the possible contribution of physicochemical properties to the gametocytocidal activity of the TCAMS dataset.

4.3.1.3 Quantitative evaluation of the physicochemical contribution to asexual and gametocyte-selective activity

Based on the suggestion that there may be a physicochemical contribution to gametocytocidal activity, the 405-compound TCAMS subset (evaluated for dose-response) was interrogated to determine the contribution of various physicochemical properties (predictor variables) to gametocyte-selective activity in a multiple linear regression approach. As asexual stage IC_{50} is used to determine TCP-5 selectivity, the contribution of the predictor variables to this response variable was also assessed. The maximum

contributors considered for both response variables included cLogP, PSA as well as the number of HBAs, HBDs, aromatic rings, amines, amides and electronegative atoms. A backward elimination approach was followed in Minitab to eliminate those properties not contributing to IC₅₀ variance. Briefly, backward elimination entails (i) selecting a significance level, (ii) fitting all possible predictor variables, (iii) considering the predictor with the highest *p*-value, (iv) if the *p*-value >significance level, removing that predictor, (v) fitting the data again and (vi) finishing once all *p*-values are <significance level.

Table 4.2: Multiple linear regression of asexual parasites versus stage V gametocyte IC₅₀ related to physicochemical descriptors.

Predictor variable	Adj SS	Rank estimate (F-ratio)	<i>p</i> -value
Asexual stages			
Aromatic rings*	12.22	13.19	0.000
Amines*	2.99	3.23	0.073
Amides*	5.43	5.86	0.016
Electronegative atoms	4.81	5.19	0.023
			<i>R</i> ² (adjusted)= 0.07
Stage V gametocytes			
Polar surface area*	2.86	3.27	0.071
Amines*	23.31	26.59	0.000
Amides*	15.97	18.22	0.000
			<i>R</i> ² (adjusted) = 0.12

Adj SS: Adjusted sum of squares; it refers to the unique portion of SS regression (variation) explained by a factor, given all other factors in the model regardless of the order in which they were entered. *If F-ratio>1.0, then the model has statistically significant predictive capability and is influenced by the number of variables (degrees of freedom) needed to achieve it. *p* <0.1.

PSA, as well as amine and amide counts, were kept as physicochemical predictor variables of stage V gametocyte IC₅₀ (Table 4.2). This was based on the significance level cut-off of *p* <0.1, as well as the adjusted sum of squares (SS) and F-ratio >1.0 observed for these descriptors. This evaluation was able to account for 12.4% of the variance observed for gametocyte-selective activity. For the asexual stage IC₅₀, aromatic ring, amine, amide and electronegative atom counts were retained as predictor variables (Table 4.2). Selection was based on the same significance level, adjusted SS and F-ratio cut-offs, and accounted for 7.4% of the variance observed for asexual stage IC₅₀.

The fine structural nuances achieved for the TCAMS dataset, and the ability to relate chemical features to TCP-5 selectivity using the SALI analysis, prompted a similar evaluation of the kinase-focussed inhibitors from Chapter 3.

4.3.2 Establishment of the cheminformatic approach using a kinase-focussed inhibitor series

The cheminformatic approach, validated in section 4.3.1, was subsequently used to interrogate the kinase-focussed inhibitors from Chapter 3 to highlight functional moieties

potentially responsible for gametocyte-selective (TCP-5) activity. The kinase-focussed compounds were subsequently profiled as either dual active (TCP-1 and TCP-5) or gametocyte (TCP-5)-selective.

4.3.2.1 Physicochemical space extraction

Data in Chapter 3 of this thesis for the kinase-focussed inhibitors indicated that these chemotypes were active towards both the proliferative asexual stages as well as the non-proliferative, transmissible gametocyte stages of the parasite. Due to the availability of early gametocyte IC_{50} data for these series, this additional level of biological information could be incorporated into the SALI analysis. To identify potential associations between chemical features and biological activity, both inter- and intra-series SALI analysis were performed. Chemotypes clustered together, and very little inter-series overlap was observed when performing a SALI neighbour analysis of the kinase-focussed inhibitor chemotypes displaying sub-micromolar late stage gametocyte IC_{50} s (Figure 4.6). This reflects the structural uniqueness of each scaffold (DTP, 2-AP, IMP, 6,9-IP and 2,6-IP) interrogated here.

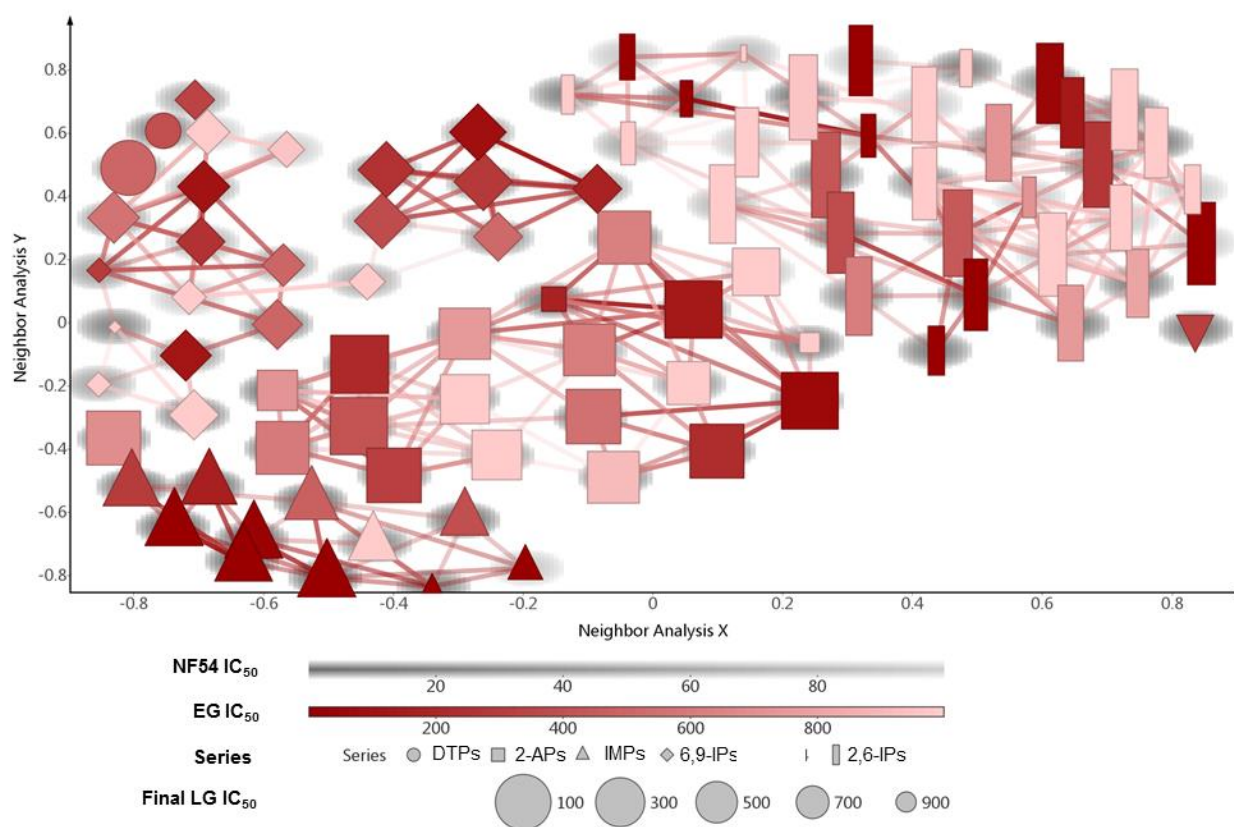


Figure 4.6: Inter-series delineation of multi-stage activity of kinase chemotypes. SALI plot of pan-reactivity associated with chemical features for each of the 90 compounds that displayed submicromolar final late (>95% stage IV/V) gametocyte IC_{50} s. Pairwise LG activity to structural feature (*SkelSphere*) analysis was performed with activity cliff analysis (Osiris DataWarrior v 4.2.2) on all five series at a stringency of 80% in structural characteristics. Increasing late (stage IV/V) potency is indicated by increasing marker size, early (stage II/III) potency by increasing colour intensity and asexual potency by increasing background colour intensity. The symbols indicate the diaminothienyl pyrimidine (circles), 2-aminopyridine (squares), imidazopyridazine (triangles), 6,9-imidazopyridine (diamonds) and 2,6-imidazopyridine (rectangles) series. Data are representative of at least three biological experiments, each performed in technical triplicates.

Within the DTP series, the thienylpyrimidine backbone was an active representative. The methylation at position R2 and the phenyl fragment at R, which were previously shown to be required for potent *in vitro* asexual activity, were confirmed here to be essential for the gametocytocidal activity of this chemotype, which was enhanced with lipophilic groups at the phenyl ring *para*-position (Figure 4.7). The morpholino group at R1 (MMV668434) may have contributed to increased hydrophilicity, as indicated by the lower cLogP value, and concomitant increases in late stage specific activity.

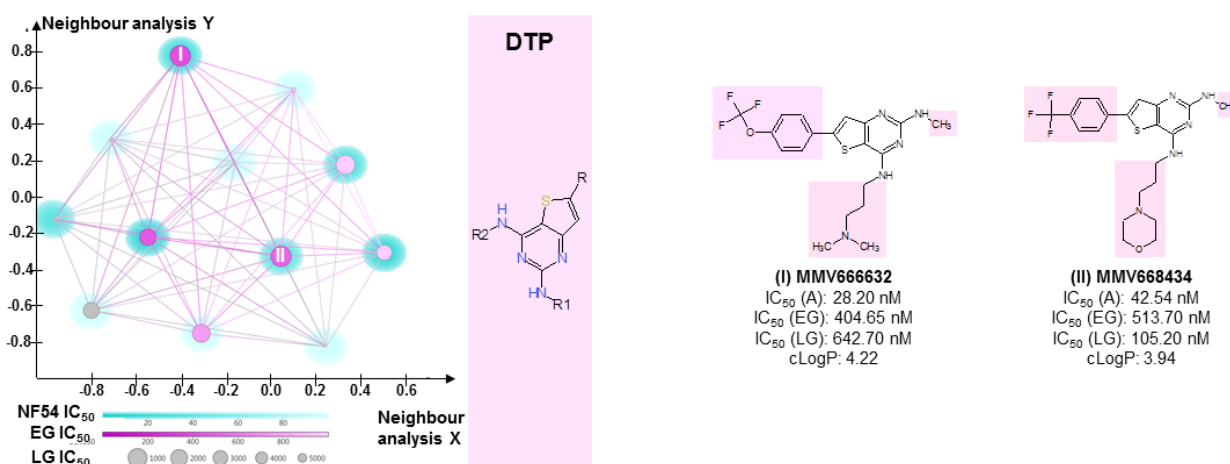


Figure 4.7: Intra-series structure activity landscape interrogation of the DTPs. Pairwise late (IV/V) stage gametocyte activity to structural feature (*Ske/Sphere*) analysis was performed with superimposed activity cliff analysis (Osiris DataWarrior V 4.2.2) at a stringency of 80% in structural characteristics. Increasing late (stage IV/V) potency is indicated by increasing marker size, early (stage II/III) potency by increasing colour intensity and asexual potency by increasing background colour intensity. R-groups are indicated in the characteristic DTP pink colouration. A = asexual parasites; EG = early stage gametocytes; LG = late (stage IV/V) gametocytes. Data are representative of at least triplicate biological experiments, \pm SEM.

Active compounds within the 2-AP series polarised into two clusters based on chemical similarity (Figure 4.8). The first cluster contained 3,5-diaryl-2-AP MMV390048 (and its 2-aminopyrazine derivatives, MMV642944 and MMV643110) and the hits MMV642942 and MMV675081, with both asexual [383] and gametocytocidal activity. Separated from the first cluster was the second cluster of 2-aminopyrazines (MMV642943, MMV674192 and MMV668647), containing R1 trifluoromethylphenyl substitutions with various amide moieties at R2. The 2-aminopyrazine backbone was identified during SAR explorations around the pyridine core and led to improvements in late stage gametocyte activity (average pyridine IC₅₀ = 140 nM; average pyrazine IC₅₀ = 49 nM). This core had lower predictive hydrophilicities (cLogP>3) with associated >10-fold activity loss against early stage gametocytes.

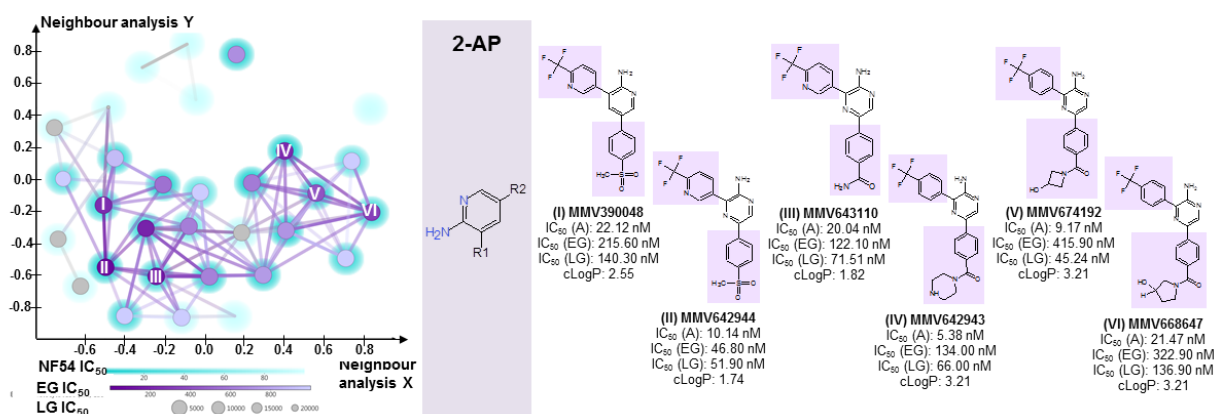


Figure 4.8: Intra-series structure activity landscape interrogation of the 2-APs. Pairwise late (IV/V) stage gametocyte activity to structural feature (*SkelSphere*) analysis was performed with superimposed activity cliff analysis (Osiris DataWarrior V 4.2.2) at a stringency of 80% in structural characteristics. Increasing late (stage IV/V) potency is indicated by increasing marker size, early (stage II/III) potency by increasing colour intensity and asexual potency by increasing background colour intensity. R-groups are indicated in the characteristic 2-AP purple colouration. A = asexual parasites; EG = early stage gametocytes; LG = late (stage IV/V) gametocytes. Data are representative of at least triplicate biological experiments, \pm SEM.

Within the IMPs, a homogenous association was observed between compound activities and chemical features. Similar to the 2-APs, *para*- and *meta*-phenyl substitutions at positions 3 and 6, respectively, of the imidazopyridazine, pyrazolopyrimidine and pyrazolopyridine cores were essential for *in vitro* asexual and gametocytocidal activity (Figure 4.9). The R2 cyclopropylsulfone and R1 methylsulfonyl improved the overall activity of the series. Moving a single nitrogen to position 5 resulted in the pyrazolopyrimidine core (MMV669810) which exhibited enhanced early and late stage gametocytocidal activity (<10 nM), still dependent on the R2 cyclopropylsulfone and R1 methylsulfonyl groups. Further core changes resulted in the pyrazolopyridines, MMV674850, MMV675615 and MMV674766. Only MMV674850 maintained equipotency, dependant on the presence of the R2 cyclopropylsulfone and R1 methylsulfonyl moieties.

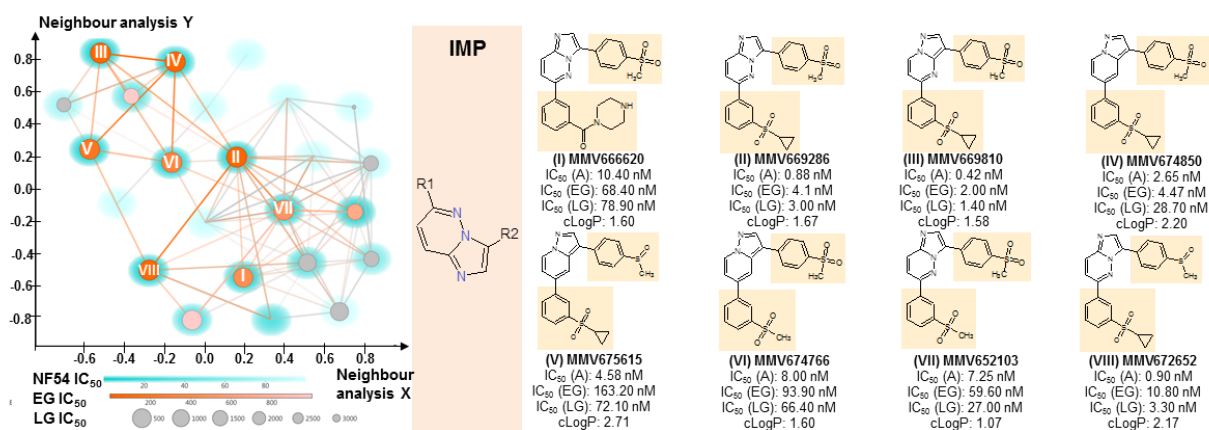


Figure 4.9: Intra-series structure activity landscape interrogation of the IMPs. Pairwise late (IV/V) stage gametocyte activity to structural feature (*SkelSphere*) analysis was performed with superimposed activity cliff analysis (Osiris DataWarrior v 4.2.2) at a stringency of 80% in structural characteristics. Increasing late (stage IV/V) potency is indicated by increasing marker size, early (stage II/III) potency by increasing colour intensity and asexual potency by increasing background colour intensity. R-groups are indicated in the characteristic IMP orange colouration. A = asexual parasites; EG = early stage gametocytes; LG = late (stage IV/V) gametocytes. Data are representative of at least triplicate biological experiments, \pm SEM.

Active representatives from the 6,9-IP series polarised into a single cluster of dimeric compounds (linked oligomers of identical monomeric compounds) and singletons of monomeric compounds (Figure 4.10). Within the dimeric compounds (I-V, Figure 4.10) the trifluoromethoxy phenyl group at R1 was crucial for dual activity. Furthermore, the presence of a 6-membered cycloalkyl with proximal and distal amines at R2 (MMV689854) led to a \sim 10-fold increase in late gametocyte-selective activity. Both early and late stage gametocytocidal activity was reduced when the stereochemistry around these amines was changed (MMV893049). Equipotency was maintained in the monomeric compound (MMV884980) with similar R-group configuration as the dimer cluster. The inclusion of an additional fluorine atom on the R1 phenyl ring or an additional linked piperidine/piperazine moiety at R2 did not affect the gametocytocidal activity of other monomers (MMV1557964 and MMV892665). The only prerequisite was the distal electron donating amine group, similar to the observation for dimers.

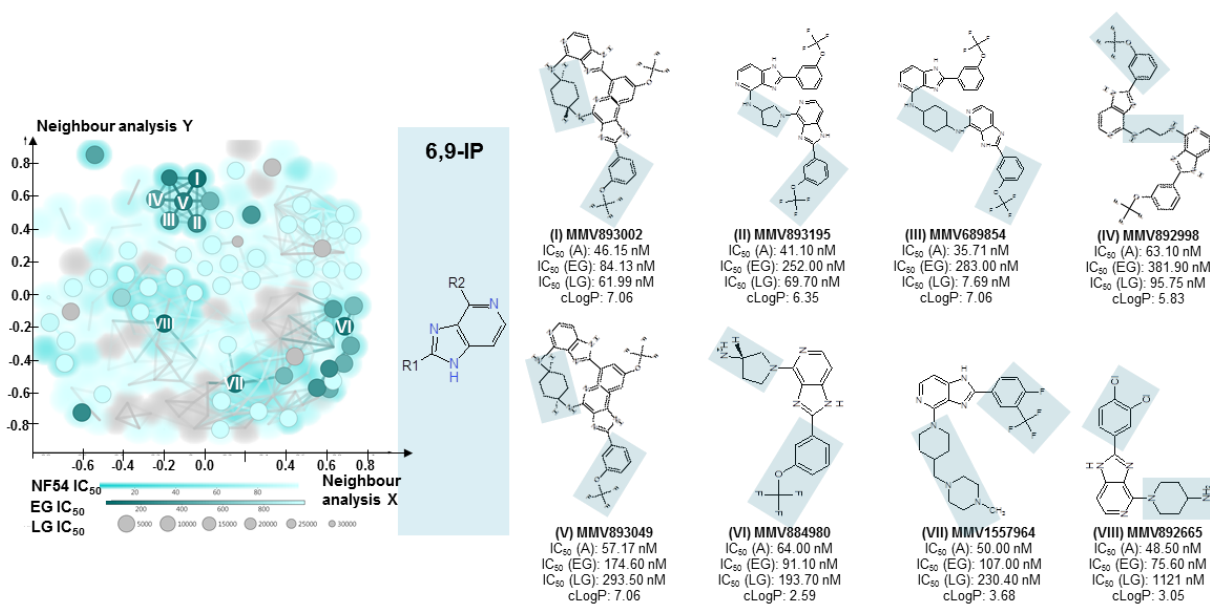


Figure 4.10: Intra-series structure activity landscape interrogation of the IMPs. Pairwise late (IV/V) stage gametocyte activity to structural feature (*SkelSphere*) analysis was performed with superimposed activity cliff analysis (Osiris DataWarrior V 4.2.2) at a stringency of 80% in structural characteristics. Increasing late (stage IV/V) potency is indicated by increasing marker size, early (stage II/III) potency by increasing colour intensity and asexual potency by increasing background colour intensity. R-groups are indicated in the characteristic 6,9-IP turquoise colouration. A = asexual parasites; EG = early stage gametocytes; LG = late (stage IV/V) gametocytes. Data are representative of at least triplicate biological experiments, \pm SEM.

For the 2,6-IPs, active compounds were scattered across the neighbour analysis landscape (Figure 4.11). The trifluoromethylphenyl moiety at R2 was crucial for late stage gametocytocidal activity, as this was lost (up to 20-fold) in MMV897780 and MMV897760 with difluorinated substituents. In contrast with the 6,9-IPs, it was crucial that the distal atom on the piperazine moiety (R1) be a neutral, HBA group (MMV688390 and MMV897780), leading to 2- to 10-fold increases in the late gametocyte specific activity of this series.

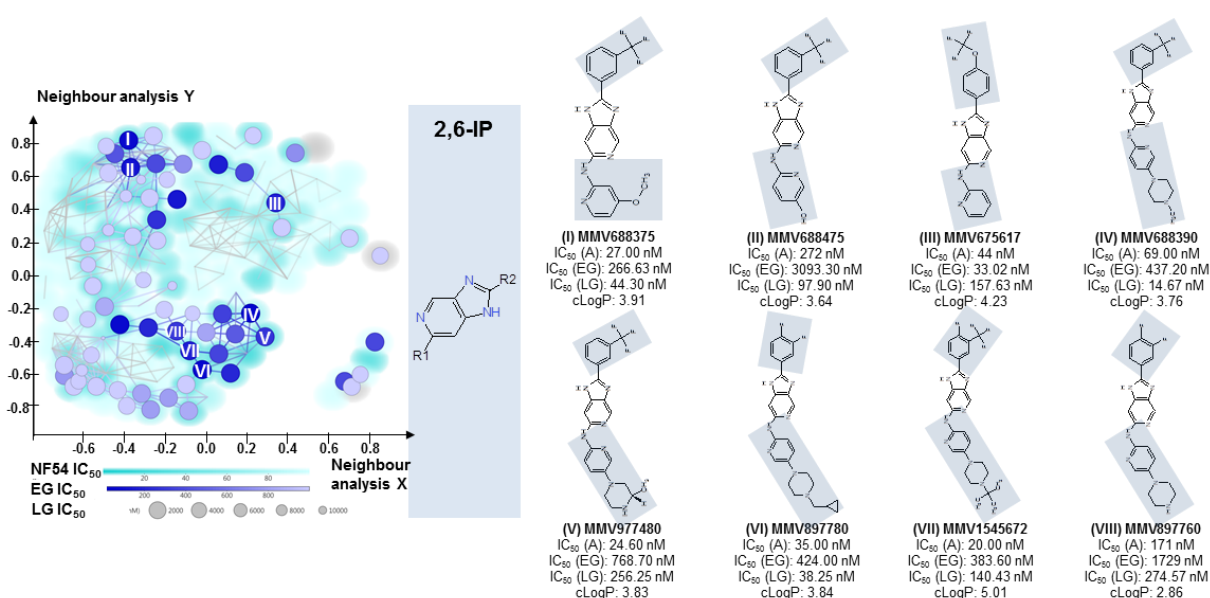


Figure 4.11: Intra-series structure activity landscape interrogation of the 2,6-IPs. Pairwise late (IV/V) stage gametocyte activity to structural feature (*SkelSphere*) analysis was performed with superimposed activity cliff analysis (Osiris DataWarrior V 4.2.2) at a stringency of 80% in structural characteristics. Increasing late (stage IV/V) potency is indicated by increasing marker size, early (stage II/III) potency by increasing colour intensity and asexual potency by increasing background colour intensity. R-groups are indicated in the characteristic 2,6-IP blue colouration. A = asexual parasites; EG = early stage gametocytes; LG = late (stage IV/V) gametocytes. Data are representative of at least triplicate biological experiments, \pm SEM.

Due to the structural similarity within each kinase-focussed scaffold, R-group deconvolution was performed to provide additional information on the functional groups responsible for dual (TCP-1 and TCP-5) or gametocyte-selective (TCP-5) activity. Strict biological selection cut-offs (late stage IV/V IC_{50} <100 nM, asexual stage IC_{50} <50 nM; Table 4.1) were imposed in order to identify potent dual active or gametocyte-selective hits.

4.3.2.2 R-group deconvolution of the kinase-focussed inhibitor series

The DTP series was excluded due to a lack of activity. For the 2-AP series, hit compounds were only identified from the 2-aminopyrazine core. Trifluoromethyl phenyl (average late stage IV/V IC_{50} = 394 nM) as well as trifluoromethyl pyridyl (average late stage IV/V IC_{50} = 359 nM) substituents at position R1 were potent with various substituents at R2 allowed (Figure 4.12). The selected hits displaying dual activity and transmission-blocking activity were confirmed on DGFA and SMFA for MMV642943 (IC_{50} DGFA (males) = 83 nM, IC_{50} DGFA (females) = 87 nM, IC_{50} SMFA = 96 nM) [274] and MMV642944 (104.57% (females) and 100.13% (males); block in transmission at 2 μ M) (data obtained from the ScienceCloud database; project number: MMV09/0002). Although it displayed an IC_{50} of >100 nM on late stage gametocytes, the transmission-blocking capacity of 2-

aminopyridine MMV390048 was also confirmed (104.30% (females) and 100.13% (males); block in transmission at 2 μ M; IC₅₀ SMFA = 111 nM) [252].

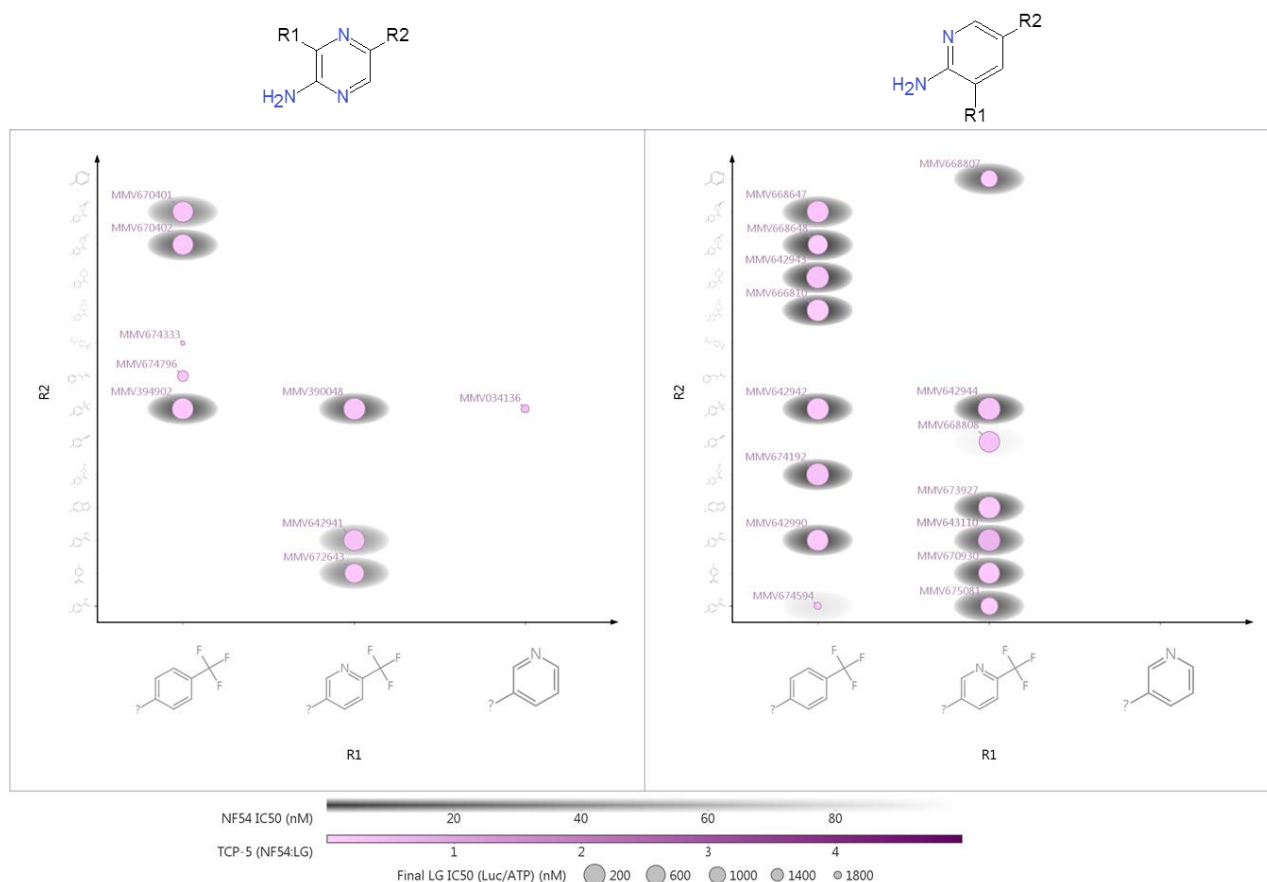


Figure 4.12: R-group deconvolution of the 2-aminopyridine and 2-aminopyrazine series. Contributions of substituents at R1 (x-axis) and R2 (y-axis) were deconvolved. The 2-aminopyridine (left) and 2-aminopyrazine (right) cores are indicated. Late stage gametocyte potency is indicated by increasing marker size, TCP-5 selectivity by increasing colour intensity and asexual potency by increasing background colour intensity. Compounds were only included if late stage gametocyte IC₅₀ \leq 2500 nM.

For the IMP scaffold, methylsulfonyl phenyl moieties at R1 were potent for all four IMP cores together with either sulfonyl or sulfoxide moieties (both electron-withdrawing groups (EWGs) at R2 (Figure 4.13). All of the hit cores (late stage IV/V IC₅₀ < 100 nM, asexual stage IC₅₀ < 50 nM) contained a cyclopropyl phenyl moiety at R1, except the pyrazolopyridine, MMV674766, which had a methylsulfonyl phenyl group in this position. A single hit compound was identified from the pyrazolopyrimidine core (MMV669810, average late stage IV/V IC₅₀ = 1.35 nM), two from the imidazopyridazine core (average late stage IV/V IC₅₀ = 662 nM) and three from the pyrazolopyridine core (average late stage IV/V IC₅₀ = 481 nM). All of these hits display dual activity with almost equipotency towards asexual parasites and late stage gametocytes, however, MMV669286 and MMV669810 do display transmission-blocking activity as confirmed by potent male and female gamete inhibition: (MMV669286: IC₅₀ (males) = 28 nM, IC₅₀ (females) = 58 nM)

and MMV669810 (IC_{50} (males) = 23 nM, IC_{50} (females) = 11 nM) (data obtained from the ScienceCloud database; project number: MMV09/0002).

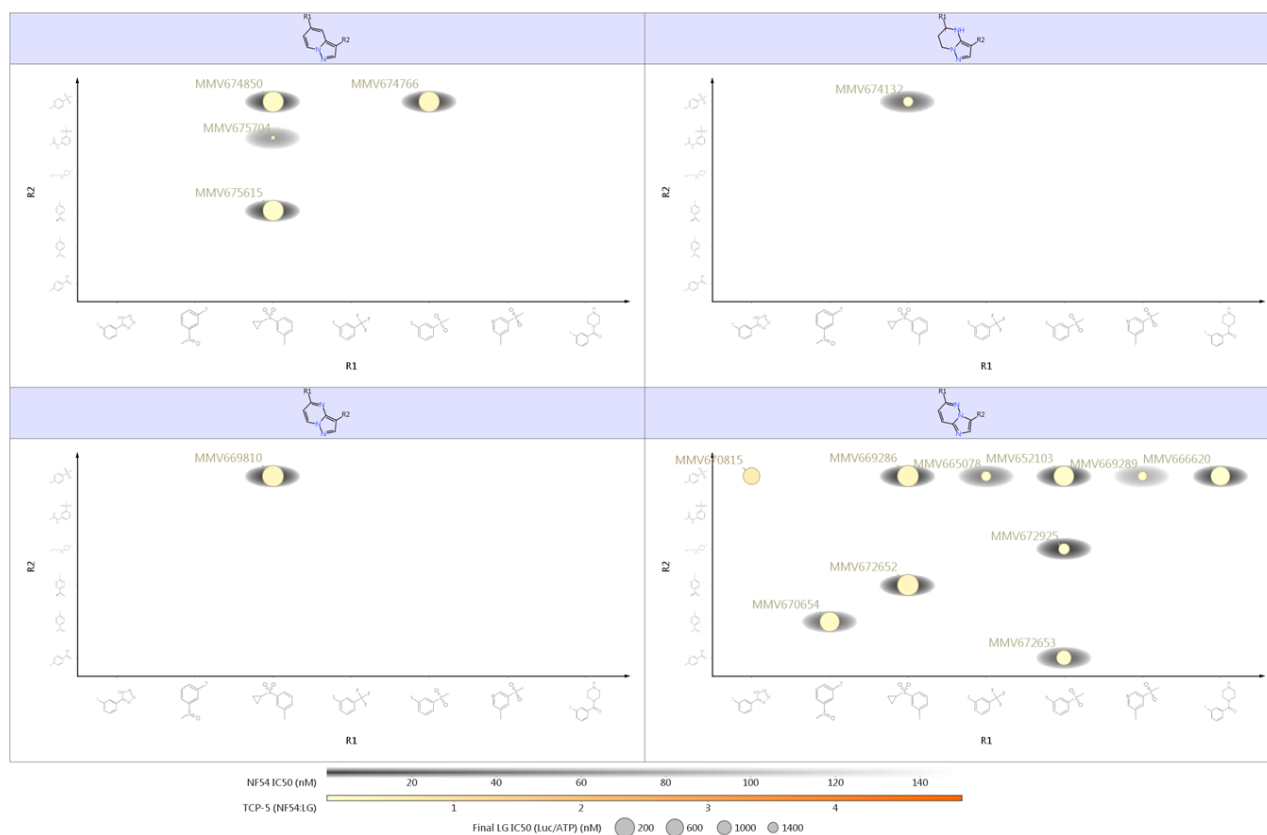


Figure 4.13: R-group deconvolution of the representative IMP cores. Contributions of substituents at R1 (x-axis) and R2 (y-axis) were deconvolved. The pyrazolopyridine (top left), tetrahydropyrazolopyrimidine (top right), pyrazolopyrimidine (bottom left) and imidazopyridazine (bottom right) cores are indicated. Late stage gametocyte potency is indicated by increasing marker size, TCP-5 selectivity by increasing colour intensity and asexual potency by increasing background colour intensity. Compounds were only included if late stage gametocyte $IC_{50} \leq 2500$ nM.

Hit compounds from the 6,9-IP core contained trifluoromethoxy phenyl groups at position R2, combined with various amine substitutions at R1 (Figure 4.14). The trifluoromethoxy phenyl scaffold maintained gametocytocidal potency (average late stage IV/V IC_{50} = 875 nM) with cyclic and primary alkyl amines, both with terminal electron donating amine groups. The four hit compounds were all dimeric with 3/4 (MMV689854, MMV893002 and MMV892998) limited by solubility concerns, as reflected by their MW and cLogP values (Table A4.2, appendix). Importantly, compound MMV689854 displayed a 4.6-fold TCP-5 selectivity, reflecting potential gametocyte-selective activity (highlighted on Figure 4.14).

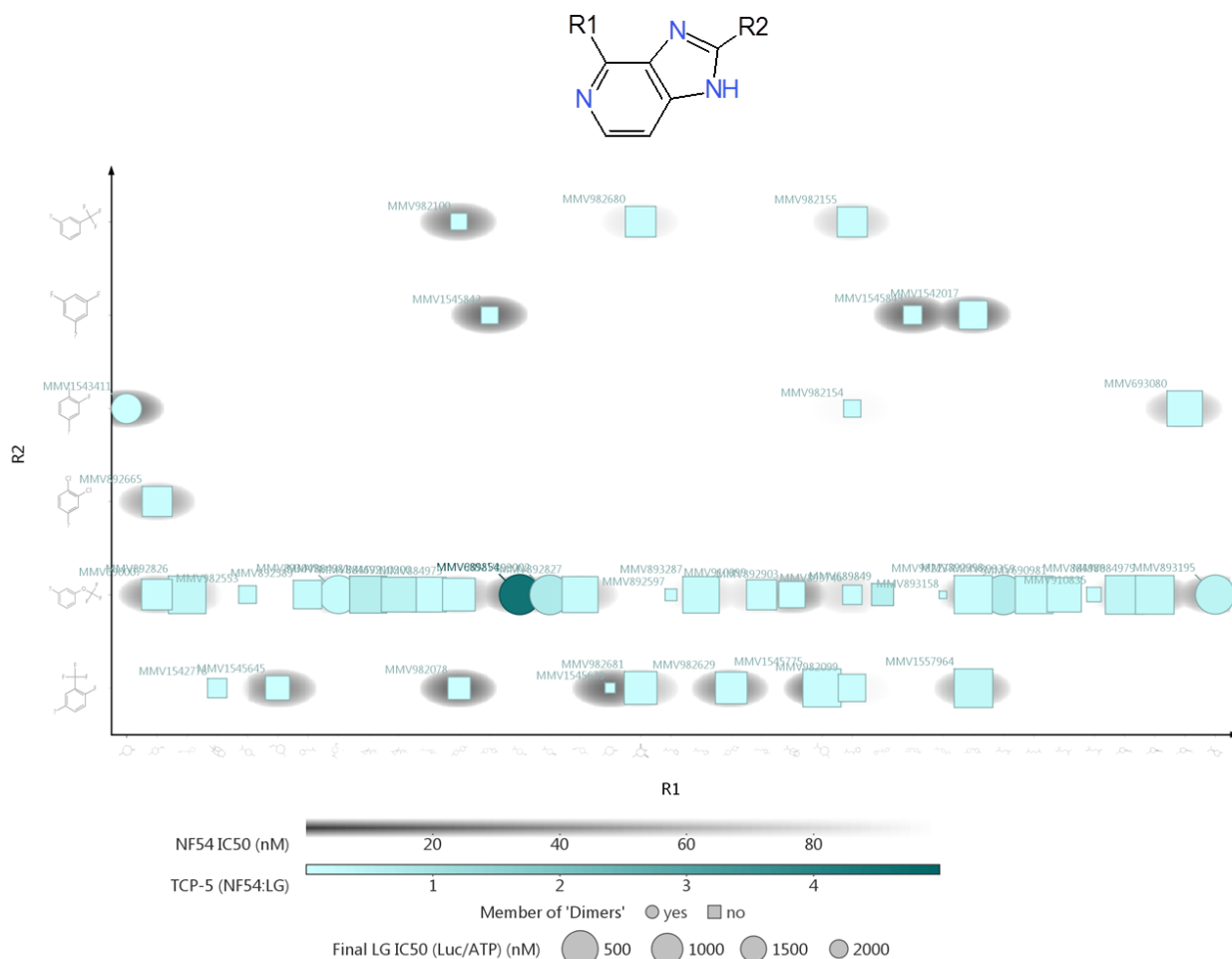


Figure 4.14: R-group deconvolution of the 6,9-IP series. Contributions of substituents at R1 (x-axis) and R2 (y-axis) were deconvolved. Late stage gametocyte potency is indicated by increasing marker size, TCP-5 selectivity by increasing colour intensity and asexual potency by increasing background colour intensity. Dimeric (circles) and monomeric (squares) compounds are indicated. Compounds were only included if late stage gametocyte $IC_{50} \leq 2500$ nM.

Compounds bearing difluorophenyl, trifluoromethyl phenyl or trifluoromethoxy phenyl substituents at R2, combined with various amine substituents at R1, were potent representatives of the 2,6-IP series (Figure 4.15). The trifluoromethoxy phenyl scaffold maintained gametocytocidal potency (average late stage IV/V $IC_{50} = 575$ nM) with pyridyl and alkyl amine containing substituents at R1. The difluoro phenyl scaffold also maintained gametocytocidal activity (average late stage IV/V $IC_{50} = 747$ nM) and bore a pyridyl moiety as well as piperazine and terminal alkane groups. MMV688390 and MMV688475 displayed TCP-5 selectivity values of 4.7 and 2.8 (highlighted on Figure 4.15).

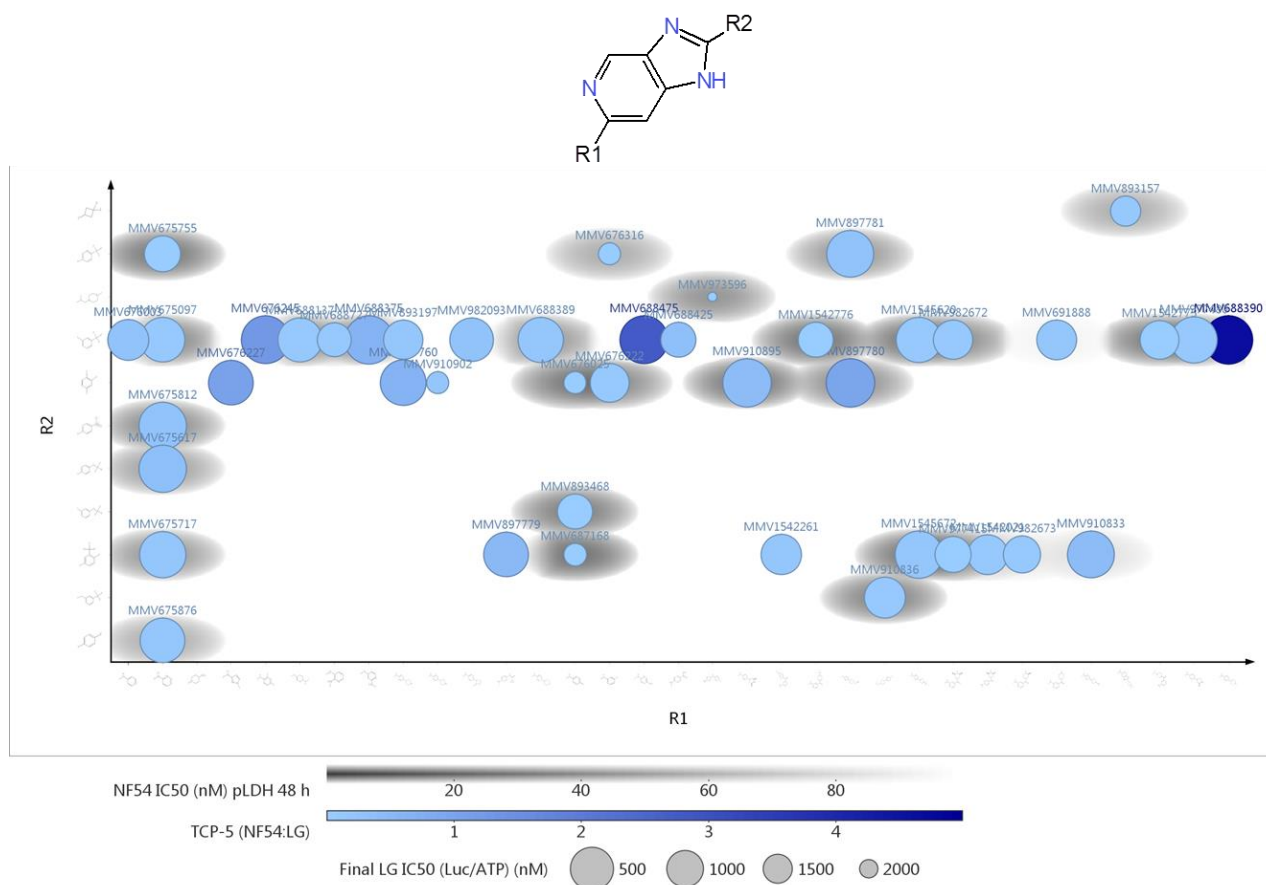


Figure 4.15: R-group deconvolution of the 2,6-IP series. Contributions of substituents at R1 (x-axis) and R2 (y-axis) were deconvolved. Late stage gametocyte potency is indicated by increasing marker size, TCP-5 selectivity by increasing colour intensity and asexual potency by increasing background colour intensity. Compounds were only included if late stage gametocyte $IC_{50} \leq 2500$ nM.

Due to the fact that one (MMV689854) and two (MMV688390 and MMV688475) late stage TCP-5 selective compounds were identified from the 6,9-IP and 2,6-IP series, these chemotypes were used as the backbone for the design of a single, unique, gametocyte-selective scaffold (Figure 4.16). The design considered core (purine-like) and functional group characteristics (R1 electron donating groups) and R2 EWGs shared between these hit compounds. Core features include the presence of the NH on the 5-membered imidazole ring, and the presence of a nitrogen at either position A (2,6-IPs) or B (6,9-IPs), position A being more representative of the nitrogen at position 1 of the ATP-purine ring. Di- or trifluorinated methyl or methoxyphenyl moieties (R2) are crucial for dual activity, and a proximal, secondary basic nitrogen (R1) or non-aromatic ring systems with distal HBA or HBD groups (R3) crucial for gametocyte-selective activity, with deviations resulting in 20- to 80-fold losses in activity and no TCP-5 selectivity.

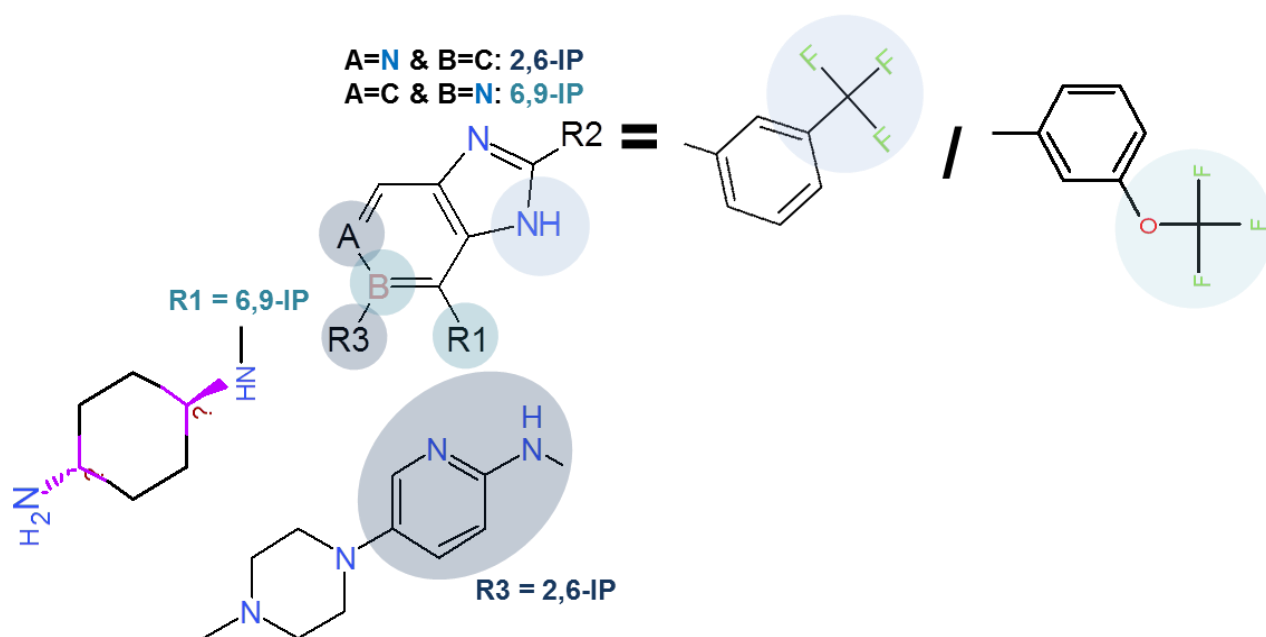


Figure 4.16: A unique, gametocyte-selective scaffold from the 6,9-IP and 2,6-IP series. Elements derived from either the 6,9-IP (turquoise) and 2,6-IP (blue) series are indicated.

4.4 Discussion

Global malaria elimination strategies require novel drugs that target both the proliferating asexual stages that cause disease symptoms, as well as the sexual gametocyte stages responsible for transmission [3]. Few of the currently available antimalarials adhere to this profile, emphasising the urgent need for drugs with both TCP-1 and TCP-5 (dual active), or TCP-5 only (gametocyte-selective) characteristics. To our knowledge, this study provides the first multifaceted cheminformatic evaluation of gametocytocidal compounds, which extends beyond the realm of chemical clustering and network analysis, but still provides SAR information in an uncomplicated way. In addition, the gametocyte-selectivity observed provides promise for the prioritisation of TCP-5 selective compounds as part of the worldwide elimination agenda.

Literature indicates that a few late stage gametocytocidal compounds have been identified [264, 436, 482, 493, 520], but only the 2,4-diaminopyrimidines, 1,2,3,4-tetrahydroacridines, 3-amino-imidazo[1,2-a]pyridines, 3H-imidazo[4,5-b]pyridines [363] and N-((4-hydroxychroman-4-yl)methyl)-sulphonamides [22] have been profiled as gametocyte selective compounds using chemical clustering. In this study, the TCAMS library [405] proved to be a valuable training set for the evaluation of various cheminformatic approaches towards the identification of dual active and gametocyte-selective compounds, since the cut-off imposed was able to isolate a TCP-5 selective subset with adequate

diversity and similarity to infer SARs. We were able to identify gametocyte-selective scaffolds with up to 5- and 47-fold TCP-5 selectivity, from a kinase-focussed library and previously published training set [405], respectively. Moreover, further interrogation of gametocyte-selective kinase inhibitors revealed a potential TCP-5 selective scaffold. Future endeavours might include derivatisation around this scaffold to decrease cytotoxicity and improve aqueous solubility, excluding any potential cross-resistance indications (including recently observed artemisinin resistance [199, 205, 581, 582]), determining *in vitro* and *in vivo* transmission-blocking activity towards clinical development and target deconvolution.

The value of the chemical clustering and our subsequent visual representation thereof, lies in the clear structural separation of gametocyte-selective clusters (cluster 1-5 and 7) from less TCP-5 selective groups, however, complete linkage clustering methods often result in bigger clusters being broken or singletons being merged with larger clusters [583], as evident from our analysis. Further cheminformatic interrogation revealed that the SALI analysis was able to delineate much finer structure-activity associations, within and between groups, when compared to that achieved during chemical clustering, since cluster 1 was separated into distinct groups during SALI analysis and the latter revealed many more disconnected singletons, some with TCP-5 selectivity. Indeed, the SALI analysis creates an easily interpreted 2D similarity map during which the similarity threshold is modulated from molecule to molecule to reduce singletons and untangle large clusters. Additionally, the map is further enhanced by superimposing activity data to indicate how much activity is gained with small changes in structure [527, 584]. The unique SALI analysis revealed 10 gametocyte-selective compounds shared amongst only three of the six clusters identified during conventional chemical clustering (23 compounds separated into six clusters). Moreover, TCAMS intra-SALI analysis was able to identify the contribution of specific substituents to TCP-5 selectivity within dual active groups. One of these scaffolds (group 3) was not highlighted during previous screens of the TCAMS library [402, 405, 493]; suggesting that this cheminformatic approach might be able to identify more gametocyte-selective chemotypes from other datasets. Importantly, the TCP-5 selectivity of gametocytocidal compounds identified from the TCAMS dataset were much higher than what has been reported [363] or highlighted in Figure 4.1, suggesting that these scaffolds might be highly selective for the sexual stages. This, together with the fact that these scaffolds were not cytotoxic improves the likelihood for further development to improve physicochemical and ADMET properties.

The SALI analysis additionally validated the contribution of the same functional groups (amines, amides and thioamides) identified during chemical clustering. The contribution of amine and amide moieties, as well as electronegative atoms and aromatic ring predictors to antiplasmodial activity, was expected in light of the known functional groups of druggable compounds [585], however, this is the first time these properties are associated to gametocyte-selectivity using a multiple linear regression analysis. Polar surface area is a unique contributor to gametocytocidal activity, has been correlated to membrane permeability [586-588] and might therefore additionally improve the access of compounds to late stage gametocytes that are already compromised by a ghost erythrocyte as well as the presence of perforins preparing these parasites for gamete egress [92, 504, 505]. Interestingly, gametocyte-selective compounds displayed variant cLogP values; this would imply limited membrane permeability and potency due to the non-linear relationship between predictive hydrophilicity, trans-cellular passage and biological distribution [589-591], however, it did not seem to affect the activity or gametocyte-selectivity of compounds. Moreover, cLogP was not identified as a physicochemical contributor to gametocytocidal activity during multiple linear regression analysis, possibly validating the lack of association to this predictor.

The 2-AP, IMPs, 6,9-IPs and 2,6-IPs all harboured either trifluoro phenyl(pyridyl) or trifluoromethoxy phenyl(pyridyl) substituents on the right-hand side of the molecule, corresponding to the proposition that halogenated phenyl rings dock efficiently into the hydrophobic pocket behind the gatekeeper residue of most kinases [275]. Although the transmission-blocking activity of MMV642943 [274], MMV390048 [252] and MMV642944 has been validated using DGFA and SMFA, the lack of TCP-5 selectivity suggests that this scaffold might be useful as dual active chemotype, with both the 2-aminopyridine and 2-aminopyrazine scaffold proven to target *Pf*PI4K and *Pv*PI4K and block transmission [252, 274]. The imidazopyridine, pyrazolopyridine and pyrazolopyrimidine cores were characterised as highly potent dual active compounds with additional activity on gametes. *Pf*PK7 [364, 592, 593], *Pf*CDPK1 [594], *Pf*CDPK4 [337, 339, 498, 513] and *Pf*PKG [161, 351, 506, 595] are validated targets of imidazopyridazine-like scaffolds, proving the promiscuity and potential polypharmacological application of this scaffold.

The IP series bore halogenated phenyls (R2) and piperazine/piperidine moieties on the left-hand side of the molecule, with either distal amines (6,9-IPs) or neutral HBA groups (2,6-IPs). Indeed, halogenated phenyls and cycloalkyls have been associated with good

antiplasmodial activity of kinase inhibitors [275, 413]. The TCP-5 selectivity of MMV689854 suggests that this 6,9-IP can serve as a potential gametocyte-selective scaffold, however, due to the dimeric nature of this compound, it will have to be derivatised to improve its physicochemical characteristics (cLogP, MW). However, the recent development of beyond rule of 5 (bRo5) drugs [596-598] suggests that the dimers can be used, providing they do not display any ADMET liabilities. IP-like scaffolds have been shown to target *Pf*PKG [161, 325, 326] and *Pf*DHODH [412], a novel target of the triazolopyrimidines DSM421 and DSM265 [245]; compounds in the MMV drug development pipeline. A gametocyte-selective scaffold was compiled from hit 6,9- and 2,6-IPs suggesting that our cheminformatic approach was indeed effective in elucidating the SARs of gametocytocidal compounds.

Although the MoA of dual active 2-APs and IMPs as well as gametocyte-selective IP-like compounds have been partly elucidated, this is based on chemoproteomic strategies or the generation of resistant mutants in asexual stage parasites [303-306]. Pre-established resistance mechanisms are transferred through gametocytes via meiotic recombination [3, 514], however, it is not yet known whether resistance can be generated in a gametocyte population under transmission-selective drug pressure. TCP-5 selective compounds might, therefore, have novel targets and MoAs, unique to the sexual stages, that can only be elucidated using metabolomics, lipidomics, *in vitro* evolution and chemogenomic methods, such as those rendered by the Malaria Drug Accelerator (MaIDA) program [599]. Moreover, the dual active and gametocyte-selective scaffolds identified from the kinase-focussed inhibitors are very different to the antimalarials currently employed [26, 206], also suggesting potentially unique MoAs, allowing combination with current antimalarials or partner drugs in the developmental pipeline [3, 26, 32, 238-244] and additionally offering the potential of avoiding resistance development due to the limited population ($\sim 10^2$ parasites) exposed to innovative drug scaffolds [266].

The identification of three TCP-5 specific compounds from the 2,6-IPs, additional to the 6,9-IP dimer, led to the identification of a unique, hybrid gametocyte-selective scaffold. Crucial features of this gametocyte-selective scaffold include (i) the nitrogen mimicking that of the ATP-purine ring which usually interacts with amide groups in the hinge region of various kinases [275], but might lead to cytotoxicity liabilities [585] as observed for this study, (ii) a halogenated phenyl or methoxyphenyl moiety at R2 crucial for docking [275], as well as (iii) heterosubstituted cycloalkanes with distal HBA or HBD groups at R1/R3,

recently shown to retain antiplasmodial activity and improve aqueous solubility [413]. Data available suggests that further optimisation of this scaffold should focus on reducing cytotoxicity. The transmission-blocking capacity of such a gametocyte-selective, TCP-5 specific drug will have to be confirmed on other life cycle stages during DGFA, SMFA and liver stage assays. Clinical development will require new pharmacokinetic and pharmacodynamic profiles, such as protracted activity and slow-release, unique to this candidate profile. Approved transmission-focussed drugs will likely be combined with a schizontocidal therapy in chemotherapeutic application [3], used prophylactically within transmission hotspots [600], or as treatment of identified gametocyte carriers in pre-elimination settings [4, 601, 602].

4.5 Conclusion

The high-level structure-activity associations provided by the SALI analysis was able to identify unique dual active (TCP-1 and TCP-5) and gametocyte-selective (TCP-5) chemotypes from a previously published diversity library, as well as a kinase-focussed library. The potent dual activity of the 2-APs and IMPs, suggests that these scaffolds might be highly selective and target a single kinase with crucial regulatory functions in both asexual and sexual stages, or hit multiple targets in different life cycle stages as well as targets essential to transmission. The gametocyte-selective activity of both IP series suggest that these chemotypes might be TCP-5 specific inhibitors, potentially targeting both the mature gametocytes and subsequent mosquito stages, leading to a block in transmission. The kinase inhibitor series interrogated here are thereby enticing chemical starting points for the development of dual active and gametocyte-selective compounds, vital tools required to achieve malaria elimination.

CHAPTER 5

CONCLUDING DISCUSSION

Despite global efforts to curb the disease, malaria remains one of the most significant causes of morbidity and mortality in sub-Saharan Africa [2]. One of the major realisations from previous attempts, is that elimination will not be achieved by focussing only on disease symptoms, but will require strategies to additionally prevent transmission of the parasite between the human host and mosquito vector [386, 415]. With various elimination agendas in hand [16-18, 23], the MMV has defined crucial benchmarks toward the development of drug candidates (TCPs) and treatment formulations (TPPs) [3]. To stop resistance spreading through meiotic recombination [3, 514] and simultaneously block transmission mediated by gametocytes [210-223], novel drugs will likely be dual active (targeting both TCP-1 and TCP-5) or selective towards mature gametocytes (TCP-5) [3].

Firstly, this thesis importantly contributed enabling technologies mediating up to high-throughput-level screening of novel chemical entities for gametocytocidal activity. Our inceptive gametocyte production protocol and complimentary hit profiling approach (published in 2015 [117] and cited 19 times [4, 240, 252, 264, 266, 274, 406, 426, 427, 448, 450, 480, 521, 603-618]), remains the most comprehensive cascade with regards to biological endpoints interrogated [4] and has contributed to various published works [240, 406, 427, 480, 521, 603, 618]. Moreover, this screening cascade contributed to the identification of novel clinical candidates with TCP-1 and TCP-5 activity: MMV390048 ([252], impact factor 2016: 16.796) and MMV642943 [274], currently in the MMV drug discovery pipeline. With the dual activity of these kinase inhibitor chemotypes as motivation, we set out to determine if a locally generated kinase-focussed inhibitor library would demonstrate potent activity against the pathogenic asexual and sexual, transmissible stages of the *P. falciparum* parasite. This study provided an in-depth evaluation of the antiplasmodial activity of the aforementioned library, the results of which was published in 2018 [619] and cited in a recent publication [604].

Roughly half of *Plasmodium* spp. kinases are vital for completion of the IDC, and those dispensable for asexual proliferation, are essential for specific transitions during sexual development [281]. Although many kinase inhibitor scaffolds have been probed for antiplasmodial [252, 274, 326, 342, 364, 366-368, 375, 376, 383, 393, 394, 402, 406, 407,

413, 414, 480, 483-486, 488, 620-628] and gametocytocidal activity [252, 274, 279, 331, 363, 370, 383, 393, 406, 407, 414, 480, 483-486, 488, 618, 622, 626, 629-632], a systematic evaluation of the kinase-inhibitor chemical space for dual asexual and gametocytocidal activity has been lacking. The potent dual activity and functional consequence of kinase inhibition observed during this study were expected in light of the known biological functions of kinases targeted by similar scaffolds [249, 252, 274, 364, 366, 368, 369, 410, 633, 634]. As an example, the lead 2-APs are known inhibitors of *PfPI4K* [252, 274], a lipid kinase catalysing the production of PIP₂ and PI3,4,5-triphosphate [595], which serve as precursors to DAG and IP₃ that maintain the Ca²⁺ gradient during the gametogenesis signalling cascade [161, 351, 506]. IMP-like scaffolds are known inhibitors of *PfPK7* [364] and *PfCDPK1* [594], kinases that are essential to the completion of erythrocytic schizogony, thereby explaining the asexual stage activity of this scaffold. The gametocytocidal component is reflected by the inhibition of *PfPKG* [161, 351, 506, 595], *PfCDPK1*, *PfCDPK4* and *PfMap-2*, kinases that are, like *PfPI4K*, involved in the Ca²⁺-regulated gametogenesis signalling cascade [498], as well as the de-repression of stored mRNAs [513] in female gametes. We propose that the equipotent dual active 2-AP and IMP series constitute tractable scaffolds with both curative and transmission-blocking properties, thereby providing the opportunity to consolidate TCP-1 and TCP-5. Moreover, their ability to target several enzymes within the same superfamily, potentiates a polypharmacological approach that might prevent resistance being conferred from asexual parasites to gametocytes [4], usually a limitation of single therapies. Transmission-blocking only compounds could overcome this caveats, but present other challenges.

The notion of targeting only the sexual stages of the malaria parasite as a way to reduce case incidence and potentiate elimination, has received increased interest in recent years [3]. This concept is underpinned by the population bottleneck presented by gametocytes [266], which suggests that this will mediate blocking transmission as well create a barrier to the spread of resistance alleles (due to the comparatively invariant characteristics of gametocyte genes [3, 269, 270, 635]). Most screens for gametocytocidal activity are performed based on pre-selection for asexual stage activity [264, 363, 405, 442, 447, 493], with only a single screen that was recently performed without this bias [22] and two studies that alluded to this selective activity [363, 405]. An urgent need therefore exists to highlight such compounds, either by screening only for TCP-5 activity, or combining screening data with an approach that can accentuate such chemotypes.

The easy-to-interpret cheminformatic approach created during this doctoral study, enabled the validation of dual active and identification of gametocyte-selective scaffolds from a diverse dataset and kinase-focussed library. This approach entailed the combination of a novel TCP-5 selectivity factor, structure-activity landscape analysis and R-group deconvolution, which together enabled uncomplicated gametocyte SAR. Applying the approach led to the interpretation of a unique TCP-5 selective scaffold from the 6,9-IP and 2,6-IP series. The IP scaffold's gametocyte-selectivity can be explained by this chemotypes' inhibition of PfPKG, a kinase that interacts with ~69 parasite proteins, thereby influencing many stage transitions during the *P. falciparum* life cycle [636], including gametogenesis [326] and ookinete motility [161]. Unfortunately, both IP series were non-amenable to further medicinal chemistry optimisations, for the reasons listed below, and subsequently discontinued. Initial attempts to truncate the dimeric 6,9-IP structures, led to reductions in potency. Although derivatives with improved *in vivo* clearance (CL; <50-100 mg/kg (ED₉₀)) could be produced from the early lead monomer, MMV1542017, by reducing the pK_a, the pharmacokinetics and bioavailability remained unfavourable (personal communication, H3D team). The novel 2,6-IP scaffold was restricted by ADMET liabilities, limited pharmacokinetics and a haemozoin formation inhibition MoA, mediated by mutations in ABC transporters ([637], personal communication, H3D team). Despite medicinal chemistry limitations, we suggest that pilot investigations should be performed to improve the selectivity and “druggability” of the gametocyte-selective scaffold, especially in light of the gametocyte (TCP-5) and liver stage (TCP-4) activities observed (personal communication, H3D team).

Should additional TCP-5, gametocyte-selective compounds be identified, they will require novel biological profiling models, independent of the constraints associated with dual active antimalarials. We suggest that this should commence with the determination of *ex vivo* efficacy and speed-of-action, followed by validation of transmission-blocking activity using direct skin feeding assays (DFA) [638] and SMFA [3], still the most predictive of transmission-blocking capacity [3, 639], even though DGFA data can be extrapolated [22, 639]. The pre-clinical development of transmission-blocking compounds will require new pharmacokinetic outlines using mouse-to-mouse transmission models (population transmission assays) [266, 640] or humanised mouse models [641, 642]. By reproducing all the stages of parasite infection in humans, these assays could act as bridge between *in vitro* assays and clinical studies, but are limited by host and parasite divergence. The human *in vivo* predictive efficacy of the abovementioned transmission-blocking assays

currently relies on field efficacy testing in endemic areas (community level reductions) [643-645], however, CHMI models are being established in order to inform the clinical development of gametocytocidal drugs, thereby filling a critical gap in transmission-blocking drug advancement [131, 132, 646].

Dosage of gametocyte-selective drugs will be driven by the free concentration in blood, sufficient to block transmission but not higher than the curative dose. The low-dose clinical activity of primaquine is a valuable reference point [266, 647], even though clinical patients receiving ACT-primaquine combinations are still infective to mosquitoes post treatment [254, 256]. To maintain transmission-blocking capacity, TCP-5 selective compounds will likely need to have protracted activity and/or a slow-release profile, or be administered over several doses due to the longevity of these stages (peak gametocytaemia ~8-12 days after infection; stage V's can circulate in the blood for ~20 days) [22, 371]. Moreover, such compounds should be specific to unique targets that can be irreversibly repressed only in gametocytes [155, 648] to prevent the selection of resistance mechanisms in asexual stages, usually transmitted to gametocytes via the associated alleles. Once clinically approved, transmission-blocking drugs with differential MoAs should be combined with a schizonticidal partner in dual active combination therapy, used prophylactically as monotherapy in a MDA scenario within transmission hotspots [600], or as treatment of identified gametocyte carriers in pre-elimination settings using a mass screening and treatment (mSAT) approach [4, 600-602]. Although mSAT is more targeted compared to MDA, it is limited by a lack of affordable and sufficiently sensitive techniques to detect submicroscopic gametocyte numbers. Both MDA and mSAT might not treat disease symptoms, but will protect populations at risk of infection. However, the implementation thereof might be hampered by political and psychological barriers to treating "healthy" individuals. Therefore, it will be crucial for investigators and regulators to agree on the most efficient clinical development and "roll-out" strategy.

As the profile of gametocytocidal compounds is currently limited to that delineated by TCP-5 [3] and only includes suggestions on dosing, efficacy, safety, co-formulation and cost, additional selection criteria are required in order to inform the initial selection of drugs with gametocyte-selective activity. The novel cheminformatic approach identified herein, not only identifies gametocyte-selective scaffolds, but will inform future TCP-5 driven screening strategies. This adds value to current phenotypic screening approaches which currently only give an indication of compound activity, but does not put this into context of

asexual stage activity or relate it to compound structural moieties. The cheminformatic approach will lead to the prioritisation of compounds that would otherwise be discarded due to asexual inactivity and/or physicochemical liabilities. Similarly, applying this strategy early-on during drug discovery, might prevent the premature discontinuation of chemical entities with gametocyte-selective potential, as was apparent for the 6,9-IP and 2,6-IP series. Additionally, as evident in Chapter 4, applying this cheminformatic approach to existing datasets might lead to the discovery of previously unidentified transmission-blocking chemical starting points.

In conclusion, this doctoral study supplied potential dual active and gametocyte-selective scaffolds from a kinase-focussed inhibitor library. It further contributed an easily-applied cheminformatic interrogation of phenotypic screening results towards highlighting TCP-5 selective scaffolds. Overall, this thesis contributed to the research community's understanding of screening for TCP-1/TCP-5 or TCP-5 driven antimalarials, and the required specifics thereof within the kinase inhibitor family. Based on our findings, we believe further interrogation of gametocyte-selective scaffolds with transmission-blocking potential, is undoubtedly warranted.

REFERENCES

1. WHO: World Malaria Report 2016. Geneva, Switzerland 2016.
2. WHO: World Malaria Report 2017. Geneva, Switzerland 2017.
3. Burrows J. N., Duparc S., Gutteridge W. E., Hooft van Huijsduijnen R., Kaszubska W., Macintyre F., Mazzuri S., Mohrle J. J., Wells T. N. C.: New developments in anti-malarial target candidate and product profiles. *Malaria Journal* 2017, 16:26.
4. Birkholtz L. M., Coetzer T. L., Mancama D., Leroy D., Alano P.: Discovering New Transmission-Blocking Antimalarial Compounds: Challenges and Opportunities. *Trends in Parasitology* 2016, 32:669-681.
5. WHO: World Malaria Report 2018. Geneva, Switzerland 2018.
6. Morrison D. A., Ellis J. T.: Effects of nucleotide sequence alignment on phylogeny estimation: a case study of 18S rDNAs of apicomplexa. *Molecular biology and evolution* 1997, 14:428 - 441.
7. CDC - Malaria - Malaria Worldwide - Impact of Malaria
[https://www.cdc.gov/malaria/malaria_worldwide/impact.html]
8. Ukpai O. M., Ubiaru P. C.: The Socio-Economic Impact of Malaria. *ABSU Journal of Environment, Science and Technology* 2012, 2:253 - 267.
9. Molina-Cruz A., Zilvermit M. M., Neafsey D. E., Hartl D. L., Barillas-Mury C.: Mosquito Vectors and the Globalization of *Plasmodium falciparum* Malaria. *Annual Review of Genetics* 2016, 50:447 - 465.
10. Burke A., Dandalo L., Munhenga G., Dahan-Moss Y., Mbokazi F., Ngxongo S., Coetzee M., Koekemoer L., Brooke B.: A new malaria vector mosquito in South Africa. *Scientific Reports* 2017, 7:43779.
11. Law Y.: Rare human outbreak of monkey malaria detected in Malaysia.: *Nature* 2018.
12. Guerra C. A., Howes R. E., Patil A. P., Gething P. W., Van Boeckel T. P., Temperley W. H., Kabaria C. W., Tatem A. J., Manh B. H., Elyazar I. R. F., Baird J. K., Snow R. W., Hay S. I.: The International Limits and Population at Risk of *Plasmodium vivax* Transmission in 2009. *PLOS Neglected Tropical Diseases* 2010, 4:e774.
13. Myrvang B.: A fifth plasmodium that can cause malaria. *Tidsskrift for Den Norske Laegeforening* 2010, 130:282-283.
14. WHO: World Health Organization: World Malaria Report. Geneva, Switzerland 2016.
15. WHO: MalERA update. World Health Organization, Geneva 2015.
16. Partnership R. B. M.: The Global Malaria Action Plan 2008.
17. RBM: Global Strategic Plan. Roll Back Malaria 2005-2015. . Roll Back Malaria Partnership, Geneva. ; 2005.
18. WHO: A framework for malaria elimination. Geneva: World Health Organization 2017.
19. WHO: World Malaria Report 2011. Geneva, Switzerland 2011.
20. Organization W. H.: World Malaria Report 2016. Geneva 2016.
21. Maharaj R., Morris N., Seocharan I., Kruger P., Moonasar D., Mabuza A., Raswiswi E., Raman J.: The feasibility of malaria elimination in South Africa. *Malaria Journal* 2012, 11:423.
22. Delves M. J., Miguel-Blanco C., Matthews H., Molina I., Ruecker A., Yahiya S., Straschil U., Abraham M., León M. L., Fischer O. J., Rueda-Zubiaurre A., Brandt J. R., Cortés Á., Barnard A., Fuchter M. J., Calderón F., Winzeler E. A., Sinden R. E., Herreros E., Gamo F. J., Baum J.: A high throughput screen for next-generation leads targeting malaria parasite transmission. *Nature Communications* 2018, 9:3805.
23. Rabinovich R. N., Drakeley C., Djimde A. A., Hall B. F., Hay S. I., Hemingway J., Kaslow D. C., Noor A., Okumu F., Steketee R., Tanner M., Wells T. N. C., Whittaker M. A., Winzeler E. A., Wirth D. F., Whitfield K., Alonso P. L.: malERA: An updated research agenda for malaria elimination and eradication. *PLoS Medicine* 2017, 14:e1002456.
24. Nilsson S. K., Childs L. M., Buckee C., Marti M.: Targeting Human Transmission Biology for Malaria Elimination. *Plos Pathogens* 2015, 11:e1004871.
25. Vaughan A. M., Mikolajczak S. A., Wilson E. M., Grompe M., Kaushansky A., Camargo N., Bial J., Ploss A., Kappe S. H.: Complete *Plasmodium falciparum* liver-stage development in liver-chimeric mice. *Journal of Clinical Investigation* 2012, 122:3618 - 3628.
26. Phillips M. A., Burrows J. N., Manyando C., van Huijsduijnen R. H., Van Voorhis W. C., Wells T. N. C.: Malaria. *Nature Reviews Disease Primers* 2017, 3:17050.
27. McGuinness D., Koram K., Bennett S., Wagner G., Nkrumah F., Riley E.: Clinical case definitions for malaria: clinical malaria associated with very low parasite densities in African infants. *Transactions of the Royal Society of Tropical Medicine and Hygiene* 1998, 92:527 - 531.
28. Wilairatana P., Tangpukdee N., Krudsood S.: Definition of hyperparasitemia in severe falciparum malaria should be updated. *Asian Pac J Trop Biomed* 2013, 3:586.

29. Karunaweera N. D., Grau G. E., Gamage P., Carter R., Mendis K. N.: Dynamics of fever and serum levels of tumor necrosis factor are closely associated during clinical paroxysms in *Plasmodium vivax* malaria. *Proceedings of the National Academy of Sciences of the United States of America* 1992, 89:3200 - 3203.
30. Wassmer S. C., Grau G. E. R.: Severe malaria: what's new on the pathogenesis front? *International Journal for Parasitology* 2017, 47:145 - 152.
31. Blumberg L. H.: Recommendations for the treatment and prevention of malaria: Update for the 2015 season in South Africa. *SAMJ: South African Medical Journal* 2015, 105:175 - 178.
32. Parasite lifecycle | Medicines for Malaria Venture [<https://www.mmv.org/malaria-medicines/parasite-lifecycle>]
33. Baker D. A.: Malaria gametocytogenesis. *Molecular & Biochemical Parasitology* 2010, 172:57 - 65.
34. Waters A. P.: Epigenetic Roulette in Blood Stream *Plasmodium*: Gambling on Sex. *Plos Pathogens* 2016, 12:e1005353.
35. Coleman B. I., Skillman K. M., Jiang R. H. Y., Childs L. M., Altenhofen L. M., Ganter M., Leung Y., Goldowitz I., Kafsack B. F. C., Marti M., Llinás M., Buckee C. O., Duraisingh M. T.: A *Plasmodium falciparum* Histone Deacetylase Regulates Antigenic Variation and Gametocyte Conversion. *Cell Host & Microbe* 2014, 16:177 - 186.
36. Brancucci N. M. B., Bertschi N. L., Zhu L., Niederwieser I., Chin W. H., Wampfler R., Freymond C., Rottmann M., Felger I., Bozdech Z., Voss T. S.: Heterochromatin protein 1 secures survival and transmission of malaria parasites. *Cell Host & Microbe* 2014, 16:165 - 176.
37. Filarsky M., Fräschka S. A., Niederwieser I., Brancucci N. M. B., Carrington E., Carrio E., Moes S., Jenoe P., Bartfai R., Voss T. S.: GDV1 induces sexual commitment of malaria parasites by antagonizing HP1-dependent gene silencing. *Science* 2018, 359:1259 - 1263.
38. Smith T. G., Lourenco P., Carter R., Walliker D., Ranford-Cartwright L. C.: Commitment to sexual differentiation in the human malaria parasite, *Plasmodium falciparum*. *Parasitology* 2000, 121 (P 2):127 - 133.
39. Ponnudurai T., Meuwissen J. H., Leeuwenberg A. D., Verhave J. P., Lensen A. H.: The production of mature gametocytes of *Plasmodium falciparum* in continuous cultures of different isolates infective to mosquitoes. *Transactions of the Royal Society of Tropical Medicine and Hygiene* 1982, 76:242 - 250.
40. Sinden R. E., Canning E. U., Bray R. S., Smalley M. E.: Gametocyte and gamete development in *Plasmodium falciparum*. . *Proceedings of the Royal Society of London* 1978, 201:375 - 399.
41. Okuda-Ashitaka E., Tachibana S., Houtani T., Minami T., Masu Y., Nishi M., Takeshima H., Sugimoto T., Ito S.: Identification and characterization of an endogenous ligand for opioid receptor homologue ROR-C: Its involvement in allodynic response to innocuous stimulus. *Molecular Brain Research* 1997, 43:96 - 104.
42. Raabe A. C., Billker O., Vial H. J., Wengelnik K.: Quantitative assessment of DNA replication to monitor microgametogenesis in *Plasmodium berghei*. . *Molecular and Biochemical Parasitology* 2009, 168:172 - 176.
43. Ponzi M., Sidén-Kiamos I., Bertuccini L., Currà C., Kroeze H., Camarda G., Pace T., Franke-Fayard B., Laurentino E. C., Louis C., Waters A. P., Janse C. J., Alano P.: Egress of *Plasmodium berghei* gametes from their host erythrocyte is mediated by the MDV-1/PEG3 protein. *Cellular Microbiology* 2009, 11:1272 - 1288.
44. Aly A. S., Vaughan A. M., Kappe S. H.: Malaria parasite development in the mosquito and infection of the mammalian host. *Annual review of microbiology* 2009, 63:195 - 221.
45. Ghosh A. K., Jacobs-Lorena M.: *Plasmodium* sporozoite invasion of the mosquito salivary gland. *Current Opinion in Microbiology* 2009, 12:394 - 400.
46. Kuehn A., Pradel G.: The Coming-Out of Malaria Gametocytes. *Journal of Biomedicine and Biotechnology* 2010.
47. Day K. P., Hayward R. E., Dyer M.: The biology of *Plasmodium falciparum* transmission stages. *Parasitology* 1998, 116:95 - 109.
48. Hawking F., Wilson M. E., Gammage K.: Evidence for cyclic development and short-lived maturity in the gametocytes of *Plasmodium falciparum*. . *Transactions of the Royal Society of Tropical Medicine and Hygiene* 1971, 65:549 - 559.
49. Josling G. A., Williamson K. C., Llinás M.: Regulation of Sexual Commitment and Gametocytogenesis in Malaria Parasites. *Annual review of microbiology* 2018, 72:null.
50. Sinden R. E., Smalley M. E.: Gametocytogenesis of *Plasmodium falciparum* in vitro: the cell-cycle. *Parasitology* 1979, 79:277 - 296.
51. Sinden R. E.: Sexual development of malarial parasites. *Advanced Parasitology* 1983, 22:153 - 216.
52. Sinden R. E.: Gametocytogenesis of *Plasmodium falciparum* in vitro: an electron microscopic study. *Parasitology* 1982, 84:1 - 11.

53. Tiburcio M., Silvestrini F., Bertuccini L., Sander A. F., Turner L., Lavstsen T., Alano P.: Early gametocytes of the malaria parasite *Plasmodium falciparum* specifically remodel the adhesive properties of infected erythrocyte surface. *Cellular Microbiology* 2013, 15:647 - 659.
54. Aguilar R., Magallon-Tejada A., Achtman A. H., Moraleda C., Joice R., Cistero P., Li Wai Suen C. S., Nhabomba A., Macete E., Mueller I., Marti M., Alonso P. L., Menendez C., Schofield L., Mayor A.: Molecular evidence for the localization of *Plasmodium falciparum* immature gametocytes in bone marrow. *Blood* 2014, 123:959 - 966.
55. Joice R., Nilsson S. K., Montgomery J., Dankwa S., Egan E., Morahan B., Seydel K. B., Bertuccini L., Alano P., Williamson K. C., Duraisingh M. T., Taylor T. E., Milner D. A., Marti M.: *Plasmodium falciparum* transmission stages accumulate in the human bone marrow. *Science Translational Medicine* 2014, 6:244re245-244re245.
56. Farfour E., Charlotte F., Settegrana C., Miyara M., Buffet P.: The extravascular compartment of the bone marrow: a niche for *Plasmodium falciparum* gametocyte maturation? *Malaria Journal* 2012, 11:285.
57. Smalley M. E., Brown J.: *Plasmodium falciparum* gametocytogenesis stimulated by lymphocytes and serum from infected Gambian children. . *Transactions of the Royal Society of Tropical Medicine and Hygiene* 1981, 25:316 - 317.
58. Lee R. S., Waters A. P., Brewer J. M.: A cryptic cycle in haematopoietic niches promotes initiation of malaria transmission and evasion of chemotherapy. *Nature Communications* 2018, 9:1689.
59. Silvestrini F., Alano P., Williams J. L.: Commitment to the production of male and female gametocytes in the human malaria parasite *Plasmodium falciparum*. *Parasitology* 2000, 121:465 - 471.
60. McRobert L., Preiser P., Sharp S., Jarra W., Kaviratne M., Taylor M. C., Renia L., Sutherland C. J.: Distinct Trafficking and Localization of STEVOR Proteins in Three Stages of the *Plasmodium falciparum* Life Cycle. *Infection and Immunity* 2004, 72:6597-6602.
61. Petter M., Bonow I., Klinkert M.-Q.: Diverse Expression Patterns of Subgroups of the rif Multigene Family during *Plasmodium falciparum* Gametocytogenesis. *Plos One* 2008, 3:e3779.
62. Meibalan E., Marti M.: Biology of Malaria Transmission. *Cold Spring Harbor Perspectives in Medicine* 2017, 7.
63. Trager W., Gill G. S., Lawrence C., Nagel R. L.: *Plasmodium falciparum*: enhanced gametocyte formation in vitro in reticulocyte-rich blood. . *Experimental Parasitology* 1999, 91:115 - 118.
64. Peatey C. L., Watson J. A., Trenholme K. R., Brown C. L., Nielson L., Guenther M., Timmins N., Watson G. S., Gardiner D. L.: Enhanced Gametocyte Formation in Erythrocyte Progenitor Cells: A Site-Specific Adaptation by *Plasmodium falciparum*. *The Journal of Infectious Diseases* 2013, 208:1170 - 1174.
65. Josling G. A., Llinas M.: Sexual development in *Plasmodium* parasites: knowing when it's time to commit. *Nature Reviews Microbiology* 2015, 13:573 - 587.
66. Dearnley M. K., Yeoman J. A., Hanssen E., Kenny S., Turnbull L., Whitchurch C. B., Tilley L., Dixon M. W. A.: Origin, composition, organization and function of the inner membrane complex of *Plasmodium falciparum* gametocytes. *Journal of Cell Science* 2012, 125:2053 - 2063.
67. Alano P., Read D., Bruce M., Aikawa M., Kaido T., Tegoshi T., Bhatti S., Smith D. K., Luo C., Hansra S., Carter R., Elliott J. F.: COS cell expression cloning of Pfg377, a *Plasmodium falciparum* gametocyte antigen associated with osmiophilic bodies. *Molecular and Biochemical Parasitology* 1995, 74:143 - 156.
68. Kehrer J., Frischknecht F., Mair G. R.: Proteomic Analysis of the *Plasmodium berghei* Gametocyte Egressome and Vesicular bioID of Osmiophilic Body Proteins Identifies Merozoite TRAP-like Protein (MTRAP) as an Essential Factor for Parasite Transmission. *Molecular & Cellular Proteomics : MCP* 2016, 15:2852 - 2862.
69. Harding C. R., Meissner M.: The inner membrane complex through development of *Toxoplasma gondii* and *Plasmodium*. *Cellular Microbiology* 2014, 16:632 - 641.
70. Kono M., Herrmann S., Loughran N. B., Cabrera A., Engelberg K., Lehmann C., Sinha D., Prinz B., Ruch U., Heussler V., Spielmann T., Parkinson J., Gilberger T. W.: Evolution and Architecture of the Inner Membrane Complex in Asexual and Sexual Stages of the Malaria Parasite. *Molecular biology and evolution* 2012, 29:2113 - 2132.
71. Boucher L. E., Bosch J.: The apicomplexan glideosome and adhesins -- structures and function. *Journal of Structural Biology* 2015, 190:93 - 114.
72. Marion H., Coralie M., W. D. M., Inga S. K., Paul M., Leann T.: Organization and function of an actin cytoskeleton in *Plasmodium falciparum* gametocytes. *Cellular Microbiology* 2015, 17:207 - 225.
73. Dearnley M., Chu T., Zhang Y., Looker O., Huang C., Klonis N., Yeoman J., Kenny S., Arora M., Osborne J. M., Chandramohanadas R., Zhang S., Dixon M. W. A., Tilley L.: Reversible host cell remodeling underpins deformability changes in malaria parasite sexual blood stages. *Proceedings of the National Academy of Sciences* 2016, 113:4800 - 4805.

74. Aingaran M., Zhang R., Law S. K., Peng Z., Undisz A., Meyer E., Diez-Silva M., Burke T. A., Spielmann T., Lim C. T., Suresh S., Dao M., Marti M.: Host cell deformability is linked to transmission in the human malaria parasite *Plasmodium falciparum*. *Cellular Microbiology* 2012, 14:983 - 993.
75. Chardome M., Janssen P. J.: Inquiry on malarial incidence by the dermal method in the region of Lubilash, Belgian Congo. *Annales de la Société Belge de Médecine Tropicale* 1952, 32:209 - 211.
76. van den Berghe B. L., Chardome M.: An easier and more accurate diagnosis of malaria and filariasis through the use of the skin scarification smear. *The American Journal of Tropical Medicine and Hygiene* 1951, 31:411 - 413.
77. Bousema T., Dinglasan R. R., Morlais I., Gouagna L. C., van Warmerdam T., Awono-Ambene P. H., Bonnet S., Diallo M., Coulibaly M., Tchuinkam T., Mulder B., Targett G., Drakeley C., Sutherland C., Robert V., Doumbo O., Touré Y., Graves P. M., Roeffen W., Sauerwein R., Birkett A., Locke E., Morin M., Wu Y., Churcher T. S.: Mosquito Feeding Assays to Determine the Infectiousness of Naturally Infected *Plasmodium falciparum* Gametocyte Carriers. *Plos One* 2012, 7:e42821.
78. Bruce M. C., Alano P., Duthie S., Carter R.: Commitment of the malaria parasite *Plasmodium falciparum* to sexual and asexual development. *Parasitology* 1990, 100 Pt 2:191 - 200.
79. Chaubey S., Grover M., Tatu U.: Endoplasmic reticulum stress triggers gametocytogenesis in the malaria parasite. *The Journal of Biological Chemistry* 2014, 289:16662 -16674.
80. Paul R. E. L., Brey P. T., Robert V.: *Plasmodium* sex determination and transmission to mosquitoes. *Trends in Parasitology* 2002, 18:32 - 38.
81. Talman A. M., Paul R. E., Sokhna C. S., Domarle O., Ariey F., Trape J. F., Robert V.: Influence of chemotherapy on the *Plasmodium* gametocyte sex ratio of mice and humans. *The American Journal of Tropical Medicine and Hygiene* 2004, 71:739 - 744.
82. Sowunmi A., Balogun S. T., Gbotosho G. O., Happi C. T.: *Plasmodium falciparum* gametocyte sex ratios in children with acute, symptomatic, uncomplicated infections treated with amodiaquine. *Malaria Journal* 2008, 7.
83. LaMonte G., Philip N., Reardon J., Lacsina J. R., Majoros W., Chapman L., Thornburg C. D., Telen M. J., Ohler U., Nicchitta C. V., Haystead T., Chi J.-T.: Translocation of sickle cell erythrocyte microRNAs into *Plasmodium falciparum* inhibits parasite translation and contributes to malaria resistance. *Cell Host & Microbe* 2012, 12:187 - 199.
84. Gautret P., Miltgen F., Gantier J. C., Chabaud A. G., Landau I.: Enhanced gametocyte formation by *Plasmodium chabaudi* in immature erythrocytes: pattern of production, sequestration, and infectivity to mosquitoes. *Journal of Parasitology* 1996, 82:900-906.
85. Ono T., Nakai T., Nakabayashi T.: Induction of gametocytogenesis in *Plasmodium falciparum* by the culture supernatant of hybridoma cells producing anti-*P. falciparum* antibody. *Biken journal* 1986, 29:77 - 81.
86. Schneeweis S., Maier W. A., Seitz H. M.: Haemolysis of infected erythrocytes--a trigger for formation of *Plasmodium falciparum* gametocytes? *Parasitol Res* 1991, 77:458 - 460.
87. Trager W., Gill G. S.: Enhanced Gametocyte Formation in Young Erythrocytes by *Plasmodium falciparum* *In Vitro*. *The Journal of Protozoology* 1992, 39:429 - 432.
88. Santra G.: Usefulness of examination of palmar creases for assessing severity of anemia in Indian perspective: A study from a tertiary care center. *International Journal of Medicine and Public Health* 2015, 5:169.
89. Lingnau A., Margos G., Maier W. A., Seitz H. M.: The effects of hormones on the gametocytogenesis of *Plasmodium falciparum* in vitro. *Applied Parasitology* 1993, 34:153 - 160.
90. Puta C., Manyando C.: Enhanced gametocyte production in Fansidar-treated *Plasmodium falciparum* malaria patients: implications for malaria transmission control programmes. *Tropical Medicine & International Health* 1997, 2:227 - 229.
91. Menezes R. A. O., Gomes M. D. S. M., Mendes A. M., Couto Á. A. R. A., Nacher M., Pimenta T. S., Sousa A. C. P., Baptista A. R. S., Jesus M. I., Enk M. J., Cunha M. G., Machado R. L. D.: Enteroparasite and vivax malaria co-infection on the Brazil-French Guiana border: Epidemiological, haematological and immunological aspects. *Plos One* 2018, 13:e0189958.
92. Mantel P. Y., Hoang A. N., Goldowitz I., Potashnikova D., Hamza B., Vorobjev I., Ghiran I., Toner M., Irimia D., Ivanov A. R., Barteneva N., Marti M.: Malaria-infected erythrocyte-derived microvesicles mediate cellular communication within the parasite population and with the host immune system. *Cell Host & Microbe* 2013, 13:521 - 534.
93. Regev-Rudzki N., Wilson D. W., Carvalho T. G., Sisquella X., Coleman B. M., Rug M., Bursac D., Angrisano F., Gee M., Hill A. F., Baum J., Cowman A. F.: Cell-cell communication between malaria-infected red blood cells via exosome-like vesicles. *Cell* 2013, 153:1120 - 1133.
94. Dyer M., Day K. P.: Commitment to gametocytogenesis in *Plasmodium falciparum*. *Parasitology Today* 2000, 16:102 - 107.

95. Buchholz K., Burke T. A., Williamson K. C., Wiegand R. C., Wirth D. F., Marti M.: A High-Throughput Screen Targeting Malaria Transmission Stages Opens New Avenues for Drug Development. *The Journal of Infectious Diseases* 2011, 203:1445 - 1453.
96. Balaji S., Babu M. M., Iyer L. M., Aravind L.: Discovery of the principal specific transcription factors of Apicomplexa and their implication for the evolution of the AP2-integrase DNA binding domains. *Nucleic Acids Research* 2005, 33:3994 - 4006.
97. Kafsack B. F. C., Rovira-Graells N., Clark T. G., Bancells C., Crowley V. M., Campino S. G., Williams A. E., Drought L. G., Kwiatkowski D. P., Baker D. A., Cortes A., Llinas M.: A transcriptional switch underlies commitment to sexual development in malaria parasites. *Nature* 2014, 507:248 - 254.
98. Sinha A., Hughes K. R., Modrzynska K. K., Otto T. D., Pfander C., Dickens N. J., Religa A. A., Bushell E., Graham A. L., Cameron R., Kafsack B. F. C., Williams A. E., Llinas M., Berriman M., Billker O., Waters A. P.: A cascade of DNA-binding proteins for sexual commitment and development in *Plasmodium*. *Nature* 2014, 507:253 - 257.
99. Campbell T. L., De Silva E. K., Olszewski K. L., Elemento O., Llinás M.: Identification and Genome-Wide Prediction of DNA Binding Specificities for the ApiAP2 Family of Regulators from the Malaria Parasite. *Plos Pathogens* 2010, 6:e1001165.
100. Flueck C.: *Plasmodium falciparum* heterochromatin protein 1 marks genomic loci linked to phenotypic variation of exported virulence factors. *Plos Pathogens* 2009, 5.
101. Zhang C., Li Z., Cui H., Jiang Y., Yang Z., Wang X., Gao H., Liu C., Zhang S., Su X.-z., Yuan J.: Systematic CRISPR-Cas9-Mediated Modifications of *Plasmodium yoelii* ApiAP2 Genes Reveal Functional Insights into Parasite Development. *mBio* 2017, 8.
102. Ikadai H., Shaw Saliba K., Kanzok S. M., McLean K. J., Tanaka T. Q., Cao J., Williamson K. C., Jacobs-Lorena M.: Transposon mutagenesis identifies genes essential for *Plasmodium falciparum* gametocytogenesis. *Proceedings of the National Academy of Sciences* 2013, 110:E1676 - E1684.
103. Lopez-Rubio J. J., Mancio-Silva L., Scherf A.: Genome-wide analysis of heterochromatin associates clonally variant gene regulation with perinuclear repressive centers in malaria parasites. *Cell Host & Microbe* 2009:179 – 190.
104. Fraschka S. A., Filarsky M., Hoo R., Niederwieser I., Yam X. Y., Brancucci N. M. B., Mohring F., Mushunje A. T., Huang X., Christensen P. R., Nosten F., Bozdech Z., Russell B., Moon R. W., Marti M., Preiser P. R., Bártfai R., Voss T. S.: Comparative Heterochromatin Profiling Reveals Conserved and Unique Epigenome Signatures Linked to Adaptation and Development of Malaria Parasites. *Cell Host & Microbe* 2018, 23:407 - 420.
105. Pérez-Toledo K., Rojas-Meza A. P., Mancio-Silva L., Hernández-Cuevas N. A., Delgadillo D. M., Vargas M., Martínez-Calvillo S., Scherf A., Hernandez-Rivas R.: *Plasmodium falciparum* heterochromatin protein 1 binds to tri-methylated histone 3 lysine 9 and is linked to mutually exclusive expression of var genes. *Nucleic Acids Research* 2009, 37:2596 - 2606.
106. Eksi S.: *Plasmodium falciparum* gametocyte development 1 (Pfgdv1) and gametocytogenesis early gene identification and commitment to sexual development. *PLoS Pathog.* 2012, 8.
107. Broadbent K. M., Broadbent J. C., Ribacke U., Wirth D., Rinn J. L., Sabeti P. C.: Strand-specific RNA sequencing in *Plasmodium falciparum* malaria identifies developmentally regulated long non-coding RNA and circular RNA. *BMC Genomics* 2015, 16:454.
108. Bechtesi D. P., Waters A. P.: Genomics and epigenetics of sexual commitment in *Plasmodium*. *International Journal for Parasitology* 2017, 47:425 - 434.
109. Rea E., Le Roch K. G., Tewari R.: Sex in *Plasmodium falciparum*: Silence Play between GDV1 and HP1. *Trends in Parasitology* 2018, 34:450 - 452.
110. Brancucci N. M. B., Gerdt J. P., Wang C., De Niz M., Philip N., Adapa S. R., Zhang M., Hitz E., Niederwieser I., Boltryk S. D., Laffitte M. C., Clark M. A., Gruring C., Ravel D., Blancke Soares A., Demas A., Bopp S., Rubio-Ruiz B., Conejo-Garcia A., Wirth D. F., Gendaszewska-Darmach E., Duraisingh M. T., Adams J. H., Voss T. S., Waters A. P., Jiang R. H. Y., Clardy J., Marti M.: Lysophosphatidylcholine Regulates Sexual Stage Differentiation in the Human Malaria Parasite *Plasmodium falciparum*. *Cell* 2017, 171:1532 - 1544
111. Lasonder E., Rijpma S. R., van Schaijk Ben C., Hoeijmakers Wieteke A., Kensche P. R., Gresnigt M. S., Italiaander A., Vos M. W., Woestenenk R., Bousema T., Mair G. R., Khan S. M., Janse C. J., Bártfai R., Sauerwein R. W.: Integrated transcriptomic and proteomic analyses of *P. falciparum* gametocytes: molecular insight into sex-specific processes and translational repression. *Nucleic Acids Research* 2016, 44:6087 - 6101.
112. Guttery D. S., Roques M., Holder A. A., Tewari R.: Commit and Transmit: Molecular Players in *Plasmodium* Sexual Development and Zygote Differentiation. *Trends in Parasitology* 2015, 31:676 - 685.

113. Khan S. M., Franke-Fayard B., Mair G. R., Lasonder E., Janse C. J., Mann M., Waters A. P.: Proteome Analysis of Separated Male and Female Gametocytes Reveals Novel Sex-Specific *Plasmodium* Biology. *Cell* 2005, 121:675 - 687.
114. Hanssen E., Knoechel C., Dearnley M., Dixon M. W. A., Le Gros M., Larabell C., Tilley L.: Soft X-ray microscopy analysis of cell volume and hemoglobin content in erythrocytes infected with asexual and sexual stages of *Plasmodium falciparum*. *Journal of Structural Biology* 2012, 177:224 - 232.
115. Young J. A., Fivelman Q. L., Blair P. L., de la Vega P., Le Roch K. G., Zhou Y., Carucci D. J., Baker D. A., Winzeler E. A.: The *Plasmodium falciparum* sexual development transcriptome: a microarray analysis using ontology-based pattern identification. *Molecular and Biochemical Parasitology* 2005, 143:67 - 79.
116. Delves M. J., Ruecker A., Straschil U., Lelièvre J., Marques S., López-Barragán M. J., Herreros E., Sinden R. E.: Male and Female *Plasmodium falciparum* Mature Gametocytes Show Different Responses to Antimalarial Drugs. *Antimicrobial Agents and Chemotherapy* 2013, 57:3268-3274.
117. Reader J., Botha M., Theron A., Lauterbach S. B., Rossouw C., Engelbrecht D., Wepener M., Smit A., Leroy D., Mancama D., Coetzer T. L., Birkholtz L. M.: Nowhere to hide: interrogating different metabolic parameters of *Plasmodium falciparum* gametocytes in a transmission blocking drug discovery pipeline towards malaria elimination. *Malaria Journal* 2015, 14:213.
118. Peatey C. L., Spicer T. P., Hodder P. S., Trenholme K. R., Gardiner D. L.: A high throughput assay for the identification of drugs against late-stage *Plasmodium falciparum* gametocytes. *Molecular and Biochemical Parasitology* 2011, 180:127 - 131.
119. Eksi S., Suri A., Williamson K. C.: Sex- and stage-specific reporter gene expression in *Plasmodium falciparum*. *Molecular and Biochemical Parasitology* 2008, 160:148 - 151.
120. Florens L., Washburn M. P., Raine J. D., Anthony R. M., Grainger M., Haynes J. D., Moch J. K., Muster N., Sacci J. B., Tabb D. L., Witney A. A., Wolters D., Wu Y., Gardner M. J., Holder A. A., Sinden R. E., Yates J. R., Carucci D. J.: A proteomic view of the *Plasmodium falciparum* life cycle. *Nature* 2002, 419:520.
121. Lasonder E., Ishihama Y., Andersen J. S., Vermunt A. M. W., Pain A., Sauerwein R. W., Eling W. M. C., Hall N., Waters A. P., Stunnenberg H. G., Mann M.: Analysis of the *Plasmodium falciparum* proteome by high-accuracy mass spectrometry. *Nature* 2002, 419:537.
122. Hayward R. E., DeRisi J. L., Alfadhli S., Kaslow D. C., Brown P. O., Rathod P. K.: Shotgun DNA microarrays and stage-specific gene expression in *Plasmodium falciparum* malaria. *Molecular Microbiology* 2000, 35:6 - 14.
123. Le Roch K. G., Zhou Y., Blair P. L., Grainger M., Moch J. K., Haynes J. D., De la Vega P., Holder A. A., Batalov S., Carucci D. J., Winzeler E. A.: Discovery of Gene Function by Expression Profiling of the Malaria Parasite Life Cycle. *Science* 2003, 301:1503 - 1508.
124. Yuda M., Iwanaga S., Kaneko I., Kato T.: Global transcriptional repression: An initial and essential step for *Plasmodium* sexual development. *Proceedings of the National Academy of Sciences* 2015, 112:12824 - 12829.
125. Scholz S. M., Simon N., Lavazec C., Dude M.-A., Templeton T. J., Pradel G.: PfCCp proteins of *Plasmodium falciparum*: Gametocyte-specific expression and role in complement-mediated inhibition of exflagellation. *International Journal for Parasitology* 2008, 38:327 - 340.
126. Simon N., Scholz S. M., Moreira C. K., Templeton T. J., Kuehn A., Dude M.-A., Pradel G.: Sexual Stage Adhesion Proteins Form Multi-protein Complexes in the Malaria Parasite *Plasmodium falciparum*. *The Journal of Biological Chemistry* 2009, 284:14537 - 14546.
127. Tiburcio M., Dixon M. W., Looker O., Younis S. Y., Tilley L., Alano P.: Specific expression and export of the *Plasmodium falciparum* Gametocyte EXported Protein-5 marks the gametocyte ring stage. *Malaria Journal* 2015, 14:334.
128. Moelans I. I. M. D., Meis J. F. G. M., Kocken C., Konings R. N. H., Schoenmakers J. G. G.: A novel protein antigen of the malaria parasite *Plasmodium falciparum*, located on the surface of gametes and sporozoites. *Molecular and Biochemical Parasitology* 1991, 45:193 - 204.
129. Bruce M. C., Carter R. N., Nakamura K.-i., Aikawa M., Carter R.: Cellular location and temporal expression of the *Plasmodium falciparum* sexual stage antigen Pfs16. *Molecular and Biochemical Parasitology* 1994, 65:11 - 22.
130. Baker D. A., Daramola O., McCrossan M. V., Harmer J., Targett G. A.: Subcellular localization of Pfs16, a *Plasmodium falciparum* gametocyte antigen. *Parasitology* 1994, 108:129 - 137.
131. Collins K. A., Wang C. Y., Adams M., Mitchell H., Rampton M., Elliott S., Reuling I. J., Bousema T., Sauerwein R., Chalon S., Mohrle J. J., McCarthy J. S.: A controlled human malaria infection model enabling evaluation of transmission-blocking interventions. *The Journal of Clinical Investigation* 2018, 128:1551 - 1562.
132. Reuling I. J., van de Schans L. A., Coffeng L. E., Lanke K., Meerstein-Kessel L., Graumans W., van Gemert G.-J., Teelen K., Siebelink-Stoter R., van de Vegte-Bolmer M., de Mast Q., van der Ven A. J., Ivinson K., Hermsen C. C., de Vlas S., Bradley J., Collins K. A., Ockenhouse C. F., McCarthy J.,

- Sauerwein R. W., Bousema T.: A randomized feasibility trial comparing four antimalarial drug regimens to induce *Plasmodium falciparum* gametocytemia in the controlled human malaria infection model. *eLife* 2018, 7:e31549.
133. Schneider P., Schoone G., Schallig H., Verhage D., Telgt D., Eling W.: Quantification of *Plasmodium falciparum* gametocytes in differential stages of development by quantitative nucleic acid sequence-based amplification. *Molecular and Biochemical Parasitology* 2004, 137:35 – 41.
 134. Sharma A., Sharma I., Kogkasuriyachai D., Kumar N.: Structure of a gametocyte protein essential for sexual development in *Plasmodium falciparum*. *Nature Structural Biology* 2003, 10:197.
 135. Anna O., Grazia C., Lucia B., Marga V. D. V. B., F. L. A. J., Robert S., Pietro A.: The *Plasmodium falciparum* protein Pfg27 is dispensable for gametocyte and gamete production, but contributes to cell integrity during gametocytogenesis. *Molecular Microbiology* 2009, 73:180 - 193.
 136. Pradel G.: Proteins of the malaria parasite sexual stages: expression, function and potential for transmission blocking strategies. *Parasitology* 2007, 134:1911 - 1929.
 137. Pradel G., Hayton K., Aravind L., Iyer L. M., Abrahamsen M. S., Bonawitz A., Mejia C., Templeton T. J.: A Multidomain Adhesion Protein Family Expressed in *Plasmodium falciparum* Is Essential for Transmission to the Mosquito. *The Journal of Experimental Medicine* 2004, 199:1533 - 1544.
 138. Pradel G., Wagner C., Mejia C., Templeton T. J.: *Plasmodium falciparum*: Co-dependent expression and co-localization of the PfCCp multi-adhesion domain proteins. *Experimental Parasitology* 2006, 112:263 - 268.
 139. Walzer K. A., Kubicki D. M., Tang X., Chi J. T.: Single-Cell Analysis Reveals Distinct Gene Expression and Heterogeneity in Male and Female *Plasmodium falciparum* Gametocytes. *mSphere* 2018, 3.
 140. Furuya T., Mu J., Hayton K., Liu A., Duan J., Nkrumah L., Joy D. A., Fidock D. A., Fujioka H., Vaidya A. B., Wellems T. E., Su X.-z.: Disruption of a *Plasmodium falciparum* gene linked to male sexual development causes early arrest in gametocytogenesis. *Proceedings of the National Academy of Sciences of the United States of America* 2005, 102:16813 - 16818.
 141. Suárez-Cortés P., Sharma V., Bertuccini L., Costa G., Bannerman N.-L., Rosa Sannella A., Williamson K., Klemba M., Levashina E. A., Lasonder E., Alano P.: Comparative Proteomics and Functional Analysis Reveal a Role of *Plasmodium falciparum* Osmiophilic Bodies in Malaria Parasite Transmission. *Molecular & Cellular Proteomics : MCP* 2016, 15:3243 - 3255.
 142. van Dijk M. R., Janse C. J., Thompson J., Waters A. P., Braks J. A. M., Dodemont H. J., Stunnenberg H. G., van Gemert G.-J., Sauerwein R. W., Eling W.: A Central Role for P48/45 in Malaria Parasite Male Gamete Fertility. *Cell*, 104:153 - 164.
 143. Saliha E., Beata C., Geert-Jan V. G., W. S. R., Wijnand E., C. W. K.: Malaria transmission-blocking antigen, Pfs230, mediates human red blood cell binding to exflagellating male parasites and oocyst production. *Molecular Microbiology* 2006, 61:991 - 998.
 144. van Schaijk B. C. L., van Dijk M. R., van de Vegte-Bolmer M., van Gemert G.-J., van Dooren M. W., Eksi S., Roeffen W. F. G., Janse C. J., Waters A. P., Sauerwein R. W.: Pfs47, paralog of the male fertility factor Pfs48/45, is a female specific surface protein in *Plasmodium falciparum*. *Molecular and Biochemical Parasitology* 2006, 149:216 - 222.
 145. Alano P.: *Plasmodium* sexual stage antigens. *Parasitology Today* 1991, 7:199 - 203
 146. Guinet F., Dvorak J. A., Fujioka H., Keister D. B., Muratova O., Kaslow D. C., Aikawa M., Vaidya A. B., Wellems T. E.: A developmental defect in *Plasmodium falciparum* male gametogenesis. *The Journal of Cell Biology* 1996, 135:269-278.
 147. Elena D., N. M. R., Lucia B., A. K. T. W., Alice L., Carolin N., Nikos P., Herwig S., Christos L., Kai M., Inga S. K.: Critical role for a stage-specific actin in male exflagellation of the malaria parasite. *Cellular Microbiology* 2011, 13:1714 - 1730.
 148. Guttery David S., Poulin B., Ramaprasad A., Wall Richard J., Ferguson David J., Brady D., Patzewitz E.-M., Whipple S., Straschil U., Wright Megan H., Mohamed Alyaa M., Radhakrishnan A., Arold Stefan T., Tate Edward W., Holder Anthony A., Wickstead B., Pain A., Tewari R.: Genome-wide Functional Analysis of *Plasmodium* Protein Phosphatases Reveals Key Regulators of Parasite Development and Differentiation. *Cell Host & Microbe* 2014, 16:128 - 140.
 149. Miao J., Li J., Fan Q., Li X., Li X., Cui L.: The Puf-family RNA-binding protein PfPuf2 regulates sexual development and sex differentiation in the malaria parasite *Plasmodium falciparum*. *Journal of Cell Science* 2010, 123:1039 - 1049.
 150. MacRae J. I., Dixon M. W. A., Dearnley M. K., Chua H. H., Chambers J. M., Kenny S., Bottova I., Tilley L., McConville M. J.: Mitochondrial metabolism of sexual and asexual blood stages of the malaria parasite *Plasmodium falciparum*. *BMC Biology* 2013, 11.
 151. Petmitr S., Krungkrai J.: Mitochondrial cytochrome b gene in two developmental stages of human malarial parasite *Plasmodium falciparum*. *Southeast Asian J Trop Med Public Health* 1995, 26:600 - 605.

152. Crofts A. R.: The cytochrome bc1 complex: function in the context of structure. *Annu Rev Physiol* 2004, 66:689 - 733.
153. Fisher N., Abd Majid R., Antoine T., Al-Helal M., Warman A. J., Johnson D. J., Lawrenson A. S., Ranson H., O'Neill P. M., Ward S. A., Biagini G. A.: Cytochrome b Mutation Y268S Conferring Atovaquone Resistance Phenotype in Malaria Parasite Results in Reduced Parasite bc(1) Catalytic Turnover and Protein Expression. *The Journal of Biological Chemistry* 2012, 287:9731-9741.
154. Siregar J. E., Kurisu G., Kobayashi T., Matsuzaki M., Sakamoto K., Mi-ichi F., Watanabe Y.-i., Hirai M., Matsuoka H., Syafruddin D., Marzuki S., Kita K.: Direct evidence for the atovaquone action on the *Plasmodium* cytochrome bc1 complex. *Parasitology International* 2015, 64:295 - 300.
155. Lamour S. D., Straschil U., Saric J., Delves M. J.: Changes in metabolic phenotypes of *Plasmodium falciparum* *in vitro* cultures during gametocyte development. *Malaria Journal* 2014, 13:468.
156. Gulati S., Eklund E. H., Ruggles K. V., Chan R. B., Jayabalasingham B., Zhou B., Mantel P.-Y., Lee M. C. S., Spottiswoode N., Coburn-Flynn O., Hjelmqvist D., Worgall T. S., Marti M., Di Paolo G., Fidock D. A.: Profiling the Essential Nature of Lipid Metabolism in Asexual Blood and Gametocyte Stages of *Plasmodium falciparum*. *Cell Host & Microbe* 2015, 18:371 - 381.
157. Tran P. N., Brown S. H. J., Rug M., Ridgway M. C., Mitchell T. W., Maier A. G.: Changes in lipid composition during sexual development of the malaria parasite *Plasmodium falciparum*. *Malaria Journal* 2016, 15:73.
158. Tibúrcio M., Niang M., Deplaine G., Perrot S., Bischoff E., Ndour P. A., Silvestrini F., Khattab A., Milon G., David P. H., Hardeman M., Vernick K. D., Sauerwein R. W., Preiser P. R., Mercereau-Puijalon O., Buffet P., Alano P., Lavazec C.: A switch in infected erythrocyte deformability at the maturation and blood circulation of *Plasmodium falciparum* transmission stages. *Blood* 2012, 119:172 - 180.
159. Besteiro S., Vo Duy S., Perigaud C., Lefebvre-Tournier I., Vial H. J.: Exploring metabolomic approaches to analyse phospholipid biosynthetic pathways in *Plasmodium*. *Parasitology* 2010, 137:1343 - 1356.
160. Bobenchik A. M., Witola W. H., Augagneur Y., Nic Lochlainn L., Garg A., Pachikara N., Choi J. Y., Zhao Y. O., Usmani-Brown S., Lee A., Adjalley S. H., Samanta S., Fidock D. A., Voelker D. R., Fikrig E., Ben Mamoun C.: *Plasmodium falciparum* phosphoethanolamine methyltransferase is essential for malaria transmission. *Proceedings of the National Academy of Sciences of the United States of America* 2013, 110:18262-18267.
161. Brochet M., Collins M. O., Smith T. K., Thompson E., Sebastian S., Volkmann K., Schwach F., Chappell L., Gomes A. R., Berriman M., Rayner J. C., Baker D. A., Choudhary J., Billker O.: Phosphoinositide Metabolism Links cGMP-Dependent Protein Kinase G to Essential Ca(2+) Signals at Key Decision Points in the Life Cycle of Malaria Parasites. *PLoS biology* 2014, 12:e1001806.
162. Organization W. H.: Global Technical Strategy for Malaria 2016 - 2030. Geneva2015.
163. WHO: Global Technical Strategy for Malaria 2016–2030. World Health Organization; 2015.
164. Organization W. H.: World Malaria Report 2017. (WHO ed. Geneva2017).
165. Cairns M., Roca-Feltrer A., Garske T., Wilson A. L., Diallo D., Milligan P. J., Ghani A. C., Greenwood B. M.: Estimating the potential public health impact of seasonal malaria chemoprevention in African children. *Nature Communications* 2012, 3:881.
166. Noor A. M., Kibuchi E., Mitto B., Coulibaly D., Doumbo O. K., Snow R. W.: Sub-National Targeting of Seasonal Malaria Chemoprevention in the Sahelian Countries of the Nouakchott Initiative. *Plos One* 2015, 10:e0136919.
167. Tagbor H., Antwi G. D., Acheampong P. R., Bart Plange C., Chandramohan D., Cairns M.: Seasonal malaria chemoprevention in an area of extended seasonal transmission in Ashanti, Ghana: an individually randomised clinical trial. *Tropical Medicine & International Health* 2016, 21:224 - 235.
168. Zongo I., Milligan P., Compaore Y. D., Some A. F., Greenwood B., Tarning J., Rosenthal P. J., Sutherland C., Nosten F., Ouedraogo J.-B.: Randomized Noninferiority Trial of Dihydroartemisinin-Piperaquine Compared with Sulfadoxine-Pyrimethamine plus Amodiaquine for Seasonal Malaria Chemoprevention in Burkina Faso. *Antimicrobial Agents and Chemotherapy* 2015, 59:4387 - 4396.
169. Wilson A. L., on behalf of the I. T.: A Systematic Review and Meta-Analysis of the Efficacy and Safety of Intermittent Preventive Treatment of Malaria in Children (IPTc). *Plos One* 2011, 6:e16976.
170. Chanda E., Remijo C. D., Pasquale H., Baba S. P., Lako R. L.: Scale-up of a programme for malaria vector control using long-lasting insecticide-treated nets: lessons from South Sudan. *Bulletin of the World Health Organization* 2014, 92:290 - 296.
171. Ojuka P., Boum Y., Denoeud-Ndam L., Nabasumba C., Muller Y., Okia M., Mwanga-Amumpaire J., De Beaudrap P., Protopopoff N., Etard J.-F.: Early biting and insecticide resistance in the malaria vector *Anopheles* might compromise the effectiveness of vector control intervention in Southwestern Uganda. *Malaria Journal* 2015, 14:148.

172. Ranson H., N'Guessan R., Lines J., Moiroux N., Nkuni Z., Corbel V.: Pyrethroid resistance in African anopheline mosquitoes: what are the implications for malaria control? *Trends in Parasitology* 2011, 27:91 - 98.
173. Protopopoff N., Matowo J., Malima R., Kavishe R., Kaaya R., Wright A., West P. A., Kleinschmidt I., Kisinza W., Masha F. W., Rowland M.: High level of resistance in the mosquito *Anopheles gambiae* to pyrethroid insecticides and reduced susceptibility to bendiocarb in north-western Tanzania. *Malaria Journal* 2013, 12:149 - 149.
174. Trape J.-F., Tall A., Diagne N., Ndiath O., Ly A. B., Faye J., Dieye-Ba F., Roucher C., Bouganali C., Badiane A., Sarr F. D., Mazenot C., Touré-Baldé A., Raoult D., Druilhe P., Mercereau-Puijalon O., Rogier C., Sokhna C.: Malaria morbidity and pyrethroid resistance after the introduction of insecticide-treated bednets and artemisinin-based combination therapies: a longitudinal study. *The Lancet Infectious Diseases* 2011, 11:925 - 932.
175. Yakob L., Cameron M., Lines J.: Combining indoor and outdoor methods for controlling malaria vectors: an ecological model of endectocide-treated livestock and insecticidal bed nets. *Malaria Journal* 2017, 16:114.
176. Sibanda M., Focke W.: Development of an insecticide impregnated polymer wall lining for malaria vector control. *Malaria Journal* 2014, 13:P80.
177. Kruger T., Sibanda M. M., Focke W. W., Bornman M. S., de Jager C.: Acceptability and effectiveness of a monofilament, polyethylene insecticide-treated wall lining for malaria control after six months in dwellings in Vhembe District, Limpopo Province, South Africa. *Malaria Journal* 2015, 14:485.
178. Bourtzis K., Lees R. S., Hendrichs J., Vreysen M. J. B.: More than one rabbit out of the hat: Radiation, transgenic and symbiont-based approaches for sustainable management of mosquito and tsetse fly populations. *Acta Tropica* 2016, 157:115 - 130.
179. Black W. C. I. V., Alphey L., James A. A.: Why RIDL is not SIT. *Trends in Parasitology*, 27:362 - 370.
180. Burt A.: Heritable strategies for controlling insect vectors of disease. *Philosophical Transactions of the Royal Society B: Biological Sciences* 2014, 369:20140217.
181. Shimp R. L., Rowe C., Reiter K., Chen B., Nguyen V., Aebig J., Rausch K. M., Kumar K., Wu Y., Jin A. J., Jones D. S., Narum D. L.: Development of a Pfs25-EPA malaria transmission blocking vaccine as a chemically conjugated nanoparticle. *Vaccine* 2013, 31:2954 - 2962.
182. Lee S.-M., Wu C.-K., Plieskatt J., McAdams D. H., Miura K., Ockenhouse C., King C. R.: Assessment of Pfs25 expressed from multiple soluble expression platforms for use as transmission-blocking vaccine candidates. *Malaria Journal* 2016, 15:405.
183. Li Y., Leneghan D. B., Miura K., Nikolaeva D., Brian I. J., Dicks M. D. J., Fyfe A. J., Zakutansky S. E., de Cassan S., Long C. A., Draper S. J., Hill A. V. S., Hill F., Biswas S.: Enhancing immunogenicity and transmission-blocking activity of malaria vaccines by fusing Pfs25 to IMX313 multimerization technology. *Scientific Reports* 2016, 6:18848.
184. Bousema T., Drakeley C.: Epidemiology and Infectivity of *Plasmodium falciparum* and *Plasmodium vivax* Gametocytes in Relation to Malaria Control and Elimination. *Clinical Microbiology Reviews* 2011, 24:377 - 410.
185. Tomas A. M., Margos G., Dimopoulos G., van Lin L. H. M., de Koning-Ward T. F., Sinha R., Lupetti P., Beetsma A. L., Rodriguez M. C., Karras M., Hager A., Mendoza J., Butcher G. A., Kafatos F., Janse C. J., Waters A. P., Sinden R. E.: P25 and P28 proteins of the malaria ookinete surface have multiple and partially redundant functions. *The EMBO Journal* 2001, 20:3975 - 3983.
186. Kapulu M. C., Da D. F., Miura K., Li Y., Blagborough A. M., Churcher T. S., Nikolaeva D., Williams A. R., Goodman A. L., Sangare I., Turner A. V., Cottingham M. G., Nicosia A., Straschil U., Tsuboi T., Gilbert S. C., Long C. A., Sinden R. E., Draper S. J., Hill A. V. S., Cohuet A., Biswas S.: Comparative Assessment of Transmission-Blocking Vaccine Candidates against *Plasmodium falciparum*. *Scientific Reports* 2015, 5:11193.
187. Wu Y., Ellis R. D., Shaffer D., Fontes E., Malkin E. M., Mahanty S., Fay M. P., Narum D., Rausch K., Miles A. P., Aebig J., Orcutt A., Muratova O., Song G., Lambert L., Zhu D., Miura K., Long C., Saul A., Miller L. H., Durbin A. P.: Phase 1 Trial of Malaria Transmission Blocking Vaccine Candidates Pfs25 and Pvs25 Formulated with Montanide ISA 51. *Plos One* 2008, 3:e2636.
188. Tachibana M., Wu Y., Iriko H., Muratova O., MacDonald N. J., Sattabongkot J., Takeo S., Otsuki H., Torii M., Tsuboi T.: N-Terminal Prodomain of Pfs230 Synthesized Using a Cell-Free System Is Sufficient To Induce Complement-Dependent Malaria Transmission-Blocking Activity. *Clinical and Vaccine Immunology : CVI* 2011, 18:1343 - 1350.
189. Chowdhury D. R., Angov E., Kariuki T., Kumar N.: A Potent Malaria Transmission Blocking Vaccine Based on Codon Harmonized Full Length Pfs48/45 Expressed in *Escherichia coli*. *Plos One* 2009, 4:e6352.

190. Chaudhury S., Ockenhouse C. F., Regules J. A., Dutta S., Wallqvist A., Jongert E., Waters N. C., Lemiale F., Bergmann-Leitner E.: The biological function of antibodies induced by the RTS,S/AS01 malaria vaccine candidate is determined by their fine specificity. *Malaria Journal* 2016, 15:301.
191. Mordmüller B., Surat G., Lagler H., Chakravarty S., Ishizuka A. S., Lalremruata A., Gmeiner M., Campo J. J., Esen M., Ruben A. J., Held J., Calle C. L., Mengue J. B., Gebu T., Ibáñez J., Sulyok M., James E. R., Billingsley P. F., Natasha K. C., Manoj A., Murshedkar T., Gunasekera A., Eappen A. G., Li T., Stafford R. E., Li M., Felgner P. L., Seder R. A., Richie T. L., Sim B. K. L., Hoffman S. L., Kremsner P. G.: Sterile protection against human malaria by chemoattenuated PfSPZ vaccine. *Nature* 2017, 542:445.
192. Kubler-Kielb J., Majadly F., Biesova Z., Mocca C. P., Guo C., Nussenzweig R., Nussenzweig V., Mishra S., Wu Y., Miller L. H., Keith J. M., Liu T.-Y., Robbins J. B., Schneerson R.: A bicomponent *Plasmodium falciparum* investigational vaccine composed of protein-peptide conjugates. *Proceedings of the National Academy of Sciences of the United States of America* 2010, 107:1172 - 1177.
193. Theisen M., Roeffen W., Singh S. K., Andersen G., Amoah L., van de Vegte-Bolmer M., Arens T., Tiendrebeogo R. W., Jones S., Bousema T., Adu B., Dziegiel M. H., Christiansen M., Sauerwein R.: A multi-stage malaria vaccine candidate targeting both transmission and asexual parasite life-cycle stages. *Vaccine* 2014, 32:2623 - 2630.
194. Smith T. A., Chitnis N., Briët O. J. T., Tanner M.: Uses of mosquito-stage transmission-blocking vaccines against *Plasmodium falciparum*. *Trends in Parasitology* 2011, 27:190 - 196.
195. Malkin E. M., Durbin A. P., Diemert D. J., Sattabongkot J., Wu Y., Miura K., Long C. A., Lambert L., Miles A. P., Wang J., Stowers A., Miller L. H., Saul A.: Phase 1 vaccine trial of Pvs25H: a transmission blocking vaccine for *Plasmodium vivax* malaria. *Vaccine* 2005, 23:3131 - 3138.
196. Cohen J., Nussenzweig V., Nussenzweig R., Vekemans J., Leach A.: From the circumsporozoite protein to the RTS, S/AS candidate vaccine. *Human Vaccines* 2010, 1:90 - 96.
197. Gonçalves D., Hunziker P.: Transmission-blocking strategies: the roadmap from laboratory bench to the community. *Malaria Journal* 2016, 15:95.
198. Nielsen C. M., Vekemans J., Lievens M., Kester K. E., Regules J. A., Ockenhouse C. F.: RTS,S malaria vaccine efficacy and immunogenicity during *Plasmodium falciparum* challenge is associated with HLA genotype. *Vaccine* 2018, 36:1637 - 1642.
199. Imwong M., Suwannasin K., Kunasol C., Sutawong K., Mayxay M., Rekol H., Smithuis F. M., Hlaing T. M., Tun K. M., van der Pluijm R. W., Tripura R., Miotto O., Menard D., Dhorda M., Day N. P. J., White N. J., Dondorp A. M.: The spread of artemisinin-resistant *Plasmodium falciparum* in the Greater Mekong subregion: a molecular epidemiology observational study. *The Lancet Infectious Diseases* 2017, 17:491 - 497.
200. Mbengue A., Bhattacharjee S., Pandharkar T., Liu H., Estiu G., Stahelin R. V., Rizk S., Njimoh D. L., Ryan Y., Chotivanich K., Nguon C., Ghorbal M., Lopez-Rubio J.-J., Pfrender M., Emrich S., Mohandas N., Dondorp A. M., Wiest O., Haldar K.: A molecular mechanism of artemisinin resistance in *Plasmodium falciparum* malaria. *Nature* 2015, 520:683 - 687.
201. Mishra N., Bharti R. S., Mallick P., Singh O. P., Srivastava B., Rana R., Phookan S., Gupta H. P., Ringwald P., Valecha N.: Emerging polymorphisms in falciparum Kelch 13 gene in Northeastern region of India. *Malaria Journal* 2016, 15:583.
202. Springer S., Zieger M., Koenig K., Kaatz M., Lademann J., Darvin M. E.: Optimization of the measurement procedure during multiphoton tomography of human skin *in vivo*. *Skin Research and Technology* 2016, 22:356 - 362.
203. Thuy-Nhien N., Tuyen N. K., Tong N. T., Vy N. T., Thanh N. V., Van H. T., Huong-Thu P., Quang H. H., Boni M. F., Dolecek C., Farrar J., Thwaites G. E., Miotto O., White N. J., Hien T. T.: K13 Propeller Mutations in *Plasmodium falciparum* Populations in Regions of Malaria Endemicity in Vietnam from 2009 to 2016. *Antimicrobial Agents and Chemotherapy* 2017, 61.
204. Thanh N. V., Thuy-Nhien N., Tuyen N. T., Tong N. T., Nha-Ca N. T., Dong L. T., Quang H. H., Farrar J., Thwaites G., White N. J., Wolbers M., Hien T. T.: Rapid decline in the susceptibility of *Plasmodium falciparum* to dihydroartemisinin-piperaquine in the south of Vietnam. *Malaria Journal* 2017, 16:27.
205. Arie F., Witkowski B., Amaratunga C., Beghain J., Langlois A.-C., Khim N., Kim S., Duru V., Bouchier C., Ma L., Lim P., Leang R., Duong S., Sreng S., Suon S., Chuor C. M., Bout D. M., Ménard S., Rogers W. O., Genton B., Fandeur T., Miotto O., Ringwald P., Le Bras J., Berry A., Barale J.-C., Fairhurst R. M., Benoit-Vical F., Mercereau-Puijalon O., Ménard D.: A molecular marker of artemisinin-resistant *Plasmodium falciparum* malaria. *Nature* 2014, 505:50 - 55.
206. Verlinden B. K., Louw A., Birkholtz L. M.: Resisting resistance: is there a solution for malaria? *Expert Opinion on Drug Discovery* 2016, 11:395-406.
207. Zyad A., Tilaoui M., Jaafari A., Oukerrou M. A., Mouse H. A.: More insights into the pharmacological effects of artemisinin. *Phytotherapy Research* 2018, 32:216 - 229.

208. Guidelines for the treatment of malaria. [<http://apps.who.int/iris/bitstream/10665/162441/>]
209. White N. J.: Antimalarial drug resistance. *Journal of Clinical Investigation* 2004, 113:1084 - 1092.
210. Gardner M. J., Hall N., Fung E., White O., Berriman M., Hyman R. W., Carlton J. M., Pain A., Nelson K. E., Bowman S., Paulsen I. T., James K., Eisen J. A., Rutherford K., Salzberg S. L., Craig A., Kyes S., Chan M. S., Nene V., Shallom S. J., Suh B., Peterson J., Angiuoli S., Pertea M., Allen J., Selengut J., Haft D., Mather M. W., Vaidya A. B., Martin D. M., Fairlamb A. H., Fraunholz M. J., Roos D. S., Ralph S. A., McFadden G. I., Cummings L. M., Subramanian G. M., Mungall C., Venter J. C., Carucci D. J., Hoffman S. L., Newbold C., Davis R. W., Fraser C. M., Barrell B.: Genome sequence of the human malaria parasite *Plasmodium falciparum*. *Nature* 2002, 419:498-511.
211. Lukens A. K., Ross L. S., Heidebrecht R., Javier Gamo F., Lafuente-Monasterio M. J., Booker M. L., Hartl D. L., Wiegand R. C., Wirth D. F.: Harnessing evolutionary fitness in *Plasmodium falciparum* for drug discovery and suppressing resistance. *Proceedings of the National Academy of Sciences of the United States of America* 2014, 111:799 - 804.
212. Taylor A. R., Flegg J. A., Holmes C. C., Guérin P. J., Sibley C. H., Conrad M. D., Dorsey G., Rosenthal P. J.: Artemether-Lumefantrine and Dihydroartemisinin-Piperaquine Exert Inverse Selective Pressure on *Plasmodium falciparum* Drug Sensitivity-Associated Haplotypes in Uganda. *Open Forum Infect Dis* 2017, 4:ofw229.
213. Sidhu A. B., Verdier-Pinard D., Fidock D. A.: Chloroquine resistance in *Plasmodium falciparum* malaria parasites conferred by *pfcr* mutations. *Science* 2002, 298:210 - 213.
214. Cooper R. A., Ferdig M. T., Su X.-Z., Ursos L. M. B., Mu J., Nomura T., Fujioka H., Fidock D. A., Roepe P. D., Wellems T. E.: Alternative Mutations at Position 76 of the Vacuolar Transmembrane Protein PfCRT Are Associated with Chloroquine Resistance and Unique Stereospecific Quinine and Quinidine Responses in *Plasmodium falciparum*. *Molecular pharmacology* 2002, 61:35 - 42.
215. Cooper R. A., Lane K. D., Deng B., Mu J., Patel J. J., Wellems T. E., Su X., Ferdig M. T.: Mutations in transmembrane domains 1, 4 and 9 of the *Plasmodium falciparum* chloroquine resistance transporter alter susceptibility to chloroquine, quinine and quinidine. *Molecular Microbiology* 2007, 63:270-282.
216. Haldar K., Bhattacharjee S., Safeukui I.: Drug resistance in *Plasmodium*. *Nature Reviews Microbiology* 2018, 16:156.
217. Veiga M. I., Dhingra S. K., Henrich P. P., Straimer J., Gnädig N., Uhlemann A.-C., Martin R. E., Lehane A. M., Fidock D. A.: Globally prevalent PfMDR1 mutations modulate *Plasmodium falciparum* susceptibility to artemisinin-based combination therapies. *Nature Communications* 2016, 7:11553.
218. Korsinczky M., Chen N., Kotecka B., Saul A., Rieckmann K., Cheng Q.: Mutations in *Plasmodium falciparum* Cytochrome b That Are Associated with Atovaquone Resistance Are Located at a Putative Drug-Binding Site. *Antimicrobial Agents and Chemotherapy* 2000, 44:2100 - 2108.
219. Shah N. K., Dhillon G. P. S., Dash A. P., Arora U., Meshnick S. R., Valecha N.: Antimalarial drug resistance of *Plasmodium falciparum* in India: changes over time and space.. *The Lancet Infectious Diseases* 2011, 11:57 - 64.
220. Costa G. L., Amaral L. C., Fontes C. J. F., Carvalho L. H., de Brito C. F. A., de Sousa T. N.: Assessment of copy number variation in genes related to drug resistance in *Plasmodium vivax* and *Plasmodium falciparum* isolates from the Brazilian Amazon and a systematic review of the literature. *Malaria Journal* 2017, 16:152.
221. Peterson D. S., Walliker D., Wellems T. E.: Evidence that a point mutation in dihydrofolate reductase-thymidylate synthase confers resistance to pyrimethamine in falciparum malaria. *Proceedings of the National Academy of Sciences of the United States of America* 1988, 85:9114 - 9118.
222. Gregson A., Plowe C. V.: Mechanisms of Resistance of Malaria Parasites to Antifolates. *Pharmacological Reviews* 2005, 57:117 - 145.
223. Mishra N., Kaitholia K., Srivastava B., Shah N. K., Narayan J. P., Dev V., Phookan S., Anvikar A. R., Rana R., Bharti R. S., Sonal G. S., Dhariwal A. C., Valecha N.: Declining efficacy of artesunate plus sulphadoxine-pyrimethamine in northeastern India. *Malaria Journal* 2014, 13:284.
224. Amato R., Lim P., Miotto O., Amaratunga C., Dek D., Pearson R. D., Almagro-Garcia J., Neal A. T., Sreng S., Suon S., Drury E., Jyothi D., Stalker J., Kwiatkowski D. P., Fairhurst R. M.: Genetic markers associated with dihydroartemisinin-piperaquine failure in *Plasmodium falciparum* malaria in Cambodia: a genotype-phenotype association study. *The Lancet. Infectious diseases* 2017, 17:164 - 173.
225. Lu F., Culleton R., Zhang M., Ramaprasad A., von Seidlein L., Zhou H., Zhu G., Tang J., Liu Y., Wang W., Cao Y., Xu S., Gu Y., Li J., Zhang C., Gao Q., Menard D., Pain A., Yang H., Zhang Q., Cao J.: Emergence of Indigenous Artemisinin-Resistant *Plasmodium falciparum* in Africa. *New England Journal of Medicine* 2017, 376:991 - 993.
226. Sutherland C. J., Lansdell P., Sanders M., Muwanguzi J., van Schalkwyk D. A., Kaur H., Nolder D., Tucker J., Bennett H. M., Otto T. D., Berriman M., Patel T. A., Lynn R., Gkrania-Klotsas E., Chiodini

- P. L.: pfk13-Independent Treatment Failure in Four Imported Cases of *Plasmodium falciparum* Malaria Treated with Artemether-Lumefantrine in the United Kingdom. *Antimicrobial Agents and Chemotherapy* 2017, 61:e02382-02316.
227. Achan J., Mwesigwa J., Edwin C. P., D'Alessandro U.: Malaria medicines to address drug resistance and support malaria elimination efforts. *Expert Rev Clin Pharmacol* 2018, 11:61 - 70.
228. Mok S., Ashley E. A., Ferreira P. E., Zhu L., Lin Z., Yeo T., Chotivanich K., Imwong M., Pukrittayakamee S., Dhorda M., Nguon C., Lim P., Amaratunga C., Suon S., Hien T. T., Htut Y., Faiz M. A., Onyamboko M. A., Mayxay M., Newton P. N., Tripura R., Woodrow C. J., Miotto O., Kwiatkowski D. P., Nosten F., Day N. P. J., Preiser P. R., White N. J., Dondorp A. M., Fairhurst R. M., Bozdech Z.: Population transcriptomics of human malaria parasites reveals the mechanism of artemisinin resistance. *Science (New York, N.Y.)* 2015, 347:431 - 435.
229. Hassett M. R., Sternberg A. R., Riegel B. E., Thomas C. J., Roepe P. D.: Heterologous Expression, Purification, and Functional Analysis of *Plasmodium falciparum* Phosphatidylinositol 3'-Kinase. *Biochemistry* 2017, 56:4335 - 4345.
230. Ismail H. M., Barton V., Phanchana M., Charoensutthivarakul S., Wong M. H. L., Hemingway J., Biagini G. A., O'Neill P. M., Ward S. A.: Artemisinin activity-based probes identify multiple molecular targets within the asexual stage of the malaria parasites *Plasmodium falciparum* 3D7. *Proceedings of the National Academy of Sciences of the United States of America* 2016, 113:2080 - 2085.
231. Wang J., Zhang C.-J., Chia W. N., Loh C. C. Y., Li Z., Lee Y. M., He Y., Yuan L.-X., Lim T. K., Liu M., Liew C. X., Lee Y. Q., Zhang J., Lu N., Lim C. T., Hua Z.-C., Liu B., Shen H.-M., Tan K. S. W., Lin Q.: Haem-activated promiscuous targeting of artemisinin in *Plasmodium falciparum*. *Nature Communications* 2015, 6:10111.
232. Global Technical Strategy for Malaria 2016–2030. [http://www.who.int/malaria/areas/global_technical_strategy/en/. 2016.]
233. [<http://www.endmalaria2040.org/>]
234. Ramachandran S., Hameed P. S., Srivastava A., Shanbhag G., Morayya S., Rautela N., Awasthy D., Kavanagh S., Bharath S., Reddy J., Panduga V., Prabhakar K. R., Saralaya R., Nanduri R., Raichurkar A., Menasinakai S., Achar V., Jimenez-Diaz M. B., Martinez M. S., Angulo-Barturen I., Ferrer S., Sanz L. M., Gamo F. J., Duffy S., Avery V. M., Waterson D., Lee M. C., Coburn-Flynn O., Fidock D. A., Iyer P. S., Narayanan S., Hosagrahara V., Sambandamurthy V. K.: N-aryl-2-aminobenzimidazoles: novel, efficacious, antimalarial lead compounds. *Journal of Medicinal Chemistry* 2014, 57:6642 - 6652.
235. Leroy D., Doerig C.: Drugging the *Plasmodium* kinome: the benefits of academia-industry synergy. *Trends in Pharmacological Sciences* 2008, 29:241-249.
236. Wells T. N., Hooft van Huijsduijnen R., Van Voorhis W. C.: Malaria medicines: a glass half full? *Nature Reviews Drug Discovery* 2015, 14:424 - 442.
237. Ouédraogo A. L., Bastiaens G. J. H., Tiono A. B., Guelbéogo W. M., Kobylinski K. C., Ouédraogo A., Barry A., Bougouma E. C., Nebie I., Ouattara M. S., Lanke K. H. W., Fleckenstein L., Sauerwein R. W., Slater H. C., Churcher T. S., Sirima S. B., Drakeley C., Bousema T.: Efficacy and Safety of the Mosquitocidal Drug Ivermectin to Prevent Malaria Transmission After Treatment: A Double-Blind, Randomized, Clinical Trial. *Clinical Infectious Diseases* 2015, 60:357 - 365.
238. Anthony M. P., Burrows J., Duparc S., Jmoehrle J., Wells T.: The global pipeline of new medicines for the control and elimination of malaria. *Malaria Journal* 2012, 11:316.
239. Le Bihan A., de Kanter R., Angulo-Barturen I., Binkert C., Boss C., Brun R., Brunner R., Buchmann S., Burrows J., Dechering K. J., Delves M., Ewerling S., Ferrer S., Fischli C., Gamo-Benito F. J., Gnädig N. F., Heidmann B., Jiménez-Díaz M. B., Leroy D., Martínez M. S., Meyer S., Moehrle J. J., Ng C. L., Noviyanti R., Ruecker A., Sanz L. M., Sauerwein R. W., Scheurer C., Schleiferboeck S., Sinden R., Snyder C., Straimer J., Wirjanata G., Marfurt J., Price R. N., Weller T., Fischli W., Fidock D. A., Clozel M., Wittlin S.: Characterization of Novel Antimalarial Compound ACT-451840: Preclinical Assessment of Activity and Dose-Efficacy Modeling. *PLoS Medicine* 2016, 13:e1002138.
240. Coertzen D., Reader J., van der Watt M., Nondaba S. H., Gibhard L., Wiesner L., Smith P., D'Alessandro S., Taramelli D., Ning Wong H., du Preez J. L., Wu R. W. K., Birkholtz L.-M., Haynes R. K.: Artemisone and artemiside - potent pan-reactive antimalarial agents that also synergize redox imbalance in *P. falciparum* transmissible gametocyte stages. *Antimicrobial Agents and Chemotherapy* 2018.
241. Shafiq N., Rajagopalan S., Kushwaha H. N., Mittal N., Chandurkar N., Bhalla A., Kaur S., Pandhi P., Puri G. D., Achuthan S., Pareek A., Singh S. K., Srivastava J. S., Gaur S. P. S., Malhotra S.: Single Ascending Dose Safety and Pharmacokinetics of CDR1-97/78: First-in-Human Study of a Novel Antimalarial Drug. *Malaria Research and Treatment* 2014, 2014:372521.
242. MMV [www.mmv.org]
243. Rueda L., Castellote I., Castro-Pichel J., Chaparro M. J., de la Rosa J. C., Garcia-Perez A., Gordo M., Jimenez-Diaz M. B., Kessler A., Macdonald S. J. F., Martinez M. S., Sanz L. M., Gamo F. J.,

- Fernandez E.: Cyclopropyl Carboxamides: A New Oral Antimalarial Series Derived from the Tres Cantos Anti-Malarial Set (TCAMS). *ACS Medicinal Chemistry Letters* 2011, 2:840 - 844.
244. Leroy D.: TCP5 and TCP6 strategy, criteria and test-cascades. MMV Partner Meeting, Geneva 2017.
245. Phillips M. A., White K. L., Kokkonda S., Deng X., White J., Mazouni F. E., Marsh K., Tomchick D. R., Manjulanagara K., Rudra K. R., Wirjanata G., Noviyanti R., Price R. N., Marfurt J., Shackelford D. M., Chiu F. C. K., Campbell M., Jimenez-Diaz M. B., Bazaga S. F., Angulo-Barturen I., Martinez M. S., Lafuente-Monasterio M., Kaminsky W., Silue K., Zeeman A.-M., Kocken C., Leroy D., Blasco B., Rossignol E., Rueckle T., Matthews D., Burrows J. N., Waterson D., Palmer M. J., Rathod P. K., Charman S. A.: A triazolopyrimidine-based dihydroorotate dehydrogenase inhibitor (DSM421) with improved drug-like properties for treatment and prevention of malaria. *ACS Infectious Diseases* 2016, 2:945 - 957.
246. Chavchich M., Van Breda K., Rowcliffe K., Diagana T. T., Edstein M. D.: The Spiroindolone KAE609 Does Not Induce Dormant Ring Stages in *Plasmodium falciparum* Parasites. *Antimicrobial Agents and Chemotherapy* 2016, 60:5167.
247. Daher W., Biot C., Fandeur T., Jouin H., Pelinski L., Viscogliosi E., Fraisse L., Pradines B., Brocard J., Khalife J., Dive D.: Assessment of *Plasmodium falciparum* resistance to ferroquine (SSR97193) in field isolates and in W2 strain under pressure. *Malaria Journal* 2006, 5:1 - 11.
248. Phyo A. P., Jittamala P., Nosten F. H., Pukrittayakamee S., Imwong M., White N. J., Duparc S., Macintyre F., Baker M., Möhrle J. J.: Antimalarial activity of artefenomel (OZ439), a novel synthetic antimalarial endoperoxide, in patients with *Plasmodium falciparum* and *Plasmodium vivax* malaria: an open-label phase 2 trial. *The Lancet Infectious Diseases* 2016, 16:61 - 69.
249. McNamara C. W., Lee M. C., Lim C. S., Lim S. H., Roland J., Simon O., Yeung B. K., Chatterjee A. K., McCormack S. L., Manary M. J., Zeeman A. M., Dechering K. J., Kumar T. S., Henrich P. P., Gagaring K., Ibanez M., Kato N., Kuhlen K. L., Fischli C., Nagle A., Rottmann M., Plouffe D. M., Bursulaya B., Meister S., Rameh L., Trappe J., Haasen D., Timmerman M., Sauerwein R. W., Suwanarusk R., Russell B., Renia L., Nosten F., Tully D. C., Kocken C. H., Glynn R. J., Bodenreider C., Fidock D. A., Diagana T. T., Winzeler E. A.: Targeting *Plasmodium* PI(4)K to eliminate malaria. *Nature* 2013, 504:248 - 253.
250. Baragana B., Hallyburton I., Lee M. C., Norcross N. R., Grimaldi R., Otto T. D., Proto W. R., Blagborough A. M., Meister S., Wirjanata G., Ruecker A., Upton L. M., Abraham T. S., Almeida M. J., Pradhan A., Porzelle A., Luksch T., Martinez M. S., Luksch T., Bolscher J. M., Woodland A., Norval S., Zuccotto F., Thomas J., Simeons F., Stojanovski L., Osuna-Cabello M., Brock P. M., Churcher T. S., Sala K. A., Zakutansky S. E., Jimenez-Diaz M. B., Sanz L. M., Riley J., Basak R., Campbell M., Avery V. M., Sauerwein R. W., Dechering K. J., Noviyanti R., Campo B., Frearson J. A., Angulo-Barturen I., Ferrer-Bazaga S., Gamo F. J., Wyatt P. G., Leroy D., Siegl P., Delves M. J., Kyle D. E., Wittlin S., Marfurt J., Price R. N., Sinden R. E., Winzeler E. A., Charman S. A., Bebrevska L., Gray D. W., Campbell S., Fairlamb A. H., Willis P. A., Rayner J. C., Fidock D. A., Read K. D., Gilbert I. H.: A novel multiple-stage antimalarial agent that inhibits protein synthesis. *Nature* 2015, 522:315 - 320.
251. Phillips M. A., Lotharius J., Marsh K., White J., Dayan A., White K. L., Njoroge J. W., El Mazouni F., Lao Y., Kokkonda S., Tomchick D. R., Deng X., Laird T., Bhatia S. N., March S., Ng C. L., Fidock D. A., Wittlin S., Lafuente-Monasterio M., Benito F. J., Alonso L. M., Martinez M. S., Jimenez-Diaz M. B., Bazaga S. F., Angulo-Barturen I., Haselden J. N., Louttit J., Cui Y., Sridhar A., Zeeman A. M., Kocken C., Sauerwein R., Dechering K., Avery V. M., Duffy S., Delves M., Sinden R., Ruecker A., Wickham K. S., Rochford R., Gahagen J., Iyer L., Riccio E., Mirsalis J., Bathurst I., Rueckle T., Ding X., Campo B., Leroy D., Rogers M. J., Rathod P. K., Burrows J. N., Charman S. A.: A long-duration dihydroorotate dehydrogenase inhibitor (DSM265) for prevention and treatment of malaria. *Science Translational Medicine* 2015, 7:296ra111.
252. Paquet T., Le Manach C., Cabrera D. G., Younis Y., Henrich P. P., Abraham T. S., Lee M. C. S., Basak R., Ghidelli-Disse S., Lafuente-Monasterio M. J., Bantscheff M., Ruecker A., Blagborough A. M., Zakutansky S. E., Zeeman A. M., White K. L., Shackelford D. M., Mannila J., Morizzi J., Scheurer C., Angulo-Barturen I., Martinez M. S., Ferrer S., Sanz L. M., Gamo F. J., Reader J., Botha M., Dechering K. J., Sauerwein R. W., Tungtaeng A., Vanachayangkul P., Lim C. S., Burrows J., Witty M. J., Marsh K. C., Bodenreider C., Rochford R., Solapure S. M., Jimenez-Diaz M. B., Wittlin S., Charman S. A., Donini C., Campo B., Birkholtz L. M., Hanson K. K., Drewes G., Kocken C. H. M., Delves M. J., Leroy D., Fidock D. A., Waterson D., Street L. J., Chibale K.: Antimalarial efficacy of MMV390048, an inhibitor of *Plasmodium* phosphatidylinositol 4-kinase. *Science Translational Medicine* 2017, 9.
253. Kondrashin A., Baranova A. M., Ashley E. A., Recht J., White N. J., Sergiev V. P.: Mass primaquine treatment to eliminate vivax malaria: lessons from the past. *Malaria Journal* 2014, 13:51.
254. Graves P. M., Choi L., Gelband H., Garner P.: Primaquine or other 8-aminoquinolines for reducing *Plasmodium falciparum* transmission. *Cochrane Database of Systematic Reviews* 2018, 2:Cd008152.

255. Lucantoni L., Avery V.: Whole-cell in vitro screening for gametocytocidal compounds. . *Future Medicinal Chemistry* 2012, 4:2337 - 2360.
256. Bousema T., Okell L., Shekalaghe S., Griffin J. T., Omar S., Sawa P., Sutherland C., Sauerwein R., Ghani A. C., Drakeley C.: Revisiting the circulation time of *Plasmodium falciparum* gametocytes: molecular detection methods to estimate the duration of gametocyte carriage and the effect of gametocytocidal drugs. *Malaria Journal* 2010, 9:136.
257. Shekalaghe S., Drakeley C., Gosling R., Ndaro A., van Meegeren M., Enevold A., Alifrangis M., Mosha F., Sauerwein R., Bousema T.: Primaquine clears submicroscopic *Plasmodium falciparum* gametocytes that persist after treatment with sulphadoxine-pyrimethamine and artesunate. *Plos One* 2007, 2:e1023.
258. Dicko A., Brown J. M., Diawara H., Baber I., Mahamar A., Soumare H. M., Sanogo K., Koita F., Keita S., Traore S. F., Chen I., Poirot E., Hwang J., McCulloch C., Lanke K., Pett H., Niemi M., Nosten F., Bousema T., Gosling R.: Primaquine to reduce transmission of *Plasmodium falciparum* malaria in Mali: a single-blind, dose-ranging, adaptive randomised phase 2 trial. *The Lancet Infectious Diseases* 2016, 16:674 - 684.
259. Goncalves B. P., Tiono A. B., Ouedraogo A., Guelbeogo W. M., Bradley J., Nebie I., Siaka D., Lanke K., Eziefula A. C., Diarra A., Pett H., Bougouma E. C., Sirima S. B., Drakeley C., Bousema T.: Single low dose primaquine to reduce gametocyte carriage and *Plasmodium falciparum* transmission after artemether-lumefantrine in children with asymptomatic infection: a randomised, double-blind, placebo-controlled trial. *BMC Medicine* 2016, 14:40.
260. Mwaiswelo R., Ngasala B., Jovel I., Aydin-Schmidt B., Gosling R., Premji Z., Mmbando B., Björkman A., Mårtensson A.: Adding a single low-dose of primaquine (0.25 mg/kg) to artemether-lumefantrine did not compromise treatment outcome of uncomplicated *Plasmodium falciparum* malaria in Tanzania: a randomized, single-blinded clinical trial. *Malaria Journal* 2016, 15:435.
261. Mwaiswelo R., Ngasala B. E., Jovel I., Gosling R., Premji Z., Poirot E., Mmbando B. P., Bjorkman A., Martensson A.: Safety of a single low-dose of primaquine in addition to standard artemether-lumefantrine regimen for treatment of acute uncomplicated *Plasmodium falciparum* malaria in Tanzania. *Malaria Journal* 2016, 15:316.
262. Tine R. C., Sylla K., Faye B. T., Poirot E., Fall F. B., Sow D., Wang D., Ndiaye M., Ndiaye J. L., Faye B., Greenwood B., Gaye O., Milligan P.: Safety and Efficacy of Adding a Single Low Dose of Primaquine to the Treatment of Adult Patients With *Plasmodium falciparum* Malaria in Senegal, to Reduce Gametocyte Carriage: A Randomized Controlled Trial. *Clinical Infectious Diseases* 2017, 65:535 - 543.
263. Johnston G. L., Gething P. W., Hay S. I., Smith D. L., Fidock D. A.: Modeling Within-Host Effects of Drugs on *Plasmodium falciparum* Transmission and Prospects for Malaria Elimination. *PLOS Computational Biology* 2014, 10:e1003434.
264. Plouffe D. M., Wree M., Du A. Y., Meister S., Li F., Patra K., Lubar A., Okitsu S. L., Flannery E. L., Kato N., Tanaseichuk O., Comer E., Zhou B., Kuhlen K., Zhou Y., Leroy D., Schreiber S. L., Scherer C. A., Vinetz J., Winzeler E. A.: High-Throughput Assay and Discovery of Small Molecules that Interrupt Malaria Transmission. *Cell Host & Microbe* 2015, 19.
265. Ruecker A., Mathias D. K., Straschil U., Churcher T. S., Dinglasan R. R., Leroy D., Sinden R. E., Delves M. J.: A male and female gametocyte functional viability assay to identify biologically relevant malaria transmission-blocking drugs. *Antimicrobial Agents and Chemotherapy* 2014, 58:7292-7302.
266. Sinden R. E.: Developing transmission-blocking strategies for malaria control. *Plos Pathogens* 2017, 13:e1006336.
267. Medley G. F., Sinden R. E., Fleck S., Billingsley P. F., Tirawanchai N., Rodriguez M. H.: Heterogeneity in patterns of malarial oocyst infections in the mosquito vector. *Parasitology* 1993, 106 (Pt 5):441 - 449.
268. Gilson P. R., Crabb B. S.: Morphology and kinetics of the three distinct phases of red blood cell invasion by *Plasmodium falciparum* merozoites. *International Journal for Parasitology* 2009, 39:91 - 96.
269. Niederwieser I., Felger I., Beck H. P.: Limited polymorphism in *Plasmodium falciparum* sexual-stage antigens. *The American Journal of Tropical Medicine and Hygiene* 2001, 64:9 - 11.
270. Hamilton W. L., Claessens A., Otto T. D., Kekre M., Fairhurst R. M., Rayner J. C., Kwiatkowski D.: Extreme mutation bias and high AT content in *Plasmodium falciparum*. *Nucleic Acids Research* 2017, 45:1889 - 1901.
271. Leroy D., Campo B., Ding X. C., Burrows J. N., Cherbuis S.: Defining the biology component of the drug discovery strategy for malaria eradication. *Trends in Parasitology* 2014, 30:478-490.
272. Vial H., Taramelli D., Boulton I. C., Ward S. A., Doerig C., Chibale K.: CRIMALDDI: platform technologies and novel anti-malarial drug targets. *Malaria Journal* 2013, 12:396-396.
273. Medicines for Malaria Venture [https://www.mmv.org/]

274. Brunschwig C., Lawrence N., Taylor D., Abay E., Njoroge M., Basarab G. S., Le Manach C., Paquet T., González Cabrera D., Nchinda A. T., de Kock C., Wiesner L., Denti P., Waterson D., Blasco B., Leroy D., Witty M. J., Donini C., Duffy J., Wittlin S., White K. L., Charman S. A., Jiménez-Díaz M. B., Angulo-Barturen I., Herreros E., Gamo F. J., Rochford R., Mancama D., Coetzer T. L., van der Watt M. E., Reader J., Birkholtz L.-M., Marsh K. C., Solapure S. M., Vanaerschot M., Fidock D. A., Fish P. V., Siegl P., Smith D. A., Wirjanata G., Noviyanti R., Price R. N., Marfurt J., Silue K. D., Street L. J., Chibale K.: UCT943, a next generation *Plasmodium falciparum* PI4K inhibitor preclinical candidate for the treatment of malaria. *Antimicrobial Agents and Chemotherapy* 2018.
275. Doerig C., Billker O., Pratt D., Endicott J.: Protein kinases as targets for antimalarial intervention: Kinomics, structure-based design, transmission-blockade, and targeting host cell enzymes. *Biochimica et Biophysica Acta* 2005, 1754:132 - 150.
276. Klebl B., Müller G., Hamacher M., Mannhold R., Kubinyi H., Folkers G.: *Protein Kinases as Drug Targets*. Wiley; 2011.
277. Manning G., Whyte D. B., Martinez R., Hunter T., Sudarsanam S.: The protein kinase complement of the human genome. *Science* 2002, 298:1912 - 1934.
278. Talevich E., Tobin A. B., Kannan N., Doerig C.: An evolutionary perspective on the kinome of malaria parasites. *Philosophical Transactions of the Royal Society B: Biological Sciences* 2012, 367:2607 - 2618.
279. Tewari R., Straschil U., Bateman A., Böhme U., Cherevach I., Gong P., Pain A., Billker O.: The Systematic Functional Analysis of *Plasmodium* Protein Kinases Identifies Essential Regulators of Mosquito Transmission. *Cell Host & Microbe* 2010, 8:377-387.
280. Roskoski R.: Classification of small molecule protein kinase inhibitors based upon the structures of their drug-enzyme complexes. *Pharmacological research* 2016, 103:26 - 48.
281. Brochet M., Tobin A. B., Billker O., Doerig C.: The Kinomics of Malaria. In *Kinomics* Edited by Kraatz H. B., Martic S.: Wiley; 2015
282. de Oliveira P. S. L., Ferraz F. A. N., Pena D. A., Pramio D. T., Morais F. A., Schechtman D.: Revisiting protein kinase–substrate interactions: Toward therapeutic development. *Science Signaling* 2016, 9:re3.
283. Hanahan D., Weinberg R. A.: Hallmarks of cancer: the next generation. *Cell* 2011, 144:646 - 674.
284. Knuutila S., Bjorkqvist A. M., Autio K., Tarkkanen M., Wolf M., Monni O., Szymanska J., Larramendy M. L., Tapper J., Pere H., El-Rifai W., Hemmer S., Wasenius V. M., Vidgren V., Zhu Y.: DNA copy number amplifications in human neoplasms: review of comparative genomic hybridization studies. *Am J Pathol* 1998, 152:1107 - 1123.
285. Kinch M. S.: An analysis of FDA-approved drugs for oncology. *Drug Discovery Today* 2014, 19:1831 - 1835.
286. Zhang J., Yang P. L., Gray N. S.: Targeting cancer with small molecule kinase inhibitors. *Nature Reviews Cancer* 2009, 9:28.
287. Kini S. G., Garg V., Prasanna S., Rajappan R., Mubeen M.: Protein Kinases as Drug Targets in Human and Animal Diseases. *Current Enzyme Inhibition* 2017, 13:99 - 108.
288. Cohen P., Alessi D. R.: Kinase Drug Discovery – What's Next in the Field? *ACS Chemical Biology* 2013, 8:96 - 104.
289. Roberts M. C., Sutcliffe J., Courvalin P., Jensen L. B., Rood J., Seppala H.: Nomenclature for Macrolide and Macrolide-Lincosamide-Streptogramin B Resistance Determinants. *Antimicrobial Agents and Chemotherapy* 1999, 43:2823 - 2830.
290. Wu P., Nielsen T. E., Clausen M. H.: FDA-approved small-molecule kinase inhibitors. *Trends in Pharmacological Sciences* 2015, 36:422 - 439.
291. Fabbro D., Cowan-Jacob S. W., Moebitz H.: Ten things you should know about protein kinases: IUPHAR Review 14. *British Journal of Pharmacology* 2015, 172:2675 - 2700.
292. Traxler P. M.: Protein tyrosine kinase inhibitors in cancer treatment. *Expert Opinion on Therapeutic Patents* 1997, 7:571 - 588.
293. Zuccotto F., Ardini E., Casale E., Angiolini M.: Through the "gatekeeper door": exploiting the active kinase conformation. *Journal of Medicinal Chemistry* 2010, 53:2681 - 2694.
294. Pargellis C., Tong L., Churchill L., Cirillo P. F., Gilmore T., Graham A. G., Grob P. M., Hickey E. R., Moss N., Pav S., Regan J.: Inhibition of p38 MAP kinase by utilizing a novel allosteric binding site. *Nature structural & molecular biology* 2002, 9:268 - 272.
295. Davidson W., Frego L., Peet G. W., Kroe R. R., Labadia M. E., Lukas S. M., Snow R. J., Jakes S., Grygon C. A., Pargellis C., Werneburg B. G.: Discovery and characterization of a substrate selective p38alpha inhibitor. *Biochemistry* 2004, 43:11658 - 11671.
296. Zhao Z., Wu H., Wang L., Liu Y., Knapp S., Liu Q., Gray N. S.: Exploration of type II binding mode: A privileged approach for kinase inhibitor focused drug discovery? *ACS Chemical Biology* 2014, 9:1230 - 1241.

297. Cox K. J., Shomin C. D., Ghosh I.: Tinkering outside the kinase ATP box: allosteric (type IV) and bivalent (type V) inhibitors of protein kinases. *Future Medicinal Chemistry* 2011, 3:29 - 43.
298. Adrian F. J., Ding Q., Sim T., Velentza A., Sloan C., Liu Y., Zhang G., Hur W., Ding S., Manley P., Mestan J., Fabbro D., Gray N. S.: Allosteric inhibitors of Bcr-abl-dependent cell proliferation. *Nature Chemical Biology* 2006, 2:95 - 102.
299. Zhang J., Adrian F. J., Jahnke W., Cowan-Jacob S. W., Li A. G., Jacob R. E., Sim T., Powers J., Dierks C., Sun F., Guo G. R., Ding Q., Okram B., Choi Y., Wojciechowski A., Deng X., Liu G., Fendrich G., Strauss A., Vajpai N., Grzesiek S., Tuntland T., Liu Y., Bursulaya B., Azam M., Manley P. W., Engen J. R., Daley G. Q., Warmuth M., Gray N. S.: Targeting Bcr-Abl by combining allosteric with ATP-binding-site inhibitors. *Nature* 2010, 463:501 - 506.
300. Schwartz P. A., Murray B. W.: Protein kinase biochemistry and drug discovery. *Bioorganic Chemistry* 2011, 39:192 - 210.
301. Anamika, Srinivasan N., Krupa A.: A genomic perspective of protein kinases in *Plasmodium falciparum*. *Proteins: Structure, Function, and Bioinformatics* 2005, 58:180 - 189.
302. Ward P., Equinet L., Packer J., Doerig C.: Protein kinases of the human malaria parasite *Plasmodium falciparum*: the kinome of a divergent eukaryote. *BMC Genomics* 2004, 5:79-79.
303. Solyakov L., Halbert J., Alam M. M., Semblat J.-P., Dorin-Semblat D., Reininger L., Bottrill A. R., Mistry S., Abdi A., Fennell C., Holland Z., Demarta C., Bouza Y., Sicard A., Nivez M.-P., Eschenlauer S., Lama T., Thomas D. C., Sharma P., Agarwal S., Kern S., Pradel G., Graciotti M., Tobin A. B., Doerig C.: Global kinomic and phospho-proteomic analyses of the human malaria parasite *Plasmodium falciparum*. *Nature Communications* 2011, 2:565.
304. Lasonder E., Green J. L., Camarda G., Talabani H., Holder A. A., Langsley G., Alano P.: The *Plasmodium falciparum* schizont phosphoproteome reveals extensive phosphatidylinositol and cAMP-protein kinase A signaling. *Journal of Proteome Research* 2012, 11:5323 - 5337.
305. Pease B. N., Huttlin E. L., Jedrychowski M. P., Talevich E., Harmon J., Dillman T., Kannan N., Doerig C., Chakrabarti R., Gygi S. P., Chakrabarti D.: Global Analysis of Protein Expression and Phosphorylation of Three Stages of *Plasmodium falciparum* Intraerythrocytic Development. *Journal of Proteome Research* 2013, 12:4028 - 4045.
306. Treeck M., Sanders J. L., Elias J. E., Boothroyd J. C.: The Phosphoproteomes of *Plasmodium falciparum* and *Toxoplasma gondii* reveal unusual adaptations within and beyond the parasites' boundaries. *Cell Host & Microbe* 2011, 10:410 - 419.
307. Niefind K., Guerra B., Ermakowa I., Issinger O.-G.: Crystal structure of human protein kinase CK2: insights into basic properties of the CK2 holoenzyme. *The EMBO Journal* 2001, 20:5320 - 5331.
308. Marti M., Good R. T., Rug M., Knuepfer E., Cowman A. F.: Targeting Malaria Virulence and Remodeling Proteins to the Host Erythrocyte. *Science* 2004, 306:1930 - 1933.
309. Schneider A. G., Mercereau-Puijalon O.: A new apicomplexa-specific protein kinase family: multiple members in *Plasmodium falciparum*, all with an export signature. *BMC Genomics* 2005, 6.
310. Nunes M. C., Okada M., Scheidig-Benatar C., Cooke B. M., Scherf A.: *Plasmodium falciparum* FIKK Kinase Members Target Distinct Components of the Erythrocyte Membrane. *Plos One* 2010, 5:e11747.
311. Nunes M. C., Goldring J. P. D., Doerig C., Scherf A.: A novel protein kinase family in *Plasmodium falciparum* is differentially transcribed and secreted to various cellular compartments of the host cell. *Molecular Microbiology* 2007, 63:391 - 403.
312. Kyes S. A., Rowe J. A., Kriek N., Newbold C. I.: Rifins: a second family of clonally variant proteins expressed on the surface of red cells infected with *Plasmodium falciparum*. *Proceedings of the National Academy of Sciences of the United States of America* 1999, 96:9333 - 9338.
313. Bonnefoy S., Guillotte M., Langsley G., Mercereau-Puijalon O.: *Plasmodium falciparum*: characterization of gene R45 encoding a trophozoite antigen containing a central block of six amino acid repeats. *Experimental Parasitology* 1992, 74:441 - 451.
314. Le Roch K., Sestier C., Dorin D., Waters N., Kappes B., Chakrabarti D., Meijer L., Doerig C.: Activation of a *Plasmodium falciparum* cdc2-related Kinase by Heterologous p25 and Cyclin H: Functional Characterization of a P. falciparum Cyclin Homologue. *Journal of Biological Chemistry* 2000, 275:8952 - 8958.
315. Li J. L., Robson K. J. H., Chen J. L., Targett G. A. T., Baker D. A.: Pfmrk, A MO15-Related Protein Kinase from *Plasmodium falciparum*. *European Journal of Biochemistry* 1996, 241:805 - 813.
316. Dorin-Semblat D., Sicard A., Doerig C., Ranford-Cartwright L., Doerig C.: Disruption of the Pfk7 Gene Impairs Schizogony and Sporogony in the Human Malaria Parasite *Plasmodium falciparum*. *Eukaryotic Cell* 2008, 7:279 - 285.
317. Jirage D., Chen Y., Caridha D., O'Neil M. T., Eyase F., Witola W. H., Mamoun C. B., Waters N. C.: The malarial CDK Pfmrk and its effector PfMAT1 phosphorylate DNA replication proteins and co-localize in the nucleus. *Molecular and Biochemical Parasitology* 2010, 172:9 - 18.

318. Rossignol M., Kolb-Cheyne I., Egly J. M.: Substrate specificity of the cdk-activating kinase (CAK) is altered upon association with TFIH. *The EMBO Journal* 1997, 16:1628 - 1637.
319. Chen Y., Jirage D., Caridha D., Kathcart A. K., Cortes E. A., Denuff R. A., Geyer J. A., Prigge S. T., Waters N. C.: Identification of an effector protein and gain-of-function mutants that activate Pfmrk, a malarial cyclin-dependent protein kinase. *Molecular and Biochemical Parasitology* 2006, 149:48 - 57.
320. Bracchi-Ricard V., Barik S., Delvecchio C., Doerig C., Chakrabarti R., Chakrabarti D.: PfPK6, a novel cyclin-dependent kinase/mitogen-activated protein kinase-related protein kinase from *Plasmodium falciparum*. *Biochemical Journal* 2000, 347:255 - 263.
321. Dorin-Semlat D., Quashie N., Halbert J., Sicard A., Doerig C., Peat E., Ranford-Cartwright L., Doerig C.: Functional characterization of both MAP kinases of the human malaria parasite *Plasmodium falciparum* by reverse genetics. *Molecular Microbiology* 2007, 65:1170 - 1180.
322. Tewari R., Dorin D., Moon R., Doerig C., Billker O.: An atypical mitogen-activated protein kinase controls cytokinesis and flagellar motility during male gamete formation in a malaria parasite. *Molecular Microbiology* 2005, 58:1253 - 1263.
323. Reininger L., Wilkes J. M., Bourgade H., Miranda-Saavedra D., Doerig C.: An essential Aurora-related kinase transiently associates with spindle pole bodies during *Plasmodium falciparum* erythrocytic schizogony. *Molecular Microbiology* 2011, 79:205-221.
324. Deng W., Baker D. A.: A novel cyclic GMP-dependent protein kinase is expressed in the ring stage of the *Plasmodium falciparum* life cycle. *Molecular Microbiology* 2002, 44:1141 - 1151.
325. Taylor H. M., McRobert L., Grainger M., Sicard A., Dluzewski A. R., Hopp C. S., Holder A. A., Baker D. A.: The malaria parasite cyclic GMP-dependent protein kinase plays a central role in blood-stage schizogony. *Eukaryotic Cell* 2010, 9:37 - 45.
326. Diaz C. A., Allocco J., Powles M. A., Yeung L., Donald R. G., Anderson J. W., Liberator P. A.: Characterization of *Plasmodium falciparum* cGMP-dependent protein kinase (PfPKG): antiparasitic activity of a PKG inhibitor. *Molecular and Biochemical Parasitology* 2006, 146:78 - 88.
327. Cheng S., Willmann M. R., Chen H., Sheen J.: Calcium Signaling through Protein Kinases. The Arabidopsis Calcium-Dependent Protein Kinase Gene Family. *Plant Physiology* 2002, 129:469 - 485.
328. Nagamune K., Moreno S. N., Chini E. N., Sibley L. D.: Calcium Regulation and Signaling in Apicomplexan Parasites. In *Molecular Mechanisms of Parasite Invasion: Subcellular Biochemistry*. Edited by Burleigh B. A., Soldati-Favre D. New York, NY: Springer New York; 2008: 70 - 81
329. Wernimont A. K., Artz J. D., Finerty P., Lin Y., Amani M., Allali-Hassani A., Senisterra G., Vedadi M., Tempel W., Mackenzie F., Chau I., Lourido S., Sibley L. D., Hui R.: Structures of apicomplexan calcium-dependent protein kinases reveal mechanism of activation by calcium. *Nature structural & molecular biology* 2010, 17:596 - 601.
330. Kato N., Sakata T., Breton G., Le Roch K. G., Nagle A., Andersen C., Bursulaya B., Henson K., Johnson J., Kumar K. A., Marr F., Mason D., McNamara C., Plouffe D., Ramachandran V., Spooner M., Tuntland T., Zhou Y., Peters E. C., Chatterjee A., Schultz P. G., Ward G. E., Gray N., Harper J., Winzeler E. A.: Gene expression signatures and small-molecule compounds link a protein kinase to *Plasmodium falciparum* motility. *Nature Chemical Biology* 2008, 4:347.
331. Billker O., Dechamps S., Tewari R., Wenig G., Franke-Fayard B., Brinkmann V.: Calcium and a Calcium-Dependent Protein Kinase Regulate Gamete Formation and Mosquito Transmission in a Malaria Parasite. *Cell*, 117:503 - 514.
332. Green J. L., Rees-Channer R. R., Howell S. A., Martin S. R., Knuepfer E., Taylor H. M., Grainger M., Holder A. A.: The Motor Complex of *Plasmodium falciparum*: Phosphorylation by a Calcium-Dependent Protein Kinase. *The Journal of Biological Chemistry* 2008, 283:30980 - 30989.
333. Coppi A., Tewari R., Bishop J. R., Bennett B. L., Lawrence R., Esko J. D., Billker O., Sinnis P.: Heparan sulfate proteoglycans provide a signal to *Plasmodium* sporozoites to stop migrating and productively invade host cells. *Cell Host Microbe* 2007, 2:316 - 327.
334. Ishino T., Orito Y., Chinzei Y., Yuda M.: A calcium-dependent protein kinase regulates *Plasmodium* ookinete access to the midgut epithelial cell. *Molecular Microbiology* 2006, 59:1175 - 1184.
335. Farber P. M., Graeser R., Franklin R. M., Kappes B.: Molecular cloning and characterization of a second calcium-dependent protein kinase of *Plasmodium falciparum*. *Molecular and Biochemical Parasitology* 1997, 87:211 - 216.
336. Li J.-L., Baker D. A., Cox L. S.: Sexual stage-specific expression of a third calcium-dependent protein kinase from *Plasmodium falciparum* 11 Nucleotide sequence data reported in this paper are available in the GenBank, EMBL and DDJB databases under the accession number AF106064. *Biochimica et Biophysica Acta (BBA) - Gene Structure and Expression* 2000, 1491:341 - 349.
337. Siden-Kiamos I., Ecker A., Nybäck S., Louis C., Sinden R. E., Billker O.: *Plasmodium berghei* calcium-dependent protein kinase 3 is required for ookinete gliding motility and mosquito midgut invasion. *Molecular Microbiology* 2006, 60:1355 - 1363.

338. Ranjan R., Ahmed A., Gourinath S., Sharma P.: Dissection of Mechanisms Involved in the Regulation of *Plasmodium falciparum* Calcium-dependent Protein Kinase 4. *The Journal of Biological Chemistry* 2009, 284:15267 - 15276.
339. Dvorin J. D., Martyn D. C., Patel S. D., Grimley J. S., Collins C. R., Hopp C. S., Bright A. T., Westenberger S., Winzeler E., Blackman M. J., Baker D. A., Wandless T. J., Duraisingh M. T.: A Plant-Like Kinase in *Plasmodium falciparum* Regulates Parasite Egress From Erythrocytes. *Science (New York, N.Y.)* 2010, 328:910 - 912.
340. Naumann K. M., Jones G. L., Saul A., Smith R.: Parasite-induced changes to localized erythrocyte membrane deformability in *Plasmodium falciparum* cultures. *Immunology And Cell Biology* 1992, 70:267.
341. ROSS-MACDONALD P. B., GRAESER R., KAPPES B., FRANKLIN R., WILLIAMSON D. H.: Isolation and expression of a gene specifying a cdc2-like protein kinase from the human malaria parasite *Plasmodium falciparum*. *European Journal of Biochemistry* 1994, 220:693 - 701.
342. Dorin D., Roch K. L., Sallicandro P., Alano P., Parzy D., Pouillet P., Meijer L., Doerig C.: Pfnk-1, a NIMA-related kinase from the human malaria parasite *Plasmodium falciparum*. *European Journal of Biochemistry* 2001, 268:2600 - 2608.
343. Lye Y. M., Chan M., Sim T.-S.: Pfnk3: An atypical activator of a MAP kinase in *Plasmodium falciparum*. *FEBS Letters* 2006, 580:6083 - 6092.
344. Dorin D., Alano P., Boccaccio I., Cicéron L., Doerig C., Sulpice R., Parzy D., Doerig C.: An Atypical Mitogen-activated Protein Kinase (MAPK) Homologue Expressed in Gametocytes of the Human Malaria Parasite *Plasmodium falciparum* : IDENTIFICATION OF A MAPK SIGNATURE. *Journal of Biological Chemistry* 1999, 274:29912 - 29920.
345. Dorin-Semblat D., Schmitt S., Semblat J.-P., Sicard A., Reininger L., Goldring D., Patterson S., Quashie N., Chakrabarti D., Meijer L., Doerig C.: *Plasmodium falciparum* NIMA-related kinase Pfnk-1: sex specificity and assessment of essentiality for the erythrocytic asexual cycle. *Microbiology* 2011, 157:2785 - 2794.
346. Reininger L., Billker O., Tewari R., Mukhopadhyay A., Fennell C., Dorin-Semblat D., Doerig C., Goldring D., Harmse L., Ranford-Cartwright L., Packer J., Doerig C.: A NIMA-related protein kinase is essential for completion of the sexual cycle of malaria parasites. *The Journal of Biological Chemistry* 2005, 280:31957 - 31964.
347. Reininger L., Tewari R., Fennell C., Holland Z., Goldring D., Ranford-Cartwright L., Billker O., Doerig C.: An Essential Role for the *Plasmodium* Nek-2 Nima-related Protein Kinase in the Sexual Development of Malaria Parasites. *The Journal of Biological Chemistry* 2009, 284:20858 - 20868.
348. Fruman D. A., Meyers R. E., Cantley L. C.: Phosphoinositide Kinases. *Annual Review of Biochemistry* 1998, 67:481 - 507.
349. Krüger T., Sanchez C. P., Lanzer M.: Complementation of *Saccharomyces cerevisiae* pik1ts by a phosphatidylinositol 4-kinase from *Plasmodium falciparum*. *Molecular and Biochemical Parasitology* 2010, 172:149 - 151.
350. Mayinger P.: Phosphoinositides and vesicular membrane traffic. *Biochimica et Biophysica Acta* 2012, 1821:1104 - 1113.
351. Raabe A. C., Wengelnik K., Billker O., Vial H. J.: Multiple roles for *Plasmodium berghei* phosphoinositide-specific phospholipase C in regulating gametocyte activation and differentiation. *Cellular Microbiology* 2011, 13:955 - 966.
352. Ogwan'g R., Mwangi J., Gachihhi G., Nwachukwu A., Roberts C. R., Martin S. K.: Use of pharmacological agents to implicate a role for phosphoinositide hydrolysis products in malaria gamete formation. *Biochemical pharmacology* 1993, 46:1601 - 1606.
353. K. Martin S., Jett M., Schneider I.: *Correlation of Phosphoinositide Hydrolysis with Exflagellation in the Malaria Microgametocyte*. 1994.
354. Carey A. F., Singer M., Bargieri D., Thiberge S., Frischknecht F., Ménard R., Amino R.: Calcium dynamics of *Plasmodium berghei* sporozoite motility. *Cellular Microbiology* 2014, 16:768 - 783.
355. Vaid A., Thomas D. C., Sharma P.: Role of Ca²⁺/Calmodulin-PfPKB Signaling Pathway in Erythrocyte Invasion by *Plasmodium falciparum*. *Journal of Biological Chemistry* 2008, 283:5589 - 5597.
356. Surolia N., Padmanaban G.: Chloroquine inhibits heme-dependent protein synthesis in *Plasmodium falciparum*. *Proceedings of the National Academy of Sciences of the United States of America* 1991, 88:4786 - 4790.
357. Zhang M., Mishra S., Sakthivel R., Rojas M., Ranjan R., Sullivan W. J., Fontoura B. M. A., Ménard R., Dever T. E., Nussenzweig V.: PK4, a eukaryotic initiation factor 2 α (eIF2 α) kinase, is essential for the development of the erythrocytic cycle of *Plasmodium*. *Proceedings of the National Academy of Sciences* 2012, 109:3956 - 3961.

358. Hanks S. K., Quinn A. M.: Protein kinase catalytic domain sequence database: identification of conserved features of primary structure and classification of family members. *Methods in enzymology* 1991, 200:38 - 62.
359. Doerig C.: Protein kinases as targets for anti-parasitic chemotherapy. *Biochimica et Biophysica Acta* 2004, 1697:155 - 168.
360. DePristo M. A., Zilversmit M. M., Hartl D. L.: On the abundance, amino acid composition, and evolutionary dynamics of low-complexity regions in proteins. *Gene* 2006, 378:19 - 30.
361. Zilversmit M. M., Volkman S. K., DePristo M. A., Wirth D. F., Awadalla P., Hartl D. L.: Low-complexity regions in *Plasmodium falciparum*: missing links in the evolution of an extreme genome. *Molecular biology and evolution* 2010, 27:2198 - 2209.
362. Hopp C. S., Bowyer P. W., Baker D. A.: The role of cGMP signalling in regulating life cycle progression of *Plasmodium*. *Microbes Infect.* 2012, 14:831 - 837.
363. Sun W., Huang X., Li H., Tawa G., Fisher E., Tanaka T. Q., Shinn P., Huang W., Williamson K. C., Zheng W.: Novel lead structures with both *Plasmodium falciparum* gametocytocidal and asexual blood stage activity identified from high throughput compound screening. *Malaria Journal* 2017, 16:147.
364. Bouloc N., Large J. M., Smiljanic E., Whalley D., Ansell K. H., Edlin C. D., Bryans J. S.: Synthesis and *in vitro* evaluation of imidazopyridazines as novel inhibitors of the malarial kinase PfPK7. *Bioorganic & Medicinal Chemistry Letters* 2008, 18:5294 - 5298.
365. Ansell K. H., Jones H. M., Whalley D., Hearn A., Taylor D. L., Patin E. C., Chapman T. M., Osborne S. A., Wallace C., Birchall K., Large J., Bouloc N., Smiljanic-Hurley E., Clough B., Moon R. W., Green J. L., Holder A. A.: Biochemical and Antiparasitic Properties of Inhibitors of the *Plasmodium falciparum* Calcium-Dependent Protein Kinase PfCDPK1. *Antimicrobial Agents and Chemotherapy* 2014, 58:6032-6043.
366. Chapman T. M., Osborne S. A., Bouloc N., Large J. M., Wallace C., Birchall K., Ansell K. H., Jones H. M., Taylor D., Clough B., Green J. L., Holder A. A.: Substituted imidazopyridazines are potent and selective inhibitors of *Plasmodium falciparum* calcium-dependent protein kinase 1 (PfCDPK1). *Bioorganic & Medicinal Chemistry Letters* 2013, 23:3064 - 3069.
367. Chapman T. M., Osborne S. A., Wallace C., Birchall K., Bouloc N., Jones H. M., Ansell K. H., Taylor D. L., Clough B., Green J. L., Holder A. A.: Optimization of an imidazopyridazine series of inhibitors of *Plasmodium falciparum* calcium-dependent protein kinase 1 (PfCDPK1). *Journal of Medicinal Chemistry* 2014, 57:3570-3587.
368. Green J. L., Moon R. W., Whalley D., Bowyer P. W., Wallace C., Rochani A., Nageshan R. K., Howell S. A., Grainger M., Jones H. M., Ansell K. H., Chapman T. M., Taylor D. L., Osborne S. A., Baker D. A., Tatu U., Holder A. A.: Imidazopyridazine Inhibitors of *Plasmodium falciparum* Calcium-Dependent Protein Kinase 1 Also Target Cyclic GMP-Dependent Protein Kinase and Heat Shock Protein 90 To Kill the Parasite at Different Stages of Intracellular Development. *Antimicrobial Agents and Chemotherapy* 2015, 60:1464-1475.
369. Large J. M., Osborne S. A., Smiljanic-Hurley E., Ansell K. H., Jones H. M., Taylor D. L., Clough B., Green J. L., Holder A. A.: Imidazopyridazines as potent inhibitors of *Plasmodium falciparum* calcium-dependent protein kinase 1 (PfCDPK1): Preparation and evaluation of pyrazole linked analogues. *Bioorganic & Medicinal Chemistry Letters* 2013, 23:6019-6024.
370. Ojo K. K., Eastman R. T., Vidadala R., Zhang Z., Rivas K. L., Choi R., Lutz J. D., Reid M. C., Fox A. M. W., Hulverson M. A., Kennedy M., Isoherranen N., Kim L. M., Comess K. M., Kempf D. J., Verlinde C. L. M. J., Su X.-z., Kappe S. H. I., Maly D. J., Fan E., Van Voorhis W. C.: A Specific Inhibitor of PfCDPK4 Blocks Malaria Transmission: Chemical-genetic Validation. *The Journal of Infectious Diseases* 2014, 209:275 - 284.
371. Vidadala R. S. R., Ojo K. K., Johnson S. M., Zhang Z., Leonard S. E., Mitra A., Choi R., Reid M. C., Keyloun K. R., Fox A. M. W., Kennedy M., Silver-Brace T., Hume J. C. C., Kappe S., Verlinde C. L. M. J., Fan E., Merritt E. A., Van Voorhis W. C., Maly D. J.: Development of potent and selective *Plasmodium falciparum* calcium-dependent protein kinase 4 (PfCDPK4) inhibitors that block the transmission of malaria to mosquitoes. *European Journal of Medicinal Chemistry* 2014, 74:562-573.
372. Huang W., Hulverson M. A., Zhang Z., Choi R., Hart K. J., Kennedy M., Vidadala R. S. R., Maly D. J., Van Voorhis W. C., Lindner S. E., Fan E., Ojo K. K.: 5-Aminopyrazole-4-carboxamide analogues are selective inhibitors of *Plasmodium falciparum* microgametocyte exflagellation and potential malaria transmission blocking agents. *Bioorganic & Medicinal Chemistry Letters* 2016, 26:5487 - 5491.
373. Vaidya A. B., Morrissey J. M., Zhang Z., Das S., Daly T. M., Otto T. D., Spillman N. J., Wyvrat M., Siegl P., Marfurt J., Wirjanata G., Sebayang B. F., Price R. N., Chatterjee A., Nagle A., Stasiak M., Charman S. A., Angulo-Barturen I., Ferrer S., Belén Jiménez-Díaz M., Martínez M. S., Gamo F. J., Avery V. M., Ruecker A., Delves M., Kirk K., Berriman M., Kortagere S., Burrows J., Fan E.,

- Bergman L. W.: Pyrazoleamide compounds are potent antimalarials that target Na(+) homeostasis in intraerythrocytic *Plasmodium falciparum*. *Nature Communications* 2014, 5:5521.
374. Lavogina D., Budu A., Enkvist E., Hopp C. S., Baker D. A., Langsley G., Garcia C. R. S., Uri A.: Targeting *Plasmodium falciparum* protein kinases with adenosine analogue–oligoarginine conjugates. *Experimental Parasitology* 2014, 138:55 - 62.
375. Buskes M. J., Harvey K. L., Richards B. J., Kalhor R., Christoff R. M., Gardhi C. K., Littler D. R., Cope E. D., Prinz B., Weiss G. E., O'Brien N. J., Crabb B. S., Deady L. W., Gilson P. R., Abbott B. M.: Antimalarial activity of novel 4-cyano-3-methylisoquinoline inhibitors against *Plasmodium falciparum*: design, synthesis and biological evaluation. *Organic & Biomolecular Chemistry* 2016, 14:4617 - 4639.
376. Caridha D., Kathcart A. K., Jirage D., Waters N. C.: Activity of substituted thiophene sulfonamides against malarial and mammalian cyclin dependent protein kinases. *Bioorganic & Medicinal Chemistry Letters* 2010, 20:3863 - 3867.
377. Bendjedou L. Z., Loaëc N., Villiers B., Prina E., Späth G. F., Galons H., Meijer L., Oumata N.: Exploration of the imidazo[1,2-b]pyridazine scaffold as a protein kinase inhibitor. *European Journal of Medicinal Chemistry* 2017, 125:696 - 709.
378. Kern S., Agarwal S., Huber K., Gehring A. P., Strödke B., Wirth C. C., Brügl T., Abodo L. O., Dandekar T., Doerig C., Fischer R., Tobin A. B., Alam M. M., Bracher F., Pradel G.: Inhibition of the SR Protein-Phosphorylating CLK Kinases of *Plasmodium falciparum* Impairs Blood Stage Replication and Malaria Transmission. *Plos One* 2014, 9:e105732.
379. Masch A., Kunick C.: Selective inhibitors of Plasmodium falciparum glycogen synthase-3 (PfGSK-3): New antimalarial agents? *Biochimica et Biophysica Acta (BBA) - Proteins and Proteomics* 2015, 1854:1644 - 1649.
380. Lin B. C., Harris D. R., Kirkman L. M. D., Perez A. M., Qian Y., Schermerhorn J. T., Hong M. Y., Winston D. S., Xu L., Brandt G. S.: FIKK Kinase, a Ser/Thr Kinase Important to Malaria Parasites, Is Inhibited by Tyrosine Kinase Inhibitors. *ACS Omega* 2017, 2:6605 - 6612.
381. Harris C. J., Hill R. D., Sheppard D. W., Slater M. J., Stouten P. F.: The design and application of target-focused compound libraries. *Combinatorial Chemistry & High Throughput Screening* 2011, 14:521 - 531.
382. Lipkin M. J., Stevens A. P., Livingstone D. J., Harris C. J.: How large does a compound screening collection need to be? *Combinatorial Chemistry & High Throughput Screening* 2008, 11:482 - 493.
383. Paquet T., Gordon R., Waterson D., Witty M. J., Chibale K.: Antimalarial aminothiazoles and aminopyridines from phenotypic whole-cell screening of a SoftFocus((R)) library. *Future Medicinal Chemistry* 2012, 4:2265-2277.
384. Baniecki M. L., Wirth D. F., Clardy J.: High-throughput *Plasmodium falciparum* growth assay for malaria drug discovery. *Antimicrobial Agents and Chemotherapy* 2007, 51:716 - 723.
385. Duffy S., Avery V. M.: Development and optimization of a novel 384-well anti-malarial imaging assay validated for high-throughput screening. *The American Journal of Tropical Medicine and Hygiene* 2012, 86:84-92.
386. Burrows J. N., Chibale K., Wells T. N.: The state of the art in anti-malarial drug discovery and development. *Current Topics in Medicinal Chemistry* 2011, 11:1226 - 1254.
387. Rosowsky A., Chen K. K., Lin M.: 2,4-Diaminothieno(2,3-d)pyrimidines as antifolates and antimalarials. 3. Synthesis of 5,6-disubstituted derivatives and related tetracyclic analogs. *Journal of Medicinal Chemistry* 1973, 16:191 - 194.
388. Rosowsky A., Chaykovsky M., Chen K. K., Lin M., Modest E. J.: 2,4-Diaminothieno(2,3-d)pyrimidines as antifolates and antimalarials. 1. Synthesis of 2,4-diamino-5,6,7,8-tetrahydrothianaphthene(2,3-d)pyrimidines and related compounds. *Journal of Medicinal Chemistry* 1973, 16:185 - 188.
389. Chaykovsky M., Lin M., Rosowsky A., Modest E. J.: 2,4-Diaminothieno(2,3-d)pyrimidines as antifolates and antimalarials. 2. Synthesis of 2,4-diaminopyrido(4',3':4,5)thieno(2,3-d)pyrimidines and 2,4-diamino-8H-thiopyrano(4',3':4,5)thieno(2,3-d)pyrimidines. *Journal of Medicinal Chemistry* 1973, 16:188 - 191.
390. Elrazaz E. Z., Serya R. A. T., Ismail N. S. M., Abou El Ella D. A., Abouzid K. A. M.: Thieno[2,3-d]pyrimidine based derivatives as kinase inhibitors and anticancer agents. *Future Journal of Pharmaceutical Sciences* 2015, 1:33 - 41.
391. Desroches J., Kieffer C., Primas N., Hutter S., Gellis A., El-Kashef H., Rathelot P., Verhaeghe P., Azas N., Vanelle P.: Discovery of new hit-molecules targeting *Plasmodium falciparum* through a global SAR study of the 4-substituted-2-trichloromethylquinazoline antiplasmodial scaffold. *European Journal of Medicinal Chemistry* 2017, 125:68 - 86.
392. Woodring J. L., Patel G., Erath J., Behera R., Lee P. J., Leed S. E., Rodriguez A., Sciotti R. J., Mensa-Wilmot K., Pollastri M. P.: Evaluation of Aromatic 6-substituted Thienopyrimidines as Scaffolds against Parasites That Cause Trypanosomiasis, Leishmaniasis, and Malaria. *MedChemComm* 2015, 6:339 - 346.

393. Gonzalez Cabrera D., Douelle F., Le Manach C., Han Z., Paquet T., Taylor D., Njoroge M., Lawrence N., Wiesner L., Waterson D., Witty M. J., Wittlin S., Street L. J., Chibale K.: Structure-Activity Relationship Studies of Orally Active Antimalarial 2,4-Diamino-thienopyrimidines. *Journal of Medicinal Chemistry* 2015, 58:7572 - 7579.
394. Le Manach C., Scheurer C., Sax S., Schleiferbock S., Cabrera D. G., Younis Y., Paquet T., Street L., Smith P., Ding X. C., Waterson D., Witty M. J., Leroy D., Chibale K., Wittlin S.: Fast in vitro methods to determine the speed of action and the stage-specificity of anti-malarials in *Plasmodium falciparum*. *Malaria Journal* 2013, 12:424.
395. Ramsden N., Wilson F.: Aminopyridine Derivates as Kinase Inhibitors., vol. WO/2008/0258202008.
396. Maltais F., Bemis W. G., Wang T.: Aminopyridines Kinase Inhibitors., vol. WO/2010/0173502010.
397. Klaus P., Matthias G., Eckhard G., P. E., Silke P., Peter S., Ronald K., Arvid S.: Tetrahydrocarbazole derivatives having improved biological action and improved solubility as ligands of Gprotein coupled receptors (GPCRs). vol. WO/2010/0173502010.
398. Yazdi H. H., Janahmadi M., Behzadi G.: The role of small-conductance Ca²⁺-activated K⁺ channels in the modulation of 4-aminopyridine-induced burst firing in rat cerebellar Purkinje cells. *Brain Research* 2007, 1156:59-66.
399. De Wael F., Jeanjot P., Moens C., Verbeuren T., Cordi A., Bouskela E., Rees J.-F., Marchand-Brynaert J.: *In vitro* and *in vivo* studies of 6,8-(diaryl)imidazo[1,2-a]pyrazin-3(7H)-ones as new antioxidants. *Bioorganic and Medicinal Chemistry* 2009, 17:4336 - 4344.
400. Charrier J. D., Durrant S. J., Golec J. M., Kay D. P., Knegtel R. M., MacCormick S., Mortimore M., O'Donnell M. E., Pinder J. L., Reaper P. M., Rutherford A. P., Wang P. S., Young S. C., Pollard J. R.: Discovery of potent and selective inhibitors of ataxia telangiectasia mutated and Rad3 related (ATR) protein kinase as potential anticancer agents. *Journal of Medicinal Chemistry* 2011, 54:2320-2330.
401. Berg S., Bergh M., Hellberg S., Hogdin K., Lo-Alfredsson Y., Soderman P., von Berg S., Weigelt T., Ormo M., Xue Y., Tucker J., Neelissen J., Jerning E., Nilsson Y., Bhat R.: Discovery of novel potent and highly selective glycogen synthase kinase-3beta (GSK3beta) inhibitors for Alzheimer's disease: design, synthesis, and characterization of pyrazines. *Journal of Medicinal Chemistry* 2012, 55:9107 - 9119.
402. Gamo F. J., Sanz L. M., Vidal J., de Cozar C., Alvarez E., Lavandera J. L., Vanderwall D. E., Green D. V., Kumar V., Hasan S., Brown J. R., Peishoff C. E., Cardon L. R., Garcia-Bustos J. F.: Thousands of chemical starting points for antimalarial lead identification. *Nature* 2010, 465:305 - 310.
403. Plouffe D., Brinker A., McNamara C., Henson K., Kato N., Kuhlen K., Nagle A., Adrian F., Matzen J. T., Anderson P., Nam T. G., Gray N. S., Chatterjee A., Janes J., Yan S. F., Trager R., Caldwell J. S., Schultz P. G., Zhou Y., Winzeler E. A.: *In silico* activity profiling reveals the mechanism of action of antimalarials discovered in a high-throughput screen. *Proceedings of the National Academy of Sciences of the United States of America* 2008, 105:9059 - 9064.
404. Meister S., Plouffe D. M., Kuhlen K. L., Bonamy G. M., Wu T., Barnes S. W., Bopp S. E., Borboa R., Bright A. T., Che J., Cohen S., Dharia N. V., Gagaring K., Gettayacamin M., Gordon P., Groessl T., Kato N., Lee M. C., McNamara C. W., Fidock D. A., Nagle A., Nam T. G., Richmond W., Roland J., Rottmann M., Zhou B., Froissard P., Glynn R. J., Mazier D., Sattabongkot J., Schultz P. G., Tuntland T., Walker J. R., Zhou Y., Chatterjee A., Diagana T. T., Winzeler E. A.: Imaging of *Plasmodium* liver stages to drive next-generation antimalarial drug discovery. *Science* 2011, 334:1372 - 1377.
405. Miguel-Blanco C., Molina I., Bardera A. I., Diaz B., de Las Heras L., Lozano S., Gonzalez C., Rodrigues J., Delves M. J., Ruecker A., Colmenarejo G., Viera S., Martinez-Martinez M. S., Fernandez E., Baum J., Sinden R. E., Herreros E.: Hundreds of dual-stage antimalarial molecules discovered by a functional gametocyte screen. *Nature Communications* 2017, 8:15160.
406. Le Manach C., Nchinda A. T., Paquet T., Gonzalez Cabrera D., Younis Y., Han Z., Bashyam S., Zabiulla M., Taylor D., Lawrence N., White K. L., Charman S. A., Waterson D., Witty M. J., Wittlin S., Botha M. E., Nondaba S. H., Reader J., Birkholtz L. M., Jimenez-Diaz M. B., Martinez M. S., Ferrer S., Angulo-Barturen I., Meister S., Antonova-Koch Y., Winzeler E. A., Street L. J., Chibale K.: Identification of a Potential Antimalarial Drug Candidate from a Series of 2-Aminopyrazines by Optimization of Aqueous Solubility and Potency across the Parasite Life Cycle. *Journal of Medicinal Chemistry* 2016, 59:9890-9905.
407. Le Manach C., Gonzalez Cabrera D., Douelle F., Nchinda A. T., Younis Y., Taylor D., Wiesner L., White K. L., Ryan E., March C., Duffy S., Avery V. M., Waterson D., Witty M. J., Wittlin S., Charman S. A., Street L. J., Chibale K.: Medicinal chemistry optimization of antiplasmodial imidazopyridazine hits from high throughput screening of a SoftFocus kinase library: part 1. *Journal of Medicinal Chemistry* 2014, 57:2789-2798.

408. Silva T. B., Bernardino A. M. R., Ferreira M. d. L. G., Rogerio K. R., Carvalho L. J. M., Boechat N., Pinheiro L. C. S.: Design, synthesis and anti-*P. falciparum* activity of pyrazolopyridine–sulfonamide derivatives. *Bioorganic & Medicinal Chemistry* 2016, 24:4492-4498.
409. Deng W., Parbhu-Patel A., Meyer D. J., Baker D. A.: The role of two novel regulatory sites in the activation of the cGMP-dependent protein kinase from *Plasmodium falciparum*. *The Biochemical Journal* 2003, 374:559 - 565.
410. Baker D. A., Stewart L. B., Large J. M., Bowyer P. W., Ansell K. H., Jimenez-Diaz M. B., El Bakkouri M., Birchall K., Dechering K. J., Boulou N. S., Coombs P. J., Whalley D., Harding D. J., Smiljanic-Hurley E., Wheldon M. C., Walker E. M., Dessens J. T., Lafuente M. J., Sanz L. M., Gamo F. J., Ferrer S. B., Hui R., Bousema T., Angulo-Barturen I., Merritt A. T., Croft S. L., Gutteridge W. E., Kettleborough C. A., Osborne S. A.: A potent series targeting the malarial cGMP-dependent protein kinase clears infection and blocks transmission. *Nature Communications* 2017, 8:430.
411. Tatipaka H. B., Gillespie J. R., Chatterjee A. K., Norcross N. R., Hulverson M. A., Ranade R. M., Nagendar P., Creason S. A., McQueen J., Duster N. A., Nagle A., Supek F., Molteni V., Wenzler T., Brun R., Glynn R., Buckner F. S., Gelb M. H.: Substituted 2-phenylimidazopyridines: a new class of drug leads for human African trypanosomiasis. *Journal of Medicinal Chemistry* 2014, 57:828 - 835.
412. Patel V., Booker M., Kramer M., Ross L., Celatka C. A., Kennedy L. M., Dvorin J. D., Duraisingh M. T., Sliz P., Wirth D. F., Clardy J.: Identification and Characterization of Small Molecule Inhibitors of *Plasmodium falciparum* Dihydroorotate Dehydrogenase. *The Journal of Biological Chemistry* 2008, 283:35078 - 35085.
413. Nchinda A. T., Le Manach C., Paquet T., González Cabrera D., Wicht K. J., Brunshwig C., Njoroge M., Abay E., Taylor D., Lawrence N., Wittlin S., Jiménez-Díaz M.-B., Santos Martínez M., Ferrer S., Angulo-Barturen I., Lafuente-Monasterio M. J., Duffy J., Burrows J., Street L. J., Chibale K.: Identification of Fast-Acting 2,6-Disubstituted Imidazopyridines That Are Efficacious in the in Vivo Humanized *Plasmodium falciparum* NODscidIL2R γ null Mouse Model of Malaria. *Journal of Medicinal Chemistry* 2018, 61:4213 - 4227.
414. Le Manach C., Paquet T., Wicht K., Nchinda A. T., Brunshwig C., Njoroge M., Gibhard L., Taylor D., Lawrence N., Wittlin S., Eyermann C. J., Basarab G. S., Duffy J., Fish P. V., Street L. J., Chibale K.: Antimalarial Lead-Optimization Studies on a 2,6-Imidazopyridine Series within a Constrained Chemical Space To Circumvent Atypical Dose–Response Curves against Multidrug Resistant Parasite Strains. *Journal of Medicinal Chemistry* 2018.
415. Burrows J. N., Leroy D., Lotharius J., Waterson D.: Challenges in antimalarial drug discovery. *Future Medicinal Chemistry* 2011, 3:1401 - 1402.
416. Sinden R. E.: Malaria. In *Parasite Biology, Pathogenesis, and Protection*. . Washington DC, USA: ASM Press; 1998.[Sherman I. W. (Series Editor)
417. Dixon M. W., Thompson J., Gardiner D. L., Trenholme K. R.: Sex in *Plasmodium*: a sign of commitment. *Trends in Parasitology* 2008, 24:168 -175.
418. Wells T. N., Alonso P. L., Gutteridge W. E.: New medicines to improve control and contribute to the eradication of malaria. . *Nature Reviews Drug Discovery* 2009, 8:879 - 891.
419. Sinden R. E.: A biologist's perspective on malaria vaccine development. . *Human Vaccines* 2010, 6:3 -11.
420. Saliba K. S., Jacobs-Lorena M.: Production of *Plasmodium falciparum* gametocytes *in vitro*. *Methods in Molecular Biology* 2013:17 - 25.
421. Dixon M. W., Peatey C. L., Gardiner D. L., Trenholme K. R.: A green fluorescent protein-based assay for determining gametocyte production in *Plasmodium falciparum*. . *Molecular and Biochemical Parasitology* 2009, 163:123 - 126.
422. Fivelman Q. L., McRobert L., Sharp S., Taylor C. J., Saeed M., Swales C. A., Sutherland C. J., Baker D. A.: Improved synchronous production of *Plasmodium falciparum* gametocytes *in vitro*. . *Molecular and Biochemical Parasitology* 2007, 154:119 - 123.
423. Roncales M., Vidal-Mas J., Leroy D., Herreros E.: Comparison and Optimization of Different Methods for the *In Vitro* Production of *Plasmodium falciparum* Gametocytes. *Journal of Parasitology Research* 2012:927148.
424. Delves M., Plouffe D., Scheurer C., Meister S., Wittlin S., Winzeler E. A., Sinden R. E., Leroy D.: The activities of current antimalarial drugs on the life cycle stages of *Plasmodium*: a comparative study with human and rodent parasites. *PLoS Medicine* 2012, 9:e1001169.
425. Peatey C. L., Leroy D., Gardiner D. L., Trenholme K. R.: Anti-malarial drugs: how effective are they against *Plasmodium falciparum* gametocytes? *Malaria Journal* 2012, 11:34.
426. D'Alessandro S., Camarda G., Corbett Y., Siciliano G., Parapini S., Cevenini L., Michelini E., Roda A., Leroy D., Taramelli D., Alano P.: A chemical susceptibility profile of the *Plasmodium falciparum* transmission stages by complementary cell-based gametocyte assays. *Journal of Antimicrobial Chemotherapy* 2016, 71:1148-1158.

427. Moyo P., Botha M. E., Nondaba S., Niemand J., Maharaj V. J., Eloff J. N., Louw A. I., Birkholtz L.: *In vitro* inhibition of *Plasmodium falciparum* early and late stage gametocyte viability by extracts from eight traditionally used South African plant species. *Journal of Ethnopharmacology* 2016, 185:235 - 242.
428. Lucantoni L., Fidock D. A., Avery V. M.: Luciferase-Based, High-Throughput Assay for Screening and Profiling Transmission-Blocking Compounds against *Plasmodium falciparum* Gametocytes. *Antimicrobial Agents and Chemotherapy* 2016, 60:2097 - 2107.
429. Trager W.: What triggers the gametocyte pathway in *Plasmodium falciparum*? *Trends in Parasitology* 2005, 21:262 - 264.
430. Ono T., Ohnishi Y., Nagamune K., Kano M.: Gametocytogenesis induction by Berenil in cultured *Plasmodium falciparum*. *Experimental Parasitology* 1993, 77:74 - 78.
431. Salcedo-Sora J. E., Caamano-Gutierrez E., Ward S. A., Biagini G. A.: The proliferating cell hypothesis: a metabolic framework for *Plasmodium* growth and development. *Trends in Parasitology, April 2014, Vol. 30, No. 4* 2014, 30:170 - 175.
432. Ono T., Nakabayashi T.: Gametocytogenesis induction by ammonium compounds in cultured *Plasmodium falciparum*. *International Journal for Parasitology* 1990, 20:615 - 618.
433. Barnes K. I., Little F., Mabuza A., Mngomezulu N., Govere J., Durrheim D., Roper C., Watkins B., White N. J.: Increased gametocytemia after treatment: an early parasitological indicator of emerging sulfadoxine-pyrimethamine resistance in falciparum malaria. *Journal of Infectious Diseases* 2008, 197:1605 - 1613.
434. Peatey C. L., Dixon M. W. A., Gardiner D. L., Trenholme K. R.: Temporal evaluation of commitment to sexual development in *Plasmodium falciparum*. *Malaria Journal* 2013, 12:1 - 17.
435. Tanaka T. Q., Williamson K. C.: A malaria gametocytocidal assay using oxidoreduction indicator, alamarBlue. *Molecular and Biochemical Parasitology* 2011, 177:160 - 163.
436. Lelievre J., Almela M. J., Lozano S., Miguel C., Franco V., Leroy D., Herreros E.: Activity of clinically relevant antimalarial drugs on *Plasmodium falciparum* mature gametocytes in an ATP bioluminescence "transmission blocking" assay. *Plos One* 2012, 7:e35019.
437. Peatey C. L., Skinner-Adams T. S., Dixon M. W., McCarthy J. S., Gardiner D. L., Trenholme K. R.: Effect of antimalarial drugs on *Plasmodium falciparum* gametocytes. *The Journal of Infectious Diseases* 2009, 200:1518 - 1521.
438. Adjalley S. H., Johnston G. L., Li T., Eastman R. T., Ekland E. H.: Quantitative assessment of *Plasmodium falciparum* sexual development reveals potent transmission-blocking activity by methylene blue. *Proceedings of the National Academy of Sciences of the United States of America* 2011, 108:1214 - 1223.
439. Duffy S., Avery V. M.: Identification of inhibitors of *Plasmodium falciparum* gametocyte development. *Malaria Journal* 2013, 12:408.
440. Chevalley S., Coste A., Lopez A., Pipy B., Valentin A.: Flow cytometry for the evaluation of anti-plasmodial activity of drugs on *Plasmodium falciparum* gametocytes. *Malaria Journal* 2010, 9.
441. LaMonte G. M., Almaliti J., Bibo-Verdugo B., Keller L., Zou B. Y., Yang J., Antonova-Koch Y., Orjuela-Sanchez P., Boyle C. A., Vigil E., Wang L., Goldgof G. M., Gerwick L., O'Donoghue A. J., Winzeler E. A., Gerwick W. H., Otilie S.: Development of a Potent Inhibitor of the *Plasmodium* Proteasome with Reduced Mammalian Toxicity. *Journal of Medicinal Chemistry* 2017, 60:6721 - 6732.
442. Miguel-Blanco C., Lelievre J., Delves M. J., Bardera A. I., Presa J. L., Lopez-Barragan M. J., Ruecker A., Marques S., Sinden R. E., Herreros E.: Imaging-based high-throughput screening assay to identify new molecules with transmission-blocking potential against *Plasmodium falciparum* female gamete formation. *Antimicrobial Agents and Chemotherapy* 2015, 59:3298 - 3305.
443. Lucantoni L., Silvestrini F., Signore M., Siciliano G., Eldering M., Decherling K. J., Avery V. M., Alano P.: A simple and predictive phenotypic High Content Imaging assay for *Plasmodium falciparum* mature gametocytes to identify malaria transmission blocking compounds. *Nature Scientific Reports* 2015, 5:16414.
444. Lucantoni L., Duffy S., Adjalley S. H., Fidock D. A., Avery V.: Identification of MMV Malaria Box Inhibitors of *Plasmodium falciparum* Early-Stage Gametocytes Using a Luciferase-Based High-Throughput Assay. *Antimicrobial Agents and Chemotherapy* 2013, 57:6050 - 6062.
445. Cevenini L., Camarda G., Michelini E., Siciliano G., Calabretta M. M., Bona R., Kumar T. R., Cara A., Branchini B. R., Fidock D. A., Roda A., Alano P.: Multicolor bioluminescence boosts malaria research: quantitative dual-color assay and single-cell imaging in *Plasmodium falciparum* parasites. *Analytical Chemistry* 2014, 86:8814 - 8821.
446. Tanaka T. Q., Dehdashti S. J., Nguyen D. T., McKew J. C., Zheng W., Williamson K. C.: A quantitative high throughput assay for identifying gametocytocidal compounds. *Molecular and Biochemical Parasitology* 2013, 188:20 - 25.

447. Sun W., Tanaka T. Q., Magle C. T., Huang W., Southall N., Huang R., Dehdashti S. J., McKew J. C., Williamson K. C., Zheng W.: Chemical signatures and new drug targets for gametocytocidal drug development. *Nature Scientific Reports* 2014, 4:1 - 11.
448. Van Voorhis W. C., Adams J. H., Adelfio R., Ah Yong V., Akabas M. H., Alano P., Alday A., Aleman Resto Y., Alsibae A., Alzualde A., Andrews K. T., Avery S. V., Avery V. M., Ayong L., Baker M., Baker S., Ben Mamoun C., Bhatia S., Bickle Q., Bounaadja L., Bowling T., Bosch J., Boucher L. E., Boyom F. F., Brea J., Brennan M., Burton A., Caffrey C. R., Camarda G., Carrasquilla M., Carter D., Belen Cassera M., Chih-Chien Cheng K., Chindaudomsate W., Chubb A., Colon B. L., Colon-Lopez D. D., Corbett Y., Crowther G. J., Cowan N., D'Alessandro S., Le Dang N., Delves M., DeRisi J. L., Du A. Y., Duffy S., Abd El-Salam El-Sayed S., Ferdig M. T., Fernandez Robledo J. A., Fidock D. A., Florent I., Fokou P. V., Galstian A., Gamo F. J., Gokool S., Gold B., Golub T., Goldgof G. M., Guha R., Guiguemde W. A., Gural N., Guy R. K., Hansen M. A., Hanson K. K., Hemphill A., Hooft van Huijsduijnen R., Horii T., Horrocks P., Hughes T. B., Huston C., Igarashi I., Ingram-Sieber K., Itoe M. A., Jadhav A., Naranuntarat Jensen A., Jensen L. T., Jiang R. H., Kaiser A., Keiser J., Ketas T., Kicka S., Kim S., Kirk K., Kumar V. P., Kyle D. E., Lafuente M. J., Landfear S., Lee N., Lee S., Lehane A. M., Li F., Little D., Liu L., Llinas M., Loza M. I., Lubar A., Lucantoni L., Lucet I., Maes L., Mancama D., Mansour N. R., March S., McGowan S., Medina Vera I., Meister S., Mercer L., Mestres J., Mfopa A. N., Misra R. N., Moon S., Moore J. P., Morais Rodrigues da Costa F., Muller J., Muriana A., Nakazawa Hewitt S., Nare B., Nathan C., Narraido N., Nawaratna S., Ojo K. K., Ortiz D., Panic G., Papadatos G., Parapini S., Patra K., Pham N., Prats S., Plouffe D. M., Poulsen S. A., Pradhan A., Quevedo C., Quinn R. J., Rice C. A., Abdo Rizk M., Ruecker A., St Onge R., Salgado Ferreira R., Samra J., Robinett N. G., Schlecht U., Schmitt M., Silva Villela F., Silvestrini F., Sinden R., Smith D. A., Soldati T., Spitzmuller A., Stamm S. M., Sullivan D. J., Sullivan W., Suresh S., Suzuki B. M., Suzuki Y., Swamidass S. J., Taramelli D., Tchokouaha L. R., Theron A., Thomas D., Tonissen K. F., Townson S., Tripathi A. K., Trofimov V., Udenze K. O., Ullah I., Vallieres C., Vigil E., Vinetz J. M., Voong Vinh P., Vu H., Watanabe N. A., Weatherby K., White P. M., Wilks A. F., Winzeler E. A., Wojcik E., Wree M., Wu W., Yokoyama N., Zollo P. H., Aba N., Blasco B., Burrows J., Laleu B., Leroy D., Spangenberg T., Wells T., Willis P. A.: Open Source Drug Discovery with the Malaria Box Compound Collection for Neglected Diseases and Beyond. *Plos Pathogens* 2016, 12:e1005763.
449. D'Alessandro S., Silvestrini F., Dechering K., Corbett Y., Parapini S., Timmerman M.: A *Plasmodium falciparum* screening assay for anti-gametocyte drugs based on parasite lactate dehydrogenase detection. *Journal of Antimicrobial Chemotherapy* 2013, 68:2048-2058.
450. Lucantoni L., Loganathan S., Avery V. M.: The need to compare: assessing the level of agreement of three high-throughput assays against *Plasmodium falciparum* mature gametocytes. *Scientific Reports* 2017, 7:45992.
451. Trager W., Jensen J. B.: Human malaria parasites in continuous culture. *Science* 1976, 193:673 - 675.
452. Allen R. J. W., Kirk K.: *Plasmodium falciparum* culture: The benefits of shaking. *Molecular and Biochemical Parasitology* 2010, 169:63 - 65.
453. Lambros C., Vanderberg J. P.: Synchronization of *Plasmodium falciparum* erythrocytic stages in culture. *Journal of Parasitology Research* 1979, 65:418 - 420.
454. Carter R., Ranford-Cartwright L. C., Alano P.: The culture and preparation of gametocytes of *Plasmodium falciparum* for immunochemical, molecular, and mosquito infectivity studies. In *Protocols in Molecular Parasitology*. Totowa, New Jersey: Humana Press Inc; 1993
455. van Schalkwyk D. A., Burrow R., Henriques G., Gadalla N. B., Beshir K. B., Hasford C., Wright S. G., Ding X. C., Chiodini P. L., Sutherland C. J.: Culture-adapted *Plasmodium falciparum* isolates from UK travellers: in vitro drug sensitivity, clonality and drug resistance markers. *Malaria Journal* 2013, 12:320.
456. Verlinden B. K., Niemand J., Snyman J., Sharma S. K., Beattie R. J., Woster P. M., Birkholtz L. M.: Discovery of novel alkylated (bis)urea and (bis)thiourea polyamine analogues with potent antimalarial activities. *Journal of Medicinal Chemistry* 2011, 54:6624-6633.
457. Happi C., Gbotosho G., Folarin O., Akinboye D., Yusuf B., Ebong O., Sowunmi A., Kyle D., Milhous W., Wirth D. F.: Polymorphisms in *Plasmodium falciparum* dhfr and dhps genes and age related *in vivo* sulfadoxine-pyrimethamine resistance in malaria-infected patients from Nigeria. *Acta Tropica* 2005, 95:183 - 193.
458. Rovira-Graells N., Gupta A. P., Planet E., Crowley V. M., Mok S., Ribas de Pouplana L., Preiser P. R., Bozdech Z., Cortés A.: Transcriptional variation in the malaria parasite *Plasmodium falciparum*. *Genome Res.* 2012, 22:925 - 938.
459. Livak K. J., Schmittgen T. D.: Analysis of relative gene expression data using real-time quantitative PCR and the 2(-Delta Delta C(T)) Method. *Methods* 2001, 25:402-408.

460. Makler M. T., Hinrichs D. J.: Measurement of the lactate dehydrogenase activity of *Plasmodium falciparum* as an assessment of parasitaemia. . *The American Journal of Tropical Medicine and Hygiene* 1993, 48:205 – 210.
461. Zhang J. H., Chung T. D., Oldenburg K. R.: A Simple Statistical Parameter for Use in Evaluation and Validation of High Throughput Screening Assays. *Journal of Biomolecular Screening* 1999, 4:67 - 73.
462. Iversen P. W., Beck B., Chen Y., Dere W., Devanarayan V., Eastwood B. J., Farmen M. W., Iturria S. J., Montrose C., Moore R. A., Weidner J. R., Sittampalam G. S.: *HTS assay validation: Assay Guidance Manual*. Bethesda (MD), USA: Eli Lilly & Co and National Centre for Advancing Translational Sciences; 2012.
463. Campino S., Benavente E. D., Assefa S., Thompson E., Drought L. G., Taylor C. J., Gorvett Z., Carret C. K., Flueck C., Ivens A. C., Kwiatkowski D. P., Alano P., Baker D. A., Clark T. G.: Genomic variation in two gametocyte non-producing *Plasmodium falciparum* clonal lines. *Malaria Journal* 2016, 15:229.
464. Bolscher J. M., Koolen K. M. J., van Gemert G. J., van de Vegte-Bolmer M. G., Bousema T., Leroy D., Sauerwein R. W., Dechering K. J.: A combination of new screening assays for prioritization of transmission-blocking antimalarials reveals distinct dynamics of marketed and experimental drugs. *Journal of Antimicrobial Chemotherapy* 2015.
465. Martín-Navarro C. M., López-Arencibia A., Sifaoui I., Reyes-Batlle M., Cabello-Vílchez A. M., Maciver S., Valladares B., Piñero J. E., Lorenzo-Morales J.: PrestoBlue and AlamarBlue are equally useful as agents to determine the viability of *Acanthamoeba* trophozoites. *Experimental Parasitology* 2014:1 - 4.
466. PrestoBlue® Cell Viability Reagent.
http://tools.lifetechnologies.com/content/sfs/manuals/PrestoBlue_Reagent_
467. Canning E. U., Sinden R. E.: Nuclear organisation in gametocytes of *Plasmodium* and hepatocystis: a cytochemical study. . *Zeitschrift Fur Parasitenkunde* 1975, 46:297 - 299.
468. Okamoto N., Spurck T. P., Goodman C. D., McFadden G. I.: Apicoplast and mitochondrion in gametocytogenesis of *Plasmodium falciparum*. . *Eukaryotic Cell* 2009, 8:128 - 132.
469. Crouch S. P., Kozlowski R., Slater K. J., Fletcher J.: The use of ATP bioluminescence as a measure of cell proliferation and cytotoxicity. . *Journal of Immunological Methods* 1993, 160:81 - 88.
470. Riss T. L., Moravec R. A., Niles A. L., Duellman S., Benink H. A., Worzella T. J., Minor L.: Cell viability assays. In *Assay Guidance Manual*. Edited by (MD) B.: USA: Eli Lilly & Co and National Centre for Advancing Translational Sciences; 2012
471. Oduola A. M., Omitowoju G. O., Sowunmi A.: *Plasmodium falciparum*: evaluation of lactate dehydrogenase in monitoring therapeutic responses to standard antimalarial drugs in Nigeria. . *Experimental Parasitology* 1997, 87:283 - 289.
472. Mueller I., Betuela I., Ginny M.: The sensitivity of the OptiMAL rapid diagnostic test to the presence of *Plasmodium falciparum* gametocytes compromises its ability to monitor treatment outcomes in an area of Papua New Guinea in which malaria is endemic. . *Journal of Clinical Microbiology* 2007, 45:627 - 630.
473. O'Neill P. M., Barton V. E., Ward S. A.: The molecular mechanism of action of artemisinin—the debate continues. . *Molecules* 2010, 15:1705 - 1721.
474. Haynes R. K., Cheu K. W., Chan H. W., Wong H. N., Li K. Y., Tang M. M., Chen M. J., Guo Z. F., Guo Z. H., Sinniah K., Witte A. B., Coghi P., Monti D.: Interactions between artemisinins and other antimalarial drugs in relation to the cofactor model—a unifying proposal for drug action. . *ChemMedChem* 2012:2204 - 2226.
475. Klonis N., Crespo-Ortiz M. P., Bottova I., Abu-Bakar N., Kenny S., Rosenthal P. J., Tilley L.: Artemisinin activity against *Plasmodium falciparum* requires hemoglobin uptake and digestion. *Proceedings of the National Academy of Sciences of the United States of America* 2011, 108:111405 - 111410.
476. Wells T. N. C., Burrows J. N., Baird J. K.: Targeting the hypnozoite reservoir of *Plasmodium vivax*: the hidden obstacle to malaria elimination. *Trends in Parasitology*, 26:145-151.
477. Dechy-Cabaret O., Benoit-Vical F.: Effects of Antimalarial Molecules on the Gametocyte Stage of *Plasmodium falciparum*: The Debate. *Journal of Medicinal Chemistry* 2012, 55:10328-10344.
478. Fowler R. E., Billingsley P. F., Pudney M., Sinden R. E.: Inhibitory action of the antimalarial compound atovaquone (566C80) against *Plasmodium berghei* ANKA in the mosquito, *Anopheles stephensi*. *Parasitology* 1994, 108:383 - 388.
479. Malo N., Hanley J. A., Cerquozzi S., Pelletier J., Nadon R.: Statistical practice in high-throughput screening data analysis. *Nature Biotechnology* 2006, 24:167.
480. Le Manach C., Paquet T., Brunschwig C., Njoroge M., Han Z., Gonzalez Cabrera D., Bashyam S., Dhinakaran R., Taylor D., Reader J., Botha M., Churchyard A., Lauterbach S., Coetzer T. L., Birkholtz L. M., Meister S., Winzeler E. A., Waterson D., Witty M. J., Wittlin S., Jimenez-Diaz M. B.,

- Santos Martinez M., Ferrer S., Angulo-Barturen I., Street L. J., Chibale K.: A Novel Pyrazolopyridine with in Vivo Activity in *Plasmodium berghei*- and *Plasmodium falciparum*-Infected Mouse Models from Structure-Activity Relationship Studies around the Core of Recently Identified Antimalarial Imidazopyridazines. *Journal of Medicinal Chemistry* 2015, 58:8713 - 8722.
481. Bowman J. D., Merino E. F., Brooks C. F., Striepen B., Carlier P. R., Cassera M. B.: Antiapicoplast and gametocytocidal screening to identify the mechanisms of action of compounds within the malaria box. *Antimicrobial Agents and Chemotherapy* 2014, 58:811-819.
482. Sanders N. G., Sullivan D. J., Mlambo G., Dimopoulos G., Tripathi A. K.: Gametocytocidal screen identifies novel chemical classes with *Plasmodium falciparum* transmission blocking activity. *Plos One* 2014, 9:e105817.
483. Gonzalez Cabrera D., Le Manach C., Douelle F., Younis Y., Feng T. S., Paquet T., Nchinda A. T., Street L. J., Taylor D., de Kock C., Wiesner L., Duffy S., White K. L., Zabiulla K. M., Sambandan Y., Bashyam S., Waterson D., Witty M. J., Charman S. A., Avery V. M., Wittlin S., Chibale K.: 2,4-Diaminothienopyrimidines as orally active antimalarial agents. *Journal of Medicinal Chemistry* 2014, 57:1014-1022.
484. Younis Y., Douelle F., Feng T. S., Gonzalez Cabrera D., Le Manach C., Nchinda A. T., Duffy S., White K. L., Shackelford D. M., Morizzi J., Mannila J., Katneni K., Bhamidipati R., Zabiulla K. M., Joseph J. T., Bashyam S., Waterson D., Witty M. J., Hardick D., Wittlin S., Avery V., Charman S. A., Chibale K.: 3,5-Diaryl-2-aminopyridines as a novel class of orally active antimalarials demonstrating single dose cure in mice and clinical candidate potential. *Journal of Medicinal Chemistry* 2012, 55:3479-3487.
485. Younis Y., Douelle F., Gonzalez Cabrera D., Le Manach C., Nchinda A. T., Paquet T., Street L. J., White K. L., Zabiulla K. M., Joseph J. T., Bashyam S., Waterson D., Witty M. J., Wittlin S., Charman S. A., Chibale K.: Structure-activity-relationship studies around the 2-amino group and pyridine core of antimalarial 3,5-diarylaminopyridines lead to a novel series of pyrazine analogues with oral *in vivo* activity. *Journal of Medicinal Chemistry* 2013, 56:8860-8871.
486. Gonzalez Cabrera D., Douelle F., Younis Y., Feng T. S., Le Manach C., Nchinda A. T., Street L. J., Scheurer C., Kamber J., White K. L., Montagnat O. D., Ryan E., Katneni K., Zabiulla K. M., Joseph J. T., Bashyam S., Waterson D., Witty M. J., Charman S. A., Wittlin S., Chibale K.: Structure-activity relationship studies of orally active antimalarial 3,5-substituted 2-aminopyridines. *Journal of Medicinal Chemistry* 2012, 55:11022 - 11030.
487. World Health Organization G.: WHO: World Malaria Report.
488. Le Manach C., Paquet T., Gonzalez Cabrera D., Younis Y., Taylor D., Wiesner L., Lawrence N., Schwager S., Waterson D., Witty M. J., Wittlin S., Street L. J., Chibale K.: Medicinal chemistry optimization of antiplasmodial imidazopyridazine hits from high throughput screening of a softfocus kinase library: part 2. *Journal of Medicinal Chemistry* 2014, 57:8839 - 8848.
489. Lipinski C. A., Lombardo F., Dominy B. W., Feeney P. J.: Experimental and computational approaches to estimate solubility and permeability in drug discovery and development settings. *Advanced Drug Delivery Reviews* 1997, 23:3 - 25.
490. Vennerstrom J. L., Arbe-Barnes S., Brun R., Charman S. A., Chiu F. C., Chollet J., Dong Y., Dorn A., Hunziker D., Matile H., McIntosh K., Padmanilayam M., Santo Tomas J., Scheurer C., Scorneaux B., Tang Y., Urwyler H., Wittlin S., Charman W. N.: Identification of an antimalarial synthetic trioxolane drug development candidate. *Nature* 2004, 430:900 - 904.
491. Clarkson C., Campbell W. E., Smith P.: *In vitro* antiplasmodial activity of abietane and totarane diterpenes isolated from *Harpagophytum procumbens* (devil's claw). *Planta Medica* 2003, 69:720 - 724.
492. Motulsky H. J.: Common misconceptions about data analysis and statistics. *Naunyn-Schmiedeberg's Archives of Pharmacology* 2014, 387:1017 - 1023.
493. Almela M. J., Lozano S., Lelievre J., Colmenarejo G., Coteron J. M., Rodrigues J., Gonzalez C., Herreros E.: A New Set of Chemical Starting Points with *Plasmodium falciparum* Transmission-Blocking Potential for Antimalarial Drug Discovery. *Plos One* 2015, 10:e0135139.
494. Kafsack B. F., Painter H. J., Llinas M.: New Agilent platform DNA microarrays for transcriptome analysis of *Plasmodium falciparum* and *Plasmodium berghei* for the malaria research community. *Malaria Journal* 2012, 11:187.
495. van Brummelen A. C., Olszewski K. L., Wilinski D., Llinás M., Louw A. I., Birkholtz L. M.: Co-inhibition of *Plasmodium falciparum* S-adenosylmethionine decarboxylase/ornithine decarboxylase reveals perturbation-specific compensatory mechanisms by transcriptome, proteome, and metabolome analyses. *The Journal of Biological Chemistry* 2009, 284:4635 - 4646.
496. (WWARN) W. A. R. N.: Data Management and Statistical Analysis Plan. WWARN; 2011.
497. Dechering K. J., Thompson J., Dodemont H. J., Eling W., Konings R. N. H.: Developmentally regulated expression of pfs16, a marker for sexual differentiation of the human malaria parasite *Plasmodium falciparum*. *Molecular and Biochemical Parasitology* 1997, 89:235 - 244.

498. Ngwa C., Ferreira de Araujo Rosa T., Pradel G.: *The Biology of Malaria Gametocytes*.2016.
499. Lopez-Barragan M. J., Lemieux J., Quinones M., Williamson K. C., Molina-Cruz A., Cui K., Barillas-Mury C., Zhao K., Su X. Z.: Directional gene expression and antisense transcripts in sexual and asexual stages of *Plasmodium falciparum*. *BMC Genomics* 2011, 12:587.
500. Hu G., Cabrera A., Kono M., Mok S., Chaal B. K., Haase S., Engelberg K., Cheemadan S., Spielmann T., Preiser P. R., Gilberger T. W., Bozdech Z.: Transcriptional profiling of growth perturbations of the human malaria parasite *Plasmodium falciparum*. *Nature Biotechnology* 2010, 28:91-98.
501. Burrows J. N., Duparc S., Gutteridge W. E., van Huijsduijnen R. H., Kaszubska W., Macintyre F., Mazzuri S., Mohrle J. J., Wells T. N. C.: Erratum to: New developments in anti-malarial target candidate and product profiles. *Malaria Journal* 2017, 16:151.
502. Jimenez-Diaz M. B., Ebert D., Salinas Y., Pradhan A., Lehane A. M., Myrand-Lapierre M. E., O'Loughlin K. G., Shackleford D. M., Justino de Almeida M., Carrillo A. K., Clark J. A., Dennis A. S., Diep J., Deng X., Duffy S., Endsley A. N., Fedewa G., Guiguemde W. A., Gomez M. G., Holbrook G., Horst J., Kim C. C., Liu J., Lee M. C., Matheny A., Martinez M. S., Miller G., Rodriguez-Alejandre A., Sanz L., Sigal M., Spillman N. J., Stein P. D., Wang Z., Zhu F., Waterson D., Knapp S., Shelat A., Avery V. M., Fidock D. A., Gamo F. J., Charman S. A., Mirsalis J. C., Ma H., Ferrer S., Kirk K., Angulo-Barturen I., Kyle D. E., DeRisi J. L., Floyd D. M., Guy R. K.: (+)-SJ733, a clinical candidate for malaria that acts through ATP4 to induce rapid host-mediated clearance of *Plasmodium*. *Proceedings of the National Academy of Sciences of the United States of America* 2014, 111:E5455-5462.
503. Tanaka T. Q., Guiguemde W. A., Barnett D. S., Maron M. I., Min J., Connelly M. C., Suryadevara P. K., Guy R. K., Williamson K. C.: Potent *Plasmodium falciparum* gametocytocidal activity of diaminoanthraquinones, lead antimalarial chemotypes identified in an antimalarial compound screen. *Antimicrobial Agents and Chemotherapy* 2015, 59:1389-1397.
504. Wirth C. C., Glushakova S., Scheuermayer M., Repnik U., Garg S., Schaack D., Kachman M. M., Weissbach T., Zimmerberg J., Dandekar T., Griffiths G., Chitnis C. E., Singh S., Fischer R., Pradel G.: Perforin-like protein PPLP2 permeabilizes the red blood cell membrane during egress of *Plasmodium falciparum* gametocytes. *Cellular Microbiology* 2014, 16:709-733.
505. Deligianni E., Morgan R. N., Bertuccini L., Wirth C. C., Silmon de Monerri N. C., Spanos L., Blackman M. J., Louis C., Pradel G., Siden-Kiamos I.: A perforin-like protein mediates disruption of the erythrocyte membrane during egress of *Plasmodium berghei* male gametocytes. *Cellular Microbiology* 2013, 15:1438-1455.
506. Raabe A., Berry L., Sollelis L., Cerdan R., Tawk L., Vial H., Billker O., Wengelnik K.: *Genetic and transcriptional analysis of phosphoinositide-specific phospholipase C in Plasmodium*.2011.
507. Arai M., Billker O., Morris H. R., Panico M., Delcroix M., Dixon D., Ley S. V., Sinden R. E.: Both mosquito-derived xanthurenic acid and a host blood-derived factor regulate gametogenesis of *Plasmodium* in the midgut of the mosquito. *Molecular and Biochemical Parasitology* 2001, 116:17 - 24.
508. Billker O., Lindo V., Panico M., Etienne A. E., Paxton T., Dell A., Rogers M., Sinden R. E., Morris H. R.: Identification of xanthurenic acid as the putative inducer of malaria development in the mosquito. *Nature* 1998, 392:289.
509. Muhia D. K., Swales C. A., Deng W., Kelly J. M., Baker D. A.: The gametocyte-activating factor xanthurenic acid stimulates an increase in membrane-associated guanylyl cyclase activity in the human malaria parasite *Plasmodium falciparum*. *Molecular Microbiology* 2001, 42:553-560.
510. Carucci D. J., Witney A. A., Muhia D. K., Warhurst D. C., Schaap P., Meima M., Li J. L., Taylor M. C., Kelly J. M., Baker D. A.: Guanylyl cyclase activity associated with putative bifunctional integral membrane proteins in *Plasmodium falciparum*. *Journal of Biological Chemistry* 2000, 275:22147-22156.
511. Rangarajan R., Bei A. K., Jethwaney D., Maldonado P., Dorin D., Sultan A. A., Doerig C.: A mitogen-activated protein kinase regulates male gametogenesis and transmission of the malaria parasite *Plasmodium berghei*. *EMBO Reports* 2005, 6:464-469.
512. Guttery D., J P Ferguson D., Poulin B., Xu Z., Straschil U., Klop O., Solyakov L., Sandrini S., Brady D., Nieduszynski C., J Janse C., Holder A., Tobin A., Tewari R.: A Putative Homologue of CDC20/CDH1 in the Malaria Parasite Is Essential for Male Gamete Development. *Plos Pathogens* 2012, 8:e1002554.
513. Sebastian S., Brochet M., Collins Mark O., Schwach F., Jones Matthew L., Goulding D., Rayner Julian C., Choudhary Jyoti S., Billker O.: A *Plasmodium* Calcium-Dependent Protein Kinase Controls Zygote Development and Transmission by Translationally Activating Repressed mRNAs. *Cell Host & Microbe* 2012, 12:9 - 19.
514. Babiker H. A., Walliker D.: Current views on the population structure of *Plasmodium falciparum*: Implications for control. *Parasitology Today* 1997, 13:262 - 267.

515. Eichner M., Diebner H. H., Molineaux L., Collins W. E., Jeffery G. M., Dietz K.: Genesis, sequestration and survival of *Plasmodium falciparum* gametocytes: parameter estimates from fitting a model to malariatherapy data. *Transactions of the Royal Society of Tropical Medicine and Hygiene* 2001, 95:497 - 501.
516. Delves M. J.: *Plasmodium* cell biology should inform strategies used in the development of antimalarial transmission-blocking drugs. *Future Medicinal Chemistry* 2012, 4:2251 - 2263.
517. Mbenda H. G. N., Zeng W., Bai Y., Siddiqui F. A., Yang Z., Cui L.: Genetic diversity of the *Plasmodium vivax* phosphatidylinositol 3-kinase gene in two regions of the China-Myanmar border. *Infection, Genetics and Evolution* 2018, 61:45 - 52.
518. Mie I., Megumi K., Shin-Ichiro T., Betty B., Miki S.-Y., Shouki Y., Nobuyuki T., Masato Y., Makoto S., Muneaki H., Osbert T. K., Alex O., Paul S. O., Mary A. A., Denis A. A., Emmanuel I. O.-A., Joseph O.-O., Makoto H., Jun O., Nirianne M. Q. P., Masatoshi K., Takafumi T., Eisaku K., Toshihiro H., Toshihiro M.: Artemisinin Resistant *Plasmodium falciparum* with High Survival Rates, Uganda, 2014–2016. *Emerging Infectious Disease journal* 2018, 24:718.
519. Vallone A., D'Alessandro S., Brogi S., Brindisi M., Chemi G., Alfano G., Lamponi S., Lee S. G., Jez J. M., Koolen K. J. M., Dechering K. J., Saponara S., Fusi F., Gorelli B., Taramelli D., Parapini S., Caldelari R., Campiani G., Gemma S., Butini S.: Antimalarial agents against both sexual and asexual parasites stages: structure-activity relationships and biological studies of the Malaria Box compound 1-[5-(4-bromo-2-chlorophenyl)furan-2-yl]-N-[(piperidin-4-yl)methyl]methanamine (MMV019918) and analogues. *European Journal of Medicinal Chemistry* 2018, 150:698 - 718.
520. Rozanne H., Dina C., Ning W. H., J. S. F., E. v. d. W. M., Janette R., H. N. S., Lyn-Marie B., K. H. R., D. N. D. D.: Activities of 11-Azaartemisinin and N-Sulfonyl Derivatives against Asexual and Transmissible Malaria Parasites. *ChemMedChem* 2017, 12:2086 - 2093.
521. Harmse R., Coertzen D., Wong H. N., Smit F. J., van der Watt M. E., Reader J., Nondaba S. H., Birkholtz L. M., Haynes R. K., N'Da D. D.: Activities of 11-Azaartemisinin and N-Sulfonyl Derivatives against Asexual and Transmissible Malaria Parasites. *ChemMedChem* 2017, 12:2086-2093.
522. Patel P. R., Sun W., Kim M., Huang X., Sanderson P. E., Tanaka T. Q., McKewa J. C., Simeonov A., Williamson K. C., Zheng W., Huang W.: In vitro evaluation of imidazo[4,5-c]quinolin-2-ones as gametocytocidal antimalarial agents. *Bioorganic & Medicinal Chemistry Letters* 2016, 26:2907 - 2911.
523. Polanski J.: *Chemoinformatics* Elsevier 2009.
524. Medina-Franco J. L.: Interrogating Novel Areas of Chemical Space for Drug Discovery using Chemoinformatics. *Drug Development Research* 2012, 73:430-438.
525. Xu J., Hagler A.: Chemoinformatics and Drug Discovery. *Molecules* 2002, 7:566.
526. Adamson G.W., Bush J. A.: A method for the automatic classification of chemical structures, Information Storage and Retrieval. In *Molecular Similarity in Drug Design*. Elsevier; 1973
527. Sander T., Freyss J., von Korff M., Rufener C.: DataWarrior: An Open-Source Program For Chemistry Aware Data Visualization And Analysis. *Journal of Chemical Information and Modeling* 2015, 55:460 - 473.
528. Penna-Coutinho J., Cortopassi W. A., Oliveira A. A., França T. C. C., Krettli A. U.: Antimalarial Activity of Potential Inhibitors of *Plasmodium falciparum* Lactate Dehydrogenase Enzyme Selected by Docking Studies. *Plos One* 2011, 6:e21237.
529. Luzhkov V. B., Selisko B., Nordqvist A., Peyrane F., Decroly E., Alvarez K., Karlen A., Canard B., Åqvist J.: Virtual screening and bioassay study of novel inhibitors for dengue virus mRNA cap (nucleoside-2'O)-methyltransferase. *Bioorganic & Medicinal Chemistry* 2007, 15:7795 - 7802.
530. Mugnaini C., Rajamaki S., Tintori C., Corelli F., Massa S., Witvrouw M., Debysen Z., Veljkovic V., Botta M.: Toward novel HIV-1 integrase binding inhibitors: Molecular modeling, synthesis, and biological studies. *Bioorganic & Medicinal Chemistry Letters* 2007, 17:5370 - 5373.
531. Sharma R., Lawrenson A. S., Fisher N. E., Warman A. J., Shone A. E., Hill A., Mbekeani A., Pidathala C., Amewu R. K., Leung S., Gibbons P., Hong D. W., Stocks P., Nixon G. L., Chadwick J., Shearer J., Gowers I., Cronk D., Parel S. P., O'Neill P. M., Ward S. A., Biagini G. A., Berry N. G.: Identification of Novel Antimalarial Chemotypes via Chemoinformatic Compound Selection Methods for a High-Throughput Screening Program against the Novel Malarial Target, PfNDH2: Increasing Hit Rate via Virtual Screening Methods. *Journal of Medicinal Chemistry* 2012, 55:3144-3154.
532. Ojha P. K., Roy K.: Chemometric modeling, docking and in silico design of triazolopyrimidine-based dihydroorotate dehydrogenase inhibitors as antimalarials. *European Journal of Medicinal Chemistry* 2010, 45:4645 - 4656.
533. Premlata K. A., Ravindra D. W., Evans C. C.: New Horizons in Antimalarial Drug Discovery in the Last Decade by Chemoinformatic Approaches. *Combinatorial Chemistry & High Throughput Screening* 2015, 18:129 - 150.

534. Baldwin J., Michnoff C. H., Malmquist N. A., White J., Roth M. G., Rathod P. K., Phillips M. A.: High-throughput Screening for Potent and Selective Inhibitors of *Plasmodium falciparum* Dihydroorotate Dehydrogenase. *Journal of Biological Chemistry* 2005, 280:21847 - 21853.
535. Heikkilä T., Ramsey C., Davies M., Galtier C., Stead A. M. W., Johnson A. P., Fishwick C. W. G., Boa A. N., McConkey G. A.: Design and Synthesis of Potent Inhibitors of the Malaria Parasite Dihydroorotate Dehydrogenase. *Journal of Medicinal Chemistry* 2007, 50:186 - 191.
536. Adi K., Pujiyanto S., Gernowo R., Pamungkas A., Putranto A. B.: Identification of *Plasmodium falciparum* phase in red blood cells using artificial neural networks. *International Journal of Applied Engineering Research* 2014, 9:13917 - 13924.
537. França T. C. C., Medeiros A. L. R. d., Santos E. C. P. d., Santos-Filho O. A., Figueroa-Villar J. D.: A complete model of the *Plasmodium falciparum* bifunctional enzyme dihydrofolate reductase-thymidylate synthase: a model to design new antimalarials. *Journal of the Brazilian Chemical Society* 2004, 15:450 - 454.
538. França T. C. C., Pascutti P. G., Ramalho T. C., Figueroa-Villar J. D.: A three-dimensional structure of *Plasmodium falciparum* serine hydroxymethyltransferase in complex with glycine and 5-formyl-tetrahydrofolate. Homology modeling and molecular dynamics. *Biophysical chemistry* 2005, 115:1 - 10.
539. França T. C. C., Wilter A., Ramalho T. C., Pascutti P. G., Figueroa-Villar J. D.: Molecular dynamics of the interaction of *Plasmodium falciparum* and human serine hydroxymethyltransferase with 5-formyl-6-hydrofolic acid analogues: design of new potential antimalarials. *Journal of the Brazilian Chemical Society* 2006, 17:1383 - 1392.
540. Leal da Silva M., Gonçalves A., Batista P., Figueroa-Villar J., Pascutti P., França T.: Design, docking studies and molecular dynamics of new potential selective inhibitors of *Plasmodium falciparum* serine hydroxymethyltransferase. *Molecular Simulation* 2010, 36:5 - 14.
541. Nicola G., Smith C. A., Lucumi E., Kuo M. R., Fidock D. A., Sacchettini J. C., Abagyan R.: Discovery of Novel Inhibitors Targeting Enoyl-Acyl Carrier Protein Reductase in *Plasmodium falciparum* by Structure-Based Virtual Screening. *Biochemical and biophysical research communications* 2007, 358:686 - 691.
542. Neha K., Tanushree B., Ponnusamy B., Koustav M., Namita S., Avadhesh S.: Design, development, synthesis, and docking analysis of 2'-substituted triclosan analogs as inhibitors for *Plasmodium falciparum* Enoyl-ACP reductase. *IUBMB life* 2009, 61:1083 - 1091.
543. Susan M. K., Jeanne A. G., William J. W., Sean T. P., Norman C. W.: Rational Inhibitor Design and Iterative Screening in the Identification of Selective Plasmodial Cyclin Dependent Kinase Inhibitors. *Combinatorial Chemistry & High Throughput Screening* 2005, 8:27 - 38.
544. Shah F., Mukherjee P., Gut J., Legac J., Rosenthal P. J., Tekwani B. L., Avery M. A.: Identification of Novel Malarial Cysteine Protease Inhibitors Using Structure-Based Virtual Screening of a Focused Cysteine Protease Inhibitor Library. *Journal of Chemical Information and Modeling* 2011, 51:852 - 864.
545. Roy A., Annessa I., Nielsen C. J. F., Tordrup D., Laursen R. R., Knudsen B. R., Desideri A., Andersen F. F.: Peptide Inhibition of Topoisomerase IB from *Plasmodium falciparum*. *Molecular Biology International* 2011, 2011.
546. Jacobsson M., Gäredal M., Schultz J., Karlén A.: Identification of *Plasmodium falciparum* Spermidine Synthase Active Site Binders through Structure-Based Virtual Screening. *Journal of Medicinal Chemistry* 2008, 51:2777 - 2786.
547. Gujjar R., Marwaha A., El Mazouni F., White J., White K. L., Creason S., Shackelford D. M., Baldwin J., Charman W. N., Buckner F. S., Charman S., Rathod P. K., Phillips M. A.: Identification of a metabolically stable triazolopyrimidine-based dihydroorotate dehydrogenase inhibitor with anti-malarial activity in mice. *Journal of Medicinal Chemistry* 2009, 52:1864 - 1872.
548. Nguyen C., Ruda G. F., Schipani A., Kasinathan G., Leal I., Musso-Buendia A., Kaiser M., Brun R., Ruiz-Pérez L. M., Sahlberg B.-L., Johansson N. G., González-Pacanowska D., Gilbert I. H.: Acyclic Nucleoside Analogues as Inhibitors of *Plasmodium falciparum* dUTPase. *Journal of Medicinal Chemistry* 2006, 49:4183 - 4195.
549. Baragaña B., McCarthy O., Sánchez P., Bosch-Navarrete C., Kaiser M., Brun R., Whittingham J. L., Roberts S. M., Zhou X.-X., Wilson K. S., Johansson N. G., González-Pacanowska D., Gilbert I. H.: β -Branched acyclic nucleoside analogues as inhibitors of *Plasmodium falciparum* dUTPase. *Bioorganic & Medicinal Chemistry* 2011, 19:2378 - 2391.
550. McCarthy O., Musso-Buendia A., Kaiser M., Brun R., Ruiz-Perez L. M., Johansson N. G., Pacanowska D. G., Gilbert I. H.: Design, synthesis and evaluation of novel uracil acetamide derivatives as potential inhibitors of *Plasmodium falciparum* dUTP nucleotidohydrolase. *European Journal of Medicinal Chemistry* 2009, 44:678 - 688.

551. Desai P. V., Patny A., Gut J., Rosenthal P. J., Tekwani B., Srivastava A., Avery M.: Identification of Novel Parasitic Cysteine Protease Inhibitors by Use of Virtual Screening. 2. The Available Chemical Directory. *Journal of Medicinal Chemistry* 2006, 49:1576 - 1584.
552. Elaziz M. A., Moemen Y. S., Hassanien A. E., Xiong S.: Quantitative Structure-Activity Relationship Model for HCVNS5B inhibitors based on an Antlion Optimizer-Adaptive Neuro-Fuzzy Inference System. *Scientific Reports* 2018, 8:1506.
553. Hossain R., Yasmin T., Hosen M. I., Nabi A. H. M. N.: In silico identification of potential epitopes present in human adenovirus proteins for vaccine design and of putative drugs for treatment against viral infection. *Journal of Immunological Methods* 2018, 455:55 - 70.
554. Putra R. P., Alkaff A. H., Nasution M. A. F., Corona A., Kantale B., Tambunan U. S. F.: Searching of flavonoid compounds as a new antiviral for Sudan Ebolavirus glycoprotein using *in silico* methods. *International Journal of GEOMATE* 2018, 15:78 - 84.
555. Marnolia A., Toepak E. P., Tambunan U. S. F.: Fragment-based lead compound design to inhibit Ebola VP35 through computational studies. *International Journal of GEOMATE* 2018, 15:65 - 71.
556. Qiu T., Wu D., Qiu J., Cao Z.: Finding the molecular scaffold of nuclear receptor inhibitors through high-throughput screening based on proteochemometric modelling. *Journal of Cheminformatics* 2018, 10:21.
557. Lawal M., Olotu F. A., Soliman M. E. S.: Across the blood-brain barrier: Neurotherapeutic screening and characterization of naringenin as a novel CRMP-2 inhibitor in the treatment of Alzheimer's disease using bioinformatics and computational tools. *Computers in Biology and Medicine* 2018, 98:168 - 177.
558. Guariento S., Tonelli M., Espinoza S., Gerasimov A. S., Gainetdinov R. R., Cichero E.: Rational design, chemical synthesis and biological evaluation of novel biguanides exploring species-specificity responsiveness of TAAR1 agonists. *European Journal of Medicinal Chemistry* 2018, 146:171 - 184.
559. Kalash L., Val C., Azuaje J., Loza M. I., Svensson F., Zoufir A., Mervin L., Ladds G., Brea J., Glen R., Sotelo E., Bender A.: Computer-aided design of multi-target ligands at A1R, A2AR and PDE10A, key proteins in neurodegenerative diseases. *Journal of Cheminformatics* 2017, 9:67.
560. Wahl J., Smieško M.: Endocrine Disruption at the Androgen Receptor: Employing Molecular Dynamics and Docking for Improved Virtual Screening and Toxicity Prediction. *International Journal of Molecular Sciences* 2018, 19:1784.
561. Wang X., Dowd C. S.: The Methylerythritol Phosphate Pathway: Promising Drug Targets in the Fight against Tuberculosis. *ACS Infectious Diseases* 2018, 4:278 - 290.
562. Shiri F., Shahraki S., Shahriari S.: Mechanistic understanding and binding analysis of a novel Schiff base palladium (II) complex with β -lactoglobulin and human serum albumin. *Journal of Molecular Liquids* 2018, 262:218 - 229.
563. Inhee C., Yoonae K., Honggun L., Kideok K., Constantin R.: Strategic Expansion and Management of Chemical Libraries for Drug Discovery. *Bulletin of the Korean Chemical Society* 2018, 39:794 - 800.
564. Gurung A. B., Mayengbam B., Bhattacharjee A.: Discovery of novel drug candidates for inhibition of soluble epoxide hydrolase of arachidonic acid cascade pathway implicated in atherosclerosis. *Computational biology and chemistry* 2018, 74:1- 11.
565. Temraz M. G., Elzahhar P. A., El-Din A. Bekhit A., Bekhit A. A., Labib H. F., Belal A. S. F.: Anti-leishmanial click modifiable thiosemicarbazones: Design, synthesis, biological evaluation and in silico studies. *European Journal of Medicinal Chemistry* 2018, 151:585 - 600.
566. Salerno L., Amata E., Romeo G., Marrazzo A., Prezzavento O., Floresta G., Sorrenti V., Barbagallo I., Rescifina A., Pittalà V.: Potholing of the hydrophobic heme oxygenase-1 western region for the search of potent and selective imidazole-based inhibitors. *European Journal of Medicinal Chemistry* 2018, 148:54 - 62.
567. Kist R., Timmers L. F. S. M., Caceres R. A.: Searching for potential mTOR inhibitors: Ligand-based drug design, docking and molecular dynamics studies of rapamycin binding site. *Journal of Molecular Graphics and Modelling* 2018, 80:251 - 263.
568. Magyari J., Barta Holló B., Vojinović-Ješić L. S., Radanović M. M., Armaković S., Armaković S. J., Molnár J., Kincses A., Gajdács M., Spengler G., Mészáros Szécsényi K.: Interactions of Schiff base compounds and their coordination complexes with the drug cisplatin. *New Journal of Chemistry* 2018, 42:5834 - 5843.
569. Hassan M., Azhar M., Abbas Q., Raza H., Moustafa A. A., Shahzadi S., Ashraf* Z., Seo* S. Y.: Finding Novel Anti-carcinomas Compounds by Targeting SFRP4 Through Molecular Modeling, Docking and Dynamic Simulation Studies. *Current Computer-Aided Drug Design* 2018, 14:160 - 173.
570. Shabana B., Katsumi S.: An Integrated Computational Approach for Plant-Based Protein Tyrosine Phosphatase Non-Receptor Type 1 Inhibitors. *Current Computer-Aided Drug Design* 2017, 13:319 - 335.

571. Quareshy M., Prusinska J., Li J., Napier R.: A cheminformatics review of auxins as herbicides. *Journal of Experimental Botany* 2018, 69:265 - 275.
572. Channar P. A. P. P. A.: Design and synthesis of 2,6-di(substituted phenyl)thiazolo[3,2-b]-1,2,4-triazoles as α -glucosidase and α -amylase inhibitors, co-relative Pharmacokinetics and 3D QSAR and risk analysis. *Biomedicine and Pharmacotherapy* 2017, 94:499 - 513.
573. Baldwin A. G., Rivers-Auty J., Daniels M. J. D., White C. S., Schwalbe C. H., Schilling T., Hammadi H., Jaiyong P., Spencer N. G., England H., Luheshi N. M., Kadirvel M., Lawrence C. B., Rothwell N. J., Harte M. K., Bryce R. A., Allan S. M., Eder C., Freeman S., Brough D.: Boron-Based Inhibitors of the NLRP3 Inflammasome. *Cell Chemical Biology* 2017, 24:1321-1335.e1325.
574. Alves V. M., Muratov E. N., Zakharov A., Muratov N. N., Andrade C. H., Tropsha A.: Chemical toxicity prediction for major classes of industrial chemicals: Is it possible to develop universal models covering cosmetics, drugs, and pesticides? *Food and Chemical Toxicology* 2018, 112:526 - 534.
575. Egieyeh S. A., Syce J., Malan S. F., Christoffels A.: Prioritization of anti-malarial hits from nature: chemo-informatic profiling of natural products with *in vitro* antiplasmodial activities and currently registered anti-malarial drugs. *Malaria Journal* 2016, 15:50.
576. Nunes R. R., Costa M. d. S., Santos B. d. R., Fonseca A. L. d., Ferreira L. S., Chagas R. C. R., Silva A. M. d., Varotti F. d. P., Taranto A. G.: Successful application of virtual screening and molecular dynamics simulations against antimalarial molecular targets. *Memórias do Instituto Oswaldo Cruz* 2016, 111:721 - 730.
577. Gurung A. B., Bhattacharjee A.: Structure based virtual screening identifies Pranlukast as a potential inhibitor against Plasmodium falciparum Adenosine Deaminase enzyme. *Gene Reports* 2017, 6:54 - 66.
578. Ghasemi J., Shiri F., Pirhadi S., Heidari Z.: Discovery of New Potential Antimalarial Compounds Using Virtual Screening of ZINC Database. *Combinatorial Chemistry & High Throughput Screening* 2015, 18:227-234.
579. Calderón F., Barros D., Bueno J. M., Coterón J. M., Fernández E., Gamo F. J., Lavandera J. L., León M. L., Macdonald S. J. F., Mallo A., Manzano P., Porrás E., Fiandor J. M., Castro J.: An Invitation to Open Innovation in Malaria Drug Discovery: 47 Quality Starting Points from the TCAMS. *ACS Medicinal Chemistry Letters* 2011, 2:741 - 746.
580. Ertl P., Rohde B., Selzer P.: Fast Calculation of Molecular Polar Surface Area as a Sum of Fragment-Based Contributions and Its Application to the Prediction of Drug Transport Properties. *Journal of Medicinal Chemistry* 2000, 43:3714 - 3717.
581. Ashley E. A., Dhorda M., Fairhurst R. M., Amaratunga C., Lim P., Suon S.: Spread of artemisinin resistance in *Plasmodium falciparum* malaria. *The New England Journal of Medicine* 2014, 371:411 - 423.
582. Dondorp A. M., Nosten F., Yi P., Das D., Phyo A. P., Tarning J., Lwin K. M., Ariey F., Hanpithakpong W., Lee S. J., Ringwald P., Silamut K., Imwong M., Chotivanich K., Lim P., Herdman T., An S. S., Yeung S., Singhasivanon P., Day N. P., Lindegardh N., Socheat D., White N. J.: Artemisinin resistance in *Plasmodium falciparum* malaria. *The New England Journal of Medicine* 2009, 361:455 - 467.
583. Loewenstein Y., Portugaly E., Fromer M., Linial M.: Efficient algorithms for accurate hierarchical clustering of huge datasets: tackling the entire protein space. *Bioinformatics (Oxford, England)* 2008, 24:i41-i49.
584. Segall M., Champness E., Leeding C., Chisholm J., Hunt P., Elliott A., Garcia-Martinez H., Foster N., Dowling S.: Breaking free from chemical spreadsheets. *Drug Discov Today* 2015, 20:1093 - 1103.
585. Zavod A. M., Knittel J. J.: Drug Design and Relationship of Functional Groups to Pharmacologic Activity. In *Foye's Principles of Medicinal Chemistry*: Wolters Kluwer;
586. Clark D. E.: Rapid calculation of polar molecular surface area and its application to the prediction of transport phenomena. 1. Prediction of intestinal absorption. *Journal of Pharmaceutical Sciences* 1999, 88:807 - 814.
587. Kelder J., Grootenhuis P. D. J., Bayada D. M., Delbressine L. P. C., Ploemen J.-P.: Polar Molecular Surface as a Dominating Determinant for Oral Absorption and Brain Penetration of Drugs. *Pharmaceutical Research* 1999, 16:1514 - 1519.
588. Palm K., Luthman K., Ungell A.-L., Strandlund G., Beigi F., Lundahl P., Artursson P.: Evaluation of Dynamic Polar Molecular Surface Area as Predictor of Drug Absorption: Comparison with Other Computational and Experimental Predictors. *Journal of Medicinal Chemistry* 1998, 41:5382 - 5392.
589. Conradi R. A., Burton P. S., Borchardt R. T.: Physico-Chemical and Biological Factors that Influence a Drug's Cellular Permeability by Passive Diffusion. In *Lipophilicity in Drug Action and Toxicology*.
590. Colmenarejo G., Alvarez-Pedraglio A., Lavandera J.-L.: Cheminformatic Models To Predict Binding Affinities to Human Serum Albumin. *Journal of Medicinal Chemistry* 2001, 44:4370 - 4378.
591. Egan W. J., Merz K. M., Baldwin J. J.: Prediction of Drug Absorption Using Multivariate Statistics. *Journal of Medicinal Chemistry* 2000, 43:3867 - 3877.

592. Dorin D., Semblat J. P., Pouillet P., Alano P., Goldring J. P., Whittle C., Patterson S., Chakrabarti D., Doerig C.: PfPK7, an atypical MEK-related protein kinase, reflects the absence of classical three-component MAPK pathways in the human malaria parasite *Plasmodium falciparum*. *Molecular Microbiology* 2005, 55:184-196.
593. Doerig C., Meijer L.: Antimalarial drug discovery: targeting protein kinases. *Expert Opinion on Therapeutic Targets* 2007, 11:279 - 290.
594. Azevedo Mauro F., Sanders Paul R., Krejany E., Nie Catherine Q., Fu P., Bach Leon A., Wunderlich G., Crabb Brendan S., Gilson Paul R.: Inhibition of *Plasmodium falciparum* CDPK1 by conditional expression of its J-domain demonstrates a key role in schizont development. *Biochemical Journal* 2013, 452:433 - 441.
595. Ebrahimzadeh Z., Mukherjee A., Richard D.: A map of the subcellular distribution of phosphoinositides in the erythrocytic cycle of the malaria parasite *Plasmodium falciparum*. *International Journal for Parasitology* 2018, 48:13 - 25.
596. Bergström C. A. S., Porter C. J. H.: Understanding the Challenge of Beyond-Rule-of-5 Compounds. *Advanced Drug Delivery Reviews* 2016, 101:1 - 5.
597. Leeson P. D., Davis A. M.: Time-Related Differences in the Physical Property Profiles of Oral Drugs. *Journal of Medicinal Chemistry* 2004, 47:6338 - 6348.
598. Leeson P. D.: Molecular inflation, attrition and the rule of five. *Advanced Drug Delivery Reviews* 2016, 101:22 - 33.
599. Cowell A. N., Istvan E. S., Lukens A. K., Gomez-Lorenzo M. G., Vanaerschot M., Sakata-Kato T., Flannery E. L., Magistrado P., Owen E., Abraham M., LaMonte G., Painter H. J., Williams R. M., Franco V., Linares M., Arriaga I., Bopp S., Corey V. C., Gnädig N. F., Coburn-Flynn O., Reimer C., Gupta P., Murithi J. M., Moura P. A., Fuchs O., Sasaki E., Kim S. W., Teng C. H., Wang L. T., Akidil A., Adjalley S., Willis P. A., Siegel D., Tanaseichuk O., Zhong Y., Zhou Y., Llinas M., Otilie S., Gamo F. J., Lee M. C. S., Goldberg D. E., Fidock D. A., Wirth D. F., Winzeler E. A.: Mapping the malaria parasite druggable genome by using *in vitro* evolution and chemogenomics. *Science* 2018, 359:191-199.
600. Chen I., Clarke S. E., Gosling R., Hamainza B., Killeen G., Magill A., O'Meara W., Price R. N., Riley E. M.: "Asymptomatic" Malaria: A Chronic and Debilitating Infection That Should Be Treated. *PLoS Medicine* 2016, 13:e1001942.
601. Griffin J. T., Hollingsworth T. D., Okell L. C., Churcher T. S., White M., Hinsley W., Bousema T., Drakeley C. J., Ferguson N. M., Basáñez M.-G., Ghani A. C.: Reducing *Plasmodium falciparum* Malaria Transmission in Africa: A Model-Based Evaluation of Intervention Strategies. *PLoS Medicine* 2010, 7:e1000324.
602. Cook J., Xu W., Msellem M., Vonk M., Bergstrom B., Gosling R., Al-Mafazy A. W., McElroy P., Molteni F., Abass A. K., Garimo I., Ramsan M., Ali A., Martensson A., Bjorkman A.: Mass screening and treatment on the basis of results of a *Plasmodium falciparum*-specific rapid diagnostic test did not reduce malaria incidence in Zanzibar. *The Journal of Infectious Diseases* 2015, 211:1476 - 1483.
603. Coetzee N., Sidoli S., van Biljon R., Painter H., Llinas M., Garcia B. A., Birkholtz L. M.: Quantitative chromatin proteomics reveals a dynamic histone post-translational modification landscape that defines asexual and sexual *Plasmodium falciparum* parasites. *Sci Rep* 2017, 7:607.
604. Cabrera D. G., Horatscheck A., Wilson C. R., Basarab G., Eyermann C. J., Chibale K.: Plasmodial Kinase Inhibitors: License to Cure? *Journal of Medicinal Chemistry* 2018, 61:8061-8077.
605. Bahamontes-Rosa N., Gomez-Lorenzo M. G., Lelièvre J., Rodriguez Alejandro A., Almela M. J., Lozano S., Herreros E., Gamo F.-J.: A novel validated assay to support the discovery of new anti-malarial gametocytocidal agents. *Malaria Journal* 2016, 15:385.
606. Vos M. W., Stone W. J. R., Koolen K. M., van Gemert G.-J., van Schaijk B., Leroy D., Sauerwein R. W., Bousema T., Dechering K. J.: A semi-automated luminescence based standard membrane feeding assay identifies novel small molecules that inhibit transmission of malaria parasites by mosquitoes. *Scientific Reports* 2015, 5:18704.
607. Duffy S., Avery V. M.: *Plasmodium falciparum* *in vitro* continuous culture conditions: A comparison of parasite susceptibility and tolerance to anti-malarial drugs throughout the asexual intra-erythrocytic life cycle. *International Journal for Parasitology: Drugs and Drug Resistance* 2017, 7:295-302.
608. Beteck R. M., Seldon R., Coertzen D., van der Watt M. E., Reader J., Mackenzie J. S., Lamprecht D. A., Abraham M., Eribez K., Müller J., Rui F., Zhu G., de Grano R. V., Williams I. D., Smit F. J., Steyn A. J. C., Winzeler E. A., Hemphill A., Birkholtz L.-M., Warner D. F., N'Da D. D., Haynes R. K.: Accessible and distinct decoquinone derivatives active against *Mycobacterium tuberculosis* and apicomplexan parasites. *Communications Chemistry* 2018, 1:62.
609. Abdel-Haleem A. M., Hefzi H., Mineta K., Gao X., Gojobori T., Palsson B. O., Lewis N. E., Jamshidi N.: Functional interrogation of *Plasmodium* genus metabolism identifies species- and stage-specific differences in nutrient essentiality and drug targeting. *PLoS Comput Biol* 2018, 14:e1005895.

610. Tambo E., Khater E. I., Chen J. H., Bergquist R., Zhou X. N.: Nobel prize for the artemisinin and ivermectin discoveries: a great boost towards elimination of the global infectious diseases of poverty. *Infect Dis Poverty* 2015, 4:58.
611. Forkuo A. D., Ansah C., Mensah K. B., Annan K., Gyan B., Theron A., Mancama D., Wright C. W.: *In vitro* anti-malarial interaction and gametocytocidal activity of cryptolepine. *Malar J* 2017, 16:496.
612. Abdul-Ghani R., Basco L. K., Beier J. C., Mahdy M. A.: Inclusion of gametocyte parameters in anti-malarial drug efficacy studies: filling a neglected gap needed for malaria elimination. *Malar J* 2015, 14:413.
613. Duffy S., Loganathan S., Holleran J. P., Avery V. M.: Large-scale production of *Plasmodium falciparum* gametocytes for malaria drug discovery. *Nature Protocols* 2016, 11:976 - 992.
614. de Lange C., Coertzen D., Smit F. J., Wentzel J. F., Wong H. N., Birkholtz L. M., Haynes R. K., N'Da D. D.: Synthesis, antimalarial activities and cytotoxicities of amino-artemisinin-1,2-disubstituted ferrocene hybrids. *Bioorg Med Chem Lett* 2018, 28:3161-3163.
615. Wadi I., Pillai C. R., Anvikar A. R., Sinha A., Nath M., Valecha N.: Methylene blue induced morphological deformations in *Plasmodium falciparum* gametocytes: implications for transmission-blocking. *Malaria Journal* 2018, 17:11.
616. Allman E. L., Painter H. J., Samra J., Carrasquilla M., Llinás M.: Metabolomic Profiling of the Malaria Box Reveals Antimalarial Target Pathways. *Antimicrobial Agents and Chemotherapy* 2016, 60:6635-6649.
617. Swann J., Corey V., Scherer C. A., Kato N., Comer E., Maetani M., Antonova-Koch Y., Reimer C., Gagaring K., Ibanez M., Plouffe D., Zeeman A. M., Kocken C. H., McNamara C. W., Schreiber S. L., Campo B., Winzeler E. A., Meister S.: High-Throughput Luciferase-Based Assay for the Discovery of Therapeutics That Prevent Malaria. *ACS Infect Dis* 2016, 2:281-293.
618. Singh K., Okombo J., Brunschwag C., Ndubi F., Barnard L., Wilkinson C., Njogu P. M., Njoroge M., Laing L., Machado M., Prudencio M., Reader J., Botha M., Nondaba S., Birkholtz L. M., Lauterbach S., Churchyard A., Coetzer T. L., Burrows J. N., Yeates C., Denti P., Wiesner L., Egan T. J., Wittlin S., Chibale K.: Antimalarial Pyrido[1,2-a]benzimidazoles: Lead Optimization, Parasite Life Cycle Stage Profile, Mechanistic Evaluation, Killing Kinetics, and *in Vivo* Oral Efficacy in a Mouse Model. *J Med Chem* 2017, 60:1432-1448.
619. van der Watt M. E., Reader J., Churchyard A., Nondaba S. H., Lauterbach S. B., Niemand J., Abayomi S., van Biljon R. A., Connacher J. I., van Wyk R. D. J., Le Manach C., Paquet T., Gonzalez Cabrera D., Brunschwag C., Theron A., Lozano-Arias S., Rodrigues J. F. I., Herrerros E., Leroy D., Duffy J., Street L. J., Chibale K., Mancama D., Coetzer T. L., Birkholtz L. M.: Potent *Plasmodium falciparum* gametocytocidal compounds identified by exploring the kinase inhibitor chemical space for dual active antimalarials. *J Antimicrob Chemother* 2018.
620. Laurent D., Jullian V., Parenty A., Knibiehler M., Dorin D., Schmitt S., Lozach O., Lebouvier N., Frostin M., Alby F., Maurel S., Doerig C., Meijer L., Sauvain M.: Antimalarial potential of xestoquinone, a protein kinase inhibitor isolated from a Vanuatu marine sponge *Xestospongia* spp. *Bioorganic & Medicinal Chemistry* 2006, 14:4477 - 4482.
621. Kirsch G., König G. M., Wright A. D., Kaminsky R.: A New Bioactive Sesterterpene and Antiplasmodial Alkaloids from the Marine Sponge *Hyrtios* cf. *erecta*. *Journal of Natural Products* 2000, 63:825-829.
622. Syin C., Parzy D., Traincard F., Boccaccio I., Joshi M. B., Lin D. T., Yang X.-M., Assemet K., Doerig C., Langsley G.: The H89 cAMP-dependent protein kinase inhibitor blocks *Plasmodium falciparum* development in infected erythrocytes. *European Journal of Biochemistry* 2001, 268:4842-4849.
623. Choubey V., Maity P., Guha M., Kumar S., Srivastava K., Puri S. K., Bandyopadhyay U.: Inhibition of *Plasmodium falciparum* Choline Kinase by Hexadecyltrimethylammonium Bromide: a Possible Antimalarial Mechanism. *Antimicrobial Agents and Chemotherapy* 2007, 51:696-706.
624. Dahari D. E., Salleh R. M., Mahmud F., Chin L. P., Embi N., Sidek H. M.: Anti-malarial Activities of Two Soil Actinomycete Isolates from Sabah via Inhibition of Glycogen Synthase Kinase 3 β . *Tropical Life Sciences Research* 2016, 27:53 - 71.
625. Gonzalez Cabrera D., Douelle F., Feng T. S., Nchinda A. T., Younis Y., White K. L., Wu Q., Ryan E., Burrows J. N., Waterson D., Witty M. J., Wittlin S., Charman S. A., Chibale K.: Novel orally active antimalarial thiazoles. *J Med Chem* 2011, 54:7713-7719.
626. Younis Y., Street L. J., Waterson D., Witty M. J., Chibale K.: Cell-based medicinal chemistry optimization of high throughput screening hits for orally active antimalarials. Part 2: hits from SoftFocus kinase and other libraries. *J Med Chem* 2013, 56:7750-7754.
627. Billker O., Lourido S., Sibley L. D.: Calcium-Dependent Signaling and Kinases in Apicomplexan Parasites. *Cell Host & Microbe* 2009, 5:612-622.
628. Hallyburton I., Grimaldi R., Woodland A., Baragana B., Luksch T., Spinks D., James D., Leroy D., Waterson D., Fairlamb A. H., Wyatt P. G., Gilbert I. H., Frearson J. A.: Screening a protein kinase inhibitor library against *Plasmodium falciparum*. *Malar J* 2017, 16:446.

629. McRobert L., Taylor C. J., Deng W., Fivelman Q. L., Cummings R. M., Polley S. D., Billker O., Baker D. A.: Gametogenesis in Malaria Parasites Is Mediated by the cGMP-Dependent Protein Kinase. *PLoS biology* 2008, 6:e139.
630. Kawamoto F., Alejo-Blanco R., Fleck S. L., Kawamoto Y., Sinden R. E.: Possible roles of Ca²⁺ and cGMP as mediators of the exflagellation of *Plasmodium berghei* and *Plasmodium falciparum*. *Molecular and Biochemical Parasitology* 1990, 42:101 - 108.
631. Kawamoto F., Fujioka H., Murakami R., Syafruddin, Hagiwara M., Ishikawa T., Hidaka H.: The roles of Ca²⁺/calmodulin- and cGMP-dependent pathways in gametogenesis of a rodent malaria parasite, *Plasmodium berghei*. *European journal of cell biology* 1993, 60:101 - 107.
632. Ojo K. K., Pfander C., Mueller N. R., Burstroem C., Larson E. T., Bryan C. M., Fox A. M. W., Reid M. C., Johnson S. M., Murphy R. C., Kennedy M., Mann H., Leibly D. J., Hewitt S. N., Verlinde C. L. M. J., Kappe S., Merritt E. A., Maly D. J., Billker O., Van Voorhis W. C.: Transmission of malaria to mosquitoes blocked by bumped kinase inhibitors. *The Journal of Clinical Investigation* 2012, 122:2301 - 2305.
633. Aher R. B., Roy K.: QSAR and pharmacophore modeling of diverse aminothiazoles and aminopyridines for antimalarial potency against multidrug-resistant *Plasmodium falciparum*. *Medicinal Chemistry Research* 2014, 23:4238 - 4249.
634. Donald R. G., Zhong T., Wiersma H., Nare B., Yao D., Lee A., Allocco J., Liberator P. A.: Anticoccidial kinase inhibitors: identification of protein kinase targets secondary to cGMP-dependent protein kinase. *Molecular and Biochemical Parasitology* 2006, 149:86 - 98.
635. Burrows J. N., van Huijsduijnen R. H., Möhrle J. J., Oeuvray C., Wells T. N. C.: Designing the next generation of medicines for malaria control and eradication. *Malar J* 2013, 12:1 - 20.
636. Alam M. M., Solyakov L., Bottrill A. R., Flueck C., Siddiqui F. A., Singh S., Mistry S., Viskaduraki M., Lee K., Hopp C. S., Chitnis C. E., Doerig C., Moon R. W., Green J. L., Holder A. A., Baker D. A., Tobin A. B.: Phosphoproteomics reveals malaria parasite Protein Kinase G as a signalling hub regulating egress and invasion. *Nature Communications* 2015, 6:7285.
637. Tran P. N., Brown S. H. J., Mitchell T. W., Matuschewski K., McMillan P. J., Kirk K., Dixon M. W. A., Maier A. G.: A female gametocyte-specific ABC transporter plays a role in lipid metabolism in the malaria parasite. *Nature Communications* 2014, 5:4773.
638. Coulibaly M. B., Gabriel E. E., Sinaba Y., Sylla D., Sacko A., Sylla L., Coulibaly B., Hume J. C. C., Baber I., Assadou M. H., Sagara I., Wu Y., Healy S. A., Doumbo O., Traore S. F., Duffy P. E.: Optimizing Direct Membrane and Direct Skin Feeding Assays for *Plasmodium falciparum* Transmission-Blocking Vaccine Trials in Bancoumana, Mali. *Am J Trop Med Hyg* 2017, 97:719-725.
639. Colmenarejo G., Lozano S., González-Cortés C., Calvo D., Sanchez-Garcia J., Matilla J.-L. P., Leroy D., Rodrigues J.: Predicting transmission blocking potential of anti-malarial compounds in the Mosquito Feeding Assay using *Plasmodium falciparum* Male Gamete Inhibition Assay. *Scientific Reports* 2018, 8:7764.
640. Blagborough A. M., Churcher T. S., Upton L. M., Ghani A. C., Gething P. W., Sinden R. E.: Transmission-blocking interventions eliminate malaria from laboratory populations. *Nature Communications* 2013, 4:1812.
641. Duffier Y., Lorthois A., Cistero P., Dupuy F., Jouvion G., Fiette L., Mazier D., Mayor A., Lavazec C., Moreno Sabater A.: A humanized mouse model for sequestration of *Plasmodium falciparum* sexual stages and in vivo evaluation of gametocytidal drugs. *Sci Rep* 2016, 6:35025.
642. Minkah N. K., Schafer C., Kappe S. H. I.: Humanized Mouse Models for the Study of Human Malaria Parasite Biology, Pathogenesis, and Immunity. *Front Immunol* 2018, 9:807.
643. Nunes J. K., Woods C., Carter T., Raphael T., Morin M. J., Diallo D., Leboulleux D., Jain S., Loucq C., Kaslow D. C., Birkett A. J.: Development of a transmission-blocking malaria vaccine: progress, challenges, and the path forward. *Vaccine* 2014, 32:5531 - 5539.
644. Birkett A. J.: Building an effective malaria vaccine pipeline to address global needs. *Vaccine* 2015, 33:7538 - 7543.
645. Tiono A. B., Ouedraogo A., Ogutu B., Diarra A., Coulibaly S., Gansane A., Sirima S. B., O'Neil G., Mukhopadhyay A., Hamed K.: A controlled, parallel, cluster-randomized trial of community-wide screening and treatment of asymptomatic carriers of *Plasmodium falciparum* in Burkina Faso. *Malar J* 2013, 12:79.
646. Griffin P., Pasay C., Elliott S., Sekuloski S., Sikulu M., Hugo L., Khoury D., Cromer D., Davenport M., Sattabongkot J., Ivinson K., Ockenhouse C., McCarthy J.: Safety and Reproducibility of a Clinical Trial System Using Induced Blood Stage *Plasmodium vivax* Infection and Its Potential as a Model to Evaluate Malaria Transmission. *PLoS Neglected Tropical Diseases* 2016, 10:e0005139.
647. Sinden R. E.: Targeting the Parasite to Suppress Malaria Transmission. *Adv Parasitol* 2017, 97:147-185.
648. Srivastava A., Philip N., Hughes K. R., Georgiou K., MacRae J. I., Barrett M. P., Creek D. J., McConville M. J., Waters A. P.: Stage-Specific Changes in *Plasmodium* Metabolism Required for

- Differentiation and Adaptation to Different Host and Vector Environments. *Plos Pathogens* 2016, 12:e1006094.
649. Li H., Sun W., Huang X., Lu X., Patel P. R., Kim M., Orr M. J., Fisher R. M., Tanaka T. Q., McKew J. C., Simeonov A., Sanderson P. E., Zheng W., Williamson K. C., Huang W.: Efficient Synthesis of 1,9-Substituted Benzo[h][1,6]naphthyridin-2(1H)-ones and Evaluation of their *Plasmodium falciparum* Gametocytocidal Activities. *ACS Combinatorial Science* 2017, 19:748 - 754.
650. D'Alessandro S., Corbett Y., Ilboudo D. P., Misiano P., Dahiya N., Abay S. M., Habluetzel A., Grande R., Gismondo M. R., Dechering K. J., Koolen K. M. J., Sauerwein R. W., Taramelli D., Basilico N., Parapini S.: Salinomycin and Other Ionophores as a New Class of Antimalarial Drugs with Transmission-Blocking Activity. *Antimicrobial Agents and Chemotherapy* 2015, 59:5135 - 5144.
651. Giulia S., T.R. S. K., Roberta B., Grazia C., Maddalena C. M., Luca C., Elisabeth D. C., Katja B., Andrea C., A. F. D., Pietro A.: A high susceptibility to redox imbalance of the transmissible stages of *Plasmodium falciparum* revealed with a luciferase-based mature gametocyte assay. *Molecular Microbiology* 2017, 104:306 - 318.
652. Mathews L. A., Keller J. M., Goodwin B. L., Guha R., Shinn P., Mull R., Thomas C. J., de Kluyver R. L., Sayers T. J., Ferrer M.: A 1536-Well Quantitative High-Throughput Screen to Identify Compounds Targeting Cancer Stem Cells. *Journal of Biomolecular Screening* 2012, 17:1231 - 1242.

APPENDIX

Table A3.1: Primary screen (1 and 5 μ M) data for late stage gametocytocidal activity. Data reflect trends in Figure 3.4. Data are representative of a single biological experiment, performed in technical triplicates.

Compound	Luciferase reporter assay		ATP assay	PrestoBlue® assay
	1 μ M	5 μ M	1 μ M	1 μ M
MMV672720	0.00	0.00	4.00	41.00
MMV672965	1.00	0.00	0.00	7.00
MMV668308	7.00	90.00	8.00	26.00
MMV669340	8.00	17.00	16.00	14.00
MMV667613	8.00	4.00	0.00	12.00
MMV672639	14.00	7.00	0.00	30.00
MMV667482	19.00	21.00	4.00	28.00
MMV668436	22.00	97.00	93.00	29.00
MMV670771	34.00	100.00	94.00	36.00
MMV668434	42.00	97.00	95.00	41.00
MMV670997	54.00	100.00	46.00	25.00
MMV666632	79.00	100.00	55.00	39.00
MMV390394	0.00	0.00	0.00	4.00
MMV674578	0.00	0.00	0.00	32.00
MMV674944	0.00	0.00	0.00	33.00
MMV674579	3.00	80.00	27.00	49.00
MMV670393	18.00	85.00	27.00	12.00
MMV674333	24.00	47.00	17.00	0.00
MMV034136	26.00	53.00	15.00	0.00
MMV674796	27.00	73.00	21.00	0.00
MMV390535	29.00	87.00	28.00	62.00
MMV668808	60.00	68.00	11.00	0.00
MMV668809	61.00	91.00	37.00	0.00
MMV672643	61.00	92.00	41.00	18.00
MMV670401	74.00	81.00	49.00	0.00
MMV668807	74.00	88.00	21.00	19.00
MMV670402	80.00	81.00	63.00	59.00
MMV394902	80.00	77.00	44.00	NA
MMV674594	81.00	85.00	49.00	31.00
MMV670930	82.00	90.00	46.00	NA
MMV642990	82.00	80.00	52.00	24.00
MMV642941	83.00	82.00	53.00	41.00
MMV643110	84.00	81.00	50.00	56.00
MMV675081	85.00	90.00	51.00	36.00
MMV666810	86.00	85.00	55.00	26.00
MMV642942	87.00	89.00	43.00	51.00
MMV673927	88.00	87.00	76.00	50.00
MMV674192	89.00	94.00	48.00	62.00
MMV390048	89.00	90.00	45.00	23.00
MMV668648	90.00	94.00	44.00	42.00

MMV642944	91.00	93.00	40.00	55.00
MMV668647	92.00	93.00	34.00	55.00
MMV642943	96.00	96.00	64.00	43.00
MMV639846	0.00	0.00	64.00	17.00
MMV674326	0.00	11.00	33.00	7.00
MMV670815	1.00	7.00	4.00	0.00
MMV672653	1.00	12.00	2.00	12.00
MMV652459	9.00	22.00	17.00	13.00
MMV652454	13.00	15.00	3.00	2.00
MMV670656	15.00	34.00	40.00	0.00
MMV665078	16.00	28.00	30.00	4.00
MMV670225	18.00	32.00	18.00	14.00
MMV666812	20.00	87.00	35.00	0.00
MMV674132	31.00	92.00	42.00	12.00
MMV675704	44.00	90.00	45.00	0.00
MMV669289	58.00	92.00	43.00	62.00
MMV672925	61.00	80.00		NA
MMV670654	74.00	90.00	72.00	58.00
MMV674766	79.00	91.00	77.00	NA
MMV675615	80.00	90.00	76.00	62.00
MMV666620	80.00	84.00	67.00	53.00
MMV652103	87.00	88.00	61.00	53.00
MMV669286	92.00	98.00	51.00	19.00
MMV674850	92.00	98.00	64.00	46.00
MMV669810	95.00	99.00	66.00	59.00
MMV672652	97.00	98.00	64.00	55.00
MMV892998	0.00	98.57	65.44	NA
MMV893359	0.00	0.00	49.95	NA
MMV032931	0.00	0.00	28.65	NA
MMV884692	0.00	100.00	32.80	NA
MMV690007	0.00	99.09	42.77	NA
MMV910899	0.00	8.72	36.27	NA
MMV892589	0.00	61.29	24.70	NA
MMV982099	0.00	95.54	23.97	NA
MMV1545645	0.00	8.10	49.84	NA
MMV982078	0.00	0.00	36.28	NA
MMV893746	0.00	80.02	32.51	NA
MMV1545843	0.00	5.72	28.04	NA
MMV982154	0.00	14.34	10.73	NA
MMV1545842	0.00	27.15	35.59	NA
MMV982100	0.00	0.00	27.35	NA
MMV892597	0.00	21.55	27.41	NA
MMV892590	0.00	34.29	17.13	NA
MMV1557966	0.00	13.86	22.66	NA
MMV893361	0.00	90.92	45.09	NA
MMV1545641	0.00	0.00	1.95	NA
MMV1558137	0.00	0.00	29.86	NA
MMV1558085	0.00	54.94	39.98	NA

MMV1545642	0.00	0.00	11.97	NA
MMV1558203	0.00	0.00	16.27	NA
MMV893729	0.00	98.55	14.12	NA
MMV689606	0.00	1.48	0.00	NA
MMV893726	0.00	98.56	9.66	NA
MMV1558899	0.00	0.00	0.00	NA
MMV1558632	0.00	27.33	0.00	NA
MMV895691	0.00	43.65	8.51	NA
MMV893360	0.00	50.01	0.00	NA
MMV689508	0.00	0.00	0.00	NA
MMV033142	0.00	0.00	5.82	NA
MMV033119	0.00	0.00	3.70	NA
MMV692813	0.00	1.65	0.00	NA
MMV692815	0.00	23.58	0.00	NA
MMV692742	0.00	33.09	0.00	NA
MMV693079	0.00	2.72	0.00	NA
MMV693082	0.00	15.76	24.80	NA
MMV693147	0.00	0.00	7.73	NA
MMV032960	0.00	11.98	0.00	NA
MMV884976	0.00	0.27	0.00	NA
MMV892576	0.00	0.00	0.00	NA
MMV892666	0.00	6.52	0.00	NA
MMV892668	0.00	7.42	0.00	NA
MMV892906	0.00	13.87	0.00	NA
MMV893362	0.00	6.51	0.93	NA
MMV893745	0.00	95.21	0.00	NA
MMV895692	0.00	7.81	11.18	NA
MMV897601	0.00	1.63	4.49	NA
MMV897602	0.00	0.00	3.56	NA
MMV897676	0.00	22.21	0.89	NA
MMV897677	0.00	6.04	5.79	NA
MMV976194	0.00	0.00	25.10	NA
MMV982079	0.00	0.00	0.00	NA
MMV982080	0.00	0.00	4.80	NA
MMV982094	0.00	0.00	0.00	NA
MMV1542777	0.00	13.04	0.00	NA
MMV1542864	0.00	9.08	6.02	NA
MMV1542865	0.00	6.45	15.97	NA
MMV1542867	0.00	4.62	3.30	NA
MMV1545577	0.00	0.00	4.71	NA
MMV1545643	0.00	0.00	5.94	NA
MMV1545644	0.00	0.00	3.08	NA
MMV1545710	0.00	0.00	0.00	NA
MMV1545711	0.00	0.00	5.71	NA
MMV1545713	0.00	0.00	0.00	NA
MMV1545714	0.00	0.00	0.00	NA
MMV1545776	0.00	1.83	1.77	NA
MMV1557858	0.00	0.00	3.35	NA

MMV1557968	0.00	10.21	0.35	NA
MMV1558002	0.00	0.00	2.11	NA
MMV1558086	0.00	0.00	9.34	NA
MMV1558296	0.00	0.00	0.00	NA
MMV1558299	0.00	0.00	0.00	NA
MMV1558346	0.00	0.00	0.00	NA
MMV1558347	0.00	0.00	1.78	NA
MMV1558619	0.00	7.13	7.50	NA
MMV693080	0.01	62.22	47.70	NA
MMV897603	0.04	8.88	5.51	NA
MMV1558135	0.15	0.00	13.33	NA
MMV1558136	0.50	44.23	67.20	NA
MMV1542778	0.79	21.82	17.70	NA
MMV982553	2.03	15.37	21.13	NA
MMV1545775	2.15	54.79	53.07	NA
MMV1558761	2.45	53.48	77.73	NA
MMV982628	2.67	35.73	0.00	NA
MMV982077	2.70	0.00	0.54	NA
MMV1558759	3.15	83.69	80.17	NA
MMV1545640	3.57	6.64	12.83	NA
MMV1558775	4.03	0.00	14.75	NA
MMV689672	4.95	5.18	0.00	NA
MMV1543409	5.06	21.41	17.62	NA
MMV1545565	5.88	22.59	2.62	NA
MMV1542123	6.11	26.58	0.00	NA
MMV1558773	6.25	30.59	46.05	NA
MMV032922	6.29	10.54	0.00	NA
MMV690983	6.69	3.69	0.00	NA
MMV1558893	6.69	0.00	0.00	NA
MMV1557964	6.89	55.97	72.43	NA
MMV893286	7.26	12.56	9.25	NA
MMV884975	7.32	46.90	47.06	NA
MMV1542913	8.03	4.70	13.70	NA
MMV1558119	8.23	0.00	14.81	NA
MMV1558774	8.42	0.00	26.98	NA
MMV1543407	9.07	10.09	9.54	NA
MMV892903	9.64	86.08	5.82	NA
MMV892665	10.12	86.03	46.69	NA
MMV892904	10.45	41.08	4.22	NA
MMV1543412	10.90	0.00	0.00	NA
MMV982238	11.76	0.00	40.98	NA
MMV897947	12.65	100.00	12.39	NA
MMV1558620	12.88	27.21	49.19	NA
MMV1545639	13.49	3.59	34.18	NA
MMV982552	13.69	22.42	1.96	NA
MMV690981	14.19	98.45	54.06	NA
MMV910897	14.58	100.00	18.82	NA
MMV892826	15.87	97.87	49.36	NA

MMV1542017	17.28	31.33	23.35	NA
MMV1542890	17.30	47.74	19.18	NA
MMV982629	21.57	63.64	41.77	NA
MMV032934	21.65	0.00	0.00	NA
MMV982680	21.72	61.15	25.76	NA
MMV982681	22.17	73.03	44.04	NA
MMV1558616	22.61	91.68	57.49	NA
MMV982624	22.67	13.87	0.00	NA
MMV1558633	23.34	21.17	2.44	NA
MMV1542016	24.87	27.49	2.08	NA
MMV982554	24.95	15.71	15.28	NA
MMV1558635	25.49	97.22	58.78	NA
MMV689849	25.68	96.94	2.29	NA
MMV910835	26.72	100.00	23.81	NA
MMV982096	27.33	29.87	16.77	NA
MMV690008	28.12	2.23	0.00	NA
MMV1558760	34.74	7.67	54.51	NA
MMV982155	35.88	97.88	35.98	NA
MMV893195	36.19	27.93	51.31	NA
MMV1558634	37.54	95.48	70.92	NA
MMV893357	37.60	64.64	51.55	NA
MMV982237	42.37	72.00	52.34	NA
MMV1558618	42.66	97.44	80.84	NA
MMV892827	43.43	97.20	48.93	NA
MMV982239	43.55	44.25	10.90	NA
MMV1543411	45.06	99.03	41.73	NA
MMV910834	46.65	100.00	0.00	NA
MMV893287	50.04	37.81	49.78	NA
MMV910901	51.05	100.00	12.55	NA
MMV884980	53.60	96.92	59.79	NA
MMV1558617	53.63	94.44	56.41	NA
MMV884979	53.77	96.95	53.54	NA
MMV893172	55.19	24.34	9.01	NA
MMV893158	56.71	13.96	6.72	NA
MMV910900	63.04	42.58	47.84	NA
MMV884981	84.18	99.84	49.93	NA
MMV893049	97.54	98.64	68.33	NA
MMV893002	99.79	99.59	61.36	NA
MMV689854	100.00	100.00	92.12	NA
MMV893358	100.00	100.00	2.08	NA
MMV1545672	0.00	96.63	88.75	NA
MMV675755	0.00	0.00	2.04	NA
MMV693083	0.00	0.93	32.11	NA
MMV676025	0.00	0.00	0.00	NA
MMV839157	0.00	54.54	30.16	NA
MMV892598	0.00	53.31	11.59	NA
MMV676026	0.00	0.00	0.00	NA
MMV689236	0.00	1.70	0.00	NA

MMV689241	0.00	0.00	0.00	NA
MMV689351	0.00	0.00	0.00	NA
MMV689352	0.00	0.00	0.00	NA
MMV689353	0.00	0.00	0.00	NA
MMV689306	0.00	0.00	0.00	NA
MMV689033	0.00	24.42	0.00	NA
MMV689053	0.00	0.00	0.00	NA
MMV689505	0.00	0.00	0.00	NA
MMV689506	0.00	0.00	0.00	NA
MMV689507	0.00	0.00	0.00	NA
MMV689572	0.00	0.00	0.00	NA
MMV689569	0.00	0.00	0.00	NA
MMV689592	0.00	0.00	0.00	NA
MMV689670	0.00	0.00	7.08	NA
MMV690006	0.00	0.00	0.00	NA
MMV690114	0.00	0.00	0.00	NA
MMV692672	0.00	0.00	0.00	NA
MMV692703	0.00	6.30	0.00	NA
MMV692741	0.00	0.00	0.00	NA
MMV693078	0.00	0.40	13.65	NA
MMV884685	0.00	21.18	29.91	NA
MMV884694	0.00	0.00	0.00	NA
MMV884972	0.00	0.00	0.00	NA
MMV884973	0.00	0.00	0.00	NA
MMV884974	0.00	0.00	0.00	NA
MMV892773	0.00	0.00	0.00	NA
MMV892999	0.00	1.45	1.23	NA
MMV893003	0.00	0.00	0.00	NA
MMV893035	0.00	0.00	0.00	NA
MMV893034	0.00	0.00	0.00	NA
MMV893385	0.00	0.00	0.00	NA
MMV893405	0.00	0.00	0.00	NA
MMV893648	0.00	26.09	11.70	NA
MMV893722	0.00	0.00	0.00	NA
MMV893727	0.00	14.74	0.00	NA
MMV893728	0.00	8.11	0.00	NA
MMV893743	0.00	4.52	0.00	NA
MMV897562	0.00	0.00	0.00	NA
MMV977402	0.00	0.00	0.00	NA
MMV1543429	0.00	0.00	0.00	NA
MMV1545646	0.00	0.00	1.59	NA
MMV1545697	0.00	0.00	2.26	NA
MMV1545716	0.00	24.28	0.35	NA
MMV675876	0.48	81.93	87.52	NA
MMV982670	0.67	8.70	9.10	NA
MMV688246	0.70	7.11	0.00	NA
MMV676248	0.76	0.14	0.00	NA
MMV689570	1.27	0.00	0.00	NA

MMV977482	1.83	13.30	4.79	NA
MMV687209	2.11	3.09	0.00	NA
MMV689573	2.13	0.00	0.00	NA
MMV1542021	2.27	79.07	49.04	NA
MMV893001	2.33	16.47	0.00	NA
MMV893468	2.68	99.78	62.67	NA
MMV675863	2.85	25.36	13.27	NA
MMV897581	3.18	91.14	59.33	NA
MMV687735	3.20	4.07	0.00	NA
MMV688389	3.24	100.00	87.31	NA
MMV688516	3.30	21.07	8.20	NA
MMV676246	3.36	2.69	0.00	NA
MMV676247	3.46	3.82	0.00	NA
MMV676218	3.48	0.99	0.00	NA
MMV973596	3.55	2.15	15.82	NA
MMV687736	3.61	3.33	0.00	NA
MMV687737	3.89	3.31	0.00	NA
MMV687208	3.92	11.65	0.00	NA
MMV675939	3.94	6.29	0.43	NA
MMV688430	4.13	7.34	0.00	NA
MMV687738	4.38	5.91	3.72	NA
MMV687168	4.91	67.52	0.00	NA
MMV676227	4.97	0.52	92.08	NA
MMV1543420	5.11	0.00	0.00	NA
MMV1542889	5.29	0.00	21.51	NA
MMV688808	5.39	40.85	0.00	NA
MMV688532	5.68	0.00	0.50	NA
MMV676003	5.87	95.99	57.17	NA
MMV676219	5.93	3.72	0.00	NA
MMV688841	6.29	83.51	19.01	NA
MMV688431	6.51	2.76	0.00	NA
MMV688842	6.54	0.00	0.00	NA
MMV1542888	6.70	0.65	6.23	NA
MMV1541929	7.18	12.11	18.21	NA
MMV977483	7.31	5.32	0.00	NA
MMV676853	7.55	8.22	0.00	NA
MMV1542776	7.63	12.35	39.97	NA
MMV688137	7.70	99.85	89.34	NA
MMV676222	7.77	25.16	66.68	NA
MMV676220	7.79	6.91	0.00	NA
MMV982092	8.08	13.77	0.00	NA
MMV977401	8.46	23.74	0.00	NA
MMV676313	8.51	12.61	0.00	NA
MMV687197	8.77	13.70	0.00	NA
MMV977416	9.00	13.69	0.00	NA
MMV1542775	9.09	10.36	43.71	NA
MMV676221	9.70	53.82	0.00	NA
MMV982672	9.71	47.58	35.74	NA

MMV1542261	10.31	31.06	45.84	NA
MMV689426	10.68	36.22	0.00	NA
MMV691888	11.32	46.53	22.53	NA
MMV676852	12.34	2.12	2.42	NA
MMV676241	12.49	15.76	0.00	NA
MMV893157	13.48	92.82	39.13	NA
MMV676316	13.52	26.45	0.76	NA
MMV893493	14.00	15.24	0.00	NA
MMV688475	14.15	93.39	85.90	NA
MMV676244	14.71	15.06	0.00	NA
MMV982673	15.03	50.89	36.07	NA
MMV689591	15.05	0.00	0.00	NA
MMV910895	15.11	4.65	68.51	NA
MMV910902	15.55	11.18	15.34	NA
MMV687196	16.26	12.18	0.00	NA
MMV688908	17.12	0.00	0.00	NA
MMV676314	17.56	38.86	0.15	NA
MMV897779	17.81	64.94	53.75	NA
MMV977484	18.21	7.99	8.91	NA
MMV897780	18.52	62.25	72.79	NA
MMV1545620	18.87	96.80	61.52	NA
MMV910833	19.14	85.19	66.69	NA
MMV1541927	19.31	39.64	9.66	NA
MMV676245	19.39	40.14	80.98	NA
MMV689781	20.25	0.00	0.00	NA
MMV688907	20.39	16.72	0.00	NA
MMV1541926	20.85	45.11	16.71	NA
MMV688425	21.31	20.00	54.52	NA
MMV897781	21.79	82.09	74.71	NA
MMV977415	22.98	36.05	35.39	NA
MMV977417	23.38	6.96	0.00	NA
MMV982093	23.48	51.52	45.10	NA
MMV973709	29.37	17.45	0.00	NA
MMV982236	29.49	45.21	0.00	NA
MMV688515	33.53	18.66	0.00	NA
MMV690004	34.05	29.03	0.00	NA
MMV688726	34.58	16.27	0.00	NA
MMV688727	34.87	100.00	79.59	NA
MMV690005	35.09	25.90	0.00	NA
MMV910836	35.10	100.00	45.05	NA
MMV977480	36.52	19.67	56.61	NA
MMV675097	36.84	100.00	95.60	NA
MMV982102	37.41	34.61	0.00	NA
MMV977445	38.55	96.02	0.00	NA
MMV675717	54.60	98.12	91.18	NA
MMV675812	67.10	97.18	92.39	NA
MMV897760	72.90	100.00	51.14	NA
MMV893197	75.30	98.80	42.68	NA

MMV675617	83.42	97.59	88.77	NA
MMV688390	83.92	100.00	95.18	NA
MMV688375	98.95	100.00	93.00	NA

Table A3.2: Biological profiles of the evaluated compounds. The DTPs series are indicated in pink, the APs in purple, the IMPs in orange, the 6,9-IPs in turquoise and the 2,6-IPs in blue. Colour intensity represents decreasing *in vitro* potency against *P. falciparum* asexual stages, early (stage II/III) gametocytes and late (stage IV/V) gametocytes. Gametocyte IC₅₀'s represent the lowest of each value obtained for the luciferase reporter or ATP bioluminescence assays (italicised values). Data are representative of at least two biological experiments, each performed in technical triplicates, ± SEM.

Compound	Pf asexual IC ₅₀ (nM)		RI	Ref	IC ₅₀ CHO cells (µM)	SI (CHO:NF54)	Gametocyte IC ₅₀ (nM)				SI (CHO:LG)
	NF54	K1					Stage II/III		Stage IV/V		
							Mean	SEM	Mean	SEM	
MMV668434	42.54	ND	ND	[393]	16.87	396.53	513.70	ND	105.20	ND	160.36
MMV666632	28.20	25.85	0.92	[483]	4.12	146.08	404.65	± 140.25	642.70	± 15.66	6.41
MMV670771	35.60	ND	ND		1.81	ND	4182.50	± 94.50	1091.00	± 71.00	1.66
MMV668436	163.91	ND	ND	[393]	2.10	12.81	781.60	± 82.90	1519.00	± 104.00	1.38
MMV670997	20.08	33.04	1.65		ND	ND	442.30	± 50.30	2193.00	± 716.00	ND
MMV667613	115.95	ND	ND	[393]	>260	>2200	ND	ND	2390.00	ND	>100
MMV667482	26.09	86.96	3.33		4.32	165.60	2960.00	± 15.00	2935.00	± 394.00	1.47
MMV668308	194.24	ND	ND	[420]	19.66	101.22	6525.00	± 742.00	5840.00	ND	3.37
MMV669340	46.76	137.81	2.95	[393]	86.31	1845.91	ND	ND	ND	ND	ND
MMV672639	167.60	ND	ND		>260	>2200	ND	ND	ND	ND	ND
MMV672720	766.70	ND	ND		220.94	288.17	ND	ND	ND	ND	ND
MMV672965	2380.00	ND	ND		>260	>2200	ND	ND	ND	ND	ND
MMV642943	5.73	5.15	0.96	[486]	18.90	3512.36	134.00	ND	66.00	ND	286.36
MMV674192	9.17	7.00	0.76	[406]	196.00	21373.64	415.90	± 42.10	45.24	± 9.09	4332.45
MMV642944	20.16	8.37	0.83	[485]	282.00	27803.44	46.80	± 22.80	51.90	± 8.50	5433.53
MMV643110	23.24	16.42	0.82	[331]	70.91	3538.71	122.10	± 12.70	71.51	± 2.38	991.61
MMV642942	10.17	8.64	0.85	[422]	254.00	24980.07	550.00	ND	134.70	± 1.20	1885.67
MMV668647	21.47	19.61	0.91	[331]	40.94	1906.44	322.90	ND	136.90	± 0.50	299.05
MMV390048	22.12	17.79	0.80	[484]	254.00	11484.97	214.60	± 16.70	140.30	± 11.40	1810.41
MMV673927	15.00	ND	ND		147.12	9808.00	697.30	± 102.00	146.05	± 26.85	1007.33
MMV666810	5.42	4.97	0.92	[423]	226.00	41663.19	602.50	± 87.90	178.70	± 7.80	1264.69
MMV670930	14.27	14.01	0.98	[422]	241.00	16886.78	639.80	± 435.00	189.90	± 28.10	1269.09
MMV394902	18.60	19.88	1.07	[421]	27.60	1483.59	919.55	± 185.45	208.60	± 4.90	132.31
MMV642941	53.02	50.23	0.95		249.00	4695.92	619.85	± 18.75	224.50	ND	1109.13
MMV642990	13.95	13.12	0.94	[331]	ND	ND	754.05	± 13.55	236.95	± 41.75	ND
MMV670401	42.11	32.75	0.78		157.63	3743.06	1168.50	± 80.50	238.40	± 5.80	661.20
MMV668808	93.76	73.25	0.78	[422]	>260	>2200	1390.00	± 136.00	342.20	± 18.50	>700
MMV668809	38.08	27.24	0.72	[422]	246.22	6465.98	2433.00	± 48.00	432.40	± 27.00	569.43
MMV670402	25.74	19.65	0.76		48.43	1881.84	1319.50	± 28.50	440.90	± 82.00	109.84
MMV672643	42.40	39.75	0.94		190.40	4490.92	1071.00	ND	460.00	± 97.00	413.91
MMV668648	6.02	ND	ND	[331]	180.52	30000.90	731.35	± 413.65	536.20	± 283.60	336.67
MMV675081	24.42	26.09	1.07	[331]	178.00	7287.68	168.00	± 14.50	845.00	± 107.00	210.65
MMV668807	26.16	19.54	0.75	[422]	>260	>2200	1835.00	± 278.00	901.25	± 108.75	>250
MMV674796	239.00	ND	ND		>260	>2200	ND	ND	1574.00	± 21.00	>150
MMV674594	89.06	91.84	1.03	[331]	278.00	3121.48	649.00	ND	1860.00	± 770.00	149.46
MMV674333	189.12	206.92	1.09		222.00	1173.86	ND	ND	1986.00	± 250.00	111.78
MMV670393	248.42	205.22	0.83		242.35	975.56	3790.00	ND	4267.00	ND	56.80
MMV390535	637.78	500.90	0.79	[421]	>260	>2200	ND	ND	22800.00	± 8000.00	>10
MMV034136	574.69	500.94	0.87	[421]	>260	>2200	1793.00	± 556.00	ND	ND	ND

MMV390394	980.13	942.34	0.96	[423]	>260	>2200	ND	ND	ND	ND	ND
MMV674578	2180.00	ND	ND		>260	>2200	ND	ND	ND	ND	ND
MMV674579	2180.00	ND	ND		>260	>2200	ND	ND	ND	ND	ND
MMV674944	2440.00	ND	ND		>260	>2200	ND	ND	ND	ND	ND
MMV669810	0.45	0.37	0.89		221.00	527537.46	2.00	± 0.80	1.40	± 0.05	157857.14
MMV669286	0.88	0.53	0.60	[488]	2.42	2740.51	4.10	± 2.40	3.00	± 0.13	805.67
MMV672652	0.56	ND	ND	[425]	2.90	3222.22	10.80	± 0.90	3.30	± 0.19	878.79
MMV652103	7.25	6.32	0.87	[407]	234.00	32269.43	59.60	± 12.98	27.00	± 2.40	8666.67
MMV674850	2.65	2.43	0.92	[480]	221.00	83344.81	4.47	± 3.63	28.70	ND	7700.35
MMV674766	7.86	ND	ND	[432]	134.00	16750.00	93.90	ND	66.40	ND	2018.07
MMV675615	4.47	3.67	0.80		17.90	3907.09	163.20	ND	72.10	ND	248.27
MMV666620	11.59	9.53	0.92	[333]	19.34	1859.64	68.40	ND	78.90	ND	245.12
MMV672925	10.20	0.94	0.09	[425]	212.00	20783.51	693.35	ND	476.80	ND	444.63
MMV670815	417.40	ND	ND	[432]	>260	>2200	ND	ND	654.75	± 46.25	>350
MMV672653	35.80	ND	ND		254.00	7094.97	ND	ND	907.27	± 237.90	279.96
MMV674132	43.71	45.89	1.05	[432]	219.00	5010.40	2604.00	ND	1453.50	± 70.50	150.67
MMV665078	59.89	45.52	0.76	[333]	240.00	4007.13	ND	ND	1462.00	± 193.00	164.16
MMV669289	95.69	81.68	0.85	[425]	>260	>2200	ND	ND	1489.00	± 10.00	>150
MMV675704	80.72	ND	ND		202.00	2502.63	ND	ND	1789.00	± 371.50	112.91
MMV670654	35.40	30.34	0.86	[425]	54.10	1528.34	35696.0	± 3711.0	7993.00	ND	6.77
MMV670656	42.84	24.80	0.58		27.60	644.23	ND	ND	ND	ND	ND
MMV652459	282.58	246.21	0.87		>260	>2200	ND	ND	ND	ND	ND
MMV674326	372.04	ND	ND		>260	>2200	ND	ND	ND	ND	ND
MMV652454	496.28	415.19	0.84	[333]	>260	>2200	ND	ND	ND	ND	ND
MMV670225	876.55	ND	ND	[432]	>260	>2200	ND	ND	ND	ND	ND
MMV639846	963.97	873.14	0.91	[333]	209.35	217.17	ND	ND	ND	ND	ND
MMV666812	2339.18	2339.18	1.00	[432]	>260	>2200	ND	ND	ND	ND	ND
MMV689854	35.71	ND	ND		ND	#REF!	283.00	± 19.70	7.69	± 1.46	53.49
MMV893002	46.15	30.94	0.67		30.94	1.44	84.13	± 15.65	61.99	± 11.34	31.20
MMV893195	41.10	56.50	1.37		56.50	1.05	252.00	± 33.80	69.65	± 22.00	25.55
MMV892998	63.10	84.00	1.33		84.00	50.00	381.90	± 15.41	95.75	± 13.23	792.39
MMV1558618	ND	25.00	ND		ND	ND	464.00	± 138.00	177.23	± 20.97	ND
MMV884980	64.00	266.00	4.16		266.00	1.97	91.10	± 1.60	193.70	± 13.36	30.78
MMV884979	51.96	288.00	5.54		288.00	2.99	571.27	± 170.36	222.30	± 10.97	57.54
MMV1557964	50.00	40.00	0.80		40.00	3.11	107.00	± 11.70	230.40	± 21.96	62.20
MMV982237	20.00	12.20	0.61		12.20	0.95	501.90	± 145.00	266.00	± 40.45	47.50
MMV1545775	20.00	ND			0.00	4.50	1291.00	± 512.00	270.80	± 198.00	225.00
MMV893049	57.17	55.20	0.97		55.20	1.21	174.60	± 24.60	293.50	± 99.30	21.16
MMV893359	45.00	249.90	5.55		249.90	5.09	525.03	± 84.24	306.23	± 74.00	113.18
MMV892826	74.42	704.00	9.46		704.00	1.64	254.47	± 48.70	321.37	± 63.89	22.04
MMV1558759	ND	ND			ND	ND	217.00	± 64.00	358.60	± 71.14	ND
MMV884981	221.80	458.00	2.06		458.00	17.23	1014.50	± 141.50	403.07	± 13.40	77.68
MMV032931	55.00	ND			0.00	19.84	15667.0	ND	440.05	± 19.55	ND
MMV892827	68.43	185.00	2.70		185.00	2.92	501.31	± 122.65	482.73	± 71.56	42.67
MMV693080	62.00	ND			0.00	3.63	327.90	ND	542.30	± 249.03	58.55
MMV910900	68.00	912.00	13.4		912.00	12.00	2330.00	ND	625.60	± 88.98	176.47
MMV884692	229.50	ND			0.00	2.64	961.30	ND	625.87	± 67.03	11.52

MMV690981	127.40	ND		0.00	30.70	2228.00	ND	660.30	± 66.88	240.97
MMV982681	66.00	226.00	3.42	226.00	40.80	1872.00	ND	830.67	± 20.59	618.18
MMV884975	63.67	91.00	1.43	91.00	3.01	293.90	± 38.85	845.53	± 47.17	47.28
MMV982629	36.00	310.00	8.61	310.00	34.20	4045.00	± 972.00	971.63	± 153.64	950.00
MMV1558616	ND	ND		ND	ND	173.00	± 68.00	1007.00	± 22.02	ND
MMV690007	40.00	ND		0.00	42.20	486.50	± 190.25	1059.80	± 89.75	1055.00
MMV982680	87.00	627.00	7.21	627.00	39.60	2504.00	ND	1064.00	ND	455.17
MMV1558136	ND	ND		0.00	ND	498.00	± 102.00	1089.00	ND	ND
MMV1558617	ND	111.00		ND	ND	196.00	± 94.00	1099.00	± 231.00	ND
MMV982155	74.00	300.00	4.05	300.00	3.62	2741.00	ND	1117.00	ND	48.92
MMV892665	48.50	129.00	2.66	129.00	1.59	75.60	± 8.20	1121.00	ND	32.78
MMV910899	82.00	455.00	5.55	455.00	19.30	2719.00	ND	1129.00	ND	235.37
MMV1543411	20.00	13.00	0.65	13.00	3.10	410.00	± 174.00	1131.00	ND	155.00
MMV1558635	ND	18.00		ND	ND	176.00	± 46.00	1181.00	± 169.33	ND
MMV1542017	23.00	41.00	1.78	41.00	24.00	ND	ND	1257.00	ND	1043.48
MMV1558761	ND	ND		ND	ND	335.00	± 67.00	1269.00	± 418.89	ND
MMV892589	147.20	250.00	1.70	ND	ND	1250.00	ND	1270.00	ND	ND
MMV982099	95.00	315.00	3.32	315.00	1.91	1822.00	ND	1357.00	ND	20.11
MMV1558634	ND	43.00		ND	ND	109.00	± 27.00	1380.00	ND	ND
MMV1558620	ND	ND		ND	ND	432.00	ND	1417.00	ND	ND
MMV892903	39.38	509.90	12.9	509.90	13.71	1001.10	± 358.92	1429.00	ND	348.15
MMV1545645	36.00	ND		0.00	7.30	1959.00	± 708.00	1602.00	ND	202.78
MMV982078	18.00	73.00	4.06	73.00	4.77	3168.00	ND	1755.00	ND	265.00
MMV1558773	ND	ND		ND	ND	174.90	± 40.00	1756.00	± 758.77	ND
MMV689849	906.80	ND		ND	ND	ND	ND	1767.00	ND	ND
MMV893746	81.00	421.00	5.20	421.00	33.90	3273.00	ND	1943.00	ND	418.52
MMV1542778	144.00	277.00	1.92	277.00	20.00	4779.00	ND	1951.00	ND	138.89
MMV1545843	20.00	ND		0.00	9.00	389.00	± 218.00	1975.00	ND	450.00
MMV1558760	ND	ND		ND	ND	161.60	± 27.00	1978.00	± 599.17	ND
MMV982553	304.00	801.00	2.63	801.00	40.00	8039.00	ND	2036.00	ND	131.58
MMV982154	97.60	461.00	4.72	461.00	2.27	7633.00	ND	2068.00	ND	23.26
MMV1558633	ND	80.00		ND	ND	1138.00	± 103.00	2069.00	ND	ND
MMV1545842	20.00	ND		0.00	20.00	1194.00	± 69.00	2073.50	ND	1000.00
MMV982100	33.00	125.00	3.79	125.00	5.79	2334.70	± 938.00	2092.00	ND	175.45
MMV910835	239.00	796.00	3.33	796.00	20.40	1308.00	ND	2198.00	ND	85.36
MMV892597	222.90	1000.00	4.49	ND	ND	1463.60	± 562.90	2321.50	± 244.50	ND
MMV1545639	21.00	ND		0.00	19.70	742.90	ND	2380.00	ND	938.10
MMV897947	94.00	338.00	3.60	338.00	45.00	ND	ND	2545.00	ND	478.72
MMV892590	143.30	192.00	1.34	ND	ND	274.30	± 30.20	2612.00	ND	ND
MMV982628	122.00	601.00	4.93	601.00	41.40	4783.00	ND	2685.00	ND	339.34
MMV1558775	ND	147.10		ND	ND	248.00	± 42.00	2782.00	ND	ND
MMV1558774	ND	61.60		ND	ND	388.40	± 73.00	2803.00	ND	ND
MMV1557966	151.00	ND		0.00	44.00	1031.00	± 293.00	2848.00	ND	291.39
MMV893361	52.00	384.60	7.40	384.60	5.18	1307.00	ND	2896.00	ND	99.65
MMV1545641	30.00	ND		0.00	41.50	2148.00	ND	2988.00	ND	1383.33
MMV1558137	ND	ND		0.00	ND	738.00	± 53.00	3121.00	ND	ND
MMV1558085	53.00	ND		0.00	3.70	555.00	± 66.00	3250.00	ND	69.81
MMV1545642	27.00	ND		0.00	25.00	1373.00	± 168.00	3328.00	ND	925.93

MMV1558203	41.00	167.00	4.07	ND	ND	953.50	±	253.00	3406.00	ND	ND
MMV893287	82.00	242.80	2.96	242.80	3.97	6458.00		ND	3457.00	ND	48.41
MMV1558135	ND	ND		0.00	ND	665.00	±	198.00	3495.00	ND	ND
MMV1558119	ND	82.00		ND	ND	1098.00	±	383.00	3548.00	ND	ND
MMV893729	133.00	300.00	2.26	ND	ND	3606.00		ND	3643.00	±	1.00
MMV910834	154.00	659.00	4.28	659.00	17.20	1423.00		ND	3730.00	ND	111.69
MMV689606	424.00	ND		0.00	128.20	4670.00		ND	3837.00	ND	302.36
MMV893726	225.00	700.00	3.11	700.00	41.70	4039.00		ND	4103.00	ND	185.33
MMV910901	82.00	364.00	4.44	364.00	44.70	2389.00		ND	4109.00	±	654.89
MMV1558899	ND	ND		ND	ND	29277.0		ND	4418.00	ND	ND
MMV1558632	ND	85.00		ND	ND	150.00		ND	4517.00	ND	ND
MMV895691	301.00	954.00	3.17	954.00	41.00	3769.00		ND	5391.00	ND	136.21
MMV893172	381.50	1000.00	2.62	1000.00	27.33	1307.00		ND	5441.00	ND	71.64
MMV1542890	20.00	77.00	3.85	77.00	17.04	5318.00		ND	5570.00	ND	852.00
MMV893357	17.00	69.91	4.11	69.91	1.37	198.00	±	35.47	6947.00	ND	80.29
MMV893360	148.00	311.40	2.10	311.40	39.85	6027.00		ND	7405.00	ND	269.26
MMV1558893	ND	ND		ND	ND	6650.00		ND	8913.00	ND	ND
MMV893158	253.20	322.60	1.27	322.60	8.72	10512.3	±	1333.5	11430.00	ND	34.42
MMV910897	449.00	764.00	1.70	764.00	44.50	ND		ND	21268.00	ND	99.11
MMV893358	334.00	ND		0.00	50.00	7154.00		ND	33279.30	±	1872.60
MMV689508	3140.00	ND		ND	ND	ND		ND	ND	ND	ND
MMV033142	384.00	ND		0.00	304.00	ND		ND	ND	ND	ND
MMV033119	2910.00	ND		ND	ND	ND		ND	ND	ND	ND
MMV032934	1437.00	ND		ND	ND	ND		ND	ND	ND	ND
MMV689672	646.00	ND		ND	ND	ND		ND	ND	ND	ND
MMV690008	962.00	ND		ND	ND	ND		ND	ND	ND	ND
MMV690983	10000.00	ND		ND	ND	ND		ND	ND	ND	ND
MMV032922	10000.00	ND		ND	ND	ND		ND	ND	ND	ND
MMV692813	10000.00	ND		ND	ND	ND		ND	ND	ND	ND
MMV692815	931.60	ND		ND	ND	5049.00		ND	ND	ND	ND
MMV692742	164.80	ND		0.00	8.23	1210.00	±	71.50	ND	ND	ND
MMV693079	10000.00	ND		ND	ND	ND		ND	ND	ND	ND
MMV693082	214.50	ND		0.00	8.10	ND		ND	ND	ND	ND
MMV693147	425.10	ND		0.00	50.00	ND		ND	ND	ND	ND
MMV032960	151.10	ND		0.00	27.93	ND		ND	ND	ND	ND
MMV884976	313.60	958.70	3.06	958.70	50.00	75.52		ND	ND	ND	ND
MMV892576	10000.00	ND		ND	ND	ND		ND	ND	ND	ND
MMV892666	337.30	718.00	2.13	718.00	31.06	ND		ND	ND	ND	ND
MMV892668	556.40	ND		ND	ND	1299.00		ND	ND	ND	ND
MMV892904	86.85	1000.00	11.5 1	1000.00	10.10	5228.00		ND	ND	ND	ND
MMV892906	180.50	402.40	2.23	402.40	43.34	ND		ND	ND	ND	ND
MMV893286	264.90	358.40	1.35	358.40	5.21	3903.00		ND	ND	ND	ND
MMV893362	163.00	501.10	3.07	501.10	19.92	ND		ND	ND	ND	ND
MMV893745	674.20	ND		ND	ND	ND		ND	ND	ND	ND
MMV895692	275.00	1000.00	3.64	1000.00	27.80	ND		ND	ND	ND	ND
MMV897601	370.00	463.00	1.25	463.00	16.00	ND		ND	ND	ND	ND
MMV897602	633.00	889.00	1.40	ND	ND	ND		ND	ND	ND	ND

MMV897603	657.00	ND		ND	ND	ND	ND	ND	ND	ND	ND
MMV897676	426.00	3000.00	7.04	3000.00	50.00	ND	ND	ND	ND	ND	ND
MMV897677	55.00	187.00	3.40	187.00	40.40	ND	ND	ND	ND	ND	ND
MMV976194	46.00	216.00	4.70	216.00	4.98	940.60	± 191.00	ND	ND	ND	ND
MMV982077	106.00	581.00	5.48	581.00	15.50	ND	ND	ND	ND	ND	ND
MMV982079	452.00	1500.00	3.32	1500.00	50.00	ND	ND	ND	ND	ND	ND
MMV982080	72.00	341.00	4.74	341.00	42.00	ND	ND	ND	ND	ND	ND
MMV982094	101.00	483.00	4.78	483.00	50.00	ND	ND	ND	ND	ND	ND
MMV982096	169.00	1175.00	6.95	1175.00	4.13	ND	ND	ND	ND	ND	ND
MMV982238	20.00	27.00	1.35	27.00	7.44	1195.00	± 69.80	ND	ND	ND	ND
MMV982239	75.70	453.00	5.98	453.00	6.50	2829.00 11392.00	ND	ND	ND	ND	ND
MMV982552	79.00	281.00	3.56	281.00	34.10	0	ND	ND	ND	ND	ND
MMV982554	31.00	264.00	8.52	264.00	33.30	ND	ND	ND	ND	ND	ND
MMV982624	78.00	433.00	5.55	433.00	40.10	ND	ND	ND	ND	ND	ND
MMV1542016	50.00	157.00	3.14	157.00	29.50	ND	ND	ND	ND	ND	ND
MMV1542123	71.00	300.00	4.23	300.00	38.60	21878.00 0	ND	ND	ND	ND	ND
MMV1542777	294.00	642.00	2.18	642.00	33.24	6081.00	ND	ND	ND	ND	ND
MMV1542864	259.00	723.00	2.79	723.00	50.00	ND	ND	ND	ND	ND	ND
MMV1542865	101.00	376.00	3.72	376.00	50.00	1650.00	ND	ND	ND	ND	ND
MMV1542867	10000.00	3000.00	0.30	3000.00	50.00	ND	ND	ND	ND	ND	ND
MMV1542913	198.00	721.00	3.64	721.00	28.80	3642.00	ND	ND	ND	ND	ND
MMV1543407	61.00	104.00	1.70	104.00	14.40	ND	ND	ND	ND	ND	ND
MMV1543409	207.00	1000.00	4.83	1000.00	7.20	ND	ND	ND	ND	ND	ND
MMV1543412	51.00	119.00	2.33	119.00	34.90	1315.00	ND	ND	ND	ND	ND
MMV1545577	220.00	478.00	2.17	478.00	32.00	3790.00	ND	ND	ND	ND	ND
MMV1545565	44.00	99.00	2.25	99.00	8.70	ND	ND	ND	ND	ND	ND
MMV1545640	80.00	ND	ND	0.00	28.00	ND	ND	ND	ND	ND	ND
MMV1545643	43.00	ND	ND	0.00	11.00	1542.00	± 159.00	ND	ND	ND	ND
MMV1545644	81.00	ND	ND	0.00	6.80	2929.00	± 477.00	ND	ND	ND	ND
MMV1545710	66.00	ND	ND	0.00	31.00	4322.00	± 932.00	ND	ND	ND	ND
MMV1545711	223.00	ND	ND	0.00	46.00	3174.00	± 427.00	ND	ND	ND	ND
MMV1545713	263.00	ND	ND	0.00	50.00	8428.00	ND	ND	ND	ND	ND
MMV1545714	290.00	ND	ND	0.00	26.00	7083.00	± 1312.00 0	ND	ND	ND	ND
MMV1545776	39.00	ND	ND	0.00	7.10	2275.00	± 680.00	ND	ND	ND	ND
MMV1557858	38.00	ND	ND	ND	ND	ND	ND	ND	ND	ND	ND
MMV1557968	209.00	ND	ND	0.00	50.00	7768.00	± 2825.00 0	ND	ND	ND	ND
MMV1558002	271.00	ND	ND	0.00	50.00	3682.00	ND	ND	ND	ND	ND
MMV1558086	210.00	ND	ND	0.00	50.00	245.30	ND	ND	ND	ND	ND
MMV1558296	ND	ND	ND	ND	ND	ND	ND	ND	ND	ND	ND
MMV1558299	209.00	289.00	1.38	ND	ND	2984.00	ND	ND	ND	ND	ND
MMV1558346	ND	ND	ND	ND	ND	ND	ND	ND	ND	ND	ND
MMV1558347	ND	ND	ND	ND	ND	ND	ND	ND	ND	ND	ND
MMV1558619	ND	ND	ND	ND	ND	4043.00	ND	ND	ND	ND	ND
MMV688390	69.00	ND	ND	0.00	5.18	437.20	± 17.29	14.67	± 1.25	75.07	
MMV897780	35.00	ND	ND	0.00	1.20	424.00	± 45.90	38.25	± 7.32	34.29	
MMV688375	27.00	ND	ND	0.00	0.70	266.63	± 14.35	44.30	± 0.56	25.93	
MMV910895	20.00	ND	ND	0.00	2.70	963.03	± 13.53	51.22	± 4.76	135.00	

MMV688475	272.00	ND	ND	0.00	269.00	3093.30	± 276.00	97.90	± 3.80	988.97
MMV676245	133.00	ND	ND	0.00	92.10	ND	ND	103.74	± 29.52	692.48
MMV1545672	20.00	ND	ND	ND	ND	383.60	± 86.00	140.43	± 50.57	ND
MMV675812	34.00	ND	ND	0.00	4.85	1139.67	± 49.69	145.40	± 14.85	142.65
MMV675617	44.00	ND	ND	0.00	7.67	33.02	± 9.23	157.63	± 13.62	174.32
MMV910833	82.00	ND	ND	0.00	22.60	1025.00	ND	195.07	± 5.19	275.61
MMV897781	40.00	ND	ND	0.00	1.20	621.77	± 66.87	195.63	± 19.08	30.00
MMV675717	40.00	ND	ND	0.00	1.96	737.15	± 50.34	239.23	± 14.13	49.00
MMV977480	24.60	ND	ND	0.00	24.78	768.70	± 263.00	256.25	± 94.95	1007.32
MMV897760	171.00	ND	ND	0.00	33.00	1729.00	ND	274.57	± 33.49	192.98
MMV688389	39.00	ND	ND	0.00	4.19	1161.00	± 31.48	317.15	± 14.35	107.44
MMV1545620	20.00	ND	ND	0.00	0.99	ND	ND	339.63	± 57.64	49.50
MMV676227	376.00	ND	ND	0.00	306.00	ND	ND	356.03	± 21.28	813.83
MMV675097	30.00	28.10	0.94	ND	ND	1970.00	± 283.00	363.60	± 32.80	ND
MMV675876	53.00	ND	ND	0.00	6.14	128.30	± 59.20	366.67	± 7.19	115.85
MMV897779	164.00	ND	ND	0.00	20.20	1124.00	ND	370.50	± 69.22	123.17
MMV688137	30.00	ND	ND	ND	ND	804.00	± 75.00	411.30	± 13.11	ND
MMV982093	118.30	ND	ND	0.00	42.90	5842.00	ND	450.50	± 31.36	362.64
MMV676003	172.00	ND	ND	0.00	8.32	2197.00	± 141.75	699.27	± 17.06	48.37
MMV910836	29.00	ND	ND	0.00	2.70	ND	ND	701.23	± 117.50	93.10
MMV1542261	117.40	ND	ND	0.00	15.21	ND	ND	744.57	± 81.78	129.56
MMV691888	93.58	ND	ND	0.00	43.50	ND	ND	774.07	± 29.72	464.84
MMV1542021	70.00	ND	ND	0.00	50.00	4553.00	ND	774.27	± 30.26	714.29
MMV893197	151.20	ND	ND	0.00	4.63	466.20	± 59.70	802.40	± 110.80	30.62
MMV982672	35.00	ND	ND	0.00	37.00	3465.00	ND	816.18	± 59.86	1057.14
MMV676222	32.00	ND	ND	0.00	5.90	3884.33	± 101.21	836.30	± 14.70	184.38
MMV1542775	26.00	ND	ND	0.00	31.00	ND	ND	842.20	± 72.63	1192.31
MMV982673	87.00	ND	ND	0.00	50.00	3577.00	ND	986.73	± 58.10	574.71
MMV977415	21.40	ND	ND	0.00	29.17	988.70	± 320.00	1037.00	ND	1363.08
MMV675755	23.00	ND	ND	0.00	9.99	97.50	± 3.10	1037.77	± 54.24	434.35
MMV675863	64.00	21.70	0.34	ND	ND	5190.33	± 5	1049.33	± 10.27	ND
MMV893468	25.10	ND	ND	0.00	34.50	373.33	± 56.00	1114.00	ND	1374.50
MMV688425	384.00	ND	ND	ND	ND	ND	ND	1130.50	± 108.50	ND
MMV1542776	20.44	ND	ND	0.00	42.00	ND	ND	1142.00	ND	2054.79
MMV688727	63.00	ND	ND	0.00	5.00	2433.50	± 2.50	1187.00	± 51.00	79.37
MMV893157	52.51	ND	ND	0.00	4.74	2117.00	ND	1440.00	ND	90.25
MMV693083	438.20	321.00	0.73	321.00	50.00	1581.00	ND	1499.00	ND	ND
MMV688841	ND	ND	ND	ND	ND	11788.0	2245.0	1726.00	± 420.00	ND
MMV982670	92.00	ND	ND	0.00	31.00	ND	ND	1801.00	ND	336.96
MMV687168	18.00	ND	ND	0.00	7.50	1094.00	± 14.00	1813.00	± 72.51	416.67
MMV910902	281.00	ND	ND	0.00	50.00	ND	ND	1834.00	± 412.17	177.94
MMV676025	25.00	ND	ND	0.00	9.29	4919.00	± 332.50	1835.67	± 156.11	371.60
MMV676316	52.00	ND	ND	0.00	31.00	ND	ND	1839.70	± 155.67	596.15
MMV982236	164.00	ND	ND	0.00	27.10	3290.00	ND	1918.00	ND	165.24
MMV973596	38.60	ND	ND	0.00	4.39	ND	ND	2237.00	ND	113.73
MMV839157	ND	ND	ND	ND	ND	2904.00	ND	2454.00	ND	ND
MMV688726	65.00	ND	ND	0.00	5.00	1971.00	± 283.00	2755.00	ND	76.92

MMV1541926	252.00	ND	ND	0.00	50.00	6592.00	ND	2773.00	ND	198.41
MMV687736	2340.00	ND	ND	0.00	278.00	ND	ND	2792.00	± 191.13	118.80
MMV687197	71.00	ND	ND	0.00	4.30	1460.00	± 11.00	2941.33	± 142.05	60.56
MMV688246	810.00	ND	ND	ND	ND	ND	ND	3090.00	ND	ND
MMV1541929	67.00	ND	ND	0.00	42.00	ND	ND	3397.00	ND	626.87
MMV687738	144.00	ND	ND	0.00	146.00	ND	ND	3501.67	± 53.14	1013.89
MMV893001	44.01	ND	ND	0.00	14.44	5708.00	± 311.50	3896.00	ND	328.11
MMV897581	196.00	ND	ND	0.00	14.40	764.43	± 50.74	4223.30	± 525.00	73.47
MMV892598	774.70	ND	ND	ND	ND	1214.00	ND	4460.00	ND	ND
MMV676221	44.00	ND	ND	0.00	4.69	3610.33	± 99.39	4975.33	± 1170.19	106.59
MMV676244	25.00	ND	ND	0.00	268.00	ND	ND	6914.67	± 978.38	10720.00
MMV676314	29.00	ND	ND	0.00	25.00	ND	ND	7279.33	± 2013.39	862.07
MMV1542889	20.00	ND	ND	0.00	35.00	4003.00	ND	7440.00	ND	1750.00
MMV676247	50.00	ND	ND	ND	ND	ND	ND	9259.00	± 427.73	ND
MMV676241	45.00	ND	ND	0.00	4.83	ND	ND	9377.00	± 611.62	107.33
MMV977445	55.10	ND	ND	0.00	30.32	4399.00	ND	11798.00	ND	550.27
MMV675939	48.00	ND	ND	0.00	124.00	9057.00	± 1363.0	ND	ND	ND
MMV676026	135.00	ND	ND	0.00	63.90	ND	ND	ND	ND	ND
MMV676218	103.00	ND	ND	0.00	61.20	ND	ND	ND	ND	ND
MMV676219	77.00	ND	ND	0.00	151.00	ND	ND	ND	ND	ND
MMV676220	154.00	ND	ND	0.00	93.80	ND	ND	ND	ND	ND
MMV676313	55.00	ND	ND	0.00	52.00	ND	ND	ND	ND	ND
MMV676852	140.00	ND	ND	0.00	281.00	ND	ND	ND	ND	ND
MMV676853	234.00	ND	ND	0.00	281.00	ND	ND	ND	ND	ND
MMV676246	46.00	ND	ND	0.00	263.00	ND	ND	ND	ND	ND
MMV676248	66.00	ND	ND	0.00	108.00	ND	ND	ND	ND	ND
MMV687196	47.00	53.30	1.13	53.30	13.20	ND	ND	ND	ND	ND
MMV687735	414.00	ND	ND	0.00	227.00	ND	ND	ND	ND	ND
MMV687737	92.00	99.00	1.08	99.00	241.00	ND	ND	ND	ND	ND
MMV687208	167.00	ND	ND	0.00	236.00	ND	ND	ND	ND	ND
MMV687209	104.00	ND	ND	0.00	237.00	ND	ND	ND	ND	ND
MMV688430	86.00	57.80	0.67	ND	ND	ND	ND	ND	ND	ND
MMV688431	100.00	ND	ND	ND	ND	ND	ND	ND	ND	ND
MMV688532	67.00	138.00	2.06	ND	ND	ND	ND	ND	ND	ND
MMV689236	63.00	148.00	2.35	ND	ND	ND	ND	ND	ND	ND
MMV689241	413.00	ND	ND	ND	ND	ND	ND	ND	ND	ND
MMV689351	351.00	ND	ND	0.00	221.00	ND	ND	ND	ND	ND
MMV689352	481.00	ND	ND	0.00	228.00	ND	ND	ND	ND	ND
MMV689353	588.00	ND	ND	ND	ND	ND	ND	ND	ND	ND
MMV689306	109.00	118.00	1.08	118.00	14.10	ND	ND	ND	ND	ND
MMV689426	59.00	ND	ND	0.00	4.73	ND	ND	ND	ND	ND
MMV689033	667.00	673.00	1.01	673.00	286.00	ND	ND	ND	ND	ND
MMV689053	712.00	ND	ND	0.00	275.00	ND	ND	ND	ND	ND
MMV689505	58.00	ND	ND	0.00	207.00	ND	ND	ND	ND	ND
MMV689506	116.00	144.00	1.24	144.00	271.00	ND	ND	ND	ND	ND
MMV689507	76.00	114.00	1.50	114.00	69.10	ND	ND	ND	ND	ND
MMV689572	473.00	ND	ND	ND	ND	ND	ND	ND	ND	ND
MMV689569	86.00	147.00	1.71	147.00	313.20	ND	ND	ND	ND	ND

MMV689570	44.00	48.90	1.11	48.90	93.90	ND	ND	ND	ND	ND
MMV689573	44.00	ND	ND	0.00	16.80	ND	ND	ND	ND	ND
MMV689592	196.00	143.00	0.73	143.00	47.20	ND	ND	ND	ND	ND
MMV689670	68.00	97.90	1.44	ND	ND	ND	ND	ND	ND	ND
MMV689591	1920.00	ND	ND	ND	ND	ND	ND	ND	ND	ND
MMV689781	217.80	386.00	1.77	386.00	371.00	ND	ND	ND	ND	ND
MMV690004	1000.00	ND	ND	ND	ND	ND	ND	ND	ND	ND
MMV690005	1000.00	ND	ND	ND	ND	ND	ND	ND	ND	ND
MMV690006	1000.00	ND	ND	ND	ND	ND	ND	ND	ND	ND
MMV690114	56.75	90.00	1.59	90.00	50.00	ND	ND	ND	ND	ND
MMV692672	1000.00	15960.0	15.9	ND	ND	ND	ND	ND	ND	ND
MMV692703	1000.00	2660.00	2.66	ND	ND	ND	ND	ND	ND	ND
MMV692741	1000.00	6006.00	6.01	ND	ND	ND	ND	ND	ND	ND
MMV693078	981.70	ND	ND	0.00	7.01	ND	ND	ND	ND	ND
MMV884685	662.20	ND	ND	0.00	50.00	ND	ND	ND	ND	ND
MMV884694	179.20	204.00	1.14	204.00	46.84	ND	ND	ND	ND	ND
MMV884972	377.30	ND	ND	0.00	50.00	ND	ND	ND	ND	ND
MMV884973	732.00	ND	ND	ND	ND	ND	ND	ND	ND	ND
MMV884974	192.00	229.00	1.19	229.00	50.00	ND	ND	ND	ND	ND
MMV892773	117.80	ND	ND	0.00	45.10	ND	ND	ND	ND	ND
MMV892999	388.10	454.00	1.17	454.00	50.00	1823.00	ND	ND	ND	ND
MMV893003	552.90	554.00	1.00	ND	ND	ND	ND	ND	ND	ND
MMV893035	416.40	417.00	1.00	417.00	50.00	ND	ND	ND	ND	ND
MMV893034	149.30	173.00	1.16	173.00	50.00	ND	ND	ND	ND	ND
MMV893385	63.00	ND	ND	ND	ND	ND	ND	ND	ND	ND
MMV893405	36.00	ND	ND	0.00	28.00	28976.0 0	ND	ND	ND	ND
MMV893493	26.60	ND	ND	0.00	50.00	ND	ND	ND	ND	ND
MMV893648	13.60	ND	ND	0.00	1.70	6581.00	ND	ND	ND	ND
MMV893722	49.40	ND	ND	0.00	37.30	ND	ND	ND	ND	ND
MMV893727	258.00	ND	ND	0.00	50.00	ND	ND	ND	ND	ND
MMV893728	30.20	ND	ND	ND	ND	ND	ND	ND	ND	ND
MMV893743	33.00	ND	ND	0.00	50.00	ND	ND	ND	ND	ND
MMV897562	2841.00	ND	ND	ND	ND	ND	ND	ND	ND	ND
MMV973709	438.40	ND	ND	0.00	50.00	ND	ND	ND	ND	ND
MMV977401	212.50	330.00	1.55	330.00	50.00	ND	ND	ND	ND	ND
MMV977402	113.90	ND	ND	0.00	50.00	ND	ND	ND	ND	ND
MMV977416	33.60	ND	ND	0.00	30.09	1822.00	ND	ND	ND	ND
MMV977417	173.00	417.00	2.41	417.00	50.00	ND	ND	ND	ND	ND
MMV977482	96.30	339.00	3.52	339.00	50.00	ND	ND	ND	ND	ND
MMV977483	21.40	ND	ND	0.00	28.47	28836.0 0	ND	ND	ND	ND
MMV977484	409.50	ND	ND	0.00	50.00	ND	ND	ND	ND	ND
MMV982092	137.90	194.00	1.41	194.00	41.60	ND	ND	ND	ND	ND
MMV982102	96.90	ND	ND	0.00	1.01	ND	ND	ND	ND	ND
MMV1541927	181.00	ND	ND	0.00	50.00	ND	ND	ND	ND	ND
MMV1542888	35.00	ND	ND	0.00	28.00	ND	ND	ND	ND	ND
MMV1543420	475.00	ND	ND	0.00	50.00	ND	ND	ND	ND	ND
MMV1543429	80.00	ND	ND	0.00	42.40	ND	ND	ND	ND	ND

MMV1545646	283.00	ND	ND	ND	ND	ND	ND	ND	ND	ND	ND
MMV1545697	271.00	ND	ND	ND	ND	ND	ND	ND	ND	ND	ND
MMV1545716	20.00	51.00	2.55	ND	ND	ND	ND	ND	ND	ND	ND
MMV688516	369.00	ND	ND	ND	ND	1375.70 ± 80.25	ND	ND	ND	ND	ND
MMV688515	1260.00	ND	ND	ND	ND	ND	ND	ND	ND	ND	ND
MMV688808	238.00	ND	ND	ND	ND	ND	ND	ND	ND	ND	ND
MMV688842	ND	ND	ND	ND	ND	ND	ND	ND	ND	ND	ND
MMV688907	891.00	ND	ND	ND	ND	ND	ND	ND	ND	ND	ND
MMV688908	554.00	ND	ND	ND	ND	ND	ND	ND	ND	ND	ND

^aPreviously published asexual stage data included as per references, for comparative purposes.

^bRI = resistance index = ratio of the IC₅₀ values of resistant to susceptible strain.

^cSI = selectivity index = ratio of IC₅₀ against asexual *P. falciparum* to IC₅₀ against mammalian cells.

Table A4.1: Chemical analysis of the 83 prioritised compounds. Cluster number refers to the clusters obtained with a complete linkage clustering algorithm (Osiris DataWarrior; Tanimoto similarity 0.55). Compounds that do not adhere to the imposed selection cutoffs (Table 4.2, main text) are indicated in red text in the corresponding row.

TCAMS ID	Cluster No	*TCP-5 specificity	MW	cLogP	H-Donors	H-Acceptors	Polar Surface Area (PSA)	Aromatic Rings	Amides	Amines	Electronegative Atoms	Selectivity index (SI)
TCMDC-125752		47.14	272.37	2.12	2	4	81.4	1	1	0	5	NA
TCMDC-125521		28.58	274.32	2.75	2	4	81.4	2	1	0	6	NA
TCMDC-125487		21.51	304.80	3.60	2	4	81.4	2	1	0	6	NA
TCMDC-123475	1	19.46	208.28	0.87	2	4	81.4	1	1	0	5	NA
TCMDC-137906		13.04	274.34	1.48	2	5	94.54	2	1	0	6	NA
TCMDC-125522		9.24	325.22	3.86	2	4	81.4	2	1	0	7	4.51
TCMDC-137783		3.99	250.36	2.02	2	4	81.4	1	1	0	5	NA
TCMDC-125854		27.54	268.34	3.35	1	4	78.94	3	1	0	5	83.90
TCMDC-124550		17.95	354.41	4.57	1	6	125.64	4	1	0	8	NA
TCMDC-125540		10.31	328.39	4.56	1	4	107.18	4	1	0	7	104.12
TCMDC-139725	2	4.03	428.53	5.47	2	6	132.1	5	2	0	8	19.36
TCMDC-124559		3.85	476.57	4.21	1	7	128.88	4	2	0	9	37.99
TCMDC-124436		3.08	399.85	4.79	0	6	107.26	3	1	0	8	NA
TCMDC-125345		1.57	341.38	3.13	1	6	101.58	3	1	0	7	70.98
TCMDC-124011	3	27.13	329.63	4.86	0	1	36.28	2	0	0	5	11.43
TCMDC-141973	4	20.69	231.29	0.88	1	4	113.36	1	0	0	6	23.58
TCMDC-135244		14.45	336.37	2.82	1	6	109.15	4	1	0	7	NA
TCMDC-124453	5	7.07	268.36	3.14	1	4	50.7	2	0	0	4	NA

TCMDC-125826		6.16	268.36	2.99	1	4	50.7	2	0	0	4	NA
TCMDC-125825		4.57	294.39	3.55	1	4	50.7	2	0	0	4	67.29
TCMDC-135243		2.28	337.36	2.15	1	7	122.04	4	1	0	8	NA
TCMDC-123745		5.88	358.82	4.18	1	4	64.16	4	1	0	5	NA
TCMDC-138557		2.96	430.89	6.52	3	8	100.01	4	2	0	9	17.99
TCMDC-125420		2.18	353.42	3.37	1	5	63.59	4	0	0	5	13.64
TCMDC-134085	6	1.36	435.58	3.55	2	5	83.81	3	1	2	6	7.04
TCMDC-134292		1.28	419.95	4.81	2	4	44.37	3	1	2	5	14.09
TCMDC-139074		1.13	303.35	4.23	0	3	39.19	3	0	0	3	5.48
TCMDC-125539		5.39	301.41	3.55	0	3	120.45	4	0	0	6	NA
TCMDC-124602	7	2.74	284.36	2.39	0	4	96.62	4	1	0	6	NA
TCMDC-137908		4.45	425.61	4.86	2	3	27.3	4	0	3	3	12.82
TCMDC-137282		3.20	592.61	7.67	2	4	42.52	4	0	2	10	2.56
TCMDC-137281		2.80	540.78	8.56	2	4	42.52	4	0	2	4	2.02
TCMDC-132052		1.81	498.70	6.39	2	6	60.98	2	0	2	6	2.82
TCMDC-137795		1.67	516.67	5.79	2	6	60.98	4	0	2	6	4.16
TCMDC-137848	8	1.51	600.83	8.38	2	6	60.98	4	0	2	6	2.13
TCMDC-137952		1.50	512.73	7.61	2	4	42.52	4	0	2	4	2.35
TCMDC-137845		1.39	600.83	8.38	2	6	60.98	4	0	2	6	1.87
TCMDC-137340		1.22	508.69	7.28	2	4	42.52	4	0	2	4	2.24
TCMDC-137319		1.12	464.68	5.81	2	4	42.52	2	0	2	4	1.87
TCMDC-137797		1.06	456.62	5.93	2	4	42.52	4	0	2	4	2.48

TCMDC-137825		1.03	572.91	9.84	2	2	74.66	4	0	2	4	2.76
TCMDC-137915		1.01	456.62	5.93	2	4	42.52	4	0	2	4	5.92
TCMDC-131270		1.00	469.06	6.21	2	4	42.52	3	0	2	5	3.65
TCMDC-124263	9	3.79	290.34	0.74	2	6	98.05	1	2	0	7	NA
TCMDC-124262		2.96	248.30	0.78	2	5	88.82	1	2	0	6	57.38
TCMDC-141154		3.50	382.89	3.05	3	5	87.82	3	1	1	6	15.99
TCMDC-141334		2.73	342.82	3.77	2	4	72.28	3	0	1	5	8.77
TCMDC-123767	10	1.67	358.73	3.10	0	5	90	3	0	0	10	NA
TCMDC-141070		1.36	453.96	3.23	4	7	102.93	3	2	1	8	39.83
TCMDC-140680		1.15	387.27	2.85	3	5	87.82	3	1	1	6	47.47
TCMDC-141060		1.05	439.94	2.88	4	7	102.93	3	2	1	8	25.69
TCMDC-139089		3.46	559.02	5.39	6	10	130.2	6	6	0	11	82.38
TCMDC-125758		3.26	277.28	2.39	3	6	89.95	4	2	0	6	4.55
TCMDC-139082	11	1.93	524.58	4.78	6	10	130.2	6	6	0	10	213.40
TCMDC-139632		1.72	584.63	4.64	6	12	148.66	6	6	0	12	307.43
TCMDC-139087		1.69	584.63	4.64	6	12	148.66	6	6	0	12	259.47
TCMDC-139099		1.06	351.40	5.19	3	5	69.39	5	3	0	5	17.73
TCMDC-132301		2.90	427.45	3.98	2	3	41.29	2	0	3	8	2.92
TCMDC-140737		1.21	502.73	5.68	2	5	43.53	3	0	3	5	8.07
TCMDC-138967	12	1.20	644.54	10.01	0	4	24.94	2	0	2	8	2.63
TCMDC-132121		1.18	420.45	3.17	2	4	65.08	2	0	3	8	5.34
TCMDC-132012		1.11	435.56	3.99	2	7	71.54	3	1	1	7	6.85

TCMDC-125142		1.07	442.59	2.66	4	6	82.98	2	0	2	6	3.42
TCMDC-140064		1.05	526.50	5.47	3	6	87.04	3	1	1	8	17.22
TCMDC-141987		1.02	494.28	4.83	4	4	64.52	2	0	2	8	4.66
TCMDC-124617	13	2.10	383.71	3.73	2	3	37.2	2	0	2	5	2.90
TCMDC-138393		1.00	437.89	4.74	1	5	50.53	4	0	2	7	8.80
TCMDC-135281		1.94	474.54	2.64	2	10	170.22	5	3	1	11	1.15
TCMDC-134441		1.80	500.62	6.83	1	3	60.58	3	1	1	7	7.86
TCMDC-134447		1.80	462.65	5.91	1	4	69.81	3	1	1	5	4.90
TCMDC-134440		1.77	461.66	5.48	1	4	63.82	3	1	2	5	4.67
TCMDC-134449		1.63	475.69	5.87	1	4	63.82	3	1	2	5	7.34
TCMDC-141698		1.52	529.03	3.70	3	8	89.07	3	2	1	9	7.09
TCMDC-134438		1.25	453.04	6.19	1	3	60.58	3	1	1	5	8.68
TCMDC-134437	14	1.22	436.58	5.68	1	3	60.58	3	1	1	5	3.75
TCMDC-134446		1.17	467.07	6.58	1	3	60.58	3	1	1	5	6.40
TCMDC-136179		1.14	581.55	3.77	4	12	172.03	5	4	1	15	5.37
TCMDC-140964		1.10	718.76	5.08	0	8	74.04	4	2	1	13	10.12
TCMDC-134442		1.09	500.62	6.83	1	3	60.58	3	1	1	7	6.18
TCMDC-124805		1.07	382.33	3.68	0	6	79.27	2	1	0	9	162.95
TCMDC-134439		1.01	448.62	5.51	1	4	69.81	3	1	1	5	8.29
TCMDC-135052		1.00	391.25	2.65	4	7	90.97	2	3	1	9	6.48
TCMDC-135917	15	1.40	380.42	1.10	1	7	114.9	3	1	0	8	21.09

*TCP-5 selectivity = Asexual stage IC₅₀/Late (stage III-V) IC₅₀

Table A4.2: Physicochemical properties of the kinase inhibitor series. The DTPs are indicated in pink, 2-APs in purple, IMPs in orange, 6,9-IPs in turquoise and the 2,6-IPs in blue. Compounds that do not adhere to the imposed selection cutoffs (Table 4.2) are indicated in red text in the corresponding row.

Compound	MW (g/mol)	cLogP	Solubility pH 6.5 (µg/ml)	PSA (Å ²)	HBA	HBD	# Aromatic rings
MMV642943	427.43	3.21	3.00	84.14	6.00	2.00	3.00
MMV674192	414.39	2.98	2.88	92.34	6.00	2.00	3.00
MMV642944	394.37	1.74	<5	107.21	6.00	1.00	3.00
MMV643110	359.31	1.82	2.44	107.78	6.00	2.00	3.00
MMV642942	393.39	2.68	3.69	94.32	5.00	1.00	3.00
MMV668647	428.41	3.32	90 uM	92.34	6.00	2.00	3.00
MMV390048	393.38	2.55	3.26	94.32	5.00	1.00	3.00
MMV673927	356.31	1.68	2.18	81.99	6.00	1.00	4.00
MMV666810	442.44	3.67	3.01	92.34	6.00	2.00	3.00
MMV670930	378.38	2.24	2.87	100.97	5.00	1.00	3.00
MMV394902	392.40	3.50	3.98	81.43	4.00	1.00	3.00
MMV642941	358.32	2.64	2.74	94.89	5.00	2.00	3.00
MMV642990	358.32	2.77	3.16	94.89	5.00	2.00	3.00
MMV670401	427.43	4.14	3.24	79.45	5.00	2.00	3.00
MMV668808	341.30	2.57	3.32	88.48	5.00	1.00	3.00
MMV668809	341.39	0.51	1.39	133.23	7.00	2.00	3.00
MMV670402	427.43	4.14	3.24	79.45	5.00	2.00	3.00
MMV672643	377.39	3.06	3.16	88.08	4.00	1.00	3.00
MMV668648	428.41	3.32	2.95	92.34	6.00	2.00	3.00
MMV675081	360.29	2.22	3.07	101.99	6.00	2.00	3.00
MMV668807	317.27	1.73	2.29	77.58	5.00	1.00	3.00
MMV674796	372.35	2.75	2.79	80.90	5.00	2.00	3.00
MMV674594	359.31	3.17	3.79	89.10	5.00	2.00	3.00
MMV674333	449.45	2.70	3.25	110.53	6.00	2.00	3.00
MMV669810	453.54	1.58	3.11	115.23	7.00	0.00	4.00
MMV669286	453.54	1.67	0.00	115.23	7.00	0.00	4.00
MMV672652	437.54	2.17	3.45	108.99	6.00	0.00	4.00
MMV652103	427.50	1.07	0.00	115.23	7.00	0.00	4.00
MMV674850	452.55	2.20	3.64	102.34	6.00	0.00	4.00
MMV674766	426.51	1.60	3.15	102.34	6.00	0.00	4.00
MMV675615	436.55	2.71	3.54	96.10	5.00	0.00	4.00
MMV666620	461.54	1.60	2.36	105.05	8.00	1.00	4.00
MMV672925	470.57	0.69	2.29	141.25	8.00	1.00	4.00
MMV670815	417.45	1.33	2.56	127.17	9.00	1.00	5.00
MMV672653	393.42	1.38	3.16	110.01	7.00	1.00	4.00
MMV674132	457.57	2.27	2.97	114.89	7.00	1.00	3.00
MMV665078	417.41	2.91	4.47	72.71	5.00	0.00	4.00
MMV669289	428.49	0.07	1.90	128.12	8.00	0.00	4.00
MMV675704	495.57	1.69	2.91	131.44	8.00	1.00	4.00
MMV689854	668.60	7.06	ND	125.66	10.00	4.00	6.00
MMV893002	668.60	7.06	5.00	125.66	10.00	4.00	6.00
MMV893195	640.50	6.35	5.00	116.87	10.00	3.00	6.00

MMV892998	614.50	5.83	5.00	125.66	10.00	4.00	6.00
MMV1558618	491.50	3.40	130.00	58.63	6.00	2.00	3.00
MMV884980	363.30	2.59	200.00	80.06	6.00	2.00	3.00
MMV884979	363.30	2.59	200.00	80.06	6.00	2.00	3.00
MMV1557964	476.50	3.68	165.00	51.29	6.00	1.00	3.00
MMV982237	474.50	3.83	200.00	60.52	7.00	1.00	3.00
MMV1545775	421.40	4.09	170.00	48.05	5.00	1.00	3.00
MMV893049	668.60	7.06	5.00	125.66	10.00	4.00	6.00
MMV893359	628.50	6.29	5.00	125.66	10.00	4.00	6.00
MMV892826	433.50	4.34	200.00	80.06	6.00	2.00	3.00
MMV1558759	475.50	4.22	ND	38.4	5.00	1.00	3.00
MMV884981	463.50	4.35	5.00	92.37	8.00	2.00	3.00
MMV032931	399.40	3.85	ND	75.72	6.00	2.00	4.00
MMV892827	391.40	3.13	200.00	80.06	6.00	2.00	3.00
MMV693080	315.30	1.70	200.00	70.83	5.00	2.00	3.00
MMV910900	457.50	3.78	195.00	84.09	7.00	3.00	4.00
MMV884692	463.50	4.35	5.00	92.37	8.00	2.00	3.00
MMV690981	365.40	2.70	184.90	66.07	6.00	2.00	3.00
MMV982681	393.40	3.38	200.00	56.84	5.00	2.00	3.00
MMV884975	460.50	3.63	190.00	60.52	7.00	1.00	3.00
MMV982629	448.50	3.23	200.00	60.08	6.00	2.00	3.00
MMV1558616	441.50	2.65	135.00	58.63	6.00	2.00	3.00
MMV690007	377.40	2.93	ND	80.06	6.00	2.00	3.00
MMV982680	375.40	3.28	200.00	56.84	5.00	2.00	3.00
MMV1558136	433.40	4.05	135.00	48.05	5.00	1.00	3.00
MMV1558617	441.50	2.65	140.00	58.63	6.00	2.00	3.00
MMV982155	398.40	3.24	5.00	78.52	6.00	3.00	4.00
MMV892665	362.30	3.05	200.00	70.83	5.00	2.00	3.00
MMV910899	461.90	4.46	50.00	74.86	6.00	3.00	4.00
MMV1543411	558.50	4.86	5.00	89.62	8.00	2.00	6.00
MMV1558635	501.60	4.89	ND	38.4	5.00	1.00	4.00
MMV1542017	426.50	2.93	200.00	51.29	6.00	1.00	3.00
MMV1558761	461.50	4.03	ND	38.4	5.00	1.00	3.00
MMV892589	398.40	4.85	5.00	62.83	5.00	2.00	4.00
MMV982099	416.40	3.34	ND	78.52	6.00	3.00	4.00
MMV1558634	467.60	4.62	140.00	38.4	5.00	1.00	3.00
MMV1558620	475.60	2.97	25.00	80.92	7.00	1.00	3.00
MMV892903	417.40	3.86	150.00	66.07	6.00	2.00	3.00
MMV1545645	407.40	3.73	200.00	48.05	5.00	1.00	3.00
MMV982078	462.50	3.48	195.00	51.29	6.00	1.00	3.00
MMV1558773	439.50	3.88	ND	38.4	5.00	1.00	3.00
MMV689849	511.50	4.96	ND	92.37	8.00	2.00	4.00
MMV893746	414.40	3.49	5.00	87.75	7.00	3.00	4.00
MMV1542778	433.40	4.10	200.00	48.05	5.00	1.00	3.00
MMV1545843	468.60	4.07	185.00	51.29	6.00	1.00	3.00
MMV1558760	411.50	3.28	ND	38.4	5.00	1.00	3.00
MMV982553	405.40	3.90	200.00	57.28	6.00	1.00	3.00

MMV982154	366.40	2.59	5.00	78.52	6.00	3.00	4.00
MMV1558633	399.50	3.66	155.00	48.05	5.00	1.00	3.00
MMV1545842	412.50	2.68	190.00	60.08	6.00	2.00	3.00
MMV982100	444.50	3.38	200.00	51.29	6.00	1.00	3.00
MMV910835	365.40	2.68	ND	66.07	6.00	2.00	3.00
MMV892597	388.30	3.06	20.00	91.51	7.00	3.00	4.00
MMV1545639	393.40	3.32	200.00	48.05	5.00	1.00	3.00
MMV688390	453.50	3.76	65.90	72.97	7.00	2.00	4.00
MMV897780	461.50	3.84	5.00	72.97	7.00	2.00	4.00
MMV688375	385.30	3.91	5.00	75.72	6.00	2.00	4.00
MMV910895	435.50	3.51	175.00	81.76	7.00	3.00	4.00
MMV688475	371.30	3.64	5.00	86.72	6.00	3.00	4.00
MMV676245	391.30	4.18	5.00	66.49	5.00	2.00	4.00
MMV1545672	513.50	5.01	ND	72.97	7.00	2.00	4.00
MMV675812	332.30	1.70	5.00	126.22	8.00	3.00	4.00
MMV675617	371.30	4.23	5.00	75.72	6.00	2.00	4.00
MMV910833	497.50	4.39	5.00	72.97	7.00	2.00	4.00
MMV897781	494.50	3.54	10.00	85.86	8.00	2.00	4.00
MMV675717	373.30	4.08	5.00	66.49	5.00	2.00	4.00
MMV977480	453.50	3.83	180.00	81.76	7.00	3.00	4.00
MMV897760	407.40	2.86	5.00	81.76	7.00	3.00	4.00
MMV688389	440.40	3.65	5.00	78.96	7.00	2.00	4.00
MMV1545620	495.50	4.91	ND	72.97	7.00	2.00	4.00
MMV676227	326.30	2.40	62.10	71.42	6.00	2.00	4.00
MMV675097	355.30	3.98	ND	66.49	5.00	2.00	4.00
MMV675876	305.30	3.23	5.00	66.49	5.00	2.00	4.00
MMV897779	456.40	4.10	5.00	95.59	7.00	3.00	4.00
MMV688137	385.30	3.91	ND	75.72	6.00	2.00	4.00
MMV982093	440.40	3.66	5.00	96.03	8.00	2.00	4.00
MMV676003	355.30	3.63	10.20	66.49	5.00	2.00	4.00
MMV910836	509.60	4.90	10.00	72.97	7.00	2.00	4.00
MMV1542261	539.50	4.65	155.00	90.04	8.00	2.00	4.00
MMV691888	481.50	3.77	124.20	90.04	8.00	2.00	4.00
MMV1542021	513.50	4.26	50.00	98.83	8.00	3.00	4.00
MMV893197	439.40	3.51	200.00	81.76	7.00	3.00	4.00
MMV982672	495.50	4.16	200.00	98.83	8.00	3.00	4.00
MMV676222	341.30	3.44	5.00	66.49	5.00	2.00	4.00
MMV1542775	509.50	4.53	110.00	90.04	8.00	2.00	4.00
MMV982673	499.50	3.94	165.00	98.83	8.00	3.00	4.00
MMV977415	513.50	4.26	200.00	98.83	8.00	3.00	4.00
MMV675755	356.30	3.04	5.00	79.38	6.00	2.00	4.00
MMV675863	323.30	ND	<5.00	ND	0.00	0.00	0.00
MMV893468	389.30	4.33	ND	75.72	6.00	2.00	4.00
MMV688425	398.30	3.07	5.00	109.58	7.00	3.00	4.00
MMV1542776	523.60	4.91	200.00	90.04	8.00	2.00	4.00
MMV688727	385.30	3.91	5.00	75.72	6.00	2.00	4.00

Table A4.3: Summary of chemical libraries and gametocyte-focussed derivatives screened for late and mature gametocytocidal activities. Gametocyte-focussed compounds are indicated by highlighting their TCP-5 selectivity factor (ratio of asexual stage IC₅₀ to Late (stage III-V) IC₅₀).

Gametocyte stage (composition)	Assay	Compound class/library ID	Hit rate achieved	TCP-5 selectivity	Active examples; IC ₅₀	SMFA	Hit class/targets	Ref
73% Stage IV/V	alamarBlue®	NPC MMV Malaria box MIPE	0.5%	NA	NSC174938; 3 nM Torin 2; 8 nM NVPAUY922; 47 nM Muduramicin; 47 nM Narasin; 50 nM	NA	Dual actives: Quinines, quinacrine, anthracyclines, dihydroergotamines Gametocyte focussed: Dibenzazepine(serotonin) D2 antagonists, HDAC, ARK1, PIKKs, Ribose-phosphate diphosphokinase, ATCase, putative transporter.	[447]
Stage III-V (73% IV/V)	alamarBlue®	Sytravon	0.3%	NCGC00134126 ; 4.0 NCGC00134124 ; 3.8 NCGC00110901 ; 3.4 NCGC00104490 ; 1.7 NCGC00134795 ; 0.2 NCGC00127017 ; 0.3	NCGC00134126; 1.19 µM NCGC00134124; 1.55 µM NCGC00110901; 10.6 v NCGC00104490; 1.29 µM NCGC00134795; 4.25 µM NCGC00127017; 11.9 µM	NA	Known scaffolds: 2,4-diaminopyrimidines 1234-tetrahydroacridine Novel scaffolds: 3-amino-imidazo[1,2-a]pyridines, 3H-imidazo[4,5-b]pyridines, 4-1H-pyrazol-5-yl piperidines	[363]
Stage III-V	alamarBlue®	LOPAC	0.5%	NA	Dibenzodolium; 0.17 µM Antabuse; 0.25 µM CyPPA; 1.17 µM Calcimycin; 1.96 µM Phenanthroline; 2.19 µM Clotrimazole; 2.44 µM Cyclosporine; 7.12 µM	NA	Ca ²⁺ activated K ⁺ channels (SK2/SK3 subtypes), aldehyde dehydrogenase	[446]
Stage III/IV/V	alamarBlue®	St. Judes DANQ derivatives	8.8% 3.8%	SJ000030570; 0.52 SJ000024933; 0.93 SJ000022283; 0.30 SJ000024948; 0.39 SJ000032726; 0.40	SJ000030570; 61 nM SJ000024933; 100 nM SJ000022283; 100 nM SJ000024948; 100 nM SJ000032726; 180 nM		Dihydronephthoquinones (DANQ) Iminobenzimidazoles (IBI)	[503]
Stage III-V	alamarBlue®	Imidazo[4,5-c]quinolin-2-	NA	12; 0.25 19; 0.26	12; 0.028 µM 19; 0.081 µM	NA	Kinase inhibitors (mTOR and PI3K)	[522]

		ones derivatives		21; 0.33 23; 0.60	21; 0.052 μ M 23; 0.042 μ M			
Stage III-V	alamarBlue®	Torin analogs: Benzo[h][1,6]naphthyridin-2-(1H)ones	NA	1; 0.34 2; 0.53 21; 0.23 26; 0.50 34; 0.21 49; 0.40	1; 35 nM 2; 103 nM 21; 73 nM 26; 33 nM 34; 99 nM 49; 20 nM	NA	Kinase inhibitors (mTOR, PI3K, Bruton's tyrosine kinase)	[649]
Stage IV/V	pLDH	Knowns	NA	NA	DHA; 17 nM Epoxomicin; 3.9 nM MB; 29.5 nM Puromycin; 202 nM	Indirect SMFA (% infected mosquitoes @ 1 μ M) DHA; 10% Epoxomicin; 0% MB; 0%	NA	[449]
Stage IV/V	pLDH	Ionophores	NA	Salinomycin; 0.3 Monensin; 5.7 Nogericin; 0.5	Salinomycin; 6.3 nM Monensin; 5.7 nM Nigericin; 0.9 nM	Salinomycin; 18 nM Monensin; 1.3 nM	K ⁺ /Na ⁺ transporters	[650]
Stage IV/V	pLDH	Azaartemisinins	NA	11; 0.02 16; 0.65 17; 0.32 18; 0.52	11; 85.1 nM 16; 8.7 nM 17; 11.9 nM 18; 25.3 nM	NA	<i>PfKelch</i> mutations; PI3K inhibition	[520]
Stage I-III Stage IV/V (>95% IV)	pLDH (resazurin endpoint)	Knowns (MMV)	NA	NA	Artemisone; 0.20 Artemether; 0.20 Artesunate; 0.45 OZ439; 1.06	Artemisone; 3.7 nM Artemether; 9.9 nM Artesunate;	Artemisinins, synthetic peroxide (OZ439)	[464]

						mM)		
Stage IV/V	NF54 ^{Pfs16} Luciferase (SteadyLite kit)	ERS_01 GDB_04	0.3% 0.6%	NA		NA		[428]
					SN00769490; 1.98 µM SN00769485; 2.03 µM SN00769494; 2.19 µM SN00771077; 1.20 µM			
Stage IV/V	3D7elo1- pfs16- CBG99 Luciferase (D-Luciferin substrate)	MMV box	NA	NA	MMV085203; 440 nM MMV019918; 540 nM MMV000248; 606 nM MMV019881; 753 nM	NA	NA	[426]
Stage IV/V	3D7elo1- pfs16- CBG99 Luciferase (D-Luciferin substrate)	MMV019918 (MMV box) derivatives	NA	1; 0.64 12; 0.53 25; 0.63 26; 0.71 45; 1.1	1; 1.2 c 12; 8.3 µM 25; 1.4 µM 26; 1.4 µM 45; 1.1 µM	IC ₅₀ SMFA 0.07 µM 0.83 µM	PfPMT inhibitors	[519]
Stage V	NF54-cg6- ULG8- CBG99	MB + ML304	NA	NA	Synergistic IC ₅₀ : 772 nM	NA	Glutathione reductase (MB) and glucose-6-phosphate dehydrogenase-6-phosphogluconolactonase (ML304) inhibitors.	[651]
Stage V	MitoTracker Red (high content imaging)	Knowns GNF Malaria box (Novartis)	NA 0.6%	NA				[264]
					KAF246; 2 nM GNF179; 3 nM KDU691; 150 nM DDD107498; 9 nM	Oocyst reducti on GNF1 79; 100% @ 15 nM KDU6 91; 100%	Carbamazide thioureas, Napthoquinones, dioxonaphthalen- acetamides, tetrahydroisoquinoline-4-carboximides, didyroidioqionolones, 2-furancarboximides	

		Broad DOS	0.4%		BRD0608; NA BRD1260; NA	@ 1 μM DDD1 07498; IC ₅₀ : 1.8 nM		
Stage IV/V	NF54 ^{Pf16-Luc-GFP} (shape, number) and MitoTracker Red. High content imaging.	MMV box	24.2%	MMV019918; 1.16 MMV007907; 1.52	MMV019918; 692 nM MMV007907; 231 nM			[439]
Stage V	MitoTracker Red (high content imaging)	Carmaphycin B	NA	0.02	IC ₅₀ : 160 nM	NA	Proteasome inhibitor	[441]
Stage V (female gamete readout)	Pfs25 Ab, Cy-3 labelled. High content imaging.	MMV 50	10.0%	NA	DHA; 0.99 μM Artesunate; 0.64 μM Artemisone; 0.94 μM Thiostrepton; 0.12 μM MB; 0.92 μM NA	NA		[442]
Stage V (female gamete readout)	Pfs25 Ab, Cy-3 labelled. High content imaging.	TCAMS	12.4%	NA		NA		
Stage V (female gamete readout)	Pfs25 Ab, Cy-3 labelled. High content imaging.	TCAMS	3.0%	TCMDC-123767; 1.69 TCMDC-125345; 1.56 TCMDC-141698; 0.65 TCMDC-141070; 0.73 TCMDC-141154; 0.28 TCMDC-124559; 0.26	TCMDC-123767; 0.16 μM TCMDC-125345; 0.36 μM TCMDC-141698; 0.44 μM TCMDC-141070; 0.53 μM TCMDC-141154; 0.21 μM TCMDC-124559; 0.5 μM	Block in transmission (IC ₉₀) TCMDC-123767; 83% TCMDC-125345; 60% TCMDC-141698; 82% TCMDC-141070; 82%	4-aminoquinolines, Diaminopyrimidines, Novel chemotypes Tie-2 tyrosine kinase receptor Dopamine-2 receptor	[405]

						141070; 88% TCMD C-141154; 93% TCMD C-124559; 15%		
Stage V (male and female gamete readout)	Exflagellation centres; Pfs25 Ab Cy-3 labelled. High content imaging.	MMV box	8.5%	NA	MMV007116; 570 nM (males) MMV667491; 183 nM (males), 174 nM (females) MMV085203; 96 nM (males)	Oocyst reduction @ 1 µM All three > 90%		[265]
Stage V (gamete readout)	Acridine orange + high content imaging (rounding up)	MMV box	9.3%	NA	Sterilizing: MMV000760, MMV000787, MMV000907, MMV396797 MMV006172; 0.455 µM MMV665980; 0.809 µM	Oocyst reduction @ 1 µM MMV006172; 98%		[443]

NPC: The National Institutes of Health (NIH) Chemical Genomics Center Pharmaceutical Collection; MIPE: Internal collection of 550 kinase inhibitors; approved drugs as well as compounds in clinical and preclinical stages [652]; Sytravon library: retired screening collection containing a diversity of novel small molecules, with an emphasis on medicinal chemistry-tractable scaffolds; LOPAC: Library Of Pharmacologically Active Compounds; St Judes; TCAMS: Tres Cantos Antimalarial Set (GlaxoSmithKline); JHU CCL: Johns Hopkins University Clinical Compound Library (version 1.3); ERS_01: commercially available, structurally diverse compounds; GDB_04: 1,225 diverse scaffolds, with 4 representative compounds for each scaffold; Broad DOS: Broad Diversity-Oriented Synthesis Library; small molecules having both skeletal and stereochemical diversity.
DANQ: Dihydronephthoquinones; ATCase, aspartate carbamoyltransferase, PfATP4:P-type cation-ATPase, RPPK: phosphoribosyl pyrophosphate synthetase, TDPE: Tyrosyl-DNA phosphodiesterase; NA: not applicable.